The DELLA Protein Family and Gibberellin Signal Transduction

A thesis presented in partial fulfilment of the requirements for the degree of

Doctor of Philosophy

in

Biochemistry

Massey University, Palmerston North

New Zealand.

Christopher Andrew Kirk

2013

Abstract

Gibberellins (GA) are plant hormones that promote important aspects of growth such as seed germination, leaf expansion, trichome initiation, transition to flowering, stem elongation, flower and fruit development. Genetic and molecular data indicate that growth and development are a default state and that the DELLA proteins are key repressors of GA-mediated growth and development. Mutant analysis indicates that GA does not directly promote growth; rather it overcomes the repression of the DELLA proteins by causing them to be degraded. The N-terminal domain of the DELLA proteins is involved in the perception of the GA signal and the C-terminal domain mediates the repression of GA responses. A GA-bound receptor recognises the DELLA proteins and interacts with an F-box E3 ligase, the DELLA proteins are then poly-ubiquitinated and degraded through the ubiquitin-26S proteasome system. However, the DELLA proteins are also post-translationally modified which affects their activity. It is believed the DELLAs are modified both with *O*-linked N-Acetyl glucosamine for stability and phosphate groups to mark them for F-box recognition. However, the precise nature, and role of these modifications is yet to be shown. DELLA-repressive action is mediated by interaction with other proteins and not through direct DNA binding. Few DELLA-interacting proteins are known.

Apple and Kiwifruit *DELLA* repressor, *GID1* GA receptor and *SLY1*/ *GID2* F-box orthologues were identified in their respective sequence databases. Relative amount and location of the orthologous transcript sequences was examined through qPCR and reporter gene experiments. Apple qPCR experiments indicated relatively high levels of *DELLA* transcripts in developmentally arrested tissues. Kiwifruit experiments present a more complicated picture, with high relative levels of *DELLA*s in the actively expanding tissues, however, concomitant with this were high relative levels of the *GID1* and *GID2* transcripts. Each transcript was found in every tissue studied and indicated complex developmental transcriptional control.

Both direct and indirect immunoprecipitation experiments utilising a novel tag were performed in GA-deficient plant backgrounds in order to isolate DELLA proteins and their interacting proteins likely targeted by DELLA repressive function. Proteins from these experiments were identified from their peptides in mass spectrometry analysis and database

query. Several transcription factors, kinases, proteins involved in RNA processing and protein components involved in hormonal signalling pathways other than GA were present.

DELLA repression complex formation was also investigated with two-dimensional electrophoresis and western blotting, and indicated a dominant repressive complex at approximately 160 kDa, with additional multiple larger complexes of up to 600 kDa.

Acknowledgments

I would like to thank my supervisors, Dr. Jasna Rakonjac, Dr. William Jones, and Dr. Toshi Foster for their advice and guidance.
David Sheerin, fellow DELLA student and Doug Hopcroft, MMIC and Dave Greenwood, PFR MARC for their assistance.
I would also like to thank my colleagues of the immunology group at Plant and Food Research for their consideration and patience.
Finally I would like to thank my family; my wife Michelle and my children Alan, Tom and Maddy for all their support.

This project was supported by grants from the Foundation for Research Science.

Table of Contents

List of Figures

List of Tables

Abbreviations

2-MEA	2-Mercaptoethanolamine.HCl .
ABA	Abscisic acid.
Bar	Bialaphos Resistance.
bHLH	Basic Helix-Loop-Helix
BMV	Brome Mosaic Virus.
BNE	Blue Native gel Electrophoresis.
bp	Base pairs
BR	Brassinosteroid.
BSA	Bovine Serum Albumin.
cDNA	complementary Deoxyribosenucleic acid.
CDS	Coding Sequences.
ChIP	Chromatin Immunoprecipitation.
C-terminal	Carboxyl end/ portion of polypeptide.
DDM	n-dodecyl β-D-maltoside.
DNA	Deoxyribose Nucleic Acid.
dNTP	Deoxynucleotide triphosphates.
DTT	1,4-Dithiothreitol.
EDTA	Ethylene-diamine-tetra-acetic acid.
EGTA	Ethylene glycol-bis(2-aminoethylether)-*N*,*N*,*N'*,*N'*-tetraacetic acid.
EMCS	Maleimidocaproyloxy]succinimide ester.
EST	Expressed Sequence Tag.
FSB	Frozen Storage Buffer.
GA	Gibberellin.
GA3	Gibberellin A3.
GDR	Genome Database for Rosaceae.
GSP	Gene Specific Primer.
IEF	Isoelectrical Focus.
IgG	Immunoglobulin G
IP	Immunoprecipitation.
IPG	Immobilised pH Gradient.
IPTG	Isopropyl β-D-1-thiogalactopyranoside.

JA	Jasmonic acid.
LB	Luria Broth.
LG	Linkage Group
mAb	monoclonal Antibody.
MBP	Maltose Binding Protein.
MG132	Z-Leu-Leu-Leu-al.
miRNA	micro Ribose Nucleic Acid.
mRNA	messenger Ribose Nucleic Acid.
N-terminal	Amino end/ portion of polypeptide.
PAC	Paclobutrazol
PBS	Phosphate Buffered Saline.
PBST	Phosphate Buffered Saline supplemented with Tween 20™ (0.1 % polysorbate-20).
PCR	Polymerase Chain Reaction.
PIPES	Piperazine-N,N'-bis(2-ethanesulfonic acid).
qPCR	quantitative PCR.
RACE	Rapid Amplification of cDNA Ends.
RE	Restriction Endonuclease type II.
RNA	Ribose Nucleic Acid.
RT	Reverse Transcription.
SAM	Shoot Apical Meristem
SDS	Sodium Dodecyl Sulphate.
SDS-PAGE	Sodium Dodecyl Sulphate Poly-Acrylamide Gel Electrophoresis.
Silwet® L-77	84 % polyalkylencoxide modified heptamethyltrisiloxane 16 % allyloxypolyethyleneglycol methyl ether.
TEMED	Tetramethyl-ethylene-diamine.
TEV	Tobacco Etch Virus.
Tris	Tris (hydroxymethyl) aminomethane.
Tween™ 20	Polysorbate-20.
uidA	β-D-Glucuronidase gene.
X-gal	5-bromo-4-chloro-3-indolyl galactopyranoside.
X-gluc	β-D-glucuronide.
YEB	Yeast Extract Broth.

1. Introduction

The study of a disease named Bakanae (translated as silly rice crop) of rice seedlings, through the early part of the 1900's, led to the discovery of the first Gibberellic Acid (GA), Gibberellin A3 (GA_3). It is named after the disease-causing organism, the fungus *Gibberella fujikuroi* (Saw). By 1956 the first evidence of gibberellins in higher plants was published, leading to acceptance that gibberellins are endogenous plant hormones (Phinney, 1983).

Gibberellins stimulate cell elongation and division, affecting many plant growth processes including seed germination and seed food reserve mobilisation, hypocotyl and stem elongation, leaf expansion, trichome development, switch to floral identity, floral organ development, pollen microspore oogenesis and fruit expansion (Sponsel, 1995).

1.1 Gibberellin biosynthesis

Throughout a particular plant there are only one or two major active forms of gibberellin or gibberellic acid. In higher plants; the most common active gibberellins are GA_1, GA_4, GA_3, or GA_7 (Hedden and Phillips, 2000). The major active forms of gibberellins differ among plants. If a plant has two active forms, these may have different levels of activity and their abundance and/or mode of activity may vary between organs and across developmental stages. Plants also contain a large number of GAs that do not act as hormones; they are either the precursors or inactivation products of the active molecules.

The major biologically active GA form is found in the concentration range of 0.1 to 100 ng per gram fresh weight (physiological range 0.1 nM to 10 μM) of floral and vegetative tissue (Phinney, 1983, Hedden and Phillips, 2000, Silverstone et al., 2001, Sun, 2010). GA_4 is the major bioactive form promoting both vegetative growth and floral initiation and maturity in *Arabidopsis* (Eriksson et al., 2006). GA_1 is the major bioactive GA in rice vegetative growth but GA_4 is the main active form in reproductive growth (Kobayashi et al., 1989).

1.1.1 Site of synthesis

Gibberellins are synthesised near the responding (expanding and differentiating) tissues, hence all target tissues produce them whilst growing, expanding and differentiating. Interestingly,

even though GA is synthesised near the vegetative shoot apical meristem (SAM), this hormone is generally excluded from the meristem. GA is, however, synthesised within the inflorescence meristem and therefore cannot be excluded from this type of SAM (Olszewski et al., 2002, Kojima et al., 2009).

GAs are not only found in tissues, but also in the phloem and xylem exudates. Therefore, GAs can be actively transported over long distances. Moreover, it has been shown directly that GA is transported from rosette leaves to the shoot apex, to facilitate flower initiation (Eriksson et al., 2006).

Not all the cells in a particular organ may be synthesising GA and therefore short distance intercellular transport also occurs. In developing flowers, expression of the genes *GA3ox3* and *GA3ox4*, encoding enzymes that mediate the final step of GA_4 synthesis, is restricted to particular tissues: stamen filament, anthers and flower receptacles. Similarly, in developing siliques, expression is restricted to the replums, funiculi, silique receptacle and the developing seeds. From these points, GAs are transported to petal and fruit endosperm, to promote growth (Hu et al., 2008).

Active GAs or (biologically inactive) GA precursors are also stored in the seed. The seed embryo does not synthesise all GA *de novo*; rather it can mobilise stored GA or GA precursors of maternal origin (Ritchie and Gilroy, 1998b). Laser microdissection of rice microspore, pollen and surrounding tapetum, followed by microarrays, was performed to look at GA biosynthesis and expression of genes that encode the proteins of the GA signalling pathway (Hirano et al., 2008). This approach showed that the signalling genes were expressed very early in development and the GA biosynthesis genes were expressed later, with little overlap. Therefore, GA is stored in pollen, without signalling components, for later use in pollen tube germination.

1.1.2 Control over synthesis

The synthesis of a bioactive GA molecule (Figure 1) is broken down into three stages by the three classes of enzymes required in the synthesis, which are localised in different compartments of a cell (Olszewski et al., 2002).

The intra-cellular transportation of the molecules can be controlled and limited at each of the three stages in the bioactive GA synthesis. GA and its precursors may also be transported out of the cell, however this process and its control are poorly understood (Kaneko et al., 2003, Ogawa et al., 2003).

The enzyme *ent*-copalyl diphosphate synthase (CPS), which catalyses the first committed step of gibberellin synthesis (Figure 1) controls the flow of catabolite into the pathway. The expression of CPS is therefore very tightly controlled. However, the key control point for the bioactive GA levels is at the final stage of synthesis, through GA20ox, GA3ox and GA2ox (Gibberellin 20-oxidase, Gibberellin 3β-hydroxylase and Gibberellin 2-oxidase) enzyme action. The major control over synthesis occurs in the form of a feed-back and feed-forward loop; where the amount of the bioactive GA affects both the rate of new bioactive GA synthesis and its turnover to an inactive form. These loops control, mainly at transcriptional level, the enzymes that catalyse two final steps in the synthesis of an active GA (GA20ox and GA3ox) and the deactivating enzyme (GA2ox). These enzymes actually comprise a family in each case, rather than a single enzyme. Each enzyme within the family has a particular expression pattern, such that it is regulated spatially (organ specific) and temporally (developmental stage) (Olszewski et al., 2002, Thomas et al., 2005, Hedden and Phillips, 2000, Yamaguchi and Kamiya, 2000, Ogawa et al., 2003, Mitchum et al., 2006). In specific instances bioactive GAs can also be controlled through other modes of inactivation: via methylation, as in *Arabidopsis* (Varbanova et al., 2007), or epoxidation as in Rice internodes (Zhu et al., 2006).

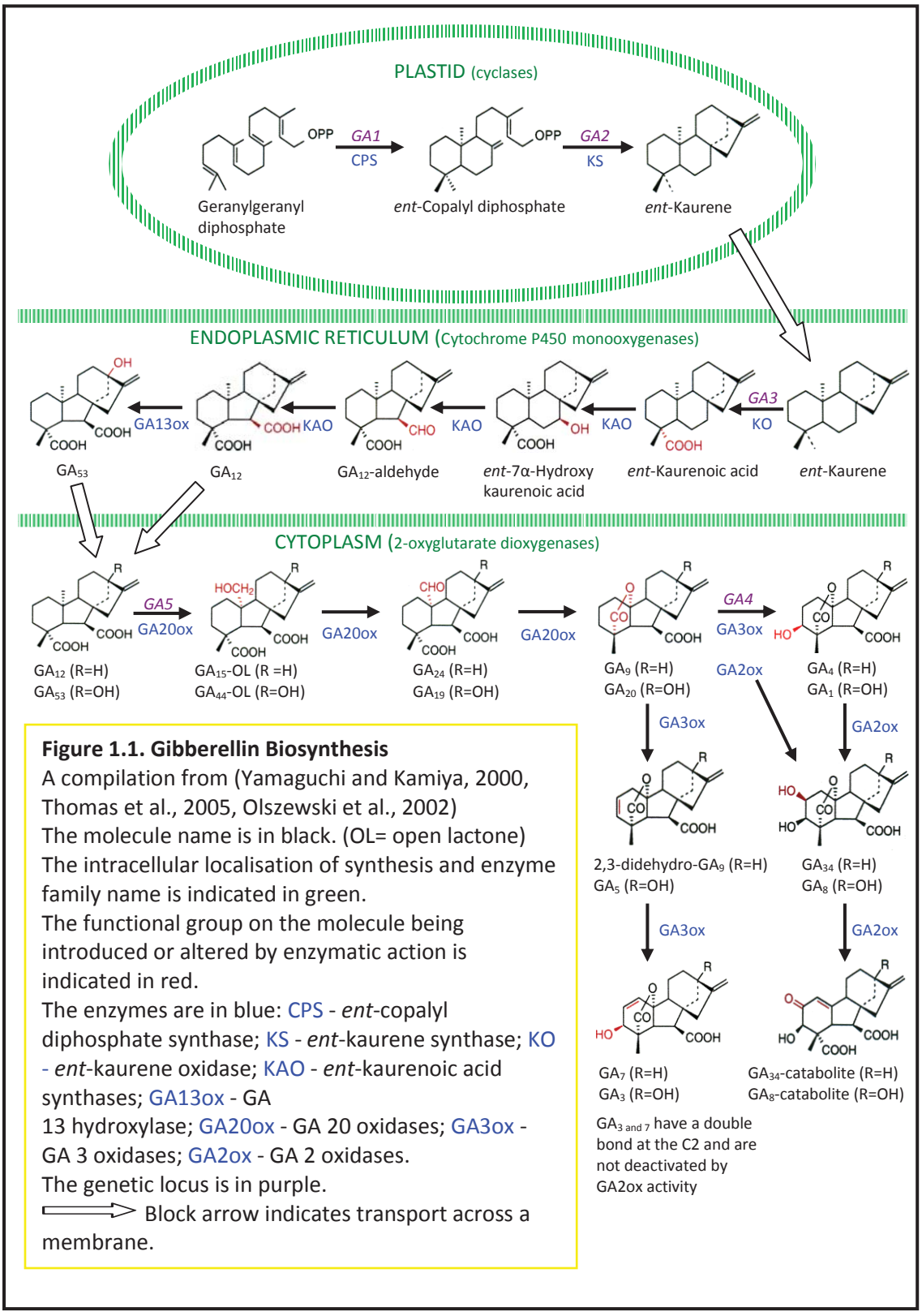

Figure 1.1. Gibberellin Biosynthesis
A compilation from (Yamaguchi and Kamiya, 2000, Thomas et al., 2005, Olszewski et al., 2002)
The molecule name is in black. (OL= open lactone)
The intracellular localisation of synthesis and enzyme family name is indicated in green.
The functional group on the molecule being introduced or altered by enzymatic action is indicated in red.
The enzymes are in blue: CPS - *ent*-copalyl diphosphate synthase; KS - *ent*-kaurene synthase; KO - *ent*-kaurene oxidase; KAO - *ent*-kaurenoic acid synthases; GA13ox - GA
13 hydroxylase; GA20ox - GA 20 oxidases; GA3ox - GA 3 oxidases; GA2ox - GA 2 oxidases.
The genetic locus is in purple.
⇨ Block arrow indicates transport across a membrane.

1.1.3 Mutations in Gibberellin biosynthetic genes and signalling pathway

Compared to wild type plants, the GA-deficient plants are dwarfed in stature (in a range from severe to semi), darker green (higher chlorophyll content), have fewer trichomes, take longer to flower (and under certain conditions they may never flower), have abnormal flower development with impaired fertility (especially male fertility; ranging from sterile to mild), fewer seeds are produced and a lower percentage of them will germinate (under what are normally favourable conditions). The phenotype of plants with null mutations of genes encoding any of the GA biosynthetic enzymes can be restored to the wild-type with exogenous application of bioactive GAs. An important mutation (in *Arabidopsis*), utilised in many studies of GA and its signalling, is the *ga1-3* mutant, a null mutation of the CPS enzyme in the *GA1* locus. Artificial control of GA biosynthesis can also be implemented by synthetic inhibitors, most commonly paclobutrazole (PAC) and uniconazole, both acting on the CPS (Koornneef et al., 1985).

1.2 The DELLA proteins

A second class of mutations can be distinguished as they cannot be restored to wild-type phenotype by exogenous application of GA. These are in components of the GA signal perception/transduction pathway and are the focus of this thesis (Figure 1.2). The core GA signalling components are the GA receptor *GID1* (*GIBBERELLIN INSENSITIVE DWARF 1*), the repressors of GA responses DELLA protein family, and the F-box 26S proteasome component *SLY1*/ *GID2* (*SLEEPY 1* and *GIBBERELLIN INSENSITIVE DWARF 2*).

GAI (*GIBBERELLIN INSENSITIVE*) was the first of the GA signalling pathway proteins to be identified and cloned. It is a member of DELLA family of proteins, named after the conserved Asp-Glu-Leu-Leu-Ala N-terminal motif. The *gai* mutant is a semi-dominant, dark green (increased chlorophyll content), dwarf plant with reduced responsiveness to exogenous GA (Koornneef et al., 1985). The mutant contained an in-frame deletion of 17 amino acids; hence it was not a simple inactivation mutant. The semi-dominant character of the mutation and analysis of the mutant responses led to a proposal that *GAI* is a 'GA de-repressible repressor' or a negative regulator of GA responses, whose repression is counteracted by GA (Peng et al., 1997).

The model proposes that the default state of a plant is growth and development, but this is held in check by DELLA activity. A balance exists between the repression of growth and all-out-development to maturity. This is done through coordinating signals (both endogenous and external) in order to achieve an optimal response and outcome for the plant. The DELLA proteins appear to be central to this balancing of competing signals from different pathways. Releasing the repression would be achieved through inactivating DELLAs.

Interestingly, the 17 amino acids deletion in the *gai* mutant was lacking the signature DELLA motif and downstream sequence, which is also highly conserved among the DELLA family of proteins, implicating the motif in the perception of GA. DELLA motif is part of a larger N-terminal domain that was found to be essential for the perception of the GA signal by the DELLA (Koornneef et al., 1985). The C-terminal domain of the DELLA proteins is involved in the repressive activity of these (Peng et al., 1997, Silverstone et al., 1997). The vast majority of dicotyledonous plants studied thus far have more than one DELLA-encoding gene, whereas grasses (like rice) have only a single DELLA ORF in their genomes. The DELLA proteins belong to a superfamily of transcription factors unique to the plant kingdom, known as GRAS proteins (for GAI, RGA, and SCARECROW) family. All GRAS proteins have the conserved C-terminal but divergent N-terminal domains (Pysh et al., 1999).

Work on DELLA proteins was stimulated by the discovery that the DELLA motif was mutated in some of the cereal "green revolution" cultivars, which with improved cultivation methods, resulted in increased crop yields that were able to feed burgeoning world population in the 1950's,'60's and '70's (Peng et al., 1999).

Figure 1.2. Phenotypes of GA biosynthesis and GA signalling mutants in Arabidopsis
Modified from (Wen and Chang, 2002).
A, Wild-type (Col-0 ecotype), **B,** Semi-dwarf (*gai*, but also representative of *ga1-3*), **C,** Severe dwarf (representative of GA-insensitive), **D,** Slender (representative of constitutive GA signalling/ GA overdose)
Yellow Scale bar 5 cm.

1.2.1 DELLA orthologues

A second *Arabidopsis* DELLA gene was identified in a screen for mutations suppressing the GA biosynthetic mutant *ga1-3* and named *RGA* (*REPRESSOR OF ga1-3*) (Silverstone et al., 1997, Silverstone et al., 1998). Experiments showed that RGA and GAI have overlapping, but not completely redundant functions in controlling the GA response pathway and that RGA had a more significant role. RGA-GFP (Green florescent protein) fusion was shown to be expressed in the nucleus of cells and was lost on GA treatment (Silverstone et al., 2001), leading to the proposal that the protein was being degraded through the ubiquitin-proteasome system. This was confirmed by Dill *et al*, who engineered the 17 amino acid DELLA motif deletion mutant of RGA fused to a GFP (RGAΔ17-GFP) and found that the mutant protein was not degraded following GA application (Dill et al., 2001).

RGA and *GAI* null mutants were shown to suppress vegetative growth defects caused through GA insufficiency in *ga1-3* mutants, supporting the role of DELLA proteins as growth repressors. However, *GAI* and *RGA* null mutants did not suppress germination and most floral defects, leading to the conclusion that *RGA* and *GAI* are involved mostly in the repression of juvenile growth and phase change (Silverstone et al., 2001, King et al., 2001, Dill and Sun, 2001). Three additional DELLA homologues were identified in the *Arabidopsis* genome (Wen and Chang, 2002, Lee et al., 2002b, Sanchez-Fernandez et al., 1998) and they were named *RGL1, RGL2,* and *RGL3* (*RGA like 1,2 and 3*) (Truong et al., 1997, Dill and Sun, 2001). All have been shown to function as nuclear localised repressors of GA signal transduction (Lee et al., 2002b, Wen and Chang, 2002, Hussain et al., 2005, Feng et al., 2008). Based on genetic analyses, *RGL2* was shown to have the most prominent role in repression of germination among the five DELLA proteins (Lee et al., 2002b). The authors proposed that *RGL2* is an integrator of environmental (water, cold spell, light quality) and endogenous (ABA and GA) signals, with the ultimate outcome of either release of the embryo for germination or maintaining its dormancy. By examining which combinations of DELLA null mutants can suppress *ga1-3* phenotypic abnormalities, it was confirmed that double null *RGA*/*GAI* fully suppresses height defects (Cheng et al., 2004, Cao et al., 2005). Furthermore, these authors concluded that RGA and GAI, with minor contributions from RGL1 and RGL2, control floral transition of the shoot apical meristem (SAM) to an inflorescence meristem (IFM). These authors also confirmed RGL2 is the predominant germination repressor, but RGA, GAI and RGL1 do contribute (listed in descending order of repressive activity). RGA and RGL2 are predominant but RGL1 does have a

role in controlling floral organ growth. RGL3 appears to have a minor role in the germination (Cao et al., 2005) and in shade-induced elongation of growth (Feng et al., 2008).

Unlike the constitutive expression of *RGA* and *GAI* (Silverstone et al., 1998), the transcript of *RGL2* was found to be inducible on seed imbibition (Lee et al., 2002b). To fully determine distribution of DELLA mRNAs in various organs of *Arabidopsis*, all five DELLA transcripts were quantified using qPCR across different tissue types throughout development (Tyler et al., 2004). This analysis showed that *RGA* and *GAI* are ubiquitously expressed, with *RGA* averaging 300 and *GAI* averaging 50 copies mRNA per 1000 mRNA copies of the housekeeping protein-encoding gene *UBQ11*. *RGL1*, *-2* and *-3* mRNAs show some tissue specificity, with *RGL2* and *-3* expressed more highly in germinating seeds and *RGL1* and *-2* expressed more highly in flowers than in other organs. *RGL2* message is very high and *RGL1* has the lowest copy number in the seeds. *RGL3* expression is the lowest overall, and is lower than all others in the flower and siliques. All *RGL* mRNAs are very low in vegetative tissues. Therefore, transcript expression profiling supports the overlap of functions seen in mutant phenotypes.

In *Arabidopsis*, genetic redundancy of the DELLA proteins is an important point to be appreciated, modulating the outcome through the different family members having slightly different functions, interactions and expression levels, depending on the organ, developmental stage, internal and external conditions (Cheng et al., 2004, Tyler et al., 2004).

RGL2 and RGA can perform interchangeable functions when they are expressed under control of the reciprocally-regulated promoters. Both proteins interact with the similar set of transcription factors, as shown by Yeast two-hybrid interaction assays (Gallego-Bartolome et al., 2010). The authors propose that differential regulation (expression pattern), as well as different pattern of the interacting transcription factors is the key to their differing physiological roles.

Rice (*Oryza sativa* L.) contains a single DELLA protein gene *SLENDER RICE 1* (*SLR1*), which is expressed throughout the plant (Ogawa et al., 2000, Ikeda et al., 2001). The lack of redundancy has facilitated the GA signalling pathway dissection in rice as a model organism (discussed in later sections). The rice genome does contain two additional protein-encoding genes of considerable homology to *SLR1*, named *SLENDER RICE LIKE 1* and *2* (*SLRL1* and *2*). However, these proteins do not have the DELLA and downstream conserved motifs (Itoh et al., 2005b). A low level of *SLRL1* transcript was found in developing flowers and elongating internodes. The

transcript level was increased in response to GA and was altered in biosynthetic and signalling mutants. Over-expression of this protein in rice results in GA-insensitive dwarfed plants. In contrast to *SLRL1*, transgenic rice plants overexpressing *SLRL2* were affected by GA. In these plants, *SLRL2* mRNA was expessed only in the embryos of immature seeds (Liu et al., 2007). When overexpressed in *Arabidopsis*, *SLRL2* caused a semi-dwarf, late flowering phenotype that was not responsive to GA. Although no function has yet been described for the native proteins, it was proposed that the SLRLs may serve to fulfil a requirement for a (constitutive) basal repression level of target genes in the presence of GA during important developmental stages of flower and embryo development.

There is a single DELLA-protein-encoding gene in barley *(Hordeum vulgare* L.), *SLENDER 1* (*SLN1*). Both the protein and mRNA of SLN1 were found in the elongation zone in the basal region of the leaves, where GA levels are highest (Chandler et al., 2002). SLN1 and GA are co-localised; therefore it is the balancing of positive and negative signalling conditions that determine the physiological outcome in this tissue. GA reduces SLN1 levels, resulting in down regulated GA synthesis through a negative feed-back regulation, *via* SLN1, of GA biosynthetic enzymes. SLN1 turnover and regulation were shown to be regulated by phosphorylation (Gubler et al., 2002). Furthermore, the role of GA in germination has been established using barley aleurone as a model (Fu et al., 2002) (please see later sections).

Maize (*Zea mays* L.) dominant dwarf mutants of the *D8* gene, a DELLA orthologue, made them important cultivars used for their sturdy stature in cropping (Peng et al., 1999, Cassani et al., 2009). These are in-frame deletion and insertion mutants affecting the N-terminal domain of the D8 protein, in particular the DELLA and downstream VHYNP motifs that are required for perception of the GA signal.

Wheat (*Triticum aestivum* L.) *REDUCED HEIGHT* (*RHT D1* and *RHT B1* alleles) DELLA orthologue mutants (N-terminal truncations including GA-response DELLA motif) were also selected and used for their reduced and sturdy stature in the ‘green revolution’(Peng et al., 1999).

GA is involved in cotton (*Gossypium hirsutum* L.) fibre development (Liao et al., 2009, Aleman et al., 2008). Epidermal cells on the surface of ovules differentiate (under auxin signalling) to become fibres and become competent to later elongate under GA signalling. There are at least two DELLA homologues in cotton, *GhSLR1a* and *-b*.

GA, along with several other phytohormones, is involved in the root nodulation-symbiosis development in a trefoil model plant from the genus Lotus (*Lotus japonicus* L.). (Maekawa et al., 2009) found that increased GA signalling, through increased expression and *SLY1* activity (*sly1-d* transgene) reduced nodule numbers.

Pea (*Pisum sativum* L.) has two DELLA orthologues, LA and CRY. LA is a dominant repressor in shoots and roots (Weston et al., 2008).

The *procera* mutant of tomato (*Solanum lycopersicum* L.) is a *DELLA* orthologue mutant whose phenotype resembles a constitutively active GA response; it is therefore a null mutant. The *procera* plant phenotype shows an increased height of the plant and altered axillary branching, with fewer leaflets that have smoother margins than the wild-type. Consistent with the phenotype the *PRO*/*SlGAI* gene product was found to have a point mutation in the C-terminal domain, in the conserved VHIID motif, that is required for the DELLA repressor function (Bassel et al., 2008, Jasinski et al., 2008). The *PRO*/*SlGAI* transcript was found in the SAM and in the vasculature of the internodes and may indicate that, in tomato, DELLAs regulate development of lateral organs and leaf morphogenesis from a very early stage. DELLAs regulate growth through cell size, not number (Jasinski et al., 2008). Silencing of *PRO* by a corresponding RNAi led to facultative parthenocarpy, along with the usual constitutive GA-signalling phenotypes of slender plant and altered flower organ morphology, anthers and styles (Marti et al., 2007). The authors concluded that DELLAs are involved in fruit development repression in the absence of pollination. The parthenocarpic fruit had abnormal morphology; hand pollination however restored a normal phenotype to the fruit, indicating a DELLA-independent signalling pathway that governs the fruit development post-pollination.

In grape (*Vitis vinifera* L.), a Pinot noir cultivar called Pinot meunier, is a dwarf that produces many flowers and trichomes. It has a mutation in DELLA orthologue *VvGAI1* (Boss and Thomas, 2002). This is a dominant gain-of-function DELLA motif mutation DEL(L→H)A. The Pinot meunier cultivar dates from the 1500's, hence this is the oldest 'green revolution' mutation. GA in grape promotes internode elongation as it does in all other plants. However, rather than promoting floral meristem induction, like in other species, GA inhibits it in the grape, by switching development toward producing tendrils. Therefore in grape, the DELLA proteins are inhibiting growth (through preventing tendril formation) as normal, but (unusually) also promote flowering. Since in the grape-vine access to the sunlight is dependent on climbing (depending on tendrils), this “anomaly” is most likely an adjustment to the vine lifestyle. Thus,

the DELLA activity is still achieving the same aim as in other plants, to prevent premature flowering under unfavourable conditions.

GA and the corresponding signalling pathway components are involved in wood formation in Aspen (*Populous* L.). GAs induce differentiation to xylem, mediated by GA signalling in the meristematic cambium and xylem fibre elongation and lignification (Mauriat and Moritz, 2009). In the root, GA inhibited lateral root primordium initiation (Gou et al., 2010, Busov et al., 2006). Consistently, over-expression of GA-unresponsive dominant N-terminal dwarfing mutants of the DELLA orthologue in Aspen caused dwarfing and promoted lateral root formation and elongation. The primary root length was not affected and transgenic plants had reduced aerial biomass and increased root biomass. Therefore, GA signalling in Aspen affects differently the aerial and root growth.

1.2.2 DELLA protein domains and their function

Analysis of DELLA protein mutations discussed above initially identified two domains; N-terminal, required for GA sensing, and C-terminal, required for repressor functions. Mutant analysis in combination with alignments of the DELLA proteins from different plant species, have identified several conserved motifs in both N- and C-terminal domains.

The first published structure-function analysis of a DELLA protein, domain deletion analysis of the rice DELLA protein SLENDER RICE 1 (SLR1), determined functions of particular domains (Itoh et al., 2002). Based on this work it was proposed that DELLA and TVHYNP motifs in the N-terminal domain, separated by a non-conserved spacer region, are involved in GA signal reception and DELLA protein stability (Figure 1.3). A third N-terminal domain segment, rich in Ser, Thr and Val and called poly S/T/V region was also identified. When this S/ T/ V region was deleted, the plants were more dwarfed compared to wild-type, hence the mutant protein was a stronger repressor of growth. The ΔS/ T/ V protein was, however, sensitive to GA. Therefore this domain may normally have a role in negative regulation of SLR1 repressor function. Given that Ser and Thr are normally targets for phosphorylation and O-glycosylation, it was proposed that the SLR1 S/ T/ V domain is a target for post-translational modification mechanisms. For *Arabidopsis* RGA*,* it was proposed that the post-translational modifications of the S/ T/ V rich region have an activation role, leading to a stronger repression of development (Silverstone et al., 1998). However, given that the poly S/ T/ V region is more pronounced in the cereal crop plants than in dicots, it was hypothesised that the DELLA proteins of dicotyledonous and

monocotyledonous plants function differently in this region (Itoh et al., 2002). The C-terminal domain commences with the leucine zipper motif, which is a well known protein-protein interaction and protein dimerisation motif. Both the repressive function and sensitivity (degradation) in response to GA were lost when the leucine zipper motif is deleted. When a truncated SLR1, containing only the N-terminal domain and lacking the C-terminal domain, was over-expressed in plants they became slender, indicating that the recombinant protein might be interfering with repressor function of the wild-type SLR1. The whole of the C-terminal domain of SLR1, including the VHIID, PFYRE and SAW motifs are involved in the repressor function. However, this region also contains GA-insensitive mutations (*Brassica rapa Brrga1-d* mutant, rice *slr1-d4*, and maize *d9-1*) which are likely interfering with targeting to the proteasome pathway (see below) (Muangprom et al., 2005, Lawit et al., 2010, Hirano et al., 2010).

In plants over-expressing DELLA proteins, the level of over-expression corresponds to the amount of growth repression, and the amount of applied GA determines the level of release from restraint, suggesting that in this situation the DELLA proteins act mostly in a quantitative manner (Itoh et al., 2002, King et al., 2001, Fu et al., 2001, Chandler et al., 2002). However, at physiological DELLA protein concentrations, post-translational modification or interacting-binding partner availability may play the dominant role in DELLA protein homeostasis and consequently developmental decisions. DELLA deletion mutants in *Arabidopsis* have also shown that there is likely a sensing mechanism that induces expression of another DELLA protein if a single DELLA protein is missing (Tyler et al., 2004, Itoh et al., 2002, McGinnis et al., 2003, Dill et al., 2004).

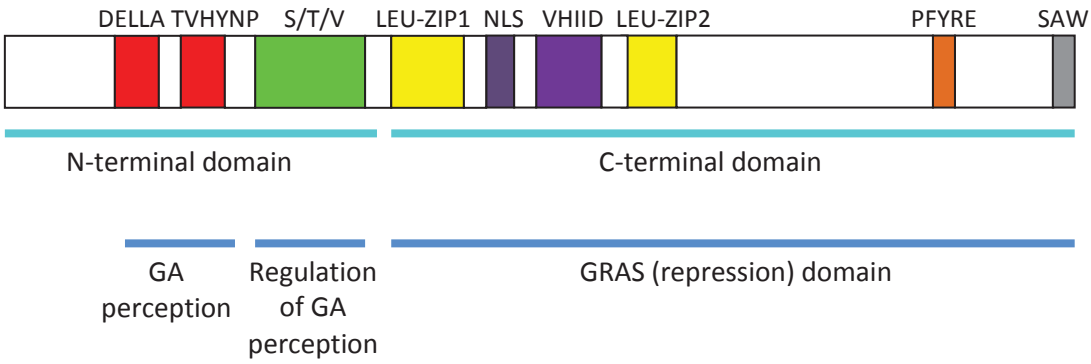

Figure 1.3. Block diagram of domains and conserved features in the DELLA proteins
From (Bolle, 2004, Peng et al., 1999)

DELLA/TVHYNP	GID1 interaction/ GA perception domain.
Poly S/T/V	GA perception? Activity and regulation domain, by post-translational modifications?
Leu Zipper domains	Protein-protein interaction domains. Repressive function
VHIID/SAW	F-box interaction? Repressive function.
PFYRE	GRAS domain highly conserved. Repressive function.

1.3 The Core Gibberellin Signalling Components

The core gibberellin signalling response proteins, in addition to DELLA proteins, are the nuclear GA receptor (*GID1*) and an F-box protein (*GID2* in rice and *SLY1* in *Arabidopsis*; Figure 1.4)

1.3.1 Perception of Gibberellin

Chemically, the gibberellins are small hydrophobic organic acids. Given that they are also uncharged at acidic pH, GAs can cross membranes without requirement of a cell surface or membrane-embedded receptor. Therefore, GAs could act directly through a receptor in the cytoplasm. However, it has not been directly demonstrated that GAs cross membranes freely, hence a cell surface receptor/transporter cannot be excluded (Ritchie et al., 2000).

Early experiments indicated GA perception took place at the plasma membrane (Gilroy and Jones, 1994, Hooley et al., 1991, Hooley et al., 1992). Three membrane GA-binding proteins were isolated, but not identified (Hooley et al., 1992, Lovegrove et al., 1998). As their role in GA perception could not be examined, it is unclear whether they were true GA receptors or simply GA-binding proteins with other unknown functions. Any membrane-associated receptor remains to be identified.

GA signalling is perturbed by a mutation in the Gα subunit of a rice G-protein heterotrimer, *DWARF1* (*D1*), implicating a G-protein-coupled transmembrane protein as a receptor. The Gα protein is located on the internal face of the plasma membrane. At low GA concentrations, in *d1* null mutants the GA signal is not transduced. However, this is the only G protein in rice and other plants, and its mutations have pleiotropic effects on signalling by multiple plant hormones (Ueguchi-Tanaka et al., 2000).

Abscisic acid (ABA) signal transduction experiments in barley aleurone cells suggest multiple receptor sites, i.e. internal (cytoplasmic) and external (plasma membrane)(Santner et al., 2009). As GA and ABA are two antagonistic phytohormones in many of their roles in developmental processes, it would seem logical for competition to exist between the two and for flexibility during growth, that they share similar features in their respective signal transduction pathways. Therefore, like ABA, GA may have both plasma membrane and cytoplasmic/nuclear receptors (Gilroy and Jones, 1994). Recently, ABA receptors have been identified as the 14 members in the family of (*PYRABACTIN RESISTANCE*) PYR proteins which,

when bound to ABA, interact with and inhibit type 2 protein phosphatases (*PP2C*) (Ma et al., 2009, Park et al., 2009).

Gibberellin binding proteins were co-purified and identified from the soluble fraction in preparations of seven day old Adzuki bean seedlings (Park et al., 2005). Subsequently, in an analysis of a rice dwarf mutant that was insensitive to GA, the group identified one of the proteins again. Their experiments found the protein to be a soluble nuclear (and in a lesser amount, cytoplasmic) GA receptor, *GIBBERELLIN INSENSITIVE DWARF 1* (*GID1*) (Ueguchi-Tanaka et al., 2005).

1.3.2 GA-dependent *GID1* interactions with DELLA proteins

The rice *gid1* mutants are severe dwarfs, unresponsive to externally applied GA. Due to a feed-back loop that regulates GA synthesis through DELLA proteins, the GA_1 levels in *gid1* mutants are 100 times that of wild-type levels. *gid1* plants accumulated high levels of the rice DELLA protein SLR1, which was not degraded following application of GA (Ueguchi-Tanaka et al., 2005). GID1 amino acid sequence shares homology to the hormone-sensitive lipase family, although it does not have the conserved catalytic residues and no esterase activity has been observed in purified recombinant GID1 proteins. GID1-GFP fluorescence was seen in the nucleus and a faint signal in the cytosol. No change in fluorescence was observed following external application of GA or of inhibitor of GA synthesis, uniconazole. GA therefore does not affect GID1 location. The authors found that recombinant GID1 only binds to biologically active GA, of which GA_4 binding is of the highest affinity ($K_d = 2 \times 10^{-7}$ M), 20 fold higher than that for GA_1 ($K_d = 4 \times 10^{-6}$ M). Therefore, a response would be fine-tuned by the changing levels, and molecules present, of GAs *in planta*. In Yeast-2-Hybrid (Y-2-H) experiments GID1 interacts with the DELLA protein SLR1 only in the presence of bioactive GAs, furthermore the presence of SLR1 enhances the binding of GA to GID1 (Ueguchi-Tanaka et al., 2005, Griffiths et al., 2006).

While rice contains only a single *GID1*, the *Arabidopsis* genome contains 3 *GID1* orthologues (named *AtGID1a*, *AtGID1b* and *AtGID1c*). The *Arabidopsis* GID1 orthologues have slightly different binding kinetics and affinities, with AtGID1a and AtGID1c more alike to each other than to AtGID1b. All three have highest affinity for GA_4 (followed by GA_3 then GA_1) and optimum at a neutral pH, but the AtGIDa and AtGIDc homologues had a much broader active range than did AtGIDb. AtGID1b had a 10 fold greater affinity for GA_4 (Ueguchi-Tanaka et al., 2005, Nakajima et al., 2006, Sheerin et al., 2011). Expression analysis showed that all three

GID1 orthologues are ubiquitously expressed in the plant, with *At*GID1a more prominently expressed compared to the other two. Null allele combinations of the three indicated some functional specificity, but also redundancy with no phenotype in mutants missing only a single allele. Using Yeast-three-hybrid interaction assay and deletion mutants it was determined that DELLAs proteins interact with the GID1 proteins in a GA-dependent manner. Using the same assay, RGA was found to require both DELLA and TVHYNP motifs, whereas GAI was found to require only the DELLA domain for interaction with GID1a (Griffiths et al., 2006, Willige et al., 2007).

A GA-dependent interaction between GID1 and SLR1 was characterised using Bimolecular fluorescence complementation (BiFC) *in planta* (Ueguchi-Tanaka et al., 2007). This approach showed that the strength of the interaction was proportional to GA concentration. A combination of alanine scanning mutagenesis and yeast-two-hybrid assay showed that, within the SLR1 N-terminal domain, the DELLA and TVHYNP motifs, but not the intervening sequences, were required for GID1 interaction. In contrast, the same approach applied to GID1 (GA receptor) showed that important residues for interaction were scattered throughout the polypeptide. The high-resolution structure of GID1-GA and *A. thaliana GID1a*-GA in complex with an N-terminal fragment of DELLA protein GAI (Murase et al., 2008) showed that GID1 proteins are structurally similar to hormone-sensitive lipases (HSLs). The authors found that GA binding in the carboxylesterase pocket of GID1 protein triggers closure of an N-terminal 'lid' which is comprised of 3 α-helices and a loop region. The solvent-exposed face of the lid forms the GAI-binding surface. The structure of the GA-binding pocket suggests that ability to bind into the GID1a pocket discriminates between bioactive and non-active GAs. The structure of the GID1a-GA complex precisely mapped the residues within the DELLA and TVHYNP motifs that form contacts between GID1 and DELLA proteins. These authors speculate that this binding induces a conformational shift in the GRAS domain that allows it to be recognised by the F-box protein; however this hypothesis has not been tested as there is no high resolution structure available of the DELLA protein GRAS domain or of a full length protein. Thermodynamics and *in silico* analysis further characterised important binding residues in the GID1 structure that interact with GA molecule side chains (Xiang et al., 2011). Further studies using binding competition of monoclonal antibodies with GID1a and *Arabidopsis* DELLA protein RGL1 N-terminal domain indicate that the Asp-Glu-Leu-Leu residues of the DELLA motif are not essential for this interaction and the fully disordered structure of the N-terminal of RGL1 goes through a 2-step conformational shift on GID1a binding (Sheerin et al., 2011).

As mentioned earlier, in plants that have multiple *GID1* and DELLA genes, such as *A. thaliana*, the site of DELLA protein expression may be the major determinant of biological function of a particular DELLA protein. However, it is also possible that some of the specificity in function of individual *A. thaliana* DELLA proteins could come from preferential interaction of a particular GID1-individual DELLA protein. To determine specificity of each GID1 with each DELLA protein in *A. thaliana*, co-immunoprecipitations of DELLA proteins with tagged GID1a, -b and -c were carried out. Each GID1 family member interacted with all five DELLAs and furthermore this interaction was stabilised in the presence of GA. The authors also used an anti-ubiquitin antibody to confirm the polyubiquitination of the immunoprecipitated DELLAs. In contrast to the wild-type, Δ17-*gai* mutant that lacks the DELLA motif was not ubiquitinated, hence GID-GA-GAI interaction is required for targeting of ubiquitin ligase. The authors also showed using *in planta* BiFC, that GID1c and RGA interact in the nucleus. Curiously, they detected GID1b binding to RGA in the absence of GA (Feng et al., 2008).

Analyses of the *GID1a*, *-b* and *-c* single and double mutant phenotypes showed redundancy, but also discovered some specificity in the *Arabidopsis GID1* homologue functions (Suzuki et al., 2009, Iuchi et al., 2007). Single mutants have the same phenotype as the wild-type plant. Of double mutants, only *gid1a*/*-c* plants showed a height defect. This is explained by the fact that *GID1b* is not expressed in the tissues required for plant growth. In contrast, *gid1a*/*-b* plants growth is not affected, however stamens do not elongate and mutants lose fertility, suggesting a dominant role of *GID1a*/*-b* in flower development. The authors proposed that this was due to low GID1c affinity for RGL2, the major DELLA protein in floral buds. However, this was not supported by biochemical analysis, which determined that GID1a/ -c affinities for DELLA proteins have only subtle differences. DELLA proteins RGL (RGL1, 2 and 3) have the highest affinity for GID1a, and GAI and RGA have highest affinity for GID1b.

In rice, an intragenic suppressor allele of a *GID1* point mutant that cannot bind GA, was discovered to be a double mutant which allows GID1 to interact with the DELLA protein SLR1 in the absence of GA (Yamamoto et al., 2010). The suppressor mutation, Pro99Ser, is located in the 'loop' region that is thought to be involved in closing the 'lid' over the GA binding pocket. The authors propose this region is therefore important in determining GA-dependent or independent activity of GID1. The loop region is quite diverse in *GID1* homologues from different plants.

1.3.3 DELLA-specific F-box protein

Following the GA signal, DELLA proteins undergo degradation. The involvement of the proteasome in DELLA degradation was first suggested when proteasome inhibitors were shown to prevent the disappearance of *SLN1* (*SLENDER 1*), the barley DELLA protein (Fu et al., 2002).

To trace the GA-response signalling pathway in rice, Matsuoka and colleagues isolated a number of GA-insensitive dwarf (*GID*) mutants. *GID1*, the GA receptor, was described earlier. The second of those mutants *GID2* (*GIBBERELLIN INSENSITIVE DWARF 2*), was an F-box protein (Sasaki et al., 2003). F-box proteins function as part of an SCF (SKP Cullin F Box containing) E3 ligase complex and are primarily involved in the substrate recognition, i.e. binding to a cognate substrate, which is then ubiquitinated (Stone and Callis, 2007, Schwechheimer and Villalobos, 2004). The *Arabidopsis* orthologue of *GID2* is *SLY1* (*SLEEPY 1*) (McGinnis et al., 2003, Steber et al., 1998). Additional homologues are *SNEEZY* (*SNE*) in *Arabidopsis* and *OsSNE* in rice. These two homologues can also act, to a certain extent, as the F-box component in GA-induced DELLA protein degradation (Strader et al., 2004, Fu et al., 2004). However, over-expression of SNE only partially rescues the null mutant of *SLY1* (*sly1-10*). In the absence of functional SLY1, over-expressed SNE was found to reduce the amount of RGA and GAI, but not RGL2 in a GA-dependent manner. The phenotypes of these plants included reduced apical dominance and a prostrate growth, which are not seen in SLY1 over-expressing plants, indicating SNE has targets in the plants, in addition to DELLA proteins (Ariizumi et al., 2011).

The F-box domain is located in the N-terminal portion of SLY1/GID2; this domain interacts with the SKP protein, a universally conserved component of SCF E3 ligase (Sasaki et al., 2003, Gomi et al., 2004, Fu et al., 2004, Dill et al., 2004). The C-terminal portion of SLY1/ GID2 contains two conserved motifs recognised in sequence alignments, the GGF and LSL (McGinnis et al., 2003). An intergenic suppressor mutation of the dwarf phenotype of *RGA ΔDELLA* motif mutation was isolated in the *SLY1* gene of *A. thaliana*. This allele, *sly1-d* (*gar2-1*), has a point mutation Glu138Lys, in the LSL motif and has increased affinity for DELLA proteins (Dill et al., 2004, Fu et al., 2004, Wilson and Somerville, 1995). This finding suggests that the LSL domain is involved in interaction with the DELLA proteins. Domain deletions in combination with yeast two-hybrid interaction assays suggest that SLY1 protein interacts with the C-terminal domain of DELLA proteins. This is further supported by finding that a *Brassica* DELLA protein dominant dwarfing mutant *Brrga1-d*, which does not interact with cognate F-box protein BrSLY1, contains a

missense mutation in the C-terminal domain, immediately downstream of the conserved VHIID motif (Muangprom et al., 2005). Other reports points to the very C-terminal end of DELLA proteins, around the SAW domain, as *sln1-c*, an expressed null (slender, null) mutant allele which has the 18 terminal amino acids deleted, is also not responsive to GA induced degradation (Gubler et al., 2002). Similarly, another mutant of the SAW motif, *slr1-d4*, is resistant to GA induced degradation (Hirano et al., 2010). It was reported that, in order for DELLA protein AtRGL1 to interact with the F-box protein, an interaction between the N- and C-terminal of the DELLA protein is required (Sheerin et al., 2011).

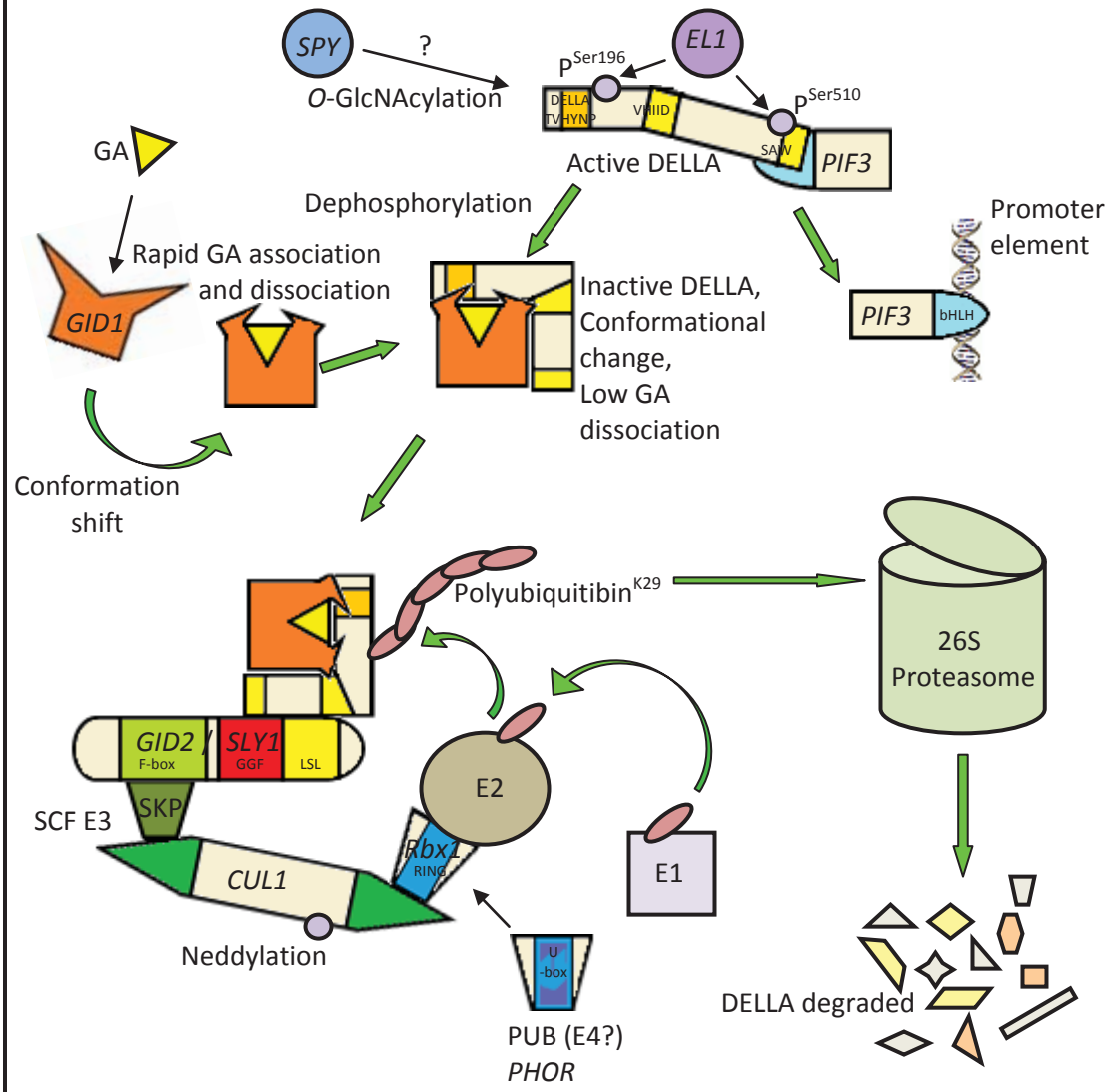

Figure 1.4. Core components of the GA Signalling Cascade
Modified from (Itoh et al., 2003, Sun, 2010)
GA is bound by its receptor, *GID1*. The recognition of DELLA proteins is greatly increased. This complex is then able to be recognised by the F-box protein, part of an SCF E3 ligase and the DELLA protein is degraded. Before GA signalling the DELLA proteins bind bHLH transcription factors such as *PIF3* and prevent this from binding DNA and promoting transcription.
E1 ubiquitin activating enzyme, E2 ubiquitin conjugating enzyme, E3 ubiquitin ligase SCF complex, SKP homologue eg. *At ASK1*, *OsSKP15*, CULLIN homologue eg. *AtCUL1*, F-box homolog eg *AtSLY1*, *OsGID2*. Rbx 1 homologue RING domain binds E2 and mediates ubiquitin transfer to substrate through the SCF E3 ligation functions.
E4 Plant U-box, a RING-type domain, may be independent of SCF.

1.3.4 The tripartite interaction

In order for the F-box protein SLY1/GID2 to bind to DELLA protein C-terminal domain, the N-terminal domain of DELLA proteins has to interact with liganded GA receptor (GID1-GA). This suggests that the N-terminal domain engagement by GID1-GA "primes" the C-terminal domain for interaction with SLY1/GID2. GID1 and GID2 proteins therefore only interact indirectly, through association with a DELLA protein. The nature of this priming event is unclear, but an undisturbed N-to-C domain link in DELLA proteins is required for efficient interaction of DELLA protein RGL1 with SLY1 in yeast three-hybrid assays (Sheerin et al., 2011), suggesting concerted conformational rearrangements between the two domains.

Yeast two- and three- hybrid assays of the *O. sativa* GID1-GA-SLR1-GID2 interactions included a GA-insensitive allele *slr1-d4* (a C-terminal SAW domain mutant, Gly576Val; (Hirano et al., 2010). These experiments showed that slr1-d4 has a reduced interaction with GID1. Furthermore, yeast three-hybrid assays revealed that slr1d-4 mutant had almost no interaction with GID2, in the presence of GID1, when compared to the interaction of wild-type SLR1-GID1-GID2. Using surface plasmon resonance the authors saw that the wild-type SLR1 C-terminal domain stabilised the interaction with GID1, reducing the disassociation rate compared with sly1-d4 mutant. They proposed that the SLR1-GID1 interaction at amino terminal DELLA and TVHYNP domains enables the C-terminal SAW domain of SLR1 to further interact with GID1 and this conformational shift forms a stable tertiary complex that can be recognised by the F-box protein, GID2. They speculate the conformational change within SLR1 due to GID1 binding prevents the suppressive function of the GRAS domain and allows binding of GID2 with no requirement for post-translational modifications. They could not map any particular region in the C-terminal domain responsible for the growth-suppressive activity using the mutants they generated in this report, hence they proposed that the complete tertiary form is important (Hirano et al., 2010).

On binding to a GA-liganded GID1, DELLA protein N-terminal region converts from an intrinsically disordered state to ordered state, changing the binding interfaces of the N-terminal domain for further interactions. Deuterium exchange mass spectroscopy, NMR and *in silico* analyses, alongside supporting evidence from antibodies of differing affinities for DELLA family proteins classified DELLAs as pre-molten globule intrinsically unstructured proteins (IUPs) and placed GAI and RGA in a separate subgroup to the RGLs (Sun et al., 2010, Sun et al.,

2012). Kinetic analysis using surface plasmon resonance modelled a two-step conformational change of the N-terminal domain from *A. thaliana* DELLA protein RGL1 upon interaction with GID1a-GA. Coupled with the structured character of the N-terminal domain in complex with GID1a-GA, these data show that upon interaction, DELLA protein N-terminal domain undergoes transition from disordered to a defined tertiary structure. This transition may have an effect on the conformation of the C-terminal domain that primes it for interaction with SLY1 (Sheerin et al., 2011).

1.3.5 Degradation-independent and modification-dependent activity

Although proteasome-mediated degradation of DELLA proteins is well-documented, some DELLA proteins were reported to be inhibited without degradation. In *A. thaliana*, during seed germination there is more RGA than RGL2 protein, however genetic analysis showed that *RGL2* is the functionally dominant repressor (Tyler et al., 2004). Therefore, the extent of repression in this case does not correlate with the amount of a particular DELLA protein. Furthermore, null mutants of the F-box protein, *sly1-2* and *sly1-10*, display a less severe dwarf phenotype than a mutation that blocks the GA biosynthetic pathway, *ga1-3.* This is even more surprising in the light of the fact that the *sly1-2* and *sly1*-10 mutants accumulate much higher levels of DELLA proteins than does the GA biosynthesis mutant *ga1-3*. Interestingly, *sly1-2* and *sly1-10* mutants retain a low-level sensitivity to GA, as indicated by functioning of the GA-dependent feedback regulation of biosynthetic gene *GA3ox* transcription, even though the DELLA (RGA) protein levels are unresponsive to GA treatment. Seeds from both *sly1-2* and *ga1–3* mutants fail to germinate unless the seed coat is manually cut after imbibition. However, *sly1-2* seeds can gain germination ability after several months of dry storage, a process known as after-ripening, and this is not accompanied by a degradation of RGL2 or the other DELLAs in the seeds. Therefore in these seeds, degradation of DELLA proteins is not a prerequisite for germination, suggesting that RGL2 is inactivated without being degraded. This in turn suggests the interaction of GA-GID1 inactivates DELLA-mediated germination repression, accounting for the reduced severity of the *sly1* phenotype compared to *ga1-3*. There is however, an unexplored possibility that the *SLY1* homologue *SNE* plays a role in degradation-independent inactivation of RGL2 and other DELLA proteins in the seed (Daviere et al., 2008, McGinnis et al., 2003, Ariizumi and Steber, 2007).

In rice, comparison of genotypes and SLR1 amount in *gid2-2*, *gid1-1* and *cps* (GA biosynthetic enzyme) mutant plants showed that the F-box protein mutant *gid2-2* has much more SLR1, but is less dwarfed than the other two, GA receptor and GA biosynthesis, mutants. (Ueguchi-Tanaka et al., 2005). These findings suggest either a bypass of DELLA regulatory function by GA, or degradation-independent GID1-GA-mediated DELLA protein inactivation.

A degradation-independent regulation of growth is observed when GA biosynthetic or signalling mutants were subjected to ACC (ethylene precursor) application. ACC caused elongation in the hypocotyl, in GA biosynthetic or signalling mutants, even though ACC caused an accumulation of RGA protein (seen through GFP-RGA) and a reduction in GA_4 levels (Vandenbussche et al., 2007b).

1.3.6 DELLA protein phosphorylation

Given that DELLA proteins integrate multiple environmental and endogenous signalling pathways, it is likely they are targets for multiple competing modifications, which modify their regulatory function and/or stability. DELLAs are phosphorylated, but there is some controversy about the consequences of the phosphorylated state (please see below). For example, there may be a different effect of phosphorylation on DELLA protein stability and function between the rice and *Arabidopsis*.

In barley aleurone, two forms of SLN1 are seen in protoplast protein extracts following SDS-PAGE and western blotting, a higher mobility form (form I) and a lower mobility form (form II) (Gubler et al., 2002). Calf intestinal phosphatase treatment of extract left only form I visible, suggesting that form II is phosphorylated. In the *sln1-d* mutant, a dominant dwarfing DELLA motif mutant, equal amounts of each form are present, but in the null mutant, *sln1-c,* which encodes a prematurely terminated SLN1 protein lacking C-terminal 18 amino acids, only form I is present. Based on these findings, phosphorylated form II is the active form tagged for degradation, and the C-terminus is required for repressor activity and phosphorylation (Fu et al., 2002). Phosphatase and kinase inhibitors were used to show that dephosphorylation of Ser/Thr residues and phosphorylation of Tyr residues are required for SLN1 degradation. Interestingly, there is also a report (Murray et al., 2003) of three forms of SLN1 in barley anthers, suggesting that further post-translational modifications are possible and they differ from those in aleurone. However, these forms have not been characterised, hence

modifications present in these forms or dependence of these forms on GA signalling are unclear.

In rice, two forms of SLR1 are seen in the *gid2-1* (F-box protein) and *gid1* (GA receptor) null mutant plants, whereas in wild-type plants form I is dominant, and form II is only barely detectable (Ueguchi-Tanaka et al., 2005, Sasaki et al., 2003). Therefore SLR1 is accumulating in the phosphorylated form in *gid1-1* and *gid2-1* plants, suggesting again that phosphate groups mark SLR1 for ubiquitination and degradation. Following immunoprecipitations of SLR1 from wild-type plants treated with specific proteasome inhibitor MG132, ubiquitinated SLR1 was detected; in contrast ubiquitination of SLR1 in *gid2-1* plants is not detectable. These observations are extended in the report that only form II of SLR1 binds GST-GID2 recombinant protein (Gomi et al., 2004). Therefore, phosphorylation of SLR1 induced by GA is necessary for GID2 proteasome targeted degradation. SLR1 is phosphorylated at serine residues only (Itoh et al., 2005a) and probably occurs across all three N-terminal domains (DELLA, TVHYNP and poly S/T/V). However, in contrast to initial reports (Sasaki et al., 2003, Gomi et al., 2004), a subsequent report (Itoh et al., 2005a) detected accumulation of both forms prior to and loss of both forms following GA treatment, there being no preference between the two forms. The latter report shows that recombinant GST-GID2 binds both SLR1 forms and Ser/Thr kinase inhibitors had no effect on GA-induced degradation.

In *Arabidopsis,* phosphorylated form II of the gai mutant protein has been identified. Following phosphatase treatment, gai could still be recognised by recombinant sly^{gar2-1} mutant protein which has increased affinity for DELLA proteins (Wilson and Somerville, 1995, Fu et al., 2004). Furthermore, only a single form of RGA in *Arabidopsis* was identified, however it has not been established of which form it represents (Dill et al., 2004). The RGL2 protein is shown to be a phospho-protein in tobacco BY2 cells, and degradation can be blocked by Ser/Thr phosphatase inhibitors (Hussain et al., 2005) but not by Ser/Thr kinase inhibitors (Hussain et al., 2007). Blocking tyrosine (Tyr) kinases inhibited degradation of *Arabidopsis* DELLAs, whereas Tyr phosphatase inhibitors had no effect. These experiments pointed to Ser/Thr dephosphorylation and Tyr phosphorylation as important in GA-induced degradation of RGL2. However, mutation-mimic experiments in which Tyr residues in RGL2 were replaced by Phe residues did not prevent degradation, hence it was unlikely that the DELLA proteins were Tyr phosphorylation targets, rather some other component(s) in GA-signalled DELLA destruction pathway. In a cell-free assay system, degradation of the *Arabidopsis* DELLAs was blocked with PP1/PP2A phosphatase inhibitors, suggesting that Ser/Thr dephosphorylation was required for

degradation (Wang et al., 2009). However, phosphorylation was not demonstrated directly on a DELLA protein. In this *in vitro* system kinase inhibitors had no effect on DELLA protein degradation.

EARLY FLOWERING 1 (*EL1*), a casein kinase 1 family Ser/Thr kinase, was shown to phosphorylate SLR1 at Ser196 and Ser510 and is required for full repressor function of SLR1. *el1* null mutants also showed defects in the feedback transcriptional regulation of *GA20ox*, *GA3ox* and *GA2ox* biosynthetic enzymes (Dai and Xue, 2010).

In summary, phosphorylation may be involved in DELLA function and it may also be involved in the regulation of DELLA abundance, however the roles of phosphorylation and dephosphorylation may vary from one plant to another and from one DELLA orthologue to another. A specific DELLA protein phosphorylation/dephosphorylation system and its components remain to be resolved (McGinnis et al., 2003).

1.3.7 *SPINDLY* (*SPY*)

The *Arabidopsis* null *SPY* mutant phenotype resembles a GA overdose phenotype; plants are able to germinate under treatment with the GA synthesis inhibitor PAC. The *SPY* null mutation also suppresses most of the gain of function *gai* mutant phenotypes, so it appears that in the absence of *SPY*, DELLA regulatory function was either bypassed, or inactivated without degradation (Swain et al., 2001, Tseng et al., 2001).

SPY (SPINDLY) is predicted to be a bifunctional protein, containing N-terminal protein-protein interaction/ scaffolding tetratricopeptide domain and C-terminal enzymatic domain, UDP-N-acetylglucosamine-peptide N-acetylglucosamyl transferase (OGT). *O*-linked N-acetyl glycosylation is thought to be competitive with phosphorylation, modifying the same Serine/Threonine (Ser/Thr) amino acid residues. This phosphorylation/glycosylation competition may be a dynamic process and is proposed to regulate responsiveness of GA signalling pathway (Jacobsen et al., 1996, Jacobsen and Olszewski, 1993, Kreppel et al., 1997, Thornton et al., 1999). *Arabidopsis* contains another OGT, called *SEC* (*SECRET AGENT*). Double null mutant of *SPY/SEC* is embryo-lethal (Hartweck et al., 2002).

SPY exists as an 850 kDa complex and functions in other pathways, hence it is not clear whether SPY directly interacts with DELLA proteins, nor has it been directly demonstrated to function as an OGT.

In rice, reducing *OsSPY* levels by RNAi and antisense knockdown changed the phosphorylated/ non-phosphorylated balance of SLR1, but not the total amount of SLR1. This indicated that SPY altered the repressor function of SLR1 by modulating its phosphorylation level, and not its turnover (Shimada et al., 2006). The authors also identified two *OsSEC* orthologues. In an *Arabidopsis* SPY null mutant, DELLA protein RGA levels were increased, confirming that SPY was not required for stability (Silverstone et al., 2007). *SPY* alleles did not alter the localisation of RGA-GFP. The dominant gain-of-function DELLA mutant Δ17-rga had increased amount in the phosphorylated form II compared to form I in the *SPY* null mutant background. These authors propose that SPY alters the activity of RGA and that normally SPY blocks phosphorylation. When no SPY (or less SPY) is present there is more phosphorylation of DELLA proteins. A possibility remains that these findings may indicate compensation, increasing the numbers of phospho-SLR1s to compensate for loss of O-GlcNAcylation. Interpretation of these findings is complicated by the fact that the role of phosphorylation in DELLA protein function is not well understood, particularly because there are multiple phosphorylation sites that could have differing effects on activity (Maymon et al., 2009). *SPY* acts in the cytosol, rather than the nucleus, where DELLA proteins are located, to repress GA responses. Therefore, all effects of SPY on DELLA phosphorylation may be indirect.

SPY has been shown to promote meristem indeterminacy (preventing the change to a floral identity) as *spy* alleles suppressed the phenotypes of canonical flower development mutants, *ap1* and *2* (*APETALA1 and APETALA2*). This effect may be achieved through modification of *KNAT1* (*KNOTTED1-LIKE IN ARABIDOPSIS THALIANA),* which in turn prevents GA action in the shoot apical meristem through GA biosynthesis control (Filardo and Swain, 2003).

SPY is also involved in circadian clock, photoperiod regulated processes with *GI* (*GIGANTEA*), and possibly acting in conjunction with a ring finger protein *PHOR* of the ubiquitin ligase SCF complex on the DELLA protein degradation. (Please see the cross talk section below) (Tseng et al., 2004, Filardo and Swain, 2003).

The SPY knockdown plants, in addition to GA responses, have a phenotype typical of altered phytohormones brassinosteriod (BR) signalling pathway (Shimada et al., 2006).

1.3.8 Evolution

All major phytohormones (auxin, cytokinin, abscisic acid, ethylene), except GA have been unambiguously identified in both mosses and liverworts (bryophytes) (Anterola and Shanle, 2008). However, these hormones do not act exactly as they do in vascular plants. Methylated GA is found in ferns, where it may function as antheridiogens, in spore formation and germination, an analogous role to that in seed plants (Hayashi et al., 2010).

To establish evolutionary origin of the GA signalling pathway, core components (*GID1, GID2/SLEEPY1* and DELLA) were searched for in representative organisms of distinct plant clades: Red and green algae (Single cells), bryophyte (*Physcomitrella patens* (Moss); non-vascular, spore forming), lycophyte (*Selaginella moellendorffii;* proto-vascular, spore forming), and angiosperm (*Arabidopsis*; vascular, flowering and seed producing). These analyses showed that the core GA signalling pathway emerged only after mosses and vascular plants have diverged (≈ 430 mya) (Vandenbussche et al., 2007a).

The *in silico* search found no true orthologues of core GA signalling pathway components in the bryophyte, *P. patens,* although they tested the best matches alongside those identified in lycophyte *S. moellendorffii*, for GID1-DELLA interactions, using yeast two-hybrid system. The *P. patens* closest orthologues of GID1 and DELLA proteins did not interact with each other nor could they rescue corresponding orthologue mutants in flowering plants. *P. patens* GID1 orthologue did, however, interact with DELLA orthologue from *S. moellendorffii* and with DELLA protein RGA from *A. thaliana*, but this interaction was not GA-dependent. S*. Moellendorffii GID1* and DELLA orthologues appear to function as they do in the flowering plants, i.e. they interact in GA-dependent manner. In *S. Moellendorffii,* applied GA_4 led to the degradation of SmDELLA protein and down-regulation of *SmGID1b*, SmGA20ox and SmGA3ox homologue transcripts. Furthermore GA synthesis inhibitor uniconazole caused a dwarf phenotype. The *SmGID1*s bound GA_4, albeit with low affinity, and showed interaction with SmDELLA homologues and *A. thaliana* RGA in yeast two-hybrid assays. The Sm*GID1* and *SmGID2* transgenes were also able to rescue the rice *gid1-3* and *gid2-1* mutant phenotypes. Furthermore, when the lycophyte *S. kraussiana* DELLA proteins were expressed in *A. thaliana*, they functioned as the flowering plant DELLA proteins. *P. patens* contain a GID1 orthologue that can bind to the lycophyte and angiosperm DELLA proteins in a GA-independent manner, but does not have a GRAS protein homologue that can interact with the GID1 orthologue (Hirano et al., 2007).

The authors concluded that GID1/DELLA GA signalling pathway evolved in a step-wise manner, with GRAS protein acquiring ability to interact with a GID1 orthologue, followed by acquiring ability to interact in a GA-dependent manner, and finally to control growth in a GA-dependent manner. They hypothesise the establishment of GA-signalling pathway was a key event in the evolution of vascular plants and their stature (Yasumura et al., 2007).

1.4 The signalling cascade

Signal transduction cascades amplify and integrate hormone signals, and co-ordinate a response with other processes (Ritchie et al., 2000). Signals that interact with GA signalling pathway may be of a chemical nature (hormones, pathogen-elicited molecules, or other cell molecules) or stimuli of non-biological origin (light, temperature or osmotic pressure; Figure 1.5). Signal transduction leads to an alteration in the cell's state, induced by a stimulus which induces changes in transcription or translation or changes in the activity of specific protein(s).

1.4.1 First response to GA, the secondary messengers

1.4.1.1 Calcium ion as a secondary messenger

Exposure of cells or tissues to GA is followed by Ca^{++} fluctuations. Ca^{++} concentration modulation in some plants is the first detectable event in response to GA application, taking place within two to five minutes from treatment. Resting Ca^{++} concentration is 100-250 nM when averaged over the whole cell and may increase two to five fold. Localised concentration peaks can be much higher, in µM range. Levels remain elevated as long as GA is present. The increase in calcium levels may be due to the influx from the extracellular space through Ca^{++} channels or due to release from intracellular stores, the ER or vacuoles. This consequently alters availability of Ca^{++} ions, the pH and charge in that compartment (Lovegrove and Hooley, 2000).

Calcium is required by many enzymes as a cofactor; e.g. for activity of chaperones that promote protein folding, or in signalling, complexed with calmodulin (CaM). The Ca^{++} ion modulation takes place in many regulatory pathways; it is often a means of cross-talk between those pathways. However, it is difficult to discern one pathway's Ca^{++} response from another's, or to determine how the Ca^{++} level transmits a signal down a specific pathway. Conflicting observations have led to the proposal that the specific temporal and spatial dynamics of Ca^{++}

levels control induction and repression responses, rather than just its concentration (Ritchie et al., 2000).

1.4.1.2 Phosphatidyl phosphoinositides

Phosphatidyl phosphoinositides are messengers both within and between cells, having the ability to cross the hydrophobic membrane boundary and also move through the hydrophilic cytosol. They are essential metabolites and are often derived from the membrane components (Stevenson et al., 2000). GA stimulates the synthesis of all the phosphatidyl phosphoinositides as well as phosphatidyl choline, a structural lipid, commencing 40 minutes after GA application to barley aleurone cells. There is also a rapid and transient increase in Phospholipase C, a phosphodiesterase, which cleaves phosphatidyl inositol (4,5) bisphosphate to Inositol (1,4,5) trisphosphate and Diacylgylcerol. The Diacylgylcerol remains in the cell membrane where it activates protein kinase C (PKC), which phosphorylates enzymes, receptors, transporters and cytoskeleton components. The Inositol (1,4,5) trisphosphate moves through the cytoplasm and triggers the release of Ca^{++} from vacuoles and activates calcium-dependent protein kinases (CDPK) (Munnik et al., 1998, Stevenson et al., 2000, Villasuso and Machado-Domenech, 2004)

A link between the central GA signalling repressor DELLAs and CDPKs, which is activated by Ca^{++} ions, is unknown. A CDPK in barley aleurone cells (*HvCDPK1*) regulates vacuolation, vacuolar secretion and vacuolar acidification, and in this way it induces mobilisation of reserve by α-amylases during germination (McCubbin et al., 2004, Ritchie and Gilroy, 1998a). Rice CDPK, *OsCDPK13*, was found to be expressed in leaf sheath; increased protein levels were seen in response to GA and cold stress. There are 27 CDPKs in rice and 34 in *Arabidopsis*. Different CDPKs may bind Ca^{++} directly to be activated or alternatively bind calcium complexes, Ca^{++}/CaM or Ca^{++}/phospholipids (Yang et al., 2003, Abbasi et al., 2004).

1.4.2 Heterotrimeric G-proteins and G-protein coupled receptors

G-protein coupled receptors (GPCR) and G-proteins are linked to many growth and developmental processes involving plant hormones, GA, BR, ABA, Cytokinins, Auxin and also light signalling. They are localised to the plasma membrane (Fujisawa et al., 2001, Assmann, 2005).

Arabidopsis has two genes encoding possible classical seven-transmembrane-domain GPCRs, *GCR1* (*G-protein coupled receptor-1*) (Josefsson and Rask, 1997) and *RGS1* (*regulator of G-protein signalling1*) (Chen et al., 2003). It is proposed that the *Arabidopsis* GPCR, *GCR1*, is

involved in flowering time and seed dormancy through the regulation of the cell cycle (Colucci et al., 2002). GPCRs transduce the signal to heterotrimeric G protein complex.

Arabidopsis has only one gene encoding each G-protein complex subunits α and β, (*GPA1*; *G-PROTEIN α 1*) (Ma et al., 1990) and (*AGB1*; *ARABIDOPSIS G-PROTEIN β 1*) (Weiss et al., 1994), whereas it has two genes encoding γ-subunits, (*AGG1*; *ARABIDOPSIS G-PROTEIN γ 1*) (Mason and Botella, 2000) and (*AGG2*; *ARABIDOPSIS G-PROTEIN γ 2*) (Mason and Botella, 2001). The *Arabidopsis GPA1* Gα protein appears to be involved in the rate of cell division, but the actual mechanism of these proteins in GA signal transduction remains unclear (Botto et al., 2009).

1.4.3 *PHOTOPERIOD RESPONSIVE 1* (*PHOR1*) family of proteins

A point of interaction of GA with the photoperiodic response, originally identified in potato (*Solanum tuberosum*), is *PHOR1* (Figure 1.4). The N-terminal domain of this protein has a U-box (UFD2-homology domain, after the yeast protein first identified) or CPI domain (has Cys, Pro, Ile conserved amino acids) and has similarities to the RING domain present in E3 ubiquitin ligases that interact with E2 ubiquitin conjugating enzymes to mediate transfer of ubiquitin to the target protein. The C-terminal domain contains seven ARM repeats (*ARMADILLO*, after the *Drosophila* protein first identified containing this repeat motif) and possibly acts as a scaffolding protein. *PHOR1* is a positive regulator of GA signalling. GA was also seen to cause migration of PHOR1 protein, in a transient fashion, from the cytoplasm to the nucleus, and the *PHOR1* transcript is also regulated in a diurnal rhythm, with peaks after transition to light and later at transition to dark (Amador et al., 2001).

Arabidopsis contains three *PHOR1* orthologues, *PLANT U-BOX27*, *-28*, and *-29* (*AtPUB27*, *-28* and *-29*). *AtPUB27* and *-28* transcripts are seen in all tissues and *AtPUB29* in the flower only (Monte et al., 2003). These proteins may function to bind E2 to transfer ubiquitin to a substrate target by an alternative pathway, independently of the standard ubiquitin ligase scaffold SCF.

1.4.4 *SHORT INTERNODES* (*SHI*)

SHORT INTERNODES (*SHI*), discovered in *A. thaliana*, is involved in the GA signalling pathway and is a negative regulator of GA response. *SHI* has a domain homology to the RING/Zn finger domain, though it has two deviations from the consensus. Database searches identified 8 *SHI* homologues in *Arabidopsis* and orthologues in other plants (Fridborg et al., 1999, Fridborg et

al., 2001). Over-expression of *SHI* resulted in elevated endogenous GA levels, dwarf phenotype, reduced apical dominance, and late but increased flowering.

1.4.5 *PAC RESISTANCE 1* (*PRE1*)

PRE1 of *Arabidopsis* is a positive regulator of GA signalling, however, its over-expression does not fully suppress the GA-resistant phenotype of dominant gain-of-function DELLA protein mutant *gai* (GA-insensitive), suggesting that *PRE1* induces only a portion of downstream effectors of GA signalling repressed by *GAI*. *PRE1* encodes a small HLH protein. As HLH is a DNA-binding motif, this protein is a putative transcription factor. There are five other *PRE1* homologues (named *PRE2-6*) in the *Arabidopsis* genome. However, *PRE1* was the only member to show GA-inducibility and responded to GA within an hour, which places its activation early in the signalling cascade (Lee et al., 2006). A transgenic line over-expressing *PRE1* demonstrated PAC resistant germination, elongated hypocotyls, earlier flowering and elevated expression of GA-responsive genes, in comparison to the wild-type. It could also suppress most of *ga2-201* (a GA biosynthetic mutant) phenotypes.

1.4.6 *erecta* (*er*)

The *ERECTA* (*ER*) mutant in the *Arabidopsis* Landsberg ecotype had been used by geneticists since the 1950's due to its compact, erect architecture and short life cycle. Many of the GA signalling mutants also show more penetrance in this background; hence the *er* ecotype (mutant) has been used most commonly to dissect the GA signalling pathway. The *ER* gene is a Ser/Thr Leucine-rich repeat receptor-like transmembrane protein kinase (LRR-RLK) (Torii et al., 1996). Its ligand is not identified but the phenotype suggests it could be involved in cell-to-cell communications, regulating cell shape and plant morphogenesis. *ER* is expressed around the shoot apical meristem (SAM).

1.4.7 *GAMYB*: GA-induced MYB transcription factor family

cis-elements were identified in the GA-induced α-amylase promoter of barley (*Hordeum vulgare*), and the sequence was called the GARC (GA response complex) (Gubler et al., 1995). In this region they identified a central consensus binding sequence (TAACAAA) for a Myb transcription factor family and identified the cognate transcription factor, *HvGAMYB*. Over-expression of *GAMYB* alone was sufficient to activate α-amylase expression in the absence of exogenous GA. Levels of *HvGAMYB* mRNA in the aleurone are very low in the absence of GA. It takes two hours following GA treatment to detect an increase in *HvGAMYB* levels and they

remain elevated for a further four hours before declining again. However, the levels of the barley DELLA protein SLN1 drop within 10 min of GA treatment to very low levels and then rise again slowly over a 12 hour period. The authors suggest that there is (are) intermediary factor(s) acting in this delay period between loss of SLN1 and increase of *HvGAMYB*. Hormone abscisic acid (ABA) had no effect on GA-induced destruction of SLN1, indicating that ABA must act downstream of *SLN1*, but upstream of *HvGAMYB.* The *HvGAMYB* induction was repressed by a gain-of-function DELLA protein mutation, *sln1-d* (Gubler et al., 1999, Gubler et al., 2002).

GAMYB homolog from grass *Lolium temulentum* was shown to be up-regulated during floral development in response to increased levels of GA, after plants are transferred to long day (LD), floral inductive conditions (Gocal et al., 1999).

In *Arabidopsis* there are three *GAMYB* orthologues, *AtGAMYB33*, *65* and *101* (Gocal et al., 2001). The level of transcription of *AtGAMYB33* increases following transfer to LD conditions, in correlation with an increase in GA biosynthesis. *LEAFY* (*LFY*) expression also correlates with *GAMYB33* levels and the two show histologically overlapping expression patterns. The promoter of *LFY* contains a possible *GAMYB* binding motif and the deletion of this motif reduces *LFY* expression in transgenic plants. *AtGAMYB33* has been shown to bind the *LFY* promoter *in vitro.* The authors conclude that it is possible that the *GAMYB*s have a role in the transition from vegetative to floral meristem.

1.4.8 Gene products acting at the GARC as a complex

There are five sequence motifs clustered together in the promoter regions of GA-responsive genes, described for the GARC (GA response complex), in the following order (in upstream-to-downstream direction): 1) The W-box also called Box 2 or O2S; 2) The Pyrimidine box; 3) The GARE (GA response element); 4) Amylase (Amy) box, also called Box 1, followed by the TATA box (Zhang et al., 2004). There is also an element (DSE) that confers a basal level of expression, downstream of the 3'UTR sequence.

Members of the WRKY protein family act at the W-box. The WRKY proteins are transcription factors identified by their WRKY domain(s), named after the conserved amino acid motif in this domain. They are nuclear-localised. In the rice α-amylase promoters, there is a double W-box consensus GATTGACTTGACC. WRKY proteins in rice include *OsWRKY51* and *OsWRKY71* (Zhang et al., 2004, Xie et al., 2006), and *ABF1* and *ABF2* in oat (Rushton et al., 1995). These WRKY

proteins have a single WRKY domain together with a Zinc-finger domain. *Arabidopsis WRKY40* is most similar to *OsWRKY71*, and there are 74 WRKY family proteins in *Arabidopsis*. *OsWRKY71* is induced by ABA; it binds the W-box and interferes with activation by *GAMYB*. *OsWRKY51* binds to *OsWRKY71* and improves the interference with *GAMYB*.

Members of the DOF (DNA binding with one finger) family of protein act at the Pyrimidine box which has the consensus sequence CCTTTT. DOF proteins have a DOF domain, which is a variant of the Zinc-finger DNA binding domain and are plant-specific transcription factors. *Os*DOF has no transcriptional activation ability of its own, but increases expression when acting with a *GAMYB* (Washio, 2003). *SAD (SCUTELLUM AND ALEURONE-EXPRESSED DOF*) (Isabel-LaMoneda et al., 2003), and *BTFB* (*BARLEY PROLAMIN BINDING FACTOR*) (Mena et al., 1998) are DOF proteins from barley that compete at the pyrimidine box. *SAD* is activating and *BTFB* is repressing α-amylase expression (Mena et al., 2002).

The GARE consensus sequence is TAACA(G/A)(G/A); it is the binding site for *GAMYB* (see above) and *HRT* (*HORDEUM REPRESSOR OF TRANSCRIPTION*) (Raventos et al., 1998). These two transcription factors compete for binding at the GARE. *GAMYB* is activating, whereas HRT is repressing transcription. Also acting on GARE is *KGM* (SER/THR KINASE ASSOCIATED WITH *GAMYB*; a Mak-kinase) and *GMPOZ* (*GAMYB ASSOCIATED POZ PROTEIN*, POZ being a protein-protein interaction domain). Both *KGM* and *GMPOZ* are transcriptional regulators (Woodger et al., 2003). *KGM* binds, but does not phosphorylate *GAMYB. KGM* may be (auto)regulated by phosphorylation and represses its *trans*-activation ability. *GMPOZ* may activate transcription of α-amylase gene indirectly, by up-regulating *GAMYB* gene expression.

The amylase box has the consensus sequence TATCCAC. A MYB protein, separate from *GAMYB*s, bind to this box. This amylase-box-binding MYB has only a single R1 DNA binding repeat, in contrast to *GAMYB*s, which also have R2 and R3 repeat. The amylase box is also a part of a sugar response complex. Three rice MYB proteins bind to the amylase box: *OsMYBS1* and *OsMYBS2*, which promote transcription and *OsMYBS3,* which represses transcription from the α-amylase promoter when sugar is present. When GA is present, all three promote activity synergistically with *GAMYB* (Lu et al., 2002).

1.4.9 MiRNA 159

The *Arabidopsis* miR159 is 21 nucleotides in length and has a near-perfect homology to the middle of *AtGAMYB 33, 65,* and *101* (and two other MYBs). The miR159 has been shown to direct cleavage of *GAMYB33* message. DELLA proteins repress both the *GAMYB33* and miR159 expression. The GA–induced DELLA degradation relieves repression of *GAMYB33* (which promotes the GA developmental processes of flowering and floral anther development and pollen dehiscence), but it also results in increase of miR159, which acts against *GAMYB*. *GAMYB* itself binds the miR159 promoter and stimulates miR159 expression. Therefore there is a complex negative feed-back loop in place which controls the *GAMYB* levels (Achard et al., 2004, Rhoades et al., 2002).

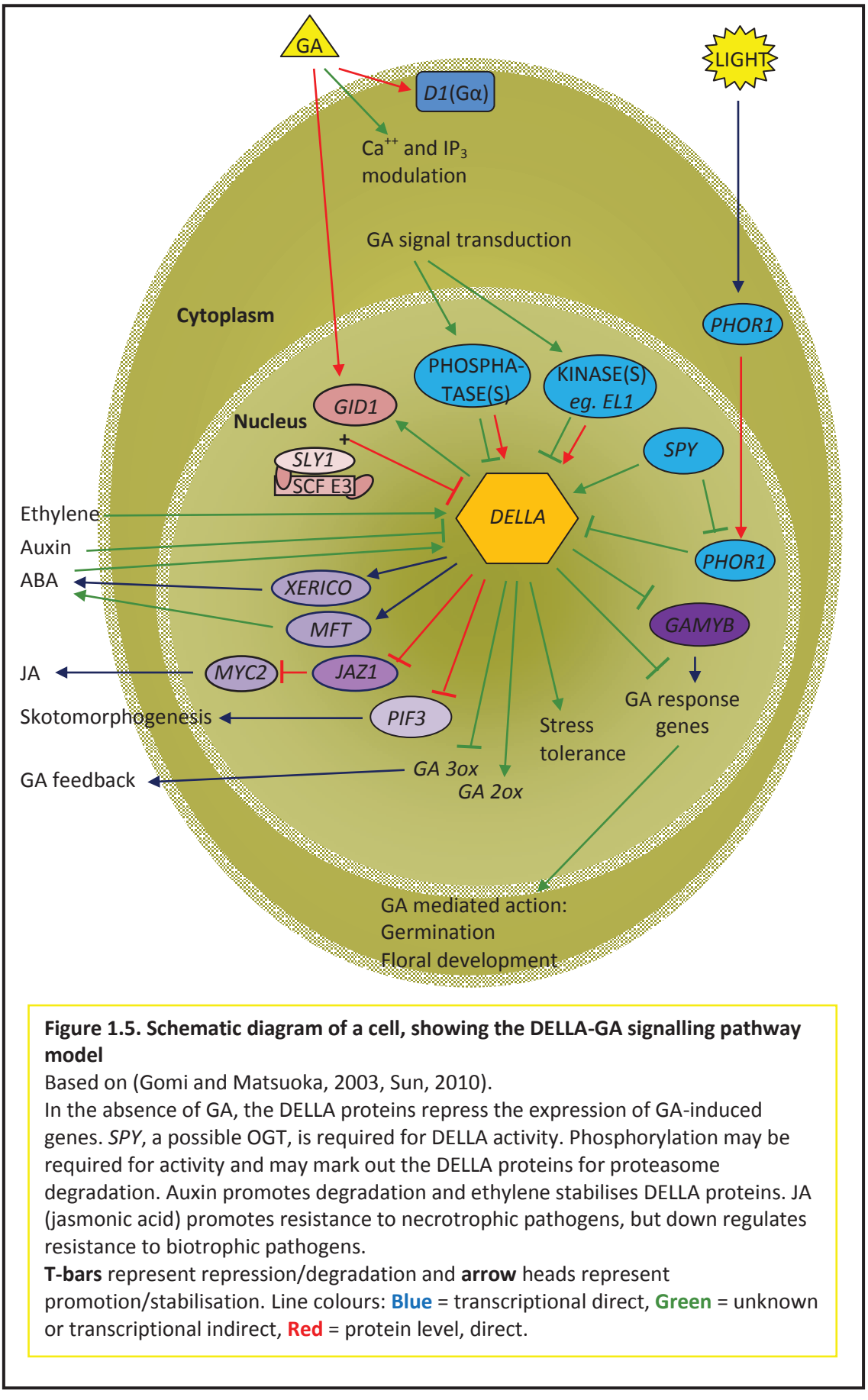

Figure 1.5. Schematic diagram of a cell, showing the DELLA-GA signalling pathway model

Based on (Gomi and Matsuoka, 2003, Sun, 2010).

In the absence of GA, the DELLA proteins repress the expression of GA-induced genes. *SPY*, a possible OGT, is required for DELLA activity. Phosphorylation may be required for activity and may mark out the DELLA proteins for proteasome degradation. Auxin promotes degradation and ethylene stabilises DELLA proteins. JA (jasmonic acid) promotes resistance to necrotrophic pathogens, but down regulates resistance to biotrophic pathogens.

T-bars represent repression/degradation and **arrow** heads represent promotion/stabilisation. Line colours: **Blue** = transcriptional direct, **Green** = unknown or transcriptional indirect, **Red** = protein level, direct.

1.5 DELLA function

Laboratory *Arabidopsis* plants can survive without four out their five DELLA proteins (Griffiths et al., 2006). Rice has a single DELLA protein without which it can survive (Ikeda et al., 2001). Different number of DELLA proteins in different plant species may indicate differential requirements and regulatory roles in development for particular DELLA protein family members and the stochastic nature of evolutionary duplications followed by accumulation of mutations. However, DELLA proteins are ubiquitous and conserved in all flowering plants and thus must be important for long-term fitness in the natural environment (Remington and Purugganan, 2002). The amount of DELLAs in the plant, tightly regulated by a narrow range of GA concentration *in planta*, seems to be important for plant viability. Too much and too little GA reduces viability (Dill and Sun, 2001).

1.5.1 Site of action

DELLA proteins are nuclear-localised repressors of elongation and growth. *A. thaliana* DELLA protein *RGA*-encoding gene is ubiquitously expressed, but the organ/ tissue/ cell in which RGA protein is active is largely unknown.

DELLA protein function has been shown to be both cell-autonomous (Boss and Thomas, 2002, Peng and Harberd, 1997, Ubeda-Tomas et al., 2008) and non-cell-autonomous, through the long distance phloem trafficking of the *gai* mRNA in tomato (Haywood et al., 2005, Huang and Yu, 2009). DELLA message trafficking from the transgenic stock (over-expressing the dominant GA-resistant mutant *gai*) to a wild-type scion leads to morphological changes in the leaves. However, (Huang and Yu, 2009) did not detect consistent trafficking for any of the other four *A. thaliana* DELLA transcripts. The important sequence motifs for trafficking in *GAI* were located between nt 995 and 2146 of the CDS (counting from the ATG).

In contrast to these findings, there is evidence of cell-autonomous function of DELLA proteins. In grape, DELLA homologue *Vvgai* is expressed only in the L1 cell layer (outermost) of the two layers in the apical meristem (Boss and Thomas, 2002), and this dominant mutant led to flower production instead of tendril development. In *Arabidopsis*, it was found that expression of *gai* was restricted to specific cell lineages, the endodermal cells in roots. The GAI control over the expansion of these cells was the primary regulator of root growth (Ubeda-Tomas et al., 2008). Evidence for autonomous action of GAI in *A. thaliana* also comes from the mosaic analysis of

Ds transposon sector mutants in *gai*/ *GAI* heterozygote. The sectors where the dominant *gai* allele was inactivated by Ds, correspond phenotypically to wild-type (pseudo-revertant sectors). This finding rules out the ability of the *gai* message in surrounding cells to migrate to the *gai*::Ds/ *GAI* effected cells, suggesting that *gai* acts cell-autonomously in *Arabidopsis* (Peng and Harberd, 1997).

1.5.2 Protein-protein interactions

DELLAs were known to interact in a GA-dependent manner, with the GA receptor *GID1*, recruiting a cognate F-box protein (*GID2* in rice and *SLY1* in *A. thaliana*), to form a tripartite interaction (Willige et al., 2007, Griffiths et al., 2006, Hirano et al., 2010). F-box protein binding targets DELLA proteins for proteasome-mediated degradation. In the absence of degradation, the tripartite interaction blocks and inactivates the C-terminal domain of DELLA proteins, disrupting their regulatory roles.

DELLA proteins likely do not directly bind DNA. They regulate transcription indirectly, by binding transcription factors. DELLA proteins, in the absence of GA, bind PIF3 (PHYTOCHROME INTERACTING FACTOR 3) protein, a basic helix-loop-helix (bHLH)-type transcription factor, and prevent it from binding its target promoters. PIF3 binds DNA to regulate other transcription factors, which in turn activate genes involved in hypocotyl expansion and skotomorphogenesis. The result of RGA-PIF3 interaction is impaired hypocotyl elongation. PIFs also interact with the light-activated form of the photoreceptor phytochrome B (phyB), and are degraded through the 26S proteasome system (Feng et al., 2008). Bimolecular fluorescence complementation (BiFC) imaging visualising direct RGA-PIF3 interaction *in vivo* in the nucleus suggests that the DELLA interaction with PIF3 does not affect PIF3 interaction with phyB*,* but rather affects PIF3's DNA-binding transcription regulation activity. In support of this, *in vitro* pre-binding of PIF3 to a G-box-containing DNA oligonucleotide inhibits RGA-PIF3 interaction. The authors confirmed that the RGA protein itself does not bind DNA using Chromatin ImmunoPrecipitation (ChIP) experiments with 38 GA-responsive promoters, all giving a negative result.

PIF4 (*PHYTOCHROME INTERACTING FACTOR 4*) is a bHLH transcription factor homologous to *PIF3* (de Lucas et al., 2008). *PIF4*, like *PIF3*, promotes cell elongation in the dark. It is negatively regulated by light through phyB -dependent proteasome-mediated protein destabilisation and by interaction with DELLA proteins, which bind to PIF4 DNA-binding surface and block its

interaction with DNA. RGA, GAI, RGL1 and RGL3 all interact with PIF3 and PIF4. RGA has a higher affinity for PIF4 than for PIF3. Given that DELLAs bind to the conserved DNA-binding domain of PIF3 and PIF4, it is possible, but not yet proven, that DELLAs may bind all members of the *PIF* bHLH subfamily of transcription factors.

Besides PIF3 and PIF4, GAI and RGL2 interact with other bHLH transcription factors of subfamily 15, *SPATULA* (*SPT*), *PHYTOCHROME INTERACTING FACTOR-LIKE 2* and *5* (*PIL2*, *PIL5*) (Gallego-Bartolome et al., 2010). *SPT* and *PIL5* inhibit GA biosynthesis at *GA3ox (1&2)* in cold (and to a lesser extent in the dark) in germination and seedling growth. However, independent investigation found that the regulation of *SPT* is independent of GA, despite its dependence on DELLA proteins (Sidaway-Lee et al., 2010). These contradictory findings indicate another complex and yet unexplored regulatory loop, or suggest that DELLAs bound to these bHLH proteins are insensitive to GA.

ALCATRAZ (*ALC*) is a bHLH transcription factor in the same subfamily as *PIF3* and *-4. ALC* is required for the specification of cells in the separation layer of the silique. This layer secretes enzymes into the replum (valve margin) to break it down and separate the two valves of the silique for seed dispersal. DELLAs (*RGA* and possibly *GAI* and *RGL2*) directly interact with *ALC* and stop its function (Arnaud et al., 2010). Overall fruit patterning in *A. thaliana* is controlled by GA; interaction of GA signalling with the DELLA-mediated inhibition of *ALC* has not been investigated.

JA ZIM-DOMAIN 1 (*JAZ1*), a repressor of Jasmonic Acid (JA) signalling, interacts with DELLA proteins. Binding to DELLA protein prevents JAZ1 from blocking MYC2, the repressor of JA signalling. From analysis of truncated of *RGA* and *JAZ* mutants, DELLA motif and the N-terminal of the two leucine zippers are the RGA domains that interact with the NT and Jaz (or tify) domains of JAZ1 (Hou et al., 2010). GA signalling leads to degradation of DELLA proteins, thereby releasing *JAZ1* from inhibition. *JAZ1* is then free to inhibit MYC2 and repress JA signalling. JA signalling is involved in necrotrophic response to pathogens, mediating necrosis; GA signalling is therefore repressing this type of response. GA also modulates the salicylic acid (SA) signalling pathway-mediated biotrophic response to pathogens. JAZ1 has also found to interact with MYB21 and MYB24 (R2R3-MYB transcription factors) that mediate the JA-regulated development of stamens in *Arabidopsis* (Song et al., 2011).

SCARECROW-LIKE 3 (*SCL3*), a GRAS superfamily protein that has a C-terminal domain conserved with DELLA proteins, interacts with some DELLA proteins. Interaction of SCL3 with RGA and possibly GAI and RGL1 attenuates DELLA activity during germination and seedling growth in the root and hypocotyl (Heo et al., 2011, Zhang et al., 2011). *SCL3* is a positive regulator of GA synthesis, up regulating *GA20ox* and *GA3ox* expression. SCL3 is a DNA binding protein; it is (auto) down regulating its own expression by binding to the *SCL3* promoters. DELLA promotes *SCL3* expression and this may be by direct promoter binding of DELLA-SCL3 complex. The root meristem and ground tissue specification is controlled by SCARECROW-SHORTROOT (SCR-SHR) GRAS protein heterodimer activity which promotes *SCL3* expression. Based on these findings it was proposed that SCR-SHR and SCL3-SCL3 and SCL3-DELLA interactions are balanced to integrate the GA signal into control of root meristematic size and activity through differentiation and elongation. SCL3 promotes GA-induced root elongation by reducing DELLA activity in the endodermal cells. SCL3 is also involved in plant development in tissues and organs other than the root, but this may be mostly DELLA-independent.

1.5.3 DNA binding

The evidence that DELLA proteins bind DNA is mixed. After identifying 14 common early response genes (down-regulated by GA and up-regulated by DELLA) in micro-arrays (Zentella et al., 2007) used ChIP assays to examine the promoters of these genes and find that DELLAs were binding to eight of the promoter regions. However, their enrichment was low, indicating that the binding was not direct, but rather through association with other transcription factors. The authors identified *XERICO* promoter as a binding site and a possible binding element they call CCT; [C/T]T[C/T][C/A]TC[T/C][C/T]TCT[C/T][C/T]T[T/C]. The *XERICO* promoter is reported to be a target for DELLAs (*RGA*, *GAI* and *RGL2*), although it is not clear whether binding is direct or indirect. *XERICO* encodes a RING-H2 zinc finger domain protein that promotes ABA biosynthesis (Piskurewicz et al., 2009), and therefore may play a part in a homeostatic mechanism between GA and ABA.

RGL2 has been shown, in ChIP assays, to bind the *MOTHER OF FT AND TFL1* (*MFT*) promoter. *MFT* regulates seed germination via the ABA signalling pathway through an unknown mechanism (Xi et al., 2010).

1.5.4 Transcriptional regulation mediated by DELLAs

DELLAs are central to the GA signalling pathway and have been shown through microarray experiments to influence many gene transcriptional levels. DELLAs are also involved in GA homeostasis via a feedback mechanism on the late GA biosynthetic genes *GA20ox* and *GA3ox*, the catabolic *GA2ox* and the receptor gene, *GID1* and may be direct targets for regulation (Silverstone et al., 2001, Fu et al., 2001, Xu et al., 1995, Zentella et al., 2007).

In rice anther development microarray data comparisons of *gid1, gid2*, *cps* (*ent*-copalyl diphosphate synthase), and *gamyb* mutants, revealed that *GAMYB* is involved in almost all instances of GA-regulated gene expression in anthers (Aya et al., 2009). In a similar fashion in the rice aleurone, almost all gibberellin responsive genes are regulated through *SLR1* and *GAMYB*, however when datasets are compared there is almost no overlap between aleurone and floral tissue (Tsuji et al., 2006). In barley aleurone, it was also found using microarrays that the *SLN1* controls almost all GA-induced genes (Chen et al., 2010).

In microarray experiments to determine DELLA-influenced processes (Cao et al., 2006) firstly compared wild-type *vs*. *ga1-3*, then *ga1-3 vs*. *ga1-3* quadruple DELLA mutant (*gai, rga, rgl1, rgl2; Δquad)* whole transcriptome profiles. They found that regulation of only approximately half of GA-regulated genes depends on DELLAs. Therefore, half are regulated independently of DELLA action through an unknown mechanism. They also compared profiles from imbibed seeds and unopened floral buds and found very different sets of regulated genes, again, despite the fact that outwardly similar cell elongation processes are occurring.

Using whole genome microarray to identify early molecular events controlled by *RGA* in flowers, Hou *et al* used a 35S-*RGA*-GR (post-translational) glucocorticoid activation construct to identify differences between *ga1-3* and *ga1-3, Δquad*, 35S-*RGA*-GR plants (Hou et al., 2008). These authors identified 806 transcripts changing greater than 1.5 fold, 4 h post-induction; 413 up-regulated and 393 down-regulated. Further to this they used cycloheximide (to prevent *de-novo* protein translation) along with steroid induction. Using this approach the authors identified 8 genes as immediate targets of *RGA* (At3g28830, At3g16750, At3g62950, At5g49450, At5g22920, At3g62230, At5g61420, and At2g17840).

These findings did not have much overlap with two other genome-wide expression studies, one investigating floral tissue, albeit using a different method (Cao et al., 2006), and another

that analysed eight day seedlings and used a similar construct (Zentella et al., 2007). Between these three studies, only three genes showed consistent regulation: *AtGID1b* (up-regulated), extracellular lipase *EXL3* (down-regulated), and an ACT domain containing protein (up-regulated).

Of the 393 down-regulated genes in (Hou et al., 2008), 171 (44 %) were metabolic enzymes. This is over-representative of this class of genes (27 % of all *Arabidopsis* genes encode metabolic enzymes). These were mostly enzymes that mediate cell wall re-modelling and modification. Therefore *RGA* is predominantly repressive on genes involved in cell expansion indicating that, in flowers at least, GA mainly affects cell expansion and not division. In contrast, down-regulation of transcription factors, at less than 6 %, is under-representation of this class. Of the 413 up-regulated genes, 35 % were metabolic (again over-representation), 11 % transcription factors (over-representation), 17 % protein-binding proteins (over-representation) and 15 % DNA-binding proteins (over-representation). Therefore, *RGA* activates regulatory genes involved in repression.

RGA-regulated genes were mostly expressed in stamens and pollen, and in petals, but very poorly expressed in carpels, sepals and pedicels. This was expected, as examination of the *ga1-3* (GA synthesis mutant) phenotype reveals deficiencies mostly in male organ sterility and the elongation of the petals.

1.6 Cross-talk with other signalling pathways

Cross-talk is defined as the points of regulatory interactions between two or more signal transduction pathways, including hormone biosynthesis pathways. GA negatively regulates the synthesis of cytokinins, brassinosteroids (BR) and jasmonic acid (JA), but can mediate both up- and down-regulation of abscisic acid (ABA), ethylene and auxin biosynthesis, depending on the context (cell and developmental stage). Hormone interactions are developmentally constrained; they may antagonise at one stage and act additively at another. Changes in the levels of one hormone will change the response to other hormones. GA biosynthesis is regulated by light, which acts through the phytochromes. Light also alters the sensitivity of developmental processes to GA (Gazzarrini and McCourt, 2003, Yamaguchi and Kamiya, 2001).

The current model of DELLA proteins is that they are general inhibitors of plant growth and that they are cooperatively regulated by GA, auxin and ethylene. However, GA appears to act

mainly through releasing DELLA protein repression, whereas both auxin and ethylene are both able to regulate growth independently of the DELLA proteins as well, leaving the centrality of the DELLA proteins in the cross-talk model an open question (Swain and Singh, 2005).

1.6.1 Photomorphogenesis

Plants sense intensity, duration, direction and wavelength of light. There are four classes of light receptors in plants. *Arabidopsis* has five phytochrome receptors, named phy*A* through to -*E*. The Phy proteins have molecular weight of approximately 125 kDa and include covalently attached bilin chromophore (N-terminal domain). Phy proteins also have a nuclear localisation domain and the C-terminal domain for dimerisation. Red light (wavelength 660 nm) activates Phy to the P_{fr} form and far red (730 nm) inactivates Phy back to the P_r form. The Phy proteins are probably Ser/Thr kinases activating or marking downstream targets through phosphorylation. Light signalling also utilises regulated degradation of signalling intermediates and these may be separated into two classes, those degraded in the light and those degraded in the dark. Plants also contain the cryptochromes and phototropins, which are sensitive to ultraviolet A and blue light wavelengths (320 to 450 nm) and zeitlupes (blue- 450 nm) (Alabadi et al., 2004, Huq, 2006, Seo et al., 2009).

In seeds, phytochrome signalling is almost solely mediated through *PIL5*. *PIL5* represses germination by binding directly to the promoters of *GAI* and *RGA* to induce expression and also to promoters of other transcriptional regulators in a cascade, to indirectly effect the germination repression. This includes *RGL2,* ABA biosynthetic and GA catabolic up-regulation, and ABA catabolic and GA biosynthetic down-regulation. *RGL2* (and not *GAI* or *RGA*) production is up-regulated by ABA through an unknown mechanism. DELLAs (*GAI*, *RGA* and *RGL2*) elevate *XERICO* expression levels and *XERICO* promotes ABA biosynthesis (also unknown mechanism). In light, *PHYB* in P_{fr} active state induces degradation of *PIL5* through the 26S proteasome system, allowing induction of GA biosynthesis and the seed germination. In the absence of GA, *RGL2* represses germination in the light, whereas the repression in the dark is mediated by *RGL2, RGA* and *GAI*. DELLAs inhibit testa rupture, but do not affect endosperm rupture (Oh et al., 2007, Piskurewicz et al., 2009, Oh et al., 2009).

Photomorphogenesis (de-etiolated growth responses) is the default developmental program following seed germination that adapts the seedling for light. The DELLA proteins are involved in the repression of photomorphogenesis (Figure 1.6), as seen by null mutant phenotypes of

gai-t6 and *rga-24* plants that show de-etiolated growth in the dark (DELLAs repress GA inhibition of photomorphogenesis). GA biosynthesis is up regulated in response to light (Huq, 2006, Alabadi et al., 2004, Fleet and Sun, 2005).

There is a three-day window after germination when GA is required in order to for etiolated growth developmental processes to be initiated. Exposure to light will induce photomorphogenesis (Alabadi et al., 2008). In the absence of GA, the (default) photomorphogenesis will be dominant in the dark. GA promotes etiolated growth in the dark through apical hook formation and hypocotyl elongation and represses photomorphogenesis.The etiolated growth in the dark is achieved by repression of default photomorphogenesis programme through *COP1* (*CONSTITUTIVE PHOTOMORPHOGENIC 1*), an E3 ubiquitin ligase, which degrades the transcription factors necessary for establishing photomorphogenesis, such as the bZIP transcription factors *HY5* (*LONG HYPOCOTYL 5*), *HYH* (*LONG HYPOCOTYL 5 HOMOLOG*), *LAF1* (*LONG AFTER FAR-RED LIGHT 1*) and *HFR1* (*LONG HYPOCOTYL IN FAR-RED LIGHT 1*) and stabilizes transcription factors required for skotomorphogenesis, such as *PIF1*, *PIF3* and *PIF4* (*PHYTOCHROME INTERCTING FACTOR 1, 3 and 4*).

Alabadi *et al* 2008 provided evidence for cross-talk between GA and light through the *COP1*-mediated pathway, and GA-signaling-regulated protein stability of *HY5* and *PIF3* activity (Alabadi et al., 2008). GA targets *HY5* to repress photomorphogenesis in darkness and regulates PIF activity to promote skotomorphogenesis.

Shade avoidance response (elongation of hypocotyl and petioles) is regulated by auxin and ethylene, mostly through DELLA-independent mechanisms, though these two hormones do affect DELLA stability. GA biosynthesis is promoted in low Red: Far Red shaded conditions, resulting in degradation of DELLA proteins. However, DELLA knockouts do not show constitutive petiole elongation, hence this appears more a secondary (though still functionally important) response rather than the main signal transduction (Pierik et al., 2009, Djakovic-Petrovic et al., 2007).

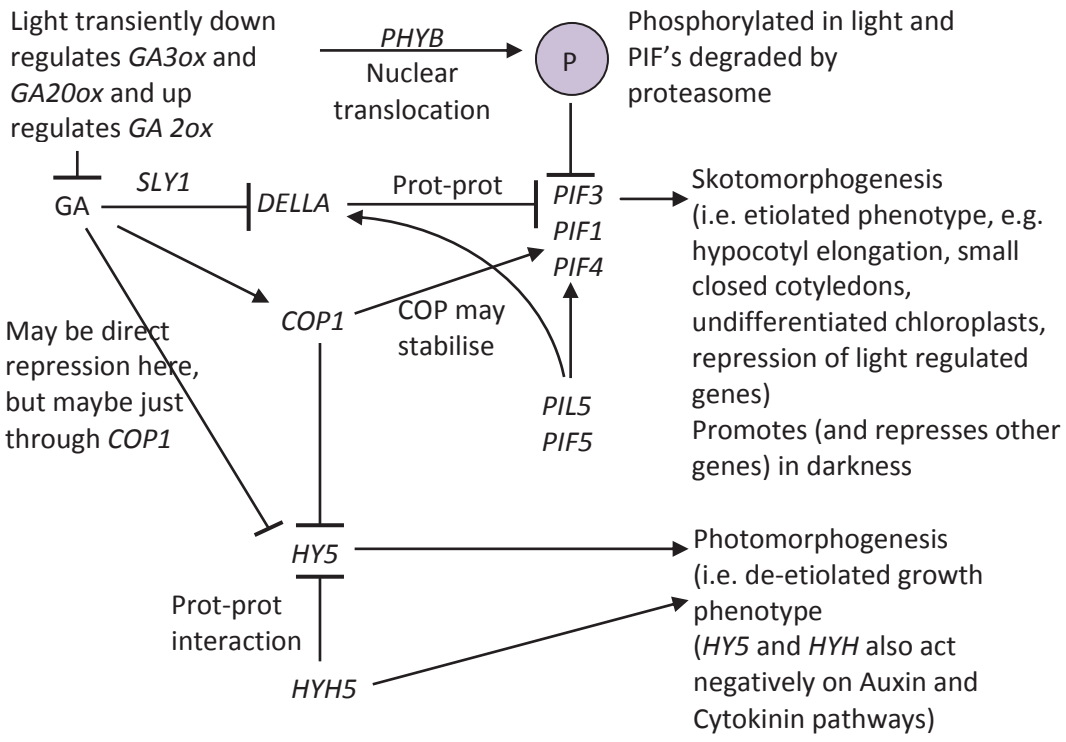

Figure 1.6. GA represses photomorphogenesis

T-bar represents repression and arrow heads promotion of signalling.

1.6.2 Flowering pathway, Floral organs and Fertilisation

A point of GA influence on the long day flowering pathway is *SOC1* whose expression is regulated by GA through opposing DELLA repression of *SOC1* (Moon et al., 2003, Bishopp et al., 2006). GA also promotes flowering through the DELLA-independent up-regulation of miR159 and *GAMYB* (in a complex feedback regulation). miR159 levels are also affected by ABA (up-regulation) and ethylene (down-regulation). Ethylene induces expression of *LFY*, the floral meristem identity gene (Achard et al., 2004). The GA pathway is the only flower-promoting pathway under short days, but it also contributes to flowering under long days.

The application of GA (to GA biosynthesis mutant, *ga1*) up-regulated the expression of the floral homeotic genes *AP3* (*APETALA 3*), *PI* (*PISTALATA*) *and AG* (*AGAMOUS*). In an inducible *RGA* construct in the *ga1-3/rgat-2/rgl2-1* null mutant background, induction of *RGA* resulted in reduced *AP3, PI* and *AG* transcript levels. GA also directly regulates genes involved in floral organ development (after the switch to reproductive development) (Yu et al., 2004). Please refer to sections 1.3.7 and 1.6.5.

GA-biosynthesis and GA-signalling mutants were reported to have a reduced fertility (Chhun et al., 2007), but their phenotypes are not identical. The GA-deficient mutant had impaired pollen germination and pollen tube growth, whereas the GA-insensitive (signalling) mutant was mainly defective in pollen maturation (development). In the GA biosynthetic mutant pollen was viable, however it failed to reach the ovule due to a short pollen tube, for whose growth *de novo* GA biosynthesis was required. In contrast, in most of the GA signalling mutants the pollen was not viable. On the developmental time scale, the transcript levels for *GID1*, *GID2*, *SLR1* and *GAMYB* were high at the pre-meiosis stage of pollen development in anthers (pollen mother-cells and tapetum), whereas expression of GA-biosynthetic genes (*CPS1*, *KS1*, *KO2*, *KAO*) occurs preferentially after meiosis.

1.6.3 Auxin

Auxin promotes cell proliferation and enlargement. It is synthesised in the growing shoot tip and transported to the root, where it promotes growth. This directional movement is called the polar auxin transport stream. Some of auxin's growth-promoting effects are mediated through the degradation of the AUX/IAA (AUXIN-RESPONSIVE PROTEIN / INDOLEACETIC ACID-INDUCED PROTEIN) proteins, mediated by the SCF^{TIR1} E3 ligase. The AUX/IAA proteins are

repressors of the ARF (AUXIN RESPONSE FACTOR) family of proteins which either activate or repress auxin-regulated gene expression. Auxin promotes GA biosynthesis (up-regulates *GA3ox* and down-regulates *GA2ox*) in the shoot and roots (O'Neill et al., 2010).

Auxin and GA have intersection during fruit formation; the auxin-induced fruit-set and development is mediated by GA action. In tomato the DELLA protein PROCERA promotes, whereas auxin down-regulates the expression of Sl*ARF7*, a repressor of ovary growth. PROCERA may be acting through a bHLH transcription factor protein like STYLE2.1 (Carrera et al., 2012). (Also see section 1.2.1 on PROCERA).

Besides its effect on GA biosynthesis, auxin also regulates growth through the modulation of the GA signal transduction pathway (Fu and Harberd, 2003). Polar auxin transport is controlled by the efflux regulator AtPIN1 (PIN-FORMED1). When the levels of AtPIN1 were reduced using RNAi knock-down approach, GFP fusion of DELLA protein RGA (RGA-GFP) was more resistant to GA-induced degradation. Also following decapitation (removal of the shoot tip, site of auxin synthesis) of plants, the RGA-GFP was again much less responsive to GA. Therefore, auxin increases susceptibility of RGA to GA-induced degradation.

1.6.4 Ethylene

Ethylene predominantly inhibits elongation but under some conditions it stimulates elongation or growth. Ethylene stimulates shoot and root differentiation, is involved in release from dormancy, stimulating flower opening, fruit ripening and fruit and leaf abscission. Ethylene is the only gaseous hormone and is produced in all tissues, depending on the developmental stage. It is also induced when the plant is under stress, such as drought or flooding and when under pest and disease attack (De Grauwe et al., 2008). Ethylene has been shown to modulate the rate of DELLA protein (RGA-GFP fusion) degradation induced by GA (Achard et al., 2003). However, in contrast to auxin, ethylene was antagonistic to GA signalling and increases DELLA stability to slow root growth.

The apical hook protects the cotyledons and SAM during germination and breaking through the soil. Ethylene, auxin, cytokinin and brassinosteroids and GA are involved in the apical hook formation. GA-induced elongation of cells is regulated by ethylene modulating RGA stability (as seen using the RGA-GFP fusion protein and monitoring fluorescence) (Vriezen et al., 2004) . Furthermore, ethylene induced hypocotyl elongation in a GA dependent manner

(Vandenbussche et al., 2007b). However, it was not entirely mediated through DELLA signalling, indicating a separate pathway GA-dependent, DELLA-independent pathway.

Ethylene and GA both appear to contribute to several other environmentally controlled developmental processes, such as germination (Chiwocha et al., 2005), hyponastic response (Pierik et al., 2004), adventitious root formation and internode elongation (Steffens et al., 2006). The molecular bases of these interactions are poorly understood.

1.6.5 Cytokinins

Cytokinins (CK) inhibit seed growth (size), germination and root growth and promote leaf development (size, chlorophyll content, and senescence delay) and shoot meristem formation and maintenance (Riefler et al., 2006). CK and GA are mostly antagonistic. GA inhibits CK signalling and CK inhibits a subset of GA responses. The leaf morphology of tomato is regulated by both CK and GA (Fleishon et al., 2011). This process was found to be DELLA-independent.

Greenboim-Wainberg *et al* found that application of GA or plants containing *spy* (null) mutant alleles can suppress the inhibition of root growth by cytokinins (Greenboim-Wainberg et al., 2005). The authors propose that SPY (or a component downstream of SPY) enhances cytokinin signalling, acting possibly on the CK phospho-relay cascade (by *O*-GlcNAc modification), and also acts negatively on GA signalling through the DELLA proteins. GA may act, through an unknown mechanism, to down-regulate SPY and hence suppress CK signalling pathway. Further to this, microarray data from seed suggest that CK down-regulates expression of genes encoding GA biosynthesis enzymes *GA20ox* and *GA3ox* and up-regulates expression of *GAI* and *RGA* (Brenner et al., 2005).

1.6.6 Abscisic Acid

Barley aleurone microarray experiments supported findings that the actions of GA and abscisic acid (ABA) are mostly antagonistic, and that their balance determines maturation of seed (embryogenesis) and continued dormancy versus germination (Chen and An, 2006). GA acts to promote germination through the induction of *GAMYB* expression, which induces expression of seed hydrolysis enzymes in germination (Gubler et al., 1995). ABA acts to promote dormancy partially through the induction of the kinase, *PKABA1*, which acts upstream of α-amylase induction to suppress expression of hydrolytic enzymes (Gomez-Cadenas et al., 1999,

Gomez-Cadenas et al., 2001). ABA also acts through the induction of two WRKY transcription factors (Xie et al., 2006).

A microarray experiment found that DELLAs may up-regulate the ABA signalling pathway by increasing expression of the E3 ligase gene *XERICO*, which promotes ABA accumulation (Zentella et al., 2007). During germination, ABA had no effect on barley DELLA (SLN1) stability (Gubler et al., 2002). However, (Achard et al., 2006) found that ABA did stabilise *A. thaliana* DELLA (RGA) to inhibit root growth, in contrast to GA that destabilises DELLA proteins. It has also been proposed that the stability of DELLA protein repression, whose outcome is mediated through cross-talk between hormones and exogenous inputs, on cotyledon expansion is the underlying control point for the coat-imposed dormancy of *Arabidopsis* seeds (Penfield et al., 2006).

1.6.7 Jasmonic acid and Salicylic acid

Plants produce chemical and physical defences against attack. SA mediates the defences against biotrophic pathogen infection and JA mediates signalling from necrotrophic pathogens, damage and wounding. There is negative cross talk between SA and JA-mediated defences (Santner et al., 2009).

DELLA proteins promote (lead to a more sensitive) jasmonic acid (JA) signalling pathway and thereby alter the balance that exists between the JA and salicylic acid (SA) defence signalling pathways (Navarro et al., 2008). This therefore affects the plant response to an attack (i.e. it weakens the SA biotrophic response). *Gibberella fujikuroi* is a necrotrophic fungus that produces GA, leading to DELLA destruction. Less DELLA weakens the JA pathway, decreases the necrotrophic response and helps the fungus colonise the plant. Examining microarray data that compared wild-type plants stimulated with a flagellin-derived peptide *FLG22* (a bacterial pathogen necrotrophic-stimulating protein) to non-stimulated *ga1-3* and wild-type plants suggested that DELLAs may up-regulate some of the WRKY transcription factors involved in plant defence and propose that DELLAs may be involved in JA perception and/or signalling. DELLA proteins promote JA signalling through direct interaction with JAZ1, a JA signalling repressor, preventing its action (please refer to section on protein-protein interactions; 1.5.2). However, GA also promotes JA biosynthesis in stamens through DAD1, a JA biosynthetic enzyme, by counteracting DELLA repression of DAD1 expression. Deficiency in JA leads to male sterility. The GA acts through JA to induce *MYB21*, *-24*, *-57*, transcription factors that promote

floral development. Null mutations of DELLA-encoding genes *RGA* and *RGL2* can restore *MYB57, -21* and *-24* levels and male fertility in *ga1-3* plants (Cheng et al., 2009).

1.6.8 Salt stress, reactive oxygen species and phosphorus

In *Arabidopsis* salt stress delays flowering in a dose-dependent manner. Under salt stress, the leaves also demonstrate morphological differences from the unstressed plants; they have a more juvenile like appearance of longer petiole with a round short blade. Overall, the salt stress causes severe full dwarfism in plants, at 100 mM NaCl (Li et al., 2007). Exogenous application of GA restores normal flowering time, indicating the GA pathway is important in this stress-response phenotype. Growth of *Arabidopsis gai-t6/rga-24/rgl1-1/rgl2-1* quadruple-DELLA null mutants (*Δquad*, containing only *RGL-3*) is less inhibited by salt than that of wild-type plant. Wild-type plants grown under salt stress conditions have reduced bioactive GA levels and increased DELLA levels (Achard et al., 2006). The increased DELLA levels were beneficial and enhanced the survival of the plants in high salt, as the *Δquad* were less salt tolerant, though the underlying mechanism is unknown. The growth response, in-part, was mediated through ABA and ethylene signalling. The ABA-treated roots accumulated DELLA proteins, whereas *Δquad* plants were resistant to ABA growth inhibition, most likely due to the lack of active DELLA proteins. Salt treatment-delayed flowering was mediated by DELLA-dependent repression of *LEAFY* (*LFY*) gene expression. In contrast to the wild-type plants, *Δquad* plants treated with salt did not have delayed flowering and had normal *LFY* levels. Besides expression of *LFY*, the salt treatment also altered transcription of other floral pathway integration genes in the wild-type: it down-regulated *CONSTANS* (*CO*) floral promoter, but up-regulated expression of floral repressor *FLOWERING LOCUS C* (*FLC*). These two genes were unaffected by salt treatment in the *Δquad* mutant background. ABA also delayed flowering in a DELLA-dependent manner, suggesting that salt acts partly through ABA signalling and ABA signalling enhances DELLA restraint. Salt also increased ethylene synthesis in wild-type and *Δquad* plants. Wild-type plants growing in an ethylene-enriched atmosphere were more inhibited than *Δquad* plants and therefore ethylene signalling can promote salt tolerance in a DELLA dependent manner.

Reactive oxygen species (ROS) are damaging to the living cells. ROS detoxification reduces cell death and increases tolerance to both abiotic and biotic stressors. ROS is thought to also act as a second messenger and is known to contribute to a reduction in root growth. DELLAs (*RGA* and *GAI*) modulate ROS (Reactive Oxygen Species) through the regulation of gene transcription

of genes encoding the ROS scavenging system enzymes *CSD1* and *CSD2* (*CU/ZN-SUPEROXIDE DISMUTASES*) (Achard et al., 2008). The authors showed that DELLA-dependent GA-responses modulate growth processes (cell elongation in root hairs) through their activities in reducing ROS accumulation. ROS basal levels were higher in *Δquad* and levels rose in *Δquad* and wild-type plant in response to salt stress. However, in *ga1-3* plants levels remained low, suggesting a possible GA-independent DELLA role in the ROS scavenging.

Phosphorus is an essential element for growth and has poor mobility and therefore low availability (due to poor solubility). Plants have mechanisms that attempt to cope with this, such as large, branched root system (root: shoot ratio), with abundant root hairs. Phosphorus starvation was found to lower bioactive GA levels and this led to an accumulation of DELLA protein RGA, as monitored by GFP-RGA fusion (Jiang et al., 2007). These authors showed, by comparing *A. thaliana* DELLA-dominant and DELLA-deficient mutant lines in the presence or absence of GA that the GA/DELLA system regulated the root hair length, root architecture and anthocyanin accumulation, but not efficiency of phosphorus uptake or expression of other genes whose transcription is known to respond to phosphorus starvation.

1.7 Research project

The DELLA proteins are unique to plants and appear to be at a cross roads of signal transduction pathways, regulating developmental responses to these combined signals.

Although the GA biosynthetic pathway is mostly elucidated, GA inactivating or storage processes are less clear. Furthermore, much remains to be identified along the GA signalling pathway. The consequence of the GA signal leading to the de-repression of development is now well founded, with a receptor, GID1 and $SCF^{GID2/SLY1}$ E3 ligase-mediated proteasome degradation of DELLA repressors demonstrated.

However finding and understanding the downstream targets of DELLA repression is only beginning. DELLA proteins bind other proteins for their transcriptional modulation function. In the instances known, they bind transcription factors and modulators of transcription factors. There is also support for function through DNA binding in complex with co-activators, though these are unknown.

Like other eukaryotic proteins involved in signalling, DELLA proteins were shown to undergo post-translational modifications – phosphorylation and ubiquitination. In addition, a putative OGT in the pathway indicates that they may also be *O*-GlcNAcylated. However, the location, number of each modification, the type of modification on particular residues and the actual role (outcome) of modifications (apart from ubiquitination) are yet to be determined.

Many plants have multiple DELLA proteins, however the distribution and roles of these proteins in development and physiology particularly in crop plants, remain unknown. The very low amount of DELLA proteins in the cells has prevented localisation of the wild-type (non-transgenic non-tagged) protein. Because of the crucial role of DELLA proteins in productivity of crops as well as their roles in overcoming environmental stress, learning about their distribution and function would provide the basis for understanding of DELLA protein function in these plants.

This thesis identified and characterised DELLA proteins of two woody crop plants, apple (*Malus domestica*, Borkhausen 1803) and kiwifruit (*Actinidia deliciosa,* Liang and Ferguson). This included genomic localisation, phylogeny, general structural comparison and transcriptional analysis of DELLA and core GA-signalling pathway components (GID1 and SLY1/ GID2 homologues). As the tools for isolating proteins from woody crop plants, including *M. domestica* and *A. deliciosa*, are not available *Arabidopsis thaliana* model plant was used to identify DELLA-interacting proteins in plants that cannot synthesise GA.

AIMS

1. Identification, characterisation and organ- and developmental-stage dependent transcriptional analysis of the core GA signalling components (DELLA, GID1 and GID2/SLY) in horticulturally important woody perennials *M. domestica* and *A. deliciosa* to understand the similarities and differences of GA signalling components from these two woody perennials with other plants that have different morphologies and life spans.
2. Identification and preliminary characterisation of DELLA-containing complexes and DELLA-interacting proteins in the model plant *A. thaliana*, to identify yet undetected players in DELLA-mediated regulation of developmental processes.

CONTRIBUTIONS:

Some sections within chapter 3 of this thesis contain data from published manuscripts that are product of team work, including C. Kirk as an author. Where applicable, contributions to figures and tables will be specified. If unspecified, the work was done exclusively by C. Kirk.

2. Material and Methods

2.1 Material

Analytical grade chemicals:

Sourced from BDH, Poole, UK: Sodium dodecyl sulphate (SDS), ammonium persulphate, ethidium bromide, ethylene-diamine-tetra-acetic acid (EDTA), sodium hydroxide, potassium acetate, glucose, maltose, sucrose, sodium chloride, potassium chloride, magnesium chloride, magnesium sulphate, potassium di-hydrogen orthophosphate, di-sodium orthophosphate, sodium di-hydrogen orthophosphate, hydrochloric acid, manganese chloride, calcium chloride, hexamine cobalt (III) chloride, glycerol, potassium hydroxide, potassium ferricyanide, potassium ferrocyanide, potassium hydroxide, bromophenol blue, sodium hypochlorite, ascorbic acid.

Sourced from Merck KGaA, Darmstadt, Germany: 40% (29.1:0.9) v/v acrylamide/ bis-acrylamide, methanol, acetic acid, ethanol.

Sourced from Sigma, St. Louis, Missouri, USA: Tris (hydroxymethyl) aminomethane (Tris), glycine, RNase A, 5-bromo-4-chloro-3-indolyl galactopyranoside (X-gal), isopropyl β-D-1-thiogalactopyranoside (IPTG), ampicillin, kanamycin, streptomycin, chloramphenicol, tetracycline, rifampicin, 1,4-dithiothreitol (DTT), Z-Leu-Leu-Leu-al (MG132), n-dodecyl β-D-maltoside (DDM), polysorbate-20 (Tween™ 20), β-mercaptoethanol, gibberellin A3 (GA_3), β-D-glucuronide (X-gluc), triton® X-100, coomassie brilliant blue R, bovine serum albumin (BSA), cyanogen bromide (BrCN), 1,6-diaminohexane, ethylene glycol-bis(2-aminoethylether)-*N*,*N*,*N*′,*N*′-tetraacetic acid (EGTA), piperazine-N,N′-bis 2-ethanesulfonic acid (PIPES), polyethylene glycol (PEG) 400 distearate, 1-hexadecanol, toluidine blue.

Sourced from Life technologies, California, USA: Tetramethyl-ethylene-diamine (TEMED), BenchMark™ protein standards, SYBR®safe DNA stain, 1kb plus DNA standard.

Sourced from Schleicher and Schuell Bioscience GmbH, Dassel, Germany: Protran nitrocellulose membrane BA83, 3MM chromatography paper.

Sourced from Thermo Scientific (Pierce), Massachusetts, Illinois, USA: *N*-e-(maleimidocaproyloxy) succinimide ester (EMCS), 2-mercaptoethanolamine.HCl (2-MEA).

Sourced from GE Healthcare, Pennsylvania, USA: ECL Advance reagent.

Sourced from Roche GambH, Penzgerg, Germany: Complete™ protease inhibitor cocktail tablets.

Sourced from Fort Richard, Auckland, New Zealand: Tryptone, yeast extract, peptone, beef extract.

Sourced from Yates, Auckland, New Zealand: Gluphosinate ammonium (Short Cut Weed killer).

Sourced from Lehle Seeds, Round Rock, USA: 84 % polyalkylencoxide modified heptamethyltrisiloxane 16 % allyloxypolyethyleneglycol methyl ether (Silwet® L-77 Vac-In-Stuff).

Sourced from Polysciences, Eppelheim GmbH, Germany: Hoechst 33258.

2.2 Methods

2.2.1 *Escherichia coli* and *Agrobacterium tumefaciens* strains and growth

All bacterial strains used in this work are listed in Table 2.1.

Escherichia coli strains DH5αFT and TOP10 (Life technologies, California, USA), were used for cloning and maintaining recombinant plasmids. Cells were propagated in Lysogeny broth (LB; 10 g/L tryptone, 5 g/L yeast extract, 10 g/L NaCl, pH7.5 NaOH) at 37 °C and was supplemented with 1.5% w/v agar for growth on plates. TUNER(DE3) or BL21(DE3) were the strains used for protein expression.

Agrobacterium tumefaciens LBA4404 or GV3101 cells were propagated on Yeast Extract Broth (YEB; 5 g/L beef extract, 5 g/L peptone, 1 g/L yeast extract, 5 g/L sucrose, 0.5 g/L magnesium sulphate) at 28 °C. For growth on plates the media had 1.5 % w/v agar added.

Media was supplemented with: ampicillin (100 µg/mL), kanamycin (50 µg/mL), chloramphenicol (25 µg/mL), tetracycline (10 µg/mL), rifampicin (100 µg/mL) or streptomycin (100 µg/mL) as appropriate to select for the transformed strains.

Bacterial strains were stored long-term at -80 °C. Overnight cultures of bacteria were prepared for storage by addition of glycerol at 15 % v/v.

Table 2.1. *Escherichia coli* and *Agrobacterium tumefaciens* strains

Strain	Genotype	Reference
E. coli		
DH5αFT	ϕ80d*lac*ZΔM15 Δ(*lac*ZYA-*arg*F) U169 *deo*R *rec*A1 *end*A1 *hsd*R17 (r_k-, m_k+) *pho*A *sup*E44 λ- *thi*-1 *gyr*A96 *rel*A1/F' *pro*AB+ *lacI*^{q}ZΔM15 Tn10 (tet^R)	Life technologies, California, USA
TOP10	F$^-$ *mcr*A Δ(*mrr-hsd*RMS-*mcr*BC) ϕ80*lac*ZΔM15 Δ*lac*X74 *rec*A1 *ara*D139 Δ(*ara leu*) 7697 *gal*U *gal*K *rps*L (Str^R) *end*A1 *nup*G	Life technologies , California, USA
BL21 (DE3)	F$^-$ *omp*T *hsd*S_B(r_B–, m_B–) *gal dcm* λ(DE3)	Merck KGaA, Darmstadt, Germany
TUNER (DE3)	F$^-$ *omp*T *hsd*S_B (r_B– m_B–) *gal dcm* *lac*Y1(DE3)	Merck KGaA, Darmstadt, Germany
A. tumefaciens		
LBA4404	Disarmed Ti plasmid pAL4404	Life technologies , California, USA
GV3101	Disarmed Ti plasmid pMP90 Rif^R	Graciously supplied by Dr. Andrew Gleave, Plant and Food Research, Auckland, NZ

R, Resistance; Δ, deletion

2.2.2 Basic recombinant DNA techniques

DNA plasmid preparations were made using alkaline lysis (Sambrook et al., 1989) or commercial kits (Qiagen GambH, Hilden, Germany) following the manufacturer's instructions. PCR amplification (Saiki et al., 1988) was, in the main, performed using Platinum Pfx DNA polymerase (Life technologies, California, USA), according to manufacturer's instructions. Oligonucleotides (synthesized by Life technologies, California, USA) are listed in Table 2.2.

Double stranded DNA was cut by using appropriate type II restriction endonucleases (New England Biolabs, Massachusetts, USA) according to manufacturer's instructions.
DNA fragments were separated by size for identification and isolation using agarose gel electrophoresis (Sambrook et al., 1989). Agarose concentration was 0.7-1.0 % w/v, depending on the size of analysed bands. Electrophoresis was typically run at 5 V/cm and the buffer used in all experiments was TAE (40 mM Tris-acetate, 1 mM EDTA; pH 8.0).

DNA and RNA concentrations were determined by spectrophotometry (Biophotometer, Eppendorf AG, Hamburg, Germany) or by fluorometry (Qubit, Life technologies, California, USA) according to manufacturer's instructions.

DNA fragments were ligated using T4 DNA ligase (Promega, Maddison, Wisconson USA), using 3 Units to ligate up to 150 ng DNA and incubated overnight at room temperature. Ligated DNA was subsequently transformed. *Escherichia coli* chemically competent cells were transformed by the heat-shock method. *Agrobacterium tumefaciens* was transformed by electroporation (MicroPulser™, Bio-Rad, California, USA) using the methods described in (Hanahan et al., 1991). Transformants were selected for on growth medium plates containing the appropriate antibiotics.

Table 2.2. Oligonucleotides.

Name	Sequence	Details
RGL2-prom for	TAAGAATGCGGCCGCCCATGACTCAGATTTTCTTTTGG	To amplify the 1.8 kb of DNA upstream of *RGL2* CDS (includes promoter), forward oligo., NotI RE site
RGL2-prom rev	TCCCCCGGGCTTTCTTGTTCTTGTGATGGTG	To amplify the 1.8 kb of DNA upstream of *RGL2* CDS (includes promoter), reverse oligo., SmaI RE site
RGL2 for	TCCCCCGGGATGAAGAGAGGATACGGAGAAAC	To amplify the *RGL2* CDS, forward oligo., SmaI RE site
RGL2 rev	GTAGTCGGTCGACGGCGAGTTTCCACGCCGAGG	To amplify the *RGL2* CDS, reverse oligo., SalI RE site
RGL2-term for	CTAGTAGGGCCCGTCGCGGCGGTAGAGATGAC	To amplify the 2 kb of DNA downstream of *RGL2* CDS (includes terminator), forward oligo. ApaI RE site
RGL2-term rev	CGGGGTACCGAATGCAGAGTAAAGTCTTAGAG	To amplify the 2 kb of DNA downstream of *RGL2* CDS (includes terminator), reverse oligo., KpnI RE site
TAP1	GACGCGTCGACGGTGGAGGTTCAATGGAATC	TAP tag forward oligo. Anneals against TAP2, SalI RE site
TAP2	TTCTTGAATCTATTTGCAGCTGAAACAGCAATAAAATTACTCAACCATCTACTA GATTCCATTGAACCTCCACC	TAP tag reverse oligo. Anneals with TAP1 and TAP3
TAP3	GCTGCAAATAGATTCAAGAAAATTTCTTCAAGTGGTGCTCTTGATTATGATATT CCTACTACAGCTTCTGAGAATCTTTACTTC	TAP tag forward oligo. Anneals with TAP2 and TAP4
TAP4	CCTCCACCGTTATTGTTATTGTTATTGTTATTGTTATTTCCTTGGAAGTAAAGAT TCTCAGAAG	TAP tag reverse oligo. Anneals with TAP3 and TAP5
TAP5	CAATAACGGTGGAGGTGGATCAGGTGGAGGTGGATCTCCTGATCAATATGAA TACAAGTATCCATAA	TAP tag forward oligo. Anneals with TAP4 and TAP6
TAP6	GACCGCTCGAGTTATGGATACTTGTATTCATATTG	TAP tag reverse oligo., anneals with TAP5, XhoI RE site
uidA for	TCCCCCGGGATGTTACGTCCTGTAGAAACC	To amplify the *uidA* (β-D-glucuronidase) CDS, forward oligo., SmaI RE site
uidA rev	CGGACCGTCGACTTGTTTGCCTCCCTGCTGCGG	To amplify the *uidA* (β-D-glucuronidase) CDS, reverse oligo., SalI RE site

Name	Sequence	Details
GR-N for	ATAAGAATGCGGCCGCATGGCTCGAAAAACAAAGAAAAAAATC	To amplify the rat glucocorticoid receptor (amino acids 497 to 794), for N-terminal fusion to DELLA, forward oligo., NotI RE site
GR-N rev	TCCCCCGGGTTTTTGATGAAACAGAAGCTTTTTG	To amplify the rat glucocorticoid receptor (amino acids 497 to 794), for N-terminal fusion to DELLA, reverse oligo, SmaI RE site
GR-point rev	GTGTTTACATTGGTCATACATGCCGGGTAGAGACATTCTCTGCTC	To induce a point mutation $C^{656}G$ in the rat glucocorticoid receptor (amino acids 497 to 794), reverse oligo.
GR-point for	GAGCAGAGAATGTCTCTACCCGGCATGTATGACCAATGTAAACAC	To induce a point mutation $C^{656}G$ in the rat glucocorticoid receptor (amino acids 497 to 794), forward oligo
GR-C for	GATCGTCGACGCTCGAAAAACAAAGAAAAAAATCAAAGGG	To amplify the rat glucocorticoid receptor (amino acids 497 to 794), for C-terminal fusion to DELLA, forward oligo, SalI RE site
GR-C rev	TCGAGTCGACTTTTTGATGAAACAGAAGCTTTTTGATA	To amplify the rat glucocorticoid receptor (amino acids 497 to 794) for C terminal fusion to DELLA, reverse oligo., SalI RE site
UidA transgene for	CACCGACATGTGGAGTGAAG	To amplify from *UidA* (Gus) into *RGL2* terminator, for confirmation of transgenic *Arabidopsis*
RGL2-term transgene rev	GGTTTCAGGCGAGTCATCTC	To amplify back from *RGL2* terminator, for confirmation of transgenic *Arabidopsis*
C-*RGL2* transgene for	CCCGATTCATCTCGGATCTA	To amplify from *RGL2* C-terminal into C-terminal GR fusion, for confirmation of transgenic *Arabidopsis*
C-GR transgene rev	AGGGTCATTTGGTCATCCAG	To amplify form C-terminal rat GR fusion into *RGL2*, for confirmation of transgenic *Arabidopsis*
N-GR transgene for	ACTCCATGCATGAGGTGGTT	To amplify from N-terminal rat GR fusion into *RGL2*, for confirmation of transgenic *Arabidopsis*
N-TAP transgene for	CCTGATCAATATGAATACAAGTAT	To amplify across N-terminal fusion TAP tag into *RGL2* for confirmation of transgenic *Arabidopsis*

Name	Sequence	Details
N-RGL2 transgene rev	AAGAACAGCAAGAAGCTCATC	To amplify back from *RGL2* to N-terminal TAP tag or rat GR fusion for confirmation of transgenic *Arabidopsis*
BAR transgene for	GTCTGCACCATCGTCAACC	To amplify *Bar* for confirmation of transgenic *Arabidopsis*, forward oligo.
BAR transgene rev	GAAGTCCAGCTGCCAGAAAC	To amplify *Bar* for confirmation of transgenic *Arabidopsis*, reverse oligo.
G05	CAATGTGGCAAAAGTGTTGC	To amplify *PP2A* in qPCR, forward oligo, amplicon start at 285bp, Tm=60.2
G06	TCTTCTGAACCACAGACTGGTC	To amplify *PP2A* in qPCR, reverse oligo, amplicon start at 285bp, Tm=59.4
G07	AAGTTGTTCTCGAGCTCCTTTG	To amplify *UPL7* in qPCR, forward oligo., amplicon start at 242bp, Tm=60.1
G08	GGCACATCACATGCAACC	To amplify *UPL7* in qPCR, reverse oligo., amplicon start at 242bp, Tm=59.4
G09	TTGCTCCCAGCAGCATG	To amplify *ACTIN 7* in qPCR, forward oligo., amplicon start at 1115bp, Tm=60.7
G10	TCCAATCCAGACACTGTATTTCC	To amplify *ACTIN 7* in qPCR, reverse oligo., amplicon start at 1115bp, Tm=60.2
G11	GTTTGCTGGTGATGATGCTC	To amplify *ACTIN7* in qPCR, forward oligo., amplicon start at 129bp, Tm=59.2
G12	CCAACCATGACACCTGTGTG	To amplify *ACTIN7* in qPCR, reverse oligo., amplicon start at 129bp, Tm=60.9
A03	AACCACAATGGGAGTGGGT	To amplify *101189*[a] *DELLA* in qPCR, forward oligo., amplicon start at 1330bp, Tm=60.1
A04	CTGGTTACTCGCCTGAGTCAAT	To amplify *101189*[a] *DELLA* in qPCR, reverse oligo., amplicon start at 1330bp, Tm=60.7
D05	CAGGAAAACGGAGTCAGACTC	To amplify *113002 DELLA* in qPCR, forward oligo., amplicon start at 532bp, Tm=58.9

Name	Sequence	Details
D06	CGACACGGCAAGGAGGT	To amplify *113002 DELLA* in qPCR, reverse oligo., amplicon start at 532bp, Tm=60.9
C02	AGAGAGAGATATGCAACATAGTGTGC	To amplify *115865 DELLA* in qPCR, forward oligo., amplicon start at 1250bp qPCR, Tm=60.2
C03	CCCCTCTAAGCCGGGA	To amplify *115865 DELLA* in qPCR, reverse oligo., amplicon start at 1250bp qPCR, Tm=59.7
A11	ACCACAATGGGAGTGGGC	To amplify *227790 DELLA* in qPCR, forward oligo., amplicon start at 1337bp, Tm=61.8
A12	CCTGGTTACTCACCTGAGTCAAC	To amplify *227790 DELLA* in qPCR, reverse oligo., amplicon start at 1337bp, Tm=60.1
E01	GCAGGAGAACGGAATCAGACTA	To amplify *49556 DELLA* in qPCR, forward oligo., amplicon start at 531bp, Tm=60.8
E02	CGGCGAGGAAGCCG	To amplify *49556 DELLA* in qPCR, reverse oligo., amplicon start at 531bp, Tm=61.3
B05	AGAGATATGCAACGTGGTGTGT	To amplify *78609 DELLA* in qPCR, forward oligo., amplicon start at 1269bp, Tm=59.5
B06	GGCCCCACTAAGCCTAGC	To amplify *78609 DELLA* in qPCR, reverse oligo., amplicon start at 1269bp, Tm=59.8
C11	CAGGAGAACGGAATCAGACTG	To amplify *79743 DELLA* in qPCR, forward oligo., amplicon start at 532bp, Tm=59.9
C12	ACGGCGAGGAAGCCA	To amplify *79743 DELLA* in qPCR, reverse oligo., amplicon start at 532bp, Tm=60.0
E07	TCTTCTCCTTCGACGTGGTC	To amplify *200355/4 GID1* in qPCR, forward oligo., amplicon start at 696bp, Tm=60.4
E08	ATGCCGAATTGGGAATTTG	To amplify *200355/4 GID1* in qPCR, reverse oligo., amplicon start at 696bp, Tm=60.7
E11	GTTTTCTCTTTCGATGTCATGATTA	To amplify *287619/17 GID1* in qPCR, forward oligo., amplicon start at 826bp, Tm=58.7

Name	Sequence	Details
E12	TTTGGAGTTCACTATAACTACGCAAG	To amplify *287619/17 GID1* in qPCR, reverse oligo., amplicon start at 826bp, Tm=60.1
F03	GGTTTTCTCTTTCGATGTCATTATG	To amplify*287619/22 GID1* in qPCR, forward oligo., amplicon start at 818bp, Tm=60.2
F04	TTCATCGACACTAGGCCGA	To amplify*287619/22 GID1* in qPCR, reverse oligo., amplicon start at 818bp, Tm=60.4
F11	AGCCGATGGCGATACGA	To amplify *SLY7 GID2* in qPCR, forward oligo., amplicon start at 18bp, Tm=61.3
F12	CCACCGCAGATCCCTCA	To amplify *SLY7 GID2* in qPCR, reverse oligo., amplicon start at 18bp, Tm=61.9
G03	CGATACGGCGGACAAGAAA	To amplify *SLY8 GID2* in qPCR, forward oligo., amplicon start at 27bp, Tm=62.1
G04	CACCAACGCAGATCCCTCT	To amplify *SLY8 GID2* in qPCR, reverse oligo., amplicon start at 27bp, Tm=61.2
F07	GAAGCCAGAAGGAGGAGAACAT	To amplify *SLY12 GID2* in qPCR, forward oligo., amplicon start at 57bp, Tm=61.1
F08	GCAAGTTCTCGTCAGCCAGA	To amplify *SLY12 GID2* in qPCR, reverse oligo., amplicon start at 57bp, Tm=61.7
BMV for	TTTGACAGACTGAGACAACT	To amplify *BMV 3a* in qPCR, forward oligo., amplicon start at 657bp, Tm=60.1
BMV rev	CCTGATCAACAGATTGTAAC	To amplify *BMV 3a* in qPCR, reverse oligo. amplicon start at 657bp, Tm=60.0
101189/98329 GSP1	TTGTGGTTCGCTTCTTGTTCT	GSP1 oligo. for 5'RACE amplification of *101189/98329*
101189/98329 GSP2	GCCTTAATCGAGGCCAATACCTT	GSP2 oligo. for 5'RACE amplification of *101189/98329*
49556 GSP1	CGAACTCGACATGGATTGTTT	GSP1 oligo. for 5'RACE amplification of *49556*
49556 GSP2	AGCTAGCTTCCAACCCACTTC	GSP2 oligo. for 5'RACE amplification of *49556*

Name	Sequence	Details
287619 GSP1	CTTTTGAGTCCTTCTGGCTTTT	GSP1 oligo. for 5'RACE amplification of *287619/17819*
287619 GSP2	ATCATAGGCACAAGGGTAATGGTTT	GSP2 oligo. for 5'RACE amplification of *287619/17819*
287619 GSP2a	TTCAGGAGCTCGCCGATAA	GSP2 oligo. for 5'RACE amplification of *287619*
200355 GSP1	AGGCAGAGGGGTAGCAGTTT	GSP1 oligo. for 5'RACE amplification of *200355*
200355 GSP2	AGGTGTCATATATGGCGCTGTTG	GSP2 oligo. for 5'RACE amplification of *200355*
200355/87170/ 112858 for	CTAGCGGCCGCATGGCCGGTARTAACGRGATCAACRTC	To amplify GID1 homologues from genomic DNA. Forward oligo, NotI RE site.
200355/87170/ 112858 rev	GAGCTGCAGTTAACAGTTRGGGTTCACAAAGCTGTTTATC	To amplify GID1 homologues from genomic DNA. Reverse oligo, PstI RE site.
287619/17819 for	CTAGCGGCCGCATGGCTGGTAGTAAAGAAGTTACTGTC	To amplify GID1 homologues from genomic DNA. Forward oligo, NotI RE site.
287619/17819 rev	GAGCTGCAGTTATGAATTAATGAAATTACTTATCTCATCC	To amplify GID1 homologues from genomic DNA. Reverse oligo, PstI RE site.
SLY GSP1	AAGTCCTTTGCCTCGGTTACT	GSP1 oligo. for 5'RACE amplification of *195089/91591*
SLY GSP2	CTCGTAGTGACGGATCGAGAG	GSP2 oligo. for 5'RACE amplification of *195089/91591*
SLY GSP2a	CGGAGGATTTCGACGGAAC	GSP2 oligo. for 5'RACE amplification of *91591*
KF *SLY1* for	GAATGCGGCCGCATGAAGCGATCGATKGAAGCCGATG	To amplify SLY1 homologues from genomic DNA. Forward oligo, NotI RE site.
KF *SLY1* rev	GGTTCTGCAGTCAANGTCCTTTGCCTCGGTTACTGAA	To amplify SLY1 homologues from genomic DNA. Reverse oligo, PstI RE site.
101189 pETM for	ATAAGAATGCGGCCGCATGAAGAGAGATCGTGRCCGCGAC	To amplify *101189* for cloning into pETM *E.coli* expression vector, forward oligo., Not I RE site
101189 pETM rev	GCATTGGTTCTGCAGCTAAGACGCAGTGGCGGCGAGTTG	To amplify *101189* for cloning into pETM *E.coli* expression vector, reverse oligo., PstI RE site
113002 pETM for	ATAAGAATGCGGCCGCATGAAGCGCGAGCACCACCG	To amplify *113002* for cloning into pETM *E.coli* expression vector, forward oligo., NotI RE site
113002 pETM rev	GCATTGGTTCTGCAGTCAACTGAGTTTCCAAGCCGAGGTGG	To amplify *113002* for cloning into pETM *E.coli* expression vector, reverse oligo., PstI RE site

Name	Sequence	Details
115865 pETM for	ATAAGAATGCGGCCGCATGGATCCGTACAGAAGCGGTAGC	To amplify *115865* for cloning into pETM *E.coli* expression vector, forward oligo., NotI RE site.
115865 pETM rev	GCATTGGTTCTGCAGTTACACCACATTATTATAAGGGTC	To amplify *115865* for cloning into pETM *E.coli* expression vector, reverse oligo., PstI RE site.
227790 pETM for	ATAAGAATGCGGCCGCATGAAGAGAGATCGCGACCGC	To amplify *227790* for cloning into pETM *E.coli* expression vector, forward oligo., NotI RE site
227790 pETM rev	GCATTGGTTCTGCAGTCACGACGCGGTGGCGGT	To amplify *227790* for cloning into pETM *E.coli* expression vector, reverse oligo., PstI RE site.
49556 pETM for	ATAAGAATGCGGCCGCATGAAGCGCGASSACCACCGCACT	To amplify *49556* for cloning into pETM *E.coli* expression vector, forward oligo., Not I RE site
49556/79743 pETM rev	GCATTGGTTCTGCAGTCAACTGAGTTTCCAAGCCGAGGT	To amplify *49556/79743* for cloning into pETM *E.coli* expression vector, reverse oligo., PstI RE site.
79743 pETM for	ATAAGAATGCGGCCGCATGAAGCGCGAGCTCCACGGCCCT	To amplify *79743* for cloning into pETM *E.coli* expression vector, forward oligo., NotI RE site.
78609 pETM for	ATAAGAATGCGGCCGCATGGGTCCGTACGAATCTGCCAT	To amplify *78609* for cloning into pETM *E.coli* expression vector, forward oligo, NotI RE site.
78609 pETM rev	GCATTGGTTCTGCAGTTACACCACATTATTATAAGGGTTAACTAAGCC	To amplify *78609* for cloning into pETM *E.coli* expression vector, reverse oligo., PstI RE site.
AdUPL7 (238886) for	TCAAATGCATTCTATAGAGGGTTGAC	To amplify 238886 to confirm kiwifruit sequence for use as reference gene in qPCR, for oligo.
AdUPL7 (238886) rev	GCATATAGAAGCTTGATTCTCATAGTGC	To amplify 238886 to confirm kiwifruit sequence for use as reference gene in qPCR, rev oligo.
AdPP2A (101815) for	GGTGCTCTTTGCATGCAATGGTTA	To amplify 101815 to confirm kiwifruit sequence for use as reference gene in qPCR, for oligo.
AdPP2A (101815) rev	CTAGCTAGACATCATGACTTGATCAAT	To amplify 101815 to confirm kiwifruit sequence for use as reference gene in qPCR, rev oligo.
AdACTIN (447680) for	CTTGTCTGTGACAATGGAACTGGAATGG	To amplify 447680 to confirm kiwifruit sequence for use as reference gene in qPCR, for oligo.

Name	Sequence	Details
AdACTIN (447680) for	GAAGCACTTCCTGTGGACGATGG	To amplify 447680 to confirm kiwifruit sequence for use as reference gene in qPCR, rev oligo.
MdRGL1b GSP1	GACTTTACGCATGGCACCTGCTTGT	GSP1 oligo. for 5′ RACE amplification of *MdRGL1b*
MdRGL1b GSP2	CTGCTTGTGAACCTGCCAGGTAGCC	GSP2 oligo. for 5′ RACE amplification of *MdRGL1b*
MdRGL2a GSP1	GATATGCAACGTGGTGGCATGTGAAG	GSP1 oligo. for 3′ RACE amplification of *MdRGL2a*
MdRGL3a GSP1	GACGACGGTGAGCTGGTTGTGGTTCTG	GSP1 oligo. for 5′ RACE amplification of *MdRGL3a*
MdRGL2a tg for	CAAGGCCAAGATTTGGGAAGA	To amplify MdRGL2a transgene in qPCR, amplicon start at 84bp, for oligo.
MdRGL2a tg rev	CGGAGAGATCGGACGGGTTGT	To amplify MdRGL2a transgene in qPCR, amplicon start at 84bp, rev oligo.
AtACTIN2 for	CTCTCCCGCTATGTATGTCGCC	To amplify *Arabidopsis ACTIN2* in qPCR, for oligo.
AtACTIN2 rev	GTGAGACACACCATCACCAG	To amplify *Arabidopsis ACTIN2* in qPCR, rev oligo.
MdRGL1b for	TGAGCAGCTTGAAGAATTTATGAGTTGT	To amplify *MdRGL1b* in qPCR, amplicon start at 219bp, for oligo.
MdRGL1b rev	CGCCGGAGCTAAAAACGGGTCGTCA	To amplify *MdRGL1b* in qPCR, amplicon start at 219bp, rev oligo.
MdRGL2b for	GCCGTGCAACTGTAACTGCACGTGAA	To amplify *MdRGL2b* in qPCR, amplicon start at 23bp, for oligo.
MdRGL2b rev	CCATGTCGTCGGACCGAACCTTGTAC	To amplify *MdRGL2b* in qPCR, amplicon start at 23bp, rev oligo.
MdRGL3b for	GCAGCGCGAGCTCCTCTTCTTCTT	To amplify *MdRGL3b* in qPCR, amplicon start at 40bp, for oligo.
MdRGL3b rev	GACCATGACGGTTTCGAGGCGTTC	To amplify *MdRGL3b* in qPCR, amplicon start at 40bp, rev oligo.
MdGAPDH	TCATTCTCTGCCCCCAGTAAGGATG	To amplify *MdGAPDH* in qPCR, for oligo.
MdGAPDH	CCAGGGGAGCAAGACAGTTGGT	To amplify *MdGAPDH* in qPCR, rev oligo.
MdRGL2a for (JR301)	CCAGGATCCATGAAGAGAGAACACTGCCATAG	To amplify (RTPCR) full length MdRGL2a for cloning pART7 and 27, forward oligo., BamHI site.

Name	Sequence	Details
MdRGL2a rev (JR333)	GGTTCTAGACTA TCA CTC CGT TGA GCT CG	To amplify (RTPCR) full length MdRGL2a for cloning pART7 and 27, reverse oligo., XbaI site.
*Md*DELLA universal-1 for	GCSGWKKYSGGRTACAAGGTYCG	Forward degenerate oligo for amplification of *Malus* orthologues.
*Md*DELLA universal-1 rev	AATTTSAGRTARGGGCAGGYCTCGTA	Reverse degenerate oligo for amplification of *Malus* orthologues.
*Md*DELLA-not L3 for	GCSGTKTTGGGRTACAAGGTTCG	Forward degenerate oligo for amplification of *Malus* orthologues.
*Md*DELLA-not L3 rev	AATTTCAGRTARGGGCAGGTCTCGTA	Reverse degenerate oligo for amplification of *Malus* orthologues.
*Md*DELLA universal-2 for	CYGTYCWYTAYAAYCCNKCBGABMT	Forward degenerate oligo for amplification of *Malus* orthologues.
*Md*DELLA universal-2 rev	ATBGCYTGRTTSGCVGTRAARTG	Reverse degenerate oligo for amplification of *Malus* orthologues.
CODEHOP 1	TGAGATCCTCCGACATGGCHGANGT	To amplify *Md*DELLAs, CODEHOP designed using All DELLAs blockmaker alignment, forward oligo., clamp, degeneracy=12.
CODEHOP 2	TGAAGTTGTTTTGTTGGACAGCYTCDGCGCA	To amplify *Md*DELLAs, CODEHOP designed using All DELLAs blockmaker alignment, reverse oligo., clamp, degeneracy=6.
CODEHOP 3	TGAGATCCTCCGACATGGCHGANGTBGC	To amplify *Md*DELLAs, CODEHOP designed using All DELLAs blockmaker alignment, reverse oligo., clamp, degeneracy=36.
CODEHOP 4	CGAACTTCAGGTAGGGGCAGSWYTCRTARAA	To amplify *Md*DELLAs, CODEHOP designed using All DELLAs blockmaker alignment, forward oligo., clamp, degeneracy=32.
CODEHOP 5	GCCTGGCTGTCGTCGGHTAYAARGT	To amplify *Md*DELLAs, CODEHOP designed using known *Md*DELLAs blockmaker alignment, forward oligo., clamp, degeneracy=12.
CODEHOP 6	CCTCCAGGATAGCTTGGTTAGCKGTRAAATG	To amplify *Md*DELLAs, CODEHOP designed using known *Md*DELLAs blockmaker alignment, reverse oligo., clamp, degeneracy=4.

Name	Sequence	Details
CODEHOP 7	CGAATGCCTGGCTGTCGTNGGHTAYAARG	To amplify *Md*DELLAs, CODEHOP designed using known *Md*DELLAs blockmaker alignment, forward oligo., clamp, degeneracy=48.
CODEHOP 8	GATTGAAGTTTTCTTGTTGCACGSHYTCDGCGCA	To amplify *Md*DELLAs, CODEHOP designed using known *Md*DELLAs blockmaker alignment, reverse oligo., clamp, degeneracy=36.

[a] EST number as designated in the Plant & Food Research *Actinidia* EST database.

2.2.3 R-tag design and vector series

An immunogenic peptide sequence was sought in order to produce a fusion tag to facilitate purification and tracking of recombinant proteins expressed in bacteria, plants and animals. Virus databases were used to aid in the approach to identify unique short peptide sequences. Chosen peptides were used as query to search the Genbank databases using BLASTp and settings for short nearly exact matches, which alter the word size and expect values to 7 and 1000 respectively (Altschul et al., 1990).

A short peptide from the Rabies virus nucleocapsid protein (gene N), was identified that produced no hits in the database sequences from other organisms. A proline residue was added to the N-terminal of the sequence. The tag was named the Rab tag (shortened to R-tag) and the full tag sequence is PDQYEYKYP. The peptide was synthesised and mice immunised against it. Following the fusion and cloning experiments a monoclonal antibody called D9 was produced and purified to be used in the experiments below (Jones et al., 2007). The monoclonal antibody (mAb) was tested using western blot experiments to confirm the absence of the peptide from the proteomes of plants, mammalian cells in culture and *E. coli*, and confirmed that no background signal was present.

The DNA sequence coding for the peptide was optimised for expression in bacteria or plants utilising the Genbank codon frequency tables. The peptide coding sequence was incorporated into a series of vectors based on a modified EMBL (European Molecular Biology Laboratory) bacterial expression vector backbone. It was used as a fusion peptide in recombinant protein experiments to either capture or track the fusion protein in purification experiments. All vectors were kanamycin resistant, expression was IPTG-inducible and driven from the T7 polymerase promoter. The expression product had the basic formula of X-Y-rTEV-MCS-Z (Figure 2.1), where X is either the fusion tag His (His tag; six consecutive Histidine residues) or the Rab peptide (R-tag); Y is maltose-binding protein (MBP), thioredoxin A (TrxA), or glutathione *S*-transferase (GST) and Z is either a GlyGlyGlyCys tag (GGGC- to facilitate *in vitro* biotinylation), His tag, R-tag or no tag (stop codon). The rTEV is the cleavage site for the Tobacco Etch virus protease. The multiple cloning site (MCS) was made up of the restriction enzyme type 2 recognition sites: 5'-Nco1, Not1, Sfi1, Nde1, EcoR1, Pst1, Kpn1, BamH1, Xho1-3'. The EMBL vector may be found at: (http://www.embl.de/pepcore/pepcore_services/strains_vectors/vectors/bacterial_expressio

n_vectors/popup_bacterial_expression_vectors/index.html). The vector series produced here facilitated the production and purification of recombinant proteins used for the production and in the screening of monoclonal antibodies produced and used in this study (Sun et al., 2008).

The R-tag peptide was also used as a fusion tag to identify recombinant proteins expressed in plants in this study.

A.

	P	D	Q	Y	E	Y	K	Y	P
Wild-type:		GAT	CAA	TAT	GAT	TAC	AAG	TAC	CCT
Bacterial:	CCG	GAT	CAG	TAT	GAA	TAC	AAA	TAT	CCG
Plant:	CCT	GAT	CAA	TAT	GAA	TAC	AAG	TAT	CCA

B.

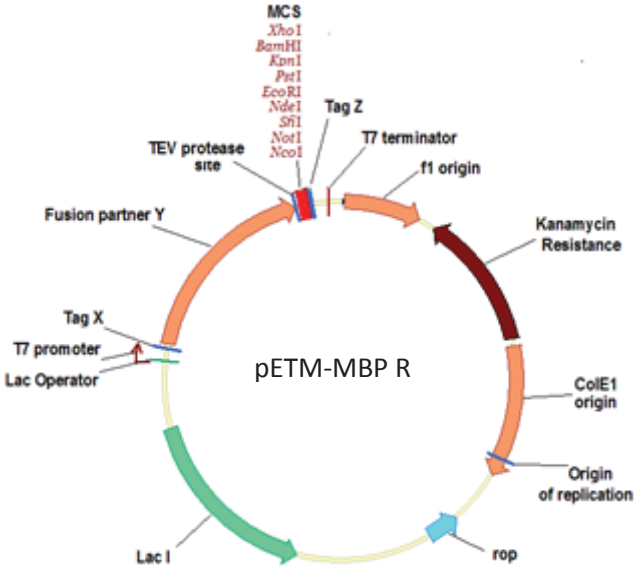

Figure 2.1. R-tag and Vector series backbone diagram
A, The R-tag sequence is an eight residue peptide that does not match any plant, mammalian or bacterial, protein in the database. This peptide is found in the nuclear coat protein of the Rabies virus. The translated peptide was optimised for expression in a plant or bacterial background. A monoclonal antibody was raised against this peptide, anti-R-tag mAb D9.
B, Schematic diagram representing the bacterial expression vector series. The plasmids series is derived from a European Molecular Biology Laboratory (EMBL) vector backbone, pETM-41. It was altered by incorporating a new MCS, different epitope tags and solubility-enhancing fusion proteins. Expression is induced by IPTG and driven by the T7 polymerase promoter.

2.2.4 Identification of *Malus x domestica* (Royal Gala apple) *DELLA* and *GID* orthologues and obtaining complete mRNAs

The Plant & Food Research *Malus domestica* sequence and EST database (Crowhurst et al., 1999-2011) was searched using BLAST with the *Arabidopsis* sequences from the conserved DELLA and TVHYNP motifs (of the N-terminal domain) and the C-terminal domain for orthologous apple sequences (Altschul et al., 1990). Six different *MdDELLA* sequences, three *MdGID1* and two *MdGID2*/ *MdSLY1* CDSs were identified. Three of the *MdDELLA* EST recombinant clones contained truncated CDSs. The missing ends were obtained using 5' and 3' rapid amplification of cDNA ends (RACE) according to the manufacturer's instructions (Life technologies, USA). Oligonucleotides are listed in Table 2.2.

The GenBank accession numbers for the DELLA genes *MdRGL1a*, *MdRGL1b, MdRGL2a*, *MdRGL2b*, *MdRGL3a*, and *MdRGL3b* are: DQ007883 to DQ00888 and the Malus GDR (Genome database for Rosaceae) protein accession numbers are: MDP0000237978, MDP0000640034, MDP0000181482, MDP0000669451, MDP0000662303 and MDP0000134341 respectively.
The Malus GDR protein accession numbers for MdGID1a, MdGID1b and MdGID1c are: MDP0000445131, MDP0000929994 and MDP0000319301 respectively.
The Malus GDR protein accession numbers for MdGID2a, MdGID2b and MdSNE are: MDP0000126528, MDP0000243435, MDP0000181892 respectively.

Total RNA was extracted from Royal Gala shoot tips using RNeasy Plant Mini kit (Qiagen GambH, Germany). First-strand cDNA was synthesised from 1 µg of total RNA, using Moloney murine leukemia virus (M-MLV) reverse transcriptase and a poly-dT primer for one hour at 37 ^{o}C. Full length cDNAs were then amplified from first strand cDNA using HiFi Taq polymerase and gene specific 5'/3' primers based on the 5'/3' RACE products. Products were cloned using a TA cloning kit (Life technologies, USA) and sequenced.

2.2.5 Degenerate primer design for identification of apple DELLA orthologues

To identify potential apple DELLA proteins in addition to those found in the Plant & Food Research database, degenerate oligonucleotides were designed from alignments of DELLA sequences using the Consensus-Degenerate Hybrid Oligonucleotide Primers (CODEHOP) programme (Rose et al., 1998).

Block Maker (Henikoff et al., 1995) calculated the alignments of amino acid sequences of known *Md*DELLA sequences and also the amino acid alignments of combined sequences from *Arabidopsis thaliana* DELLAs and *Md*DELLAs through the web based programmes at http://bioinformatics.weizmann.ac.il/blocks/blockmkr/www/make_blocks.html and http://bioinformatics.weizmann.ac.il/blocks/codehop.html.
The amino acid sequence alignments were inputted into the CODEHOP programme according to the programme instructions. The oligonucleotides produced are composed of a nondegenerate 5' portion (the clamp) and a degenerate 3' portion. Two levels of degeneracy were selected for use in the 3' portion. The oligonucleotides, CODEHOP 1 through 8, are listed in Table 2.2.

Degenerate primers were also designed without using CODEHOP based on the DELLA nucleotide alignments obtained using the ClustalW algorithm within the Vector NTi software package (Life technologies, California, USA). The primers, *Md*DELLA universal-1 for and rev, *Md*DELLA universal-2 for and rev, *Md*DELLA-not L3 for and rev (listed in Table 2.2).

For preparation of DNA, *Malus domestica* Pacific Rose apple young leaf tissue was harvested into liquid nitrogen and ground with mortar and pestle. Genomic DNA was prepared (DNeasy plant, Qiagen GambH, Hilden, Germany) according to the manufacturer's instructions. Possible *Md*DELLA orthologues were amplified by PCR and the products were separated by agarose gel electrophoresis, isolated using minElute gel extraction kit (Qiagen GambH, Hilden, Germany) and cloned into pGEM-T easy (Promega, Madison, Wisconsin, USA) or pCR-blunt II TOPO (Life technologies, California, USA) vectors for sequencing.

2.2.6 Identification of *Actinidia deliciosa* (Hayward kiwifruit) DELLA and *GID* orthologues and obtaining complete mRNAs

The Plant & Food Research *Actinidia* sequence and EST database (Crowhurst et al., 1999-2011) was searched using BLAST for orthologous sequences to coding sequences (CDSs) of known DELLA proteins (Altschul et al., 1990). For several mRNAs the 5' portion of the CDS was missing from the database, hence the rapid amplification of cDNA ends (RACE) was used to recover the 5' portions of the CDSs and mRNA (Frohman et al., 1988). *Actinidia deliciosa* (Hayward kiwifruit) tissue was picked directly into liquid nitrogen and stored at -80 °C. Total RNA was extracted from *Actinidia deliciosa* tissue using RNeasy Plant kit according to the

manufacturer's instructions (Qiagen GambH, Hilden, Germany) and quantified by spectrophotometry (Biophotometer, Eppendorf AG, Hamburg, Germany). First strand cDNA synthesis was performed on 5 µg total RNA using the gene-specific antisense primer 1 (GSP1). The cDNA was purified and dC-tailed before PCR amplification with Taq DNA polymerase (Life technologies, California, USA) using GSP2 primer and the Abridged anchor primer from the kit, according to manufacturer's instructions (5' RACE system, Life technologies, California, USA). A schematic representation of this method is shown in Figure 2.2. A gene-specific antisense primer (GSP1), complementary to known 3' portion of the EST sequence from the database was used to prime cDNA synthesis. A poly-C tail was synthesised at the 5' end of the synthesised cDNA to serve as an "anchor" site for amplification of the cDNA. This tailed cDNA is amplified by PCR, using a poly-G forward primer (complementary to the cDNA poly-C tail) and a nested gene-specific primer (GSP2) that is more proximal to the 5' region than GSP1. The sequences of primers are listed in Table 2.2.

The primers used were 101189 GSP1 and 2, 49556 GSP1 and 2, 287619 GSP1 and 2 and 2a, 200355 GSP1 and 2, SLY GSP1 and 1 and 2a (Table 2.2). Amplification products were separated by agarose gel electrophoresis; dominant DNA bands were isolated with minElute gel extraction kit (Qiagen GambH, Hilden, Germany). DNA fragments were cloned into pGEM-T easy vector (Promega, Madison, Wisconsin, USA) for sequencing. The sequences of the CDSs were submitted to the GenBank using the BankIt tool. The GenBank accession numbers for *A. deliciosa* DELLA genes *AdRGL1a*, *AdRGL1b*, *AdRGL1c*, *AdRGL2a*, *AdRGL2b*, *AdRGL3a*, and *AdRGL3b* CDSs are KF588651 to KF588657 respectively. The accession numbers of the *A. deliciosa GID1* homologues *AdGID1a*, *AdGID1b* and *AdGID1c* are KF588661, KF588662 and KF588663 rspectively. The accession numbers for the *A. deliciosa SLY1/ GID2* homologues *AdSLY1/7*, *AdSLY1/8* and *AdSLY1/12* are KF588658, KF588659 and KF588660 respectively.

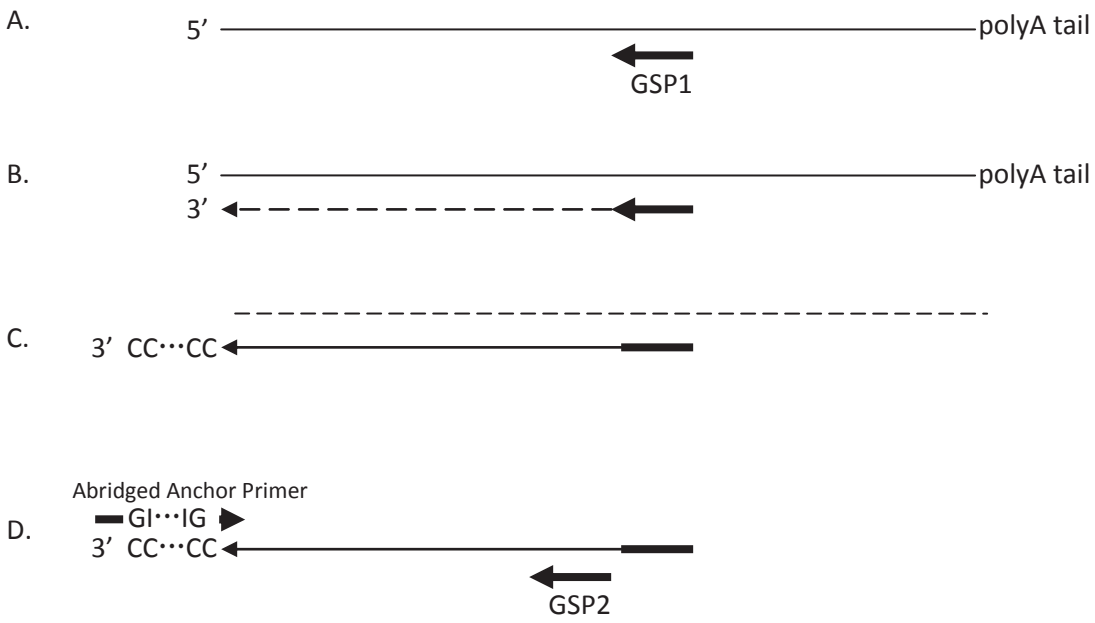

Figure 2.2. 5’ RACE procedure and the principle of anchored PCR
A schematic diagram representing the main steps involved for the amplification and future sequence determination of an unknown 5’ mRNA sequence, using a single known 3’ sequence.
A, and **B**, representation of a single mRNA species within a pool of possible targets and the first strand synthesis (reverse transcription) of cDNA, primed from GSP1, a gene-specific antisense primer. Note that this experiment used total RNA as a starting point.
C, RNA is degraded with RNases H and T1 and a 3’ polyC tail is synthesised through the action of the enzyme Terminal deoxynucleotidyl transferase on to the cDNA.
D, PCR amplification with a nested gene specific (GSP2) primer and the Abridged Anchor primer that is complementary to the 3’ tail of cDNA.

2.2.7 Plasmid constructs

All bacterial and binary plasmid constructs used in this thesis are detailed in Table 2.3 and the oligonucleotides are listed in Table 2.2.

AtRGL2 (At3g03450) transgene cassette contained the coding sequence (CDS) of *Arabidopsis thaliana RGL2* (this and other DELLA genes do not contain introns). The cassette also contained 1.8 kb of DNA upstream of the *RGL2* coding sequence (including the promoters) and 2.2 kb of DNA downstream of the *RGL2* coding sequence, altogether 5.5 kb. The chromosomal segments corresponding to upstream, coding and downstream region were PCR amplified separately from *Arabidopsis thaliana* Landsberg *erecta* (L*er*) genomic DNA using three pairs of primers: RGL2-prom for and rev, RGL2 for and rev, RGL2-term for and rev, all listed in Table 2.2. The obtained amplicons were cloned into pGREEN II-0229. A novel combination tag (TAPR) was constructed by modifying the published TAP tag (Rohila et al., 2004, Rigaut et al., 1999). For construction of the N-terminal or C-terminal TAPR tag, synthesised oligonucleotides TAP1 through 6 were annealed to the 5' or 3' end, respectively, of amplified and phosphorylated *AtRGL2* CDS.

The β-D-glucuronidase (Gus) gene (*uidA*) from *E. coli* was amplified from pRT99 Gus plasmid using primers *uidA* for and rev.

Expression constructs of *Actinidia deliciosa* DELLA proteins (AdDELLAs) were constructed by inserting the full-length CDSs into the pETM-MBP R vectors. The full-length CDSs were amplified using *Actinidia deliciosa* genomic DNA as a template (DELLA genes have no introns). The primers used for CDS amplification were: 101189 pETM for and rev, 113002 pETM for and rev, 115865 pETM for and rev, 227790 pETM for and rev, 49556 pETM for, 79743 pETM for, 49556/79743 rev, 78609 for and rev (Table 2.2). Expression constructs were made in pETM backbone vectors as described (Sun et al., 2008).

Apple *MdRGL2a* full length CDS was RT-PCR amplified from total RNA prepared from apple shoot tips (RNeasy plant, Qiagen GambH and Superscript II, Life technologies, USA). The amplified fragment was separated by agarose gel electrophoresis, isolated with minElute gel extraction (Qiagen GambH) and restriction digested Bam HI/ XbaI (New England Biolabs) for cloning into pART 7. The construct was moved by Not I restriction into Ti binary vector pART 27 (Gleave, 1992b) for plant transformation (see section 2.2.11).

All constructs were confirmed by dideoxynucleotide sequencing (Institute of Molecular Biosciences Genome Services, Massey University, Palmerston North, New Zealand).

Table 2.3. Plasmid Constructs

Name	Description	Reference
pETM MBPR	*E. coli* expression vector; Kan^R, T7 promoter, N-terminal MBP protein fusion, MCS, and C-terminal R-tag peptide fusion	Modified from EMBL, Heidelberg, Germany, this study.
pGREEN II-0229	Ti Binary vector; Kan^R, T-DNA bordered cassette containing *Bar* and MCS	(Hellens et al., 2000)
pSOUP	Helper plasmid for pGREEN II *in A. tumefaciens*; Tet^R	(Hellens et al., 2000)
pART 7	Stepwise construction vector; Amp^R, 35Spromoter-MCS-*ocs* 3'. Excise and clone Not1 to pART27	(Gleave, 1992a)
pART 27	Ti Binary vector; Str^R, T-DNA bordered cassette containing Not1 RE site and Kan^R	(Gleave, 1992a)
pGEM-T easy	*E. coli* plasmid for cloning of PCR products with A overhangs, supplied in a linearised form with 3'-T overhangs; Amp^R, *LacZ*, MCS	Promega, Wisconsin, USA
pCR-blunt IITOPO	*E. coli* plasmid for cloning of PCR products with blunt ends, supplied in a linearised form with blunt ends; Kan^R, *LacZ*, MCS	Life technologies, California, USA
pPMB 4087	*101189*[a] *Ad*DELLA[b] in pETM-MBP R, Kan^R	This study
pPMB 4090	*113002 Ad*DELLA in pETM-MBP R, Kan^R	This study
pPMB 4088	*115865 Ad*DELLA in pETM-MBP R, Kan^R	This study
pPMB 4097	*227790 Ad*DELLA in pETM-MBP R, Kan^R	This study
pPMB 4091	*49556 Ad*DELLA in pETM-MBP R, Kan^R	This study
pPMB 4089	*78609 Ad*DELLA in pETM-MBP R, Kan^R	This study
pPMB 4092	*79743 Ad*DELLA in pETM-MBP R, Kan^R	This study
pPMB 0402	*RGL2prom-RGL2*-TAPR tag-*RGL2term* :: pGREENII-0229	This study
pPMB 0389	*RGL2prom-UidA*-TAPR tag-*RGL2term* :: pGREENII-0229	This study
pPMB 4033	*RGL2prom*-TAPR tag-*RGL2-RGL2term* :: pGREENII-0229	This study
pPMB 0260	*MdRGL2a*::pART7	(Foster et al., 2007)
pPMB 0261	*35Sprom-MdRGL2a-OCS 3'*::pART27	(Foster et al., 2007)

[a]EST number as designated by the Plant & Food Research *Actinidia* EST database
[b]AdDELLA, *Actinidia deliciosa* DELLA orthologues.

2.2.8 Apple sample collection, RNA preparation and qPCR

Samples were collected from Royal Gala and Pacific Rose mature trees at midday and immediately frozen in liquid nitrogen. The tissues that were collected from Royal Gala in early summer were: arrested buds (these are expected to be floral), growing shoot tips and expanding leaves. The tissues from Pacific Rose that were collected in autumn were arrested terminal buds. These buds were expected to be either vegetative or floral, depending on the tree cycle. Pacific Rose is a biennial bearing cultivar, with alternating floral and vegetative years, and the trees are in a known cycle prior to collection. Seeds were vernalised, and imbibed for either 3 or 8 days prior to sample freezing. Vernalisation was for 8 weeks at 4 ^{o}C.

Total RNA was extracted from 100 mg tissue (RNeasy, Qiagen GambH, Germany). Reverse transcription synthesis was performed using M-MLV enzyme and primed with a poly-dT primer. 1 µL of the cDNA sample was used as a template for the real-time PCR, using the LightCycler fast start DNA master SYBR I green kit in the LightCycler real-time thermocycler (Roche GambH, Germany).

The primers for detecting transcripts of *MdRGL1b*, *MdRGL2b*, *MdRGL3b* and *MdGAPDH* are listed in Table 2.2. Primers were used at 1 µM each in a 10 µl reaction volume. PCR parameters were: initial denaturation at 95 ^{o}C for 10 min then 40 cycles of 95 ^{o}C 10 s, 68 ^{o}C 5 s, 72 ^{o}C 10 s (annealing temperature was 60 ^{o}C for *MdGAPDH* primers). Each PCR product was analysed by agarose gel electrophoresis and the melting curve was examined to verify the presence of a single amplicon of the correct size. Every mRNA of interest was quantified by a separate experiment. To eliminate variation due to the differences in total mRNA amount in the samples, the *MdDELLA* mRNA copy number was normalised to that of *MdGAPDH*, which is relatively constant in all tissue types and developmental stages (Iskandar et al., 2004). A preliminary analysis indicated that the expression level of the a/b gene pairs was very similar. Therefore, due to the limited amount of RNA samples, quantification of only the “b” gene was carried out in triplicate.

2.2.9 *Actinidia deliciosa* tissue collection, mRNA preparation, reverse transcription and qPCR

Actinidia deliciosa (Hayward kiwifruit) tissue was picked between 1 and 3 pm directly into liquid nitrogen and stored at -80 °C. The samples of different biological replicas were collected

on different days; dormant buds 36 days apart, breaking buds 6 days apart, expanding leaves 38 days apart, shoot tips 7 days apart, male floral buds 20 days apart, female floral buds 20 days apart, styles (female flower) 12 days apart, and fruit cortex 18 days apart. Also, they were collected from different vines, albeit from the same row of vines in the orchard.

2.2.9.1 Quality controls in qPCR

To ascertain that the RNA template for qPCR was of sufficient integrity across the set of samples prepared from a range of tissues and to monitor the level of genomic DNA (gDNA) contamination, the total RNA preparations were analysed by capillary electrophoresis using the Agilent 2100 Bioanalyzer (Figure 2.3). This analysis showed that the RNA was of very good quality, giving RIN scores within recommended range (> 8.0) and showing minimal genomic DNA contamination. However, after experimentation it was decided to prepare mRNA directly from the study tissues and use as the template for the reverse transcription (RT) for qPCR experiments. The mRNA was prepared directly from tissues using poly-dT magnetic beads as per the manufacturer's instructions (mRNA direct, Life technologies, USA) and quantified by fluorometry (Qubit, Life technologies, USA). A total of 20 ng mRNA per RT reaction was found to be sufficient amount of template yielding acceptable quantitation cycle values (or crossing points (Cp)) in the mid-section of the amplification cycle count.

Contaminating genomic DNA (gDNA) was removed using DNase I, and was controlled for in the qPCR analysis by using a non-reverse transcribed RNA template in the PCR reactions. It was found that, although complete elimination of gDNA was not possible, the levels were low enough to not contribute significantly to the signal generated from mRNA as a template. A cut-off point for the acceptance of data for analysis was set at eight cycles. Such that, if the difference in the quantitation cycle (Cp) values between the 'no-reverse transcription' (no-RT) control and RT experimental data was greater than eight then the Cp data was accepted to originate primarily from the mRNA, and not from a contaminating gDNA amplicon. These eight cycles represent a 256-fold difference (2^8, efficiency of amplification raised by cycle number) or 1/256, or 0.4 % template contribution coming from the gDNA contamination.

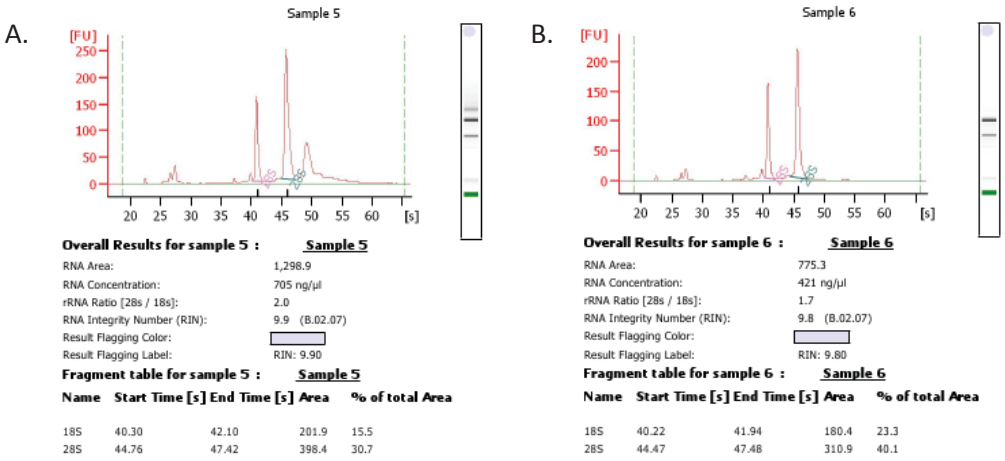

Figure 2.3. Bioanalyzer RNA integrity data
An example of the data generated from the Aligent 2100 Bioanalyzer. In this example the total RNA preparation is from *A. deliciosa* expanding leaves.
A, Before DNase I treatment. **B,** After DNase I treatment.
16S and 28S RNA peaks labelled, and a ratio calculated. The third peak (of higher molecular weight) detected in the electrophoresis seen only in A., represents DNA contamination of the RNA preparation. The RIN number given would be considered very good for all experimentally confirmed tissues.

Reverse transcription (RT) was performed on 200 ng of kiwifruit mRNA and a 10 pg control spike of Brome Mosaic Virus RNA (BMV *RNA3a*; Genbank accession number J02042.1) and on 'No RNA' control (Baltimore, 1970). 'No RT enzyme' control reactions were also performed on 200 ng kiwifruit mRNA and 10 pg BMV RNA. Reactions were incubated according to the manufacturer's instructions (Transcriptor first strand cDNA synthesis kit, Roche GambH, Germany). Conditions were: RNA and oligo dT preincubation of 65 °C for 10 minutes before RT enzyme and dNTPs were added and incubated at 55 °C for 30 minutes. A final enzyme denaturing step of 5 min at 85 °C was included.

A volume of 1 µL from the reverse transcription and control reactions was used in each qPCR reaction, according to the manufacturer's instructions. Primers were used at 500 nM each in a 20 µL reaction volume (Lightcycler 480 system, SYBR green I master, Roche GambH, Germany)(Zipper et al., 2004). Conditions for the real-time PCR are given in Table 2.4.

Throughout quantification, plate to plate variability was controlled by including, in each qPCR plate, an identical aliquot of a single identical stock of reverse-transcribed RNA. As the input template is exactly the same in each case, variability in the PCR reaction is detected. The plate-to-plate variation was very low. Plate set-up is shown in Figure 2.4.

The reverse transcription reaction can introduce substantial variation into a qPCR amplification result. This was controlled for by maintaining a standardised method for quantification of the mRNA template (picoGreen) and using the same quantity of mRNA (20 ng), and the same priming strategy (poly T only) in each reaction. The reaction-to-reaction variation was also minimised by using the same batch of dNTPs and reverse transcriptase enzyme throughout the experiment.

As the amplicon positions on the target transcripts were located at various distances from the poly-T priming point, the full progression of the reverse transcriptase enzyme along a transcript was confirmed by using two priming sites one kilobase apart, in the 5'-terminal and 3'-terminal positions within the ACTIN2/7 transcript.

A control spike of 10 pg of BMV (Brome Mosaic Virus) RNA (gene *3a*, Genbank accession number J02042.1; Appendix Figure 6.2) was introduced into each reverse transcription reaction to control for inhibition of the reaction by any unforeseen mechanism and from contamination with unknown metabolites within the RNA template preparations which could

have been different in different tissues. Substantial variation of tissue-to-tissue inhibition was found and controlled for by the qPCR analysis programme QPCR (Hellemans et al., 2007, Pabinger et al., 2009), through normalisation.

	1	2	3	4	5	6	7	8	9	10	11	12
A	PP2A reference a	PP2A reference b	PP2A reference c	49556 Target a	49556 Target b	49556 Target c	SLY 12 Target a	SLY 12 Target b	SLY 12 Target c	PP2A No RT	ACTIN C No RT	79743 No RT
B	UPL7 reference a	UPL7 reference b	UPL7 reference c	78609 Target a	78609 Target b	78609 Target c	BMV Standard a	BMV Standard b	BMV Standard c	UPL7 No RT	ACTIN N No RT	200355/4 No RT
C	ACTIN C reference a	ACTIN C reference b	ACTIN C reference c	79743 Target a	79743 Target b	79743 Target c	PP2A Calibrator a	PP2A Calibrator b	101189 No RNA	SLY 7 No RNA	101189 No RT	287619/17 No RT
D	ACTIN N reference a	ACTIN N reference b	ACTIN N reference c	200355/4 Target a	200355/4 Target b	200355/4 Target c	UPL7 Calibrator a	UPL7 Calibrator b	113002 No RNA	SLY 8 No RNA	113002 No RT	287619/22 No RT
E	101189 Target a	101189 Target b	101189 Target c	287619/17 Target a	287619/17 Target b	287619/17 Target c	ACTIN C Calibrator a	ACTIN C Calibrator b	115865 No RNA	SLY 12 No RNA	115865 No RT	SLY 7 No RT
F	113002 Target a	113002 Target b	113002 Target c	287619/22 Target a	287619/22 Target b	287619/22 Target c	ACTIN N Calibrator a	ACTIN N Calibrator b	227790 No RNA	200355/4 No RNA	227790 No RT	SLY 8 No RT
G	115865 Target a	115865 Target b	115865 Target c	SLY 7 Target a	SLY 7 Target b	SLY 7 Target c	UPL7 No RNA	ACTIN C No RNA	49556 No RNA	287619/17 No RNA	49556 No RT	SLY 12 No RT
H	227790 Target a	227790 Target b	227790 Target c	SLY 8 Target a	SLY 8 Target b	SLY 8 Target c	PP2A No RNA	79743 No RNA	78609 No RNA	287619/22 No RNA	78609 No RT	BMV No RT

Figure 2.4. qPCR Plate set up
qPCR experimental plate loading setup as a gene maximisation approach. All plates in the experiment were set up in an identical fashion. Each plate quantified a single tissue's mRNA for all analysed genes and contained all controls (except for the calibrator wells; see below).
Grey, the 4 reference gene amplicons (3 different genes), in technical triplicates. **Blue**, the target amplicons: 7 *AdDELLA*, 3 *AdGID1* and 3 *AdSLY1*, in technical triplicates. **Red**, the RNA Brome mosaic virus spike, in technical triplicate. **Yellow**, the experimental plate calibration wells (4 amplicons), in technical duplicates. **Green**, the negative controls; **pale green** is the 'no template' control, **bright green** is 'no-reverse transcriptase' control, in technical duplicates.
The template in each well of the plate, except for the **yellow** wells, is from one preparation and cDNA synthesis of a tissue type. The **yellow** wells contain template cDNA is from a single preparation, run on all plates (expanding leaf mRNA). The same preparation was aliquoted and stored for use on each of the 16 plates in the experiment. The **red** wells contained an additional RNA spike, into the plate tissue RNA, prior to the synthesis to cDNA.

The primers used were G05 and G06 (for amplification of *AdPP2A*), G07 and G08 (for amplification of *AdUPL7*), G09 and G10 (for amplification of *AdACTIN7* 3' amplicon), G11 and G12 (for amplification of *AdACTIN7* 5' amplicon), D05 and D06 (for amplification of *AdRGL1a*), E01 and E02 (for amplification of *AdRGL1b*), C11 and C12 (for amplification of *AdRGL1c*), A03 and A04 (for amplification of *AdRGL2a*), A11 and A12 (for amplification of *AdRGL2b*), C02 and C03 (for amplification of *AdRGL3a*), B05 and B06 (for amplification of *AdRGL3b*), E11 and E12 (for amplification of AdGID1a), E07 and E08 (for amplification of *AdGID1b*), F03 and F04 (for amplification of *AdGID1c*), F11 and F12 (for amplification of *AdGID2a*), F07 and F08 (for amplification of *AdGID2b*), G03 and G04 (for amplification of *AdGID2c*), BMV for and rev, and are listed in Table 2.2. Oligonucleotides for qPCR and 5' RACE were screened for through Primer3 software: http://frodo.wi.mit.edu/primer3/ (Rozen and Skaletsky, 1999). Reference genes for qPCR; *PP2A*, *UPL7* and *ACTIN7* were used on the basis of findings in (Czechowski et al., 2005).

Table 2.4. Conditions for the real-time PCR

	Temperature (°C)	Acquisition mode	Hold (Min : sec)	Ramp rate (°C /second)	Acquisitions per °C
Pre-incubation	95	None	10:00	4.4	-
Amplification	95	None	00:10	4.4	-
	59	None	00:00	2.2	-
	72	Single	00:06	4.4	-
Melting curve	95	None	00:05	4.4	-
	65	None	01:00	2.2	-
	97	Continuous	-	-	5
Cooling	40	None	00:10	1.5	-

2.2.10 *Arabidopsis* growth

All *Arabidopsis thaliana* lines used are listed in Table 2.5. *Arabidopsis thaliana* seeds were stratified at 4 °C for 4 days in water except for *ga1-3* mutants for which water was supplemented with 100 µM gibberellin A3 (GA3). The stratified seeds were transferred to moistened seed-raising mix for germination. Plants were grown in a glasshouse in soil under long-day conditions of 16 hour light and 8 hour dark cycle (approximately 1000 to 15 000 lux) at 22°C.

2.2.11 Plant transformation

Recombinant plasmids derived from the plant transformation binary vectors pART 27 or pGREEN II and helper plasmid pSOUP were introduced into *Agrobacterium tumefaciens* strains LBA4404 or GV3101 by electroporation. Clonal-purified transformants were grown over-night at 28 °C in 10 mL YEB supplemented with appropriate antibiotics. Following centrifugation, the *Agrobacterium* cell pellet was resuspended in 5 % sucrose and 0.02 % v/v Silwet L-77 (Lehle seeds, Round Rock, USA). *Arabidopsis thaliana* plants (lines listed in Table 2.5 and appropriate Results section) were transformed by conjugation, using *Agrobacterium* containing the plasmid constructs as a donor, by the floral dip method (Clough and Bent, 1998). The plants were dipped 3 times over 6 days and were initially at an unopened inflorescence stage. The transgenic plants were selected in soil by spraying seedlings at a four leaf stage with 20 mg/L glufosinate ammonium (*DL*-Phosphinothricin) or 50 mg/L kanamycin. The *ga1-3* line spraying solution also contained 100 µM GA3 to allow plants to flower successfully.

The *Arabidopsis* plant transformation of the apple transgene was carried out at Plant & Food Research Mt. Albert facility. Plants of T_3 and subsequent generations from the viable progeny of recovered kanamycin resistant transgenic plants were examined for the presence of transgenic cassette.

Table 2.5. *Arabidopsis* line genotypes

Genotype	Background	Reference
Wild type, L*er*	Landsberg-*erecta*	-
Wild type, col-0	Columbia	-
ga1-3	Landsberg-*erecta*	(Koornneef and Veen, 1980)
rgl2-1	Landsberg-*erecta*	(Lee et al., 2002b)
ga1-3, *gai-t6*, *rga-t2*, *rgl1-1*, *rgl2-1* (*Δglobal*)	Landsberg-*erecta*	(Cao et al., 2005)
gai-t6, *rga-t2*, *rgl1-1*, *rgl2-1* (*Δquad*)	Landsberg-*erecta*	(Achard et al., 2006)

2.2.12 *Arabidopsis* DNA extraction and transgene confirmation

Arabidopsis thaliana leaf tissue was punched out by closing a 0.5 mL microcentrifuge lid on leaf tissue. The leaf disc fell directly into the DNA extraction buffer. Tubes were stored on ice until all samples were collected. The DNA was isolated using the sucrose preparation method (Berendzen et al., 2005). The transgenic cassette inserted into the *A. thaliana* genome was detected by diagnostic PCR in which one primer was complementary to the non-*Arabidopsis* portion of the construct, the TAPR tag, and the second primer was complementary to the *AtRGL2* CDS or 3' untranslated 'terminator' sequences. The *BAR* gene encoding the selective marker was also PCR amplified from each plant. The oligonucleotides used were N-TAP transgene for, N-*RGL2* transgene rev, C-*RGL2* transgene for, *RGL2*-term transgene rev, *BAR* transgene for and rev, all listed in Table 2.2. No transgenes were identified for transgenic cassettes containing the 35S CaMV promoter. Transgenes containing cassettes: *RGL2prom-UidA-TAPR tag-RGL2term (UidA-TAPR), RGL2prom-TAPR tag-RGL2-RGL2term (TAPR-AtRGL2)* and *RGL2prom-RGL2-TAPR tag-RGL2term (AtRGL2-TAPR)* were obtained successfully in *A. thaliana ga1-3* and *Δquad* mutants, and were used in further analysis. The remaining transgenic constructs were not further transformed or analysed.

For quantification of *MdRGL2a* transcript in the transgenic *A. thaliana* lines, total RNA was extracted from leaves of mature *Arabidopsis* plants, the first strand cDNA synthesis carried out and transgene expression levels were analysed by quantitative real-time PCR as described in section 2.2.8. The *MdRGL2a*-specific primers are in Table 2.2. In this experiment, *MdRGL2a* cDNA levels were normalised relative to *AtACTIN* cDNA. Phenotypic analysis was performed on T_3 and subsequent generations. For analysis of leaf size and plant height, plants were grown for 25 days in long-day conditions (16 hr light/ 8 hr dark), one plant per pot. Plant height was measured along the primary inflorescence axis and the maximum rosette diameter was measured for 10-20 plants per line. Plants were grown in 8 hr light/16 hrs dark to determine time to flowering in short-day (SD) conditions. Flowering was scored when petals were first visible.

2.2.13 *Arabidopsis* protein extraction

Inflorescence tissue of 4-5 week old *A. thaliana* was plucked with forceps, immediately frozen in liquid nitrogen and stored at -80 °C. Frozen tissue was subsequently crushed using the rolling pin method in ice-cold extraction buffer [100 mM phosphate buffer pH 7.4 (77 mM

Na_2HPO_4, 23 mM NaH_2PO_4), 140 mM NaCl, 1 mM EDTA, 5 mM 1,4-Dithiothreitol (DTT), 20 µM MG132, 1% w/v n-Dodecyl β -D-maltoside (DDM), 1X Complete™ protease inhibitors] at a ratio of 2 to 3 µL per mg of tissue. Buffer-insoluble proteins and plant debris were removed by centrifugation at 20,000 x g for 30 min at 4 °C. The supernatant, containing buffer-soluble extracted proteins, was stored at -80 °C until use.

2.2.14 *GUS* reporter gene activity staining

Inflorescence tissue of 4 to 5 week old transgenic *Arabidopsis* containing the pRGL2-*UidA*-TAP (pPMB 0389) construct were plucked with forceps into microcentrifuge tubes in an ice bath until all samples were collected. The tissue was washed with the stain buffer prior to incubation in stain solution [100 mM phosphate buffer pH 7.2 (68 mM Na_2HPO_4, 32 mM NaH_2PO_4), 1 mM potassium ferrocyanide, 1 mM potassium ferricyanide, 0.05 % Triton X-100, 2 mM X-Gluc]. The stain solution was infiltrated into the tissue under low vacuum for 15 min, and then incubated over-night at 37 °C. The stain solution was then removed and the tissue equilibrated with and ethanol series; 20 %, 35 % and 50 % for 30 min each. The tissue was fixed with FAA (50 % ethanol, 10 % glacial acetic acid, 5 % formaldehyde) for 30 min before storing the tissue in 70 % ethanol and/ or examination of the reporter signal.

2.2.15 Monoclonal antibodies

Anti-DELLA monoclonal antibodies (mAbs) were developed and supplied by William Jones, Plant and Food Research, New Zealand (Sun et al., 2010). The mouse mAbs: BC9, AD7, and BB7 were raised against recombinant N-terminal domains of *Arabidopsis thaliana* DELLA proteins. The mouse monoclonal antibodies 5E1 and 6C8 were raised against a synthetic peptide, DELLAVLGYK (mAbs 5E1 and 6C8) and mAb G10 against the C-terminal conserved motif CPYLKFAHFTANQ .

Monoclonal antibody D9 specific for the R-tag (Section 2.2.3) was raised against a synthetic peptide that does not occur in plants (Jones et al., 2007).

2.2.16 Immunoprecipitation

Direct, indirect and on-column immunoprecipitation were used to immunoprecipitate DELLA proteins using cognate monoclonal antibodies. In direct immunoprecipitation, mAb were covalently attached to the surface of superparamagnetic iron oxide-dextran beads (Miltenyi et al., 1990). First, dextran on the surface of the beads was activated by incubation with

cyanogen bromide (BrCN) and reacted with an excess of 1, 6-diaminohexane to form amide bonds with one of the diaminohexane amino groups. The second amino group of the diaminohexane is reacted with a succinamidyl ester group of the hexan linker *N*-(e-maleimidocaproyloxy) succinimide ester (EMCS). The maleimidyl group was reacted with monoclonal antibodies which had been reduced with 2-mercaptoethanolamine.HCl (2-MEA) to form a thioester covalent attachment. After antibody conjugation the beads were magnetically separated from the solution in a MS column (Miltenyi Biotech GmbH, Bergisch Gladbach, Germany), washed to remove unreacted components and suspended in PBS in the absence of magnetic field. Absorbance of the antibody-conjugated beads was read at 450 nm (UV-1201 spectrophotometer, Shimadzu Corp., Kyoto, Japan) to determine their density. The bead density was adjusted to OD_{450}=10 with PBS and stored at 4 °C in the dark. Before usage in immunoprecipitation experiments mAb-conjugated beads were washed with buffer used for preparation of plant protein (plant protein extraction buffer) on µMacs columns, then incubated with plant protein extract at 4 °C for 4 h. The beads were magnetically immobilised on a µMacs column and washed repeatedly with degassed extract buffer. Beads were recovered in minimal volume of extract buffer by removing the column off the magnet. The beads were then mixed with SDS sample buffer (25 mM Tris-HCl pH 6.8, 10 % v/v glycerol, 1 % w/v SDS, 15 mM DTT, 0.05 % w/v bromophenol blue) and non-covalently bound proteins were eluted by heating at 100 °C for 5 min.

For indirect immunoprecipitation, beads with immobilised secondary antibodies (rat anti-mouse IgG1) were used to capture mAb-antigen complexes. To obtain these complexes, mAbs against DELLA proteins were incubated at 4 °C with plant protein extract for 30 minutes before the addition of M-450 rat anti-mouse IgG1 beads (Life technologies, California, USA) and incubated for a further 30 minutes. The beads were washed 3 times with extraction buffer on the magnetic particle concentrator for microcentrifuge tubes (MPC-E; Life technologies, California, USA). They were then mixed with SDS sample buffer and heat-denatured at 95 °C for 5 min.

For on-column (pull-down) immunoprecipitation, mAb D9 (anti-R tag) was immobilised on a HiTrap™ NHS-activated column (GE Healthcare, Pennsylvania, USA) via amino covalent linkage (Jones et al., 2007). Protein extract from transgenic plants expressing RGL2–TAPR tag was loaded onto the column at 1 mL/min and circulated at 4 °C over-night. In this experiment the plant extraction buffer (50 mM Tris-HCl pH 7.4, 140 mM NaCl, 50 mM sodium ascorbate, 1 % w/v DDM, 1X Complete™ protease inhibitor cocktail without EDTA, 20 µM MG132) did not

contain phosphate or EDTA because Ca^{++} was used in later steps. The column was washed with 15 bed volumes of extract buffer before loading with 2 µg/mL rTEV (Tobacco Etch virus) protease and incubating at 4 °C over-night. The column was eluted with 1 bed volume of the Tris-based EDTA-free plant extraction buffer 3 times and the D9 column was regenerated. Eluate was subjected to calmodulin affinity chromatography to further purify the fusion which contained the calmodulin-binding tag. First, 2 mM calcium was added to the eluate and loaded onto a pre-equilibrated calmodulin column (Calmodulin sepharose 4B, GE Healthcare, Pennsylvania, USA) and circulated at 4 °C for 2 hours. The column was washed with 10 bed volumes of plant extraction buffer. Any bound protein was eluted 3 successive times with 1 bed volume of 2 mM EGTA to the plant extraction buffer. Finally, the column was regenerated according to manufacturer's instructions.

Eluted proteins from all immunoprecipitations were separated by SDS-PAGE (10 % acrylamide). Separated proteins were analysed by staining, western blotting and/ or mass spectrometry. For western blotting, proteins transferred to nitrocellulose membrane (Schleicher and Schuell Bioscience GmbH, Dassel, Germany) by electro-blotting and probed using anti-DELLA and anti-R tag mAbs. For mass spectrometry, protein bands were excised from acrylamide gels and processed as described below (section 2.2.20).

2.2.17 Recombinant protein expression

An N-terminal His tag and a maltose binding protein (MBP) tag were fused to kiwifruit DELLA proteins. The fusion proteins were expressed and purified in the pETM-MBP R vector (Section 2.2.3) as previously described (Sun et al., 2008), except that protein expression was induced at 28 °C with 300 µM IPTG for 3 hours. The cells were harvested by centrifugation and stored at -20 °C. Cell pellets were resuspended in ice cold extraction buffer (20 mM Tris/HCl, pH 8.0, 100 mM NaCl, 1 mM EDTA, 1 X Complete™ protease inhibitor cocktail, 20 µM Z-leu-leu-leu-al (MG132)) and lysed by sonication, 10 sec pulses at 4 °C. Fusion proteins were affinity purified using immobilised amylose resin (New England Biolabs, Massachusetts, USA), and concentrated using 10 kDa cut-off Vivaspin centrifugal concentrators (Sartorius, Aubagne, France). Protein concentrations were determined by spectrophotometry (Biophotometer, Eppendorf AG, Hamburg, Germany) using sequence-derived extinction coefficients (Vector NTi, Life technologies, California, USA).

2.2.18 Protein electrophoresis

To prepare samples for denaturing sodium dodecyl sulphate polyacrylamide gel electrophoresis (SDS-PAGE), proteins were denatured by heating at 95 °C for 5 min in the denaturing sample buffer (1 % SDS, 25 mM Tris-HCl pH 6.8, 15 mM DTT, 10 % v/v glycerol, 0.05 % w/v bromophenol blue) and separated by 10 to 15 % w/v acrylamide SDS-PAGE, as previously described (Laemmli, 1970).

Native protein samples were separated by using; blue-native PAGE on 4-12 % w/v acrylamide gradient gels (Life technologies, California, USA) (Wittig et al., 2006), or high-resolution clear native electrophoresis (hrCNE) (Wittig et al., 2007) on 4-12 % w/v gradient polyacrylamide gels. Alternatively, proteins were separated by the native glycine buffer acrylamide electrophoresis (100 mM Tris / 100 mM glycine 7.5 % w/v (Reid and Bieleski, 1968).

Proteins were isoelectrically focused (IEF) (O'Farrell, 1975) on a 7cm pH 3-6 ReadyStrip™ immobilised pH gradient (IPG) strip using the Protean® IEF cell (Bio-Rad, California, USA) according to the manufacturer's instructions.

Native proteins were also isoelectrically focused in the liquid-phase in 8 % ampholytes pH 4-6, 25 % v/v glycerol, 1 % w/v DDM, 5 mM EDTA, 5 mM DTT, 1X Complete™ protease inhibitors, 20 µM proteasome inhibitor MG132. Anode buffer for IEF was 0.5 M acetic acid and cathode buffer was 0.5 M ethanolamine. A Rotofor® Liquid-Phase IEF Cell (Bio-Rad, California, USA) was running at 1 W, maximum at 350 V and 10 mA for 3½ hours according to the manufacturer's instructions.

Proteins were detected by staining with coomassie brilliant blue G250 (Life technologies, California, USA), coomassie brilliant blue R or SYPRO® ruby gel stain (Bio-Rad, California, USA).

2.2 19 Western blotting

Western blotting was performed as previously described (Sambrook et al., 1989). Un-stained proteins separated by poly-acrylamide gel electrophoresis were transferred to nitrocellulose membrane (Schleicher and Schuell Bioscience, Dassel, Germany) at 6 °C in transfer buffer (100 mM Tris, 100 mM glycine, 10 % v/v methanol) at 30 V, 45 mA over-night. Membranes were blocked with 5% w/v skim milk powder in phosphate buffered saline (PBS; 8.1 mM Na_2HPO_4,

1.5 mM KH_2PO_4, 137 mM NaCl, 2.7 mM KCl, pH 7.4), supplemented with 0.1 % v/v Tween™-20 (PBST). Membranes were incubated for 1 hour at room temperature with 1 µg/mL primary antibody in blocking buffer. The membrane was rinsed 3 times by MQ water and once in PBS for 5 min. Incubation with horse radish peroxidise-labelled secondary antibodies (Sigma, anti-mouse IgG (Fc) A9309 or (Fab) A2034 at 1:40000 dilution) in blocking buffer. Membranes were washed as above and developed using ECL Advance detection reagent (GE Healthcare, Pennsylvania, USA). Chemiluminescence signal was detected using an Intelligent dark box LAS3000 (Fujifilm, Tokyo, Japan).

2.2.20 Mass spectrometry

Mass spectrometry was performed by Dr. Dave Greenwood, Plant and Food Research, Auckland, New Zealand using the University of Auckland Fourier transform-ion cyclotron resonance (FT-ICR) mass spectrometer (LTQ-FT, Thermo, Massachusetts, USA).
Following immunoprecipitation experiments, protein bands from eluted samples resolved by SDS-PAGE, were visualised with SYPRO® ruby gel stain (Bio-Rad, California, USA) and excised from the SDS-PAGE gels. In-gel tryptic digests were made according to manufacturer's instructions (Sequencing grade Trypsin, Roche, GambH, Penzgerg, Germany). The peptides were separated by reversed phase chromatography on a C-18 stable bond column (Agilent, California, USA) and the eluate was passed directly into the mass spectrometer for electrospray ionisation tandem mass spectrometry (LC-ESI MS/MS). A parallel experiment was performed on each extracted gel band digest whereby for each duty cycle high resolution accurate mass data was obtained in the ICR cell on peptide ions at 100,000 resolution in a full scan from 300-2000 m/z followed by MS/MS in the ion trap on the top 5 ions with dynamic exclusion enabled. An ESI source voltage of 3.8 kV and a capillary temp of 225 °C were used. Peptide mass fragment (MS/MS) data (.RAW files) were analysed using TurboSEQUEST (Thermo, Massachusetts, USA) with a processed FASTA database digested *in silico* with trypsin. Allowance was made for posttranslational modifications for carboxyamidomethylation on cysteine, deamidation on asparagine and glutamine, and oxidation of methionine. A false discovery rate of 1% was considered acceptable.

2.1.21 *A. thaliana* tissue fixation and embedding

In all fixation methods, inflorescence was picked directly into the fixative solution.
For LR White resin (London Resin Co. Ltd., Reading, UK) embedding; inflorescence tissue was fixed in 0.1 % v/v glutaraldehyde with 2 % w/v formaldehyde in PBS using low vacuum

infiltration and incubated at room temperature for 2 h. The fixed tissue was then subjected to a series of ethanol dehydration steps of 10 minutes each, at 25 %, 50 %, 75 %, 90 %, and finally 2 changes of 100 % ethanol, before placing in LR White resin. The LR White resin was changed twice each day, over 2 days before polymerising in gelatine capsules at 60 °C over-night. The gelatine casing was removed and the LR White capsules trimmed with a razor blade down to a pyramid shape, close to the embedded sample. Sections of 0.5 µm thickness were cut by a glass knife on a microtome (Leica ultracut R, Leica mikrosysteme GmbH, Austria). Sections were taken off the knife edge with forceps and floated onto a drop of water on a microscope slide. The water was then evaporated on a heating block at 80 °C to secure the section to the slide. The section was stained with 0.05 % toluidine blue in 100 mM phosphate buffer to monitor sectioning progress through the sample. At the desired point a diamond knife was switched in, replacing the glass knife, then further 0.1 µm or 0.5 µm sections were cut and dried down onto formvar resin coated nickel grids (Agar scientific, England) for the transmission electron microscope (TEM) work or onto Polysine™ microscope slides (Erie scientific company, USA) for light microscopy.

For wax (9:1 ratio PEG 400 distearate : 1-hexadecanol) embedding; inflorescence tissue was fixed in 4 % v/v paraformaldehyde in PBS under low vacuum for 1 hour at room temperature. After fixation the tissue was washed 3 times for 5 minutes each with MTSB buffer [50 mM piperazine-N,N′-bis(2-ethanesulfonic acid) (PIPES), 0.5 mM EGTA, 0.5 mM magnesium sulphate, 9 mM potassium hydroxide] and washed for 15 minutes with PBS. The tissue was dehydrated through a series of ethanol steps, incubated for 1 h each, from 25 %, 50 %, 75 % to 96 % ethanol. Tissue was washed in 96 % ethanol at 37 °C for 10 minutes before the wax infiltration series, starting with 33 % wax (in ethanol) then 50 %, 66 % and 100 % wax at 37 °C, 1 h each. The tissue was transferred with forceps and dispersed evenly over the bottom of a small Petri dish in fresh wax and allowed to solidify at room temperature before incubating at 4 °C for 20 minutes (Paciorek et al., 2006). Wax blocks were trimmed and 8 µm sections were cut through tissue on a microtome (Leica Jung RM2045, Leica mikrosysteme GmbH, Austria). Strips of sections were relaxed by floating on MilliQ filtered water before being lifted onto Superfrost® Plus microscope slides (Erie scientific company, USA) and allowed to dry.

2.2.22 Immunolocalisation

For fluorescent light microscopy (LM), the wax-embedded sections on a microscope slide were encircled using a PAP pen (Daido Sangyo, Tokyo, Japan). Sections were de-waxed by immersion

in 99 % ethanol for 10 minutes before being rehydrated in steps of 10 min each: 90 % ethanol (in water), 50 % ethanol, then to PBS. Slides of sections were incubated with target retrieval solution (Dako Cytomation, USA) at 95 °C for 20 min and allowed to cool naturally to room temperature. They were washed with MQ water, followed by PBS supplemented with 0.1 % Tween™ 20 (PBST) for 5 minutes each. Incubated with Image-iT™ FX signal enhancer (Life technologies, USA) for 30 minutes before reducing non-specific binding with blocker (0.1 % BSA-c™ (Aurion, Wageningen, The Netherlands) in PBST) for 1 hour. Primary antibody (20 µg/mL) was incubated in blocker at 4 °C overnight. Slides were washed 2 times with 1 mL of PBST. Secondary antibody, Alexa 594- or Alexa 488-labelled goat anti-mouse IgG antibody (Life technologies, USA), was used at a dilution of 1 in 20. The slides were incubated in secondary antibody in blocker solution for 1 h and washed as described above. Sections were mounted under a coverslip in prolong gold DAPI (Life technologies, USA) nuclear stain. Immunoprobed sections were viewed with Olympus BX51, Olympus, Tokyo, Japan microscope under appropriate illumination for excitation of the fluorophores used and images were captured with a digital camera.

For transmission electron microscopy (TEM), inflorescence was embedded in LR White resin. The sections were incubated with 50 mM glycine in PBS for 15 minutes. Non-specific binding was blocked with 5% BSA, 0.1 % gelatine (cold water fish skin), 5 % goat serum in PBS (Aurion, The Netherlands) for 30 minutes. Subsequently, sections were subjected to 2 washes with incubation buffer (0.1 % BSA-c™ (Aurion, The Netherlands) in PBS) for 5 minutes each, before incubating with 20 µg/mL primary monoclonal antibody in incubation buffer for 1 hour. The sections were washed 6 times, for 5 min each, in incubation buffer. Sections were then incubated in 1:50 dilution of secondary antibody, goat anti-mouse IgG ultra-small gold (Aurion, The Netherlands) for 2 h. Sections were washed as described above, and subjected to a further 3 washes in PBS (5 min each), followed by post-fixing in 2 % v/v glutaraldehyde in PBS for 5 minutes. Sections were washed twice, 5 min each, in PBS and in MQ water. Silver enhance R-Gent SE-EM (Aurion, The Netherlands) was incubated for 25 min before the final wash series of MQ water for 5 times of 2 minutes each. The grids were allowed to dry and viewed by TEM (CM-10, Philips, The Netherlands) at 60 kV and the images captured by a digital camera.

For (non-fluorescent) light microscopy the LR white embedded sections were subjected to a target retrieval step of either 2M HCl at room temperature for 10 min or 1 mM EDTA pH 8.0 at 95 °C for 20 min or Dako target retrieval solution (a modified 10 mM citrate pH 6.1 buffer) at 95 °C for 20 min. The catalysed signal amplification (CSA) system (DakoCytomation, USA) was

used according to the manufacturer's instructions to visualise any antigen. The section was counter stained with 5 µg/mL Hoechst 33258 and mounted in citifluor AF1 (Citifluor Ltd., UK) under a coverslip.

3. Core Gibberellin signalling components

3.1 Apple proteins involved in gibberellic acid signalling

Apple is an economically important crop worth approximately 400 million dollars for the New Zealand economy each year. To maximise production and fruit quality its development is manipulated, physically through pruning and fruit thinning and chemically through the use of exogenous application of GA or GA inhibitors to synchronise flowering time and enhance fruit development. As DELLA proteins play a significant role in GA regulated processes there is potential that by understanding the functions of apple DELLA proteins it may be possible to screen for cultivars that have reduced requirement for these labour-intensive husbandry practices.

Together with DELLA proteins, two other proteins form the core gibberellin signalling components: the GA receptor (GID1 and GID1-like proteins) and a DELLA-specific F-box protein (GID2 or SLY1 proteins) that take part in ubiquitination and subsequent degradation of DELLA proteins upon reception of the GA signal (Alvey and Harberd, 2005).

3.1.1 Apple DELLA genes identified

The Plant & Food Research *Malus* EST database containing 164, 000 sequences (NB. originally the HortResearch EST database) was searched with the canonical domain I and II motifs (DELLA and TVHYNP) from *Arabidopsis* using the BLAST algorithm. Six DELLA-encoding genes were identified by this search, of which three were full-length cDNAs and the remaining three were truncated at either the 5′ or 3′ end. The missing ends were obtained by RACE (Rapid Amplification of cDNA Ends) and full-length cDNAs were amplified from Royal Gala cDNA using primers based on the sequences of appropriate 5′ or 3′ RACE products. The six *DELLA* genes cluster into three pairs and were designated *MdRGL1a*, *MdRGL1b*, *MdRGL2a*, *MdRGL2b*, *MdRGL3a*, and *MdRGL3b*, for *Malus domestica RGA*-like (Figures 3.1 and 3.2). The GenBank and GDR protein accession numbers are given in chapter 2, section 2.2.4. Each a/b pair shares 91-93% homology at the amino acid level, reflecting the presumed allopolyploid origins of the Maloideae (Evans and Campbell, 2002). The homologous pairs are more divergent from one another than they are to

the same allele from different cultivars, which tend to be 98-99% homologous to one another (data not shown). The MdRGL1a/b, MdRGL2a/b and MdRGL3a/b ORFs are 1.9, 1.7 and 1.6 kb respectively. Based on PCR analysis of genomic DNA, none of these genes contain introns, which is consistent with DELLA-encoding genes from other plant species (data not shown). The group of six genes and proteins are referred to as *MdDELLA* and MdDELLA, respectively.

The predicted molecular mass of MdRGL1a/b, MdRGL2a/b and MdRGL3a/b proteins are 70, 64, and 60 kDa respectively. A multiple alignment indicates that the N-termini of these proteins have the two signature motifs, DELLA and TVHYNP, which define the DELLA subfamily and are necessary for GA-induced degradation of DELLA proteins. MdRGL3a/b diverge from the consensus sequence within the DELLA domain with substitutions to 7 of 27 amino acids. The C-termini of the MdDELLAs have five highly conserved motifs (LHRI, VHIID, LHRII, PFYRE, and SAW) that are shared by the larger family of GRAS proteins (Figure 3.1). Overall, these proteins share 67-69 % (MdRGL1a/b vs. MdRGL2a/b), 47-48 % (MdRGL1a/b vs. MdRGL3a/b), and 47-50 % (MdRGL2a/b vs. MdRGL3a/b) homology to one another (Figure 3.2). The MdDELLAs are most divergent over their N-termini, and are highly homologous over their C-termini. Alignment with *Arabidopsis* DELLA proteins showed that MdRGL1a/b and MdRGL2a/b are 62-63% homologous to AtGAI and AtRGA. MdRGL3a/b pair is the most divergent, sharing 45-51% homology with all of the *Arabidopsis* DELLA proteins (Figure 3.14).

To investigate whether there are additional DELLA genes in apple, degenerate primers were designed using CODEHOP algorithm (Rose et al., 2003) and used to amplify *MdDELLA* genes from Royal Gala chromosomal DNA under stringent primer hybridisation conditions (Figure 3.3). The three amplicons were purified, cloned individually and the obtained clones sequenced. The known (a and b) pairs of the three *MdDELLAs*, but no other products were all identified using this approach. Under low-stringency primer annealing conditions other minor products were obtained. 29 of these products within the expected size range were sequenced, but none were new apple *DELLA* genes. When the draft apple genome database became available it was searched for further DELLA CDS (Velasco et al., 2010). The draft genome sequence was initially searched using a word search with the DELLA term and subsequently with tBLASTn and BLASTp searches using the N-terminal domain of the known *Malus* DELLA orthologues as queries. No new DELLA CDS were identified in these searches. In conclusion, the apple genome encodes three distinct DELLA proteins, each represented by two closely related variants due to genome duplication. The identification of five DELLA genes in *Malus domestica* has also been reported in (Song et al., 2012).

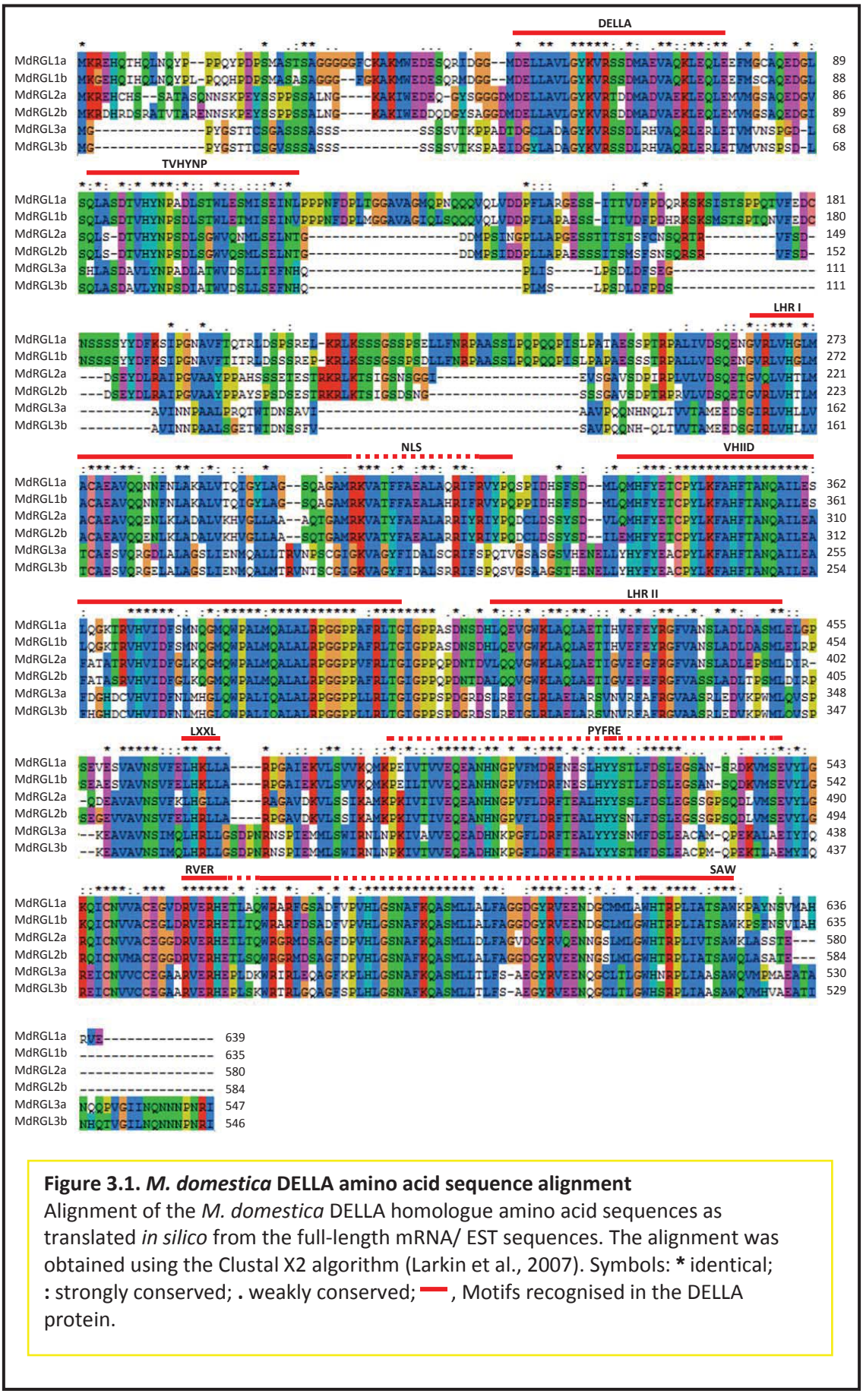

Figure 3.1. *M. domestica* DELLA amino acid sequence alignment
Alignment of the *M. domestica* DELLA homologue amino acid sequences as translated *in silico* from the full-length mRNA/ EST sequences. The alignment was obtained using the Clustal X2 algorithm (Larkin et al., 2007). Symbols: ***** identical; **:** strongly conserved; **.** weakly conserved; ▬, Motifs recognised in the DELLA protein.

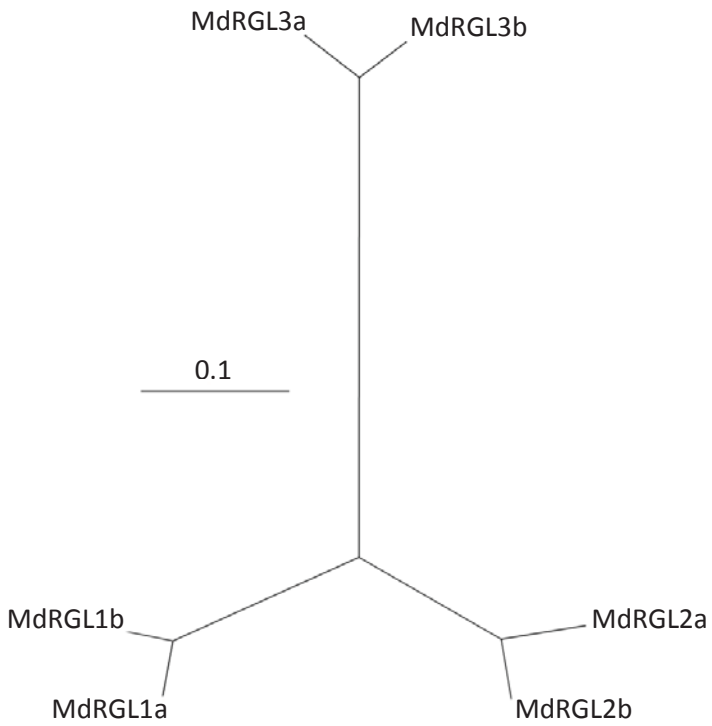

Figure 3.2. Unrooted tree view of *M. domestica* DELLA homologues
Produced from a ClustalX2 amino acid alignment (Larkin et al., 2007) of *in silico* translated full-length *Malus* DELLA homologue genomic sequence. Unrooted tree view produced in TreeView 1.6.6 (Page, 1996). Scale bar is 0.1 amino acid substitution per site.

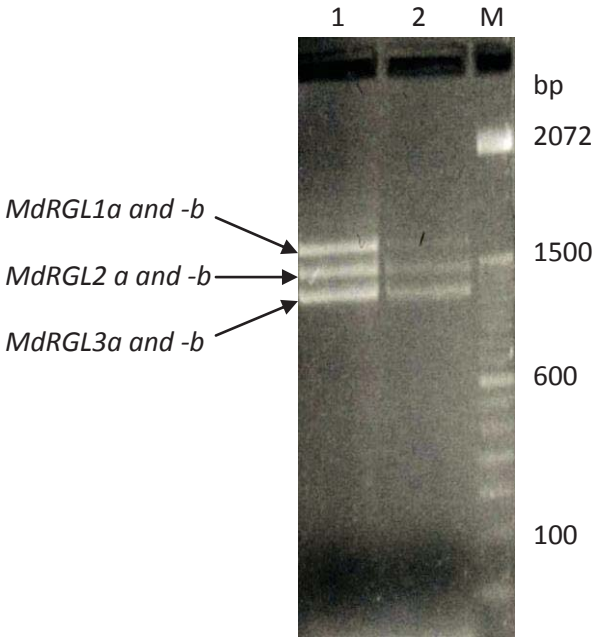

Figure 3.3 PCR amplification with degenerate primers designed to amplify DELLA CDS

PCR using CODEHOP-designed degenerate primers was performed on genomic DNA extracted from apple. Amplification products were separated by agarose electrophoresis; each band was purified and sent for commercial sequencing. Lanes: **1**, amplification using lower stringency primer annealing; **2**, higher stringency primer annealing (please see section 2.2.5); **M**, marker lane, 100 bp ladder (Life Technologies).

3.1.2 Apple GID1 and GID2/ SLY orthologues

Given the low conservation of the MdDELLA sequences in the N-terminal region, and the cooperative nature by which the GA signal is processed by the GID1-GA-DELLA-GID2(SLY1) complex, we undertook to identify, in addition to DELLAs, genes encoding GID1 and GID2(SLY1) homologues in apple.

The apple (*Malus x domestica*) database at Plant and Food Research (Crowhurst et al., 1999-2011) and the Rosaceae database (GDR)(Jung et al., 2008) were mined for GID1/ 2 sequences. The databases were searched using word search terms GID, SLY, GA receptor and GA F-box and with BLASTn, tBLASTn and BLASTp (Altschul et al., 1990) using *Arabidopsis* and rice orthologous sequences as queries. Based on the DELLA protein data and the apple genome structure, it was expected that there will be duplicated sequences.

For the GID1 orthologues, like the DELLA proteins, one protein is further diverged from two more closely related proteins (see Figures 3.4 and 3.5). The proteins share 71 % (both MdGID1a and c vs. MdGID1b) and 90 % (MdGID1a vs. MdGID1c) homology. The *Malus* GDR protein accession numbers are given in chapter 2, section 2.2.4. Like other GID1 homologues, these GA receptors share the conserved motifs of the hormone sensitive lipase (HSL) family and have the mutation of the critical catalytic site amino acid (Histidine to Isoleucine or Valine) that renders them enzymatically inactive on their substrate (GA) and characterises them as members of the GA receptor HSL subfamily.

The apple GID2/ SLY1 DELLA-specific F-box protein orthologues found by searching the available databases share the same domain organisation and contain the hallmark SLY1 motifs GGF and LSL motifs downstream of the F-box domain (McGinnis et al., 2003). Two complete MdGID2 homologues with 86 % amino acid identity were found; they were labelled as a and b variants. Additional incomplete sequences were found in the Plant & Food Research database and these may indicate further diverged orthologues but these could not be resolved further due to the fragmented nature in the databases. The partial sequences were not further investigated. An F-box protein orthologous to *A. thaliana* distant SLY1 paralogue, SNE, was also identified in the *M. domestica* genome. The *Malus* SNE orthologue had 24 % homology with the MdGID2a/ b homologues. The *Malus* GDR protein accession numbers are listed in chapter 2, section 2.2.4. The SNE F-box proteins are related to SLY1 proteins and may be implicated in

GA signalling (please see Chapter 1). Apple SNE orthologue sequence was included in the analysis (see Figures 3.6 and 3.7).

The location of the apple *DELLA*, *GID1* and *GID2* orthologous CDS on the integrated physical and genetic map linkage groups (chromosomes) corresponds to the homologous pairings of the linkage groups (LG), identified through marker mapping, that likely represents the most recent genome-wide duplication event (Han et al., 2011, Velasco et al., 2010). Unfortunately *MdRGL1a* and *–b* are unanchored, however *MdRGL2a* and *–b* lie on LG9 and LG17 respectively, and *MdRGL3a* and *–b* lie on LG15 and LG2 respectively. *MdGID1a* and *MdGID1c* lie on LG4 and LG12 respectively. *MdGID2a* and *MdGID2b* lie on LG 8 and LG 15 respectively. These are homologous pairs of linkage groups that are identified by Velasco *et al* (LGs; 1-7, 2-15, 3-11, 4-12, 5-10, 6-14, 8-15, 9-17, 13-16) though genetic mapping techniques. *MdGID1b*, the further diverged GA receptor orthologue, is on LG3 and *MdSNE* is on LG17.

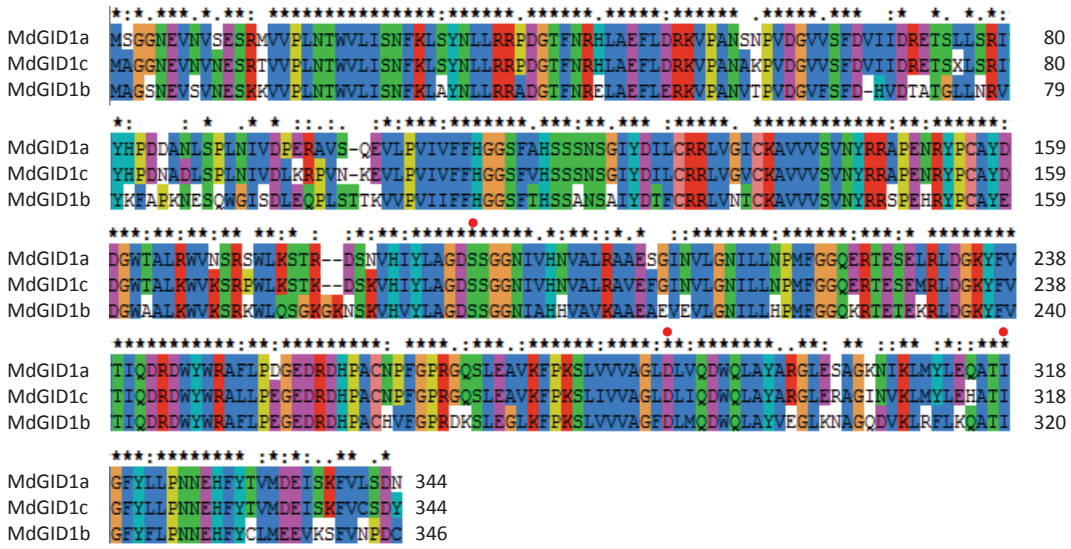

Figure 3.4. *Malus x domestica* GID1 homologue amino acid sequence alignment
Alignment of the *Malus* GID1 homologue amino acid sequences mined from the Plant & Food and GDR databases (Crowhurst et al., 1999-2011, Jung et al., 2008). The alignment was obtained using the Clustal X2 algorithm (Larkin et al., 2007). Symbols: * identical; : strongly conserved; **.** weakly conserved. • Catalytic triad residue for HSL, C-terminal residue not H.

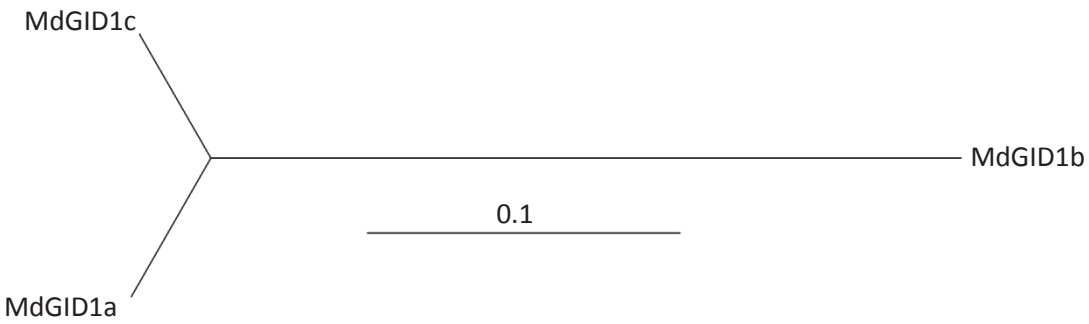

Figure 3.5. Unrooted tree view of *M. domestica* GID1 homologues
Produced from a ClustalX2 amino acid alignment (Larkin et al., 2007) of *in silico* translated full-length *Malus* DELLA homologue genomic sequence. Unrooted tree view produced in TreeView 1.6.6 (Page, 1996). Scale bar is 0.1 amino acid substitution per site.

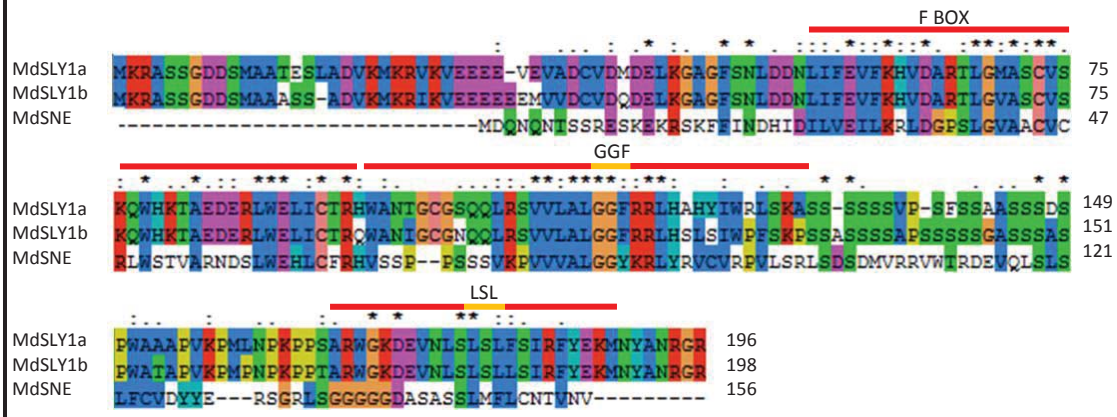

Figure 3.6. *M. domestica* GID2/ SLY1 and SNE1 homologue amino acid sequence alignment

Alignment of the *A. deliciosa SLY1* homologue amino acid sequences as translated *in silico* from the full-length mRNA/ EST sequences. The alignment was obtained using the Clustal X2 algorithm (Larkin et al., 2007). Symbols: ***** identical; **:** strongly conserved; **.** weakly conserved. ; ▬, Motifs recognised in the GID1 protein.

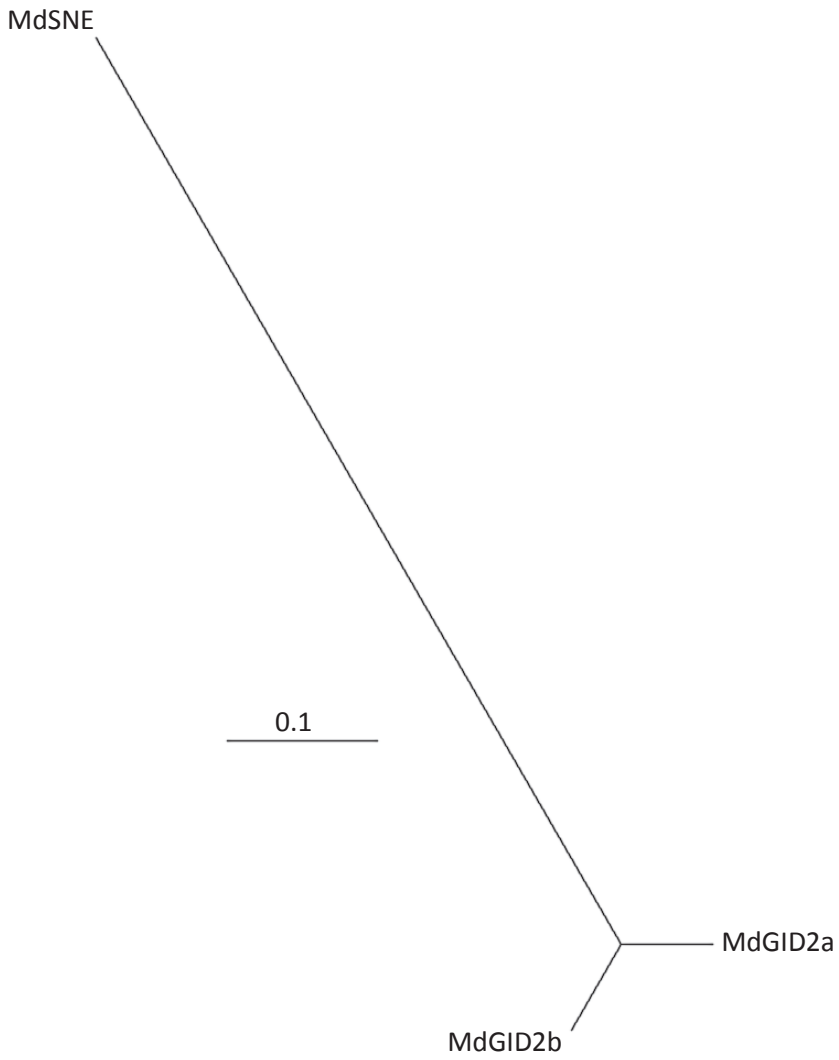

Figure 3.7. Unrooted tree view of *M. domestica* GID2/ SLY homologues
Produced from a ClustalX2 amino acid alignment (Larkin et al., 2007) of *in silico* translated full-length *Malus* DELLA homologue genomic sequence. Unrooted tree view produced in TreeView 1.6.6 (Page, 1996). Scale bar is 0.1 amino acid substitution per site.

3.1.3 Apple DELLA expression analysis

Individual *MdDELLA* transcripts in various tissues were determined by real-time quantitative PCR. An initial screen of the six *MdDELLA* transcripts indicated that all were expressed in all investigated tissues, and there was little difference between the -a and -b gene pairing. A qPCR experiment was performed on the -b gene variant to examine the relative expression pattern of the *MdDELLA*s compared to the reference gene *GAPDH* in selected tissues: actively growing shoot tips, expanding leaves, spur-type shoots (shoots that have arrested growth before the end of the full growth season), shoot tips and floral buds arrested at the end of the season, and germinating seeds.

In early summer, spur-type shoots cease leaf initiation and enter a period of developmental arrest, whereas extension shoots continue to initiate leaves and undergo internode extension for another 4-8 weeks (Fulford, 1965, Fulford, 1966). The spur-type shoots had over ten times more *MdDELLA* transcripts compared to the level in actively growing shoots and the expanding leaves. The level of *MdRGL3b* was twice that of *MdRGL1b* or *MdRGL2b*. At this same time-point, all six *MdDELLA*s are expressed at very low levels in the apices of actively growing shoots and in young expanding leaves. These findings are consistent with current understanding of DELLAs as repressors of growth and also indicate a possible dominant role for *MdRGL3* in maintaining developmental arrest in the spur-type shoot meristem.

Once the vegetative growth at the end of the growth season ceases, all terminal buds have either arrested as vegetative meristems, or have undergone floral development (Foster et al., 2003). In autumn, the levels of all three *MdDELLA* transcripts are elevated in the shoot tips to over ten times the levels present during growth earlier in the season. However, in the floral bud tissue at the end of season, the *MdDELLA* transcripts are at a moderately low level, approximately two times that of the shoot tissue during growth, indicating that the DELLAs may have a more prominent role in restricting growth in vegetative buds compared to floral buds.

All three *MdDELLA* transcripts and in particular *MdRGL2b,* are much less abundant in the expanding leaves and growing apices relative to vegetative and floral buds. This may indicate a specific inhibitory role for the *MdRGL2b*, requiring almost complete obliteration of this message in expanding tissues.

MdDELLA transcripts were quantified in 3- or 8- day germinating seeds (that were vernalised for 8 weeks prior to germination). The relative expression levels of all *MdDELLA*s were low in germinating seeds, at levels that were very similar to those in expanding leaves during the growth season. This is in contrast with *Arabidopsis DELLA*s (especially the relative levels reported for *AtRGL2* and *-3*), which are highly abundant in seeds at an equivalent developmental stage (Tyler et al., 2004). It is possible that in apple seeds *MdDELLA* mRNAs have high turnover, hence the amount of message found by qPCR appears small (Figure 3.8) (Foster et al., 2007).

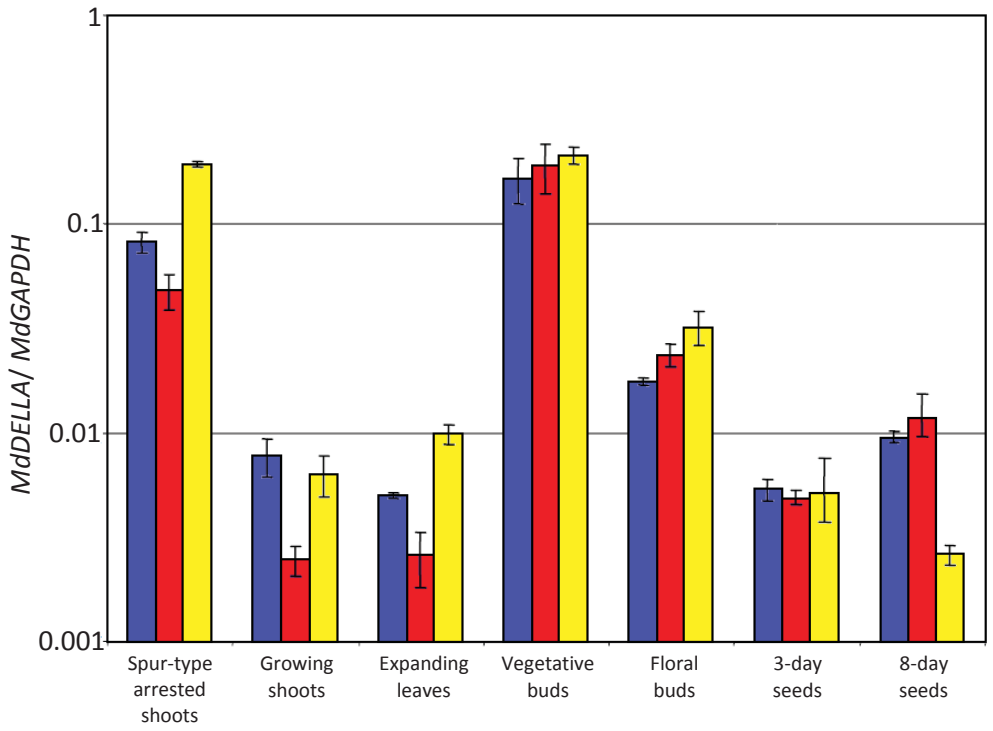

Figure 3.8. Relative transcript levels of *MdDELLA*s across tissue types
Bar graphs representing the relative transcript levels of *MdRGL1b*, *MdRGL2b* and *MdRGL3b* normalised to *MdGAPDH* in different tissues and developmental stages. Tissue for RNA was isolated in early summer from growing shoots, expanding leaves and arrested spur-type shoots. Tissue was again harvested in autumn after the fruit harvest from dormant vegetative and floral buds. Seeds were vernalised then imbibed for either three or eight days before harvesting.
KEY: *MdRGL1*, *MdRGL2*, *MdRGL3*.
Experiment was performed by T. Foster and J. Rakonjac.

3.1.4 Apple DELLA function

Transgenic *Arabidopsis* lines (Columbia ecotype) were constructed to determine if MdDELLAs function analogously to DELLA proteins in *Arabidopsis*. The transgenic cassette contained the full length *MdRGL2a* under the control of 35S CaMV promoter and followed by the Octopine synthase terminator, in a vector containing a kanamycin resistance marker. Transgenic plants were selected under kanamycin treatment and six independent transgenic lines of T3 and subsequent generation plants were phenotypically assessed (see sections 2.2.10, 2.2.11 and 2.2.12). *MdRGL2a* was selected for over-expression analysis because it has conserved DELLA family motifs (Figure 3.1) and down-regulation of *MdRGL2* expression in growing shoots and expanding leaves is most pronounced among the three *MdDELLAs* (Figure 3.8). The transgenic plants showed the phenotypes of impaired GA responses, as reported from over-expression of an active xeno *DELLA* repressor protein in *A. thaliana* (Ait-ali et al., 2003, Fu et al., 2001): reduced height, leaf size and rosette diameter and very delayed flowering with most of the plants expressing *MdRGL2a* not flowering by 140 days in the short day (SD) regimen (the data is presented is as percent flowering by 94 days in SD). They were also tested for the hypocotyl elongation response to exogenous application of GA_3. As expected for constitutively expressed DELLAs, the transgenic plants had a lowered elongation response relative to the wild-type *A. thaliana* control plants (Figure 3.9). The extent of *MdRGL2a* over-expression among the transgenic lines correlates with all measured phenotypic effects (Figure 3.9 Ai). This demonstrates that an apple DELLA homologue in *A. thaliana* is at least partially functionally conserved and acts as a repressor of developmental GA-regulated processes (Foster et al., 2007). Partially dominant effect of the transgenes is consistent with a highly conserved C-terminal domain between *Arabidopsis* and apple DELLA proteins, as this domain is mediating the repression of downstream GA-responses. Furthermore, besides the over-expression effect which contributes to partial GA-insensitivity of the transgenic lines (especially line 5), differences in the N-terminal domain primary amino acid sequences between MdRGL2a and *A. thaliana* DELLAs are expected to confer low responsiveness to the GA signal, as this signal is mediated through very specific interactions between amino acid residues of the liganded GA receptor (GID1-GA) and the C α helix and AB loop of DELLA proteins (Please see DELLA protein modelling in Section 4).

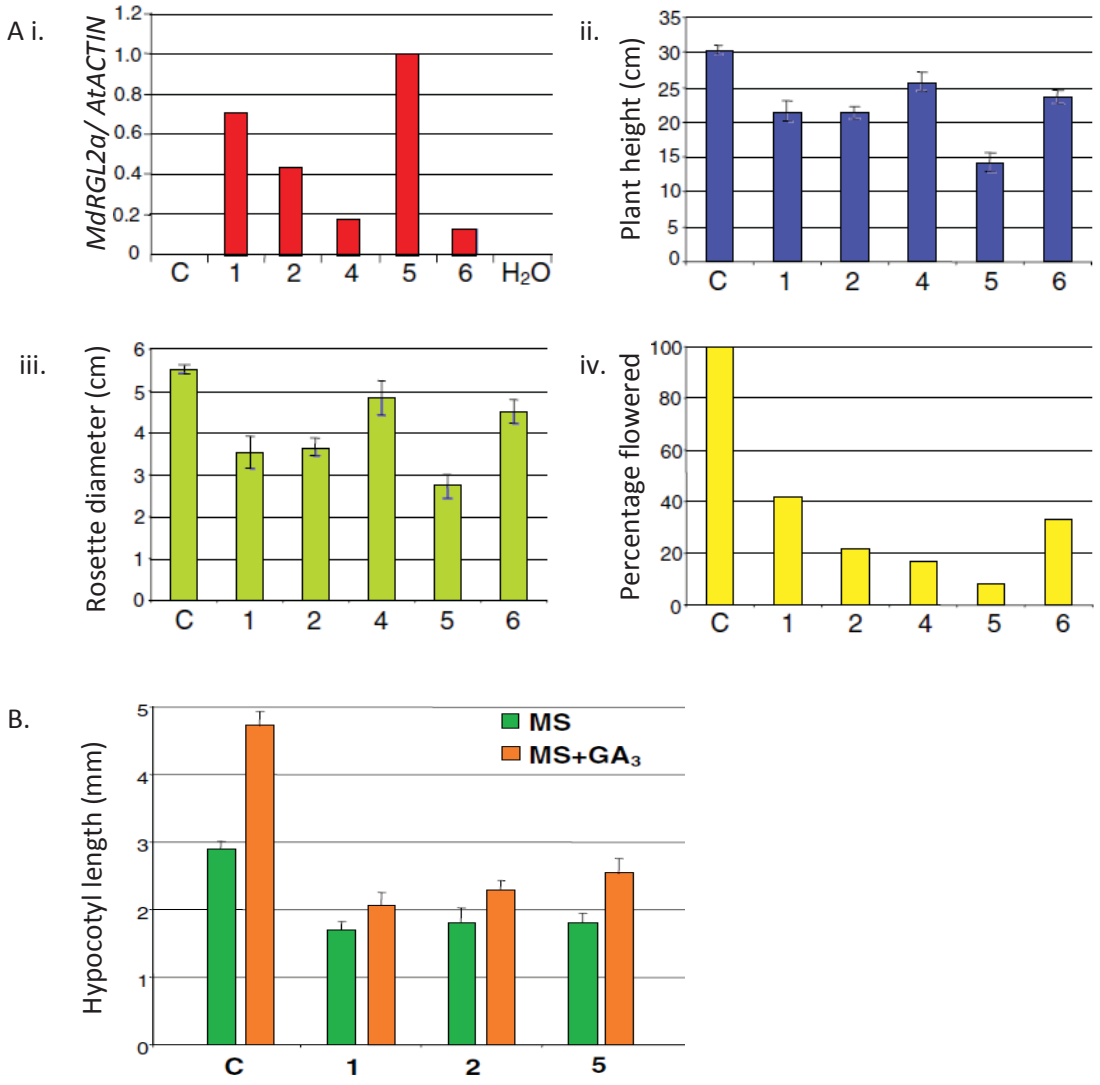

Figure 3.9. Phenotypes of transgenic *A. thaliana* expressing Apple DELLA MdRGL2a transgene

A, Six independent transformation lines were scored for transgene expression level, and plant height and rosette diameter phenotypes after 25 days under 16 h light/ 8 h dark (LD) conditions. The percentage of plants to flower after 94 days was scored under 8 h light/ 16 h dark (SD) conditions. A total of 20 plants were measured. **I,** Relative expression level of *MdRGL2a/ AtACTIN*, **ii,** Plant height (of primary inflorescence), **iii,** Rosette diameter, **iv,** Percentage of plants flowering after 94 days **B,** Three of the transgenic lines were scored for hypocotyl length of the germinating seeds. They were measured after 7 days in the presence or absence of 100 µM GA_3. **C,** control plant (wild-type Co).

Transgenic plants were constructed by the Plant and Food Institute Facility (Mt. Albert). T. Foster carried out phenotypic analysis.

3.2 Kiwifruit proteins involved in gibberellic acid signalling

Kiwifruit (*Actinidia spp.*) is an economically important plant for New Zealand. It is a long-lived perennial vine that grows in two year cycles. An axillary bud, initiated in the first growth season, can remain dormant over winter and break in the following spring season for renewed growth. Two types of shoot may be produced, terminating and non-terminating. Growth cessation occurs in terminating shoots soon after breaking; the shoot tip aborts and the cane dies. Other shoots continue to grow and do not terminate growth until the end of the season. Vine growth is via twining and not by use of tendrils.

The shoot buds, new shoots and leaves are densely covered in red hairs. Leaves are large rounded ovals with long petioles. Kiwifruit floral buds are set in the axils of the leaves and require a period of low temperatures during the winter dormancy for full floral break in spring. The flowers are born either in threes or as a single. Kiwifruit is a dioecious plant. Female flowers have a whorl of fused styles surrounded by a thin whorl of sterile stamens. Male flowers are a little smaller than female flowers and they have a central vestigial style whorl surrounded by a mass of stamens. Petals are white to pale yellow. Pollination is via insect vectors. The fruit is produced on one year old and older canes. The fruit are a large rounded oblong with juicy green (*A. deliciosa*) or yellow (*A. chinensis*) flesh and covered in a tough hairy brown skin. Small dark seeds are dispersed radiating from a central pale cortex.

Many aspects of plant growth and development are regulated, at least in part, by gibberellin and the signalling pathway responding to this phytohormone. The key components of this signalling pathway have been studied in cereals as well as the model plant *Arabidopsis thaliana*, but very little is known about these proteins in the woody perennials. Work has been done with *Populus spp.* and indicates dominant dwarfing gain-of-function mutations in DELLA proteins similar to those observed in rice and *A. thaliana*. However, novel functions, with a likely role in wood formation (Mauriat and Moritz, 2009) and dormancy (Druart et al., 2007) have also been observed. Some information about gibberellin signalling in the grape vine, *Vitis vinifera*, indicates that one ancient line used in the wine production contains a dominant mutation in a DELLA protein resulting in greater flower production over tendril formation (Boss and Thomas, 2002). The kiwifruit vine is, however, very different from the grape vine in many of its growth aspects. To compare kiwifruit with the grape vine and other woody perennials,

this section characterised the key components of the gibberellin signalling pathway in the kiwifruit *(A. deliciosa*). The key proteins involved in gibberellin signalling that were sought for were the nuclear gibberellin receptor (GID1 protein family), the gene expression regulator (DELLA protein family) and the DELLA-specific F-box protein which mediates DELLA degradation upon the GA signal (SLY1 or GID2 protein family).

3.2.1 Identification of the key gibberellin signalling pathway proteins in the Plant and Food Research kiwifruit EST database

Plant & Food Research expressed sequence tag (EST) database which contains sequences of the 3' moieties of cDNAs derived from multiple tissues of apple and kiwifruit (Crowhurst et al., 1999-2011) was used as a sequence source to identify the *A. deliciosa* homologues of key gibberellin signalling pathway components. The non-redundant (nr) EST data base was mined for orthologous sequences to known *DELLA*, *GID1* and *GID2*/ *SLY1* genes and proteins from other plants. To identify the orthologues of these proteins that have already been annotated as such in the database, a word search was first carried out. Secondly, a sequence alignment-based search using the BLAST (Basic Local Alignment Search Tool) algorithm was performed (Altschul et al., 1990). Several different protein queries were used to search the translated nucleotide database (translation of all 6 reading frames). In particular, conserved amino acid sequence motifs or particular domains of *Arabidopsis* or cereal sequences were used as queries. Given that the database contained only 3' moieties of cDNA sequence, the complete sequences were derived from the inserts of the recombinant cDNA clone bank from which the EST database is derived. However, as many of the EST clone inserts still lacked the 5' end of the corresponding mRNAs (and therefore the 5' end of a CDS), they did not contain the complete coding sequences (CDS) or mRNAs. To obtain the complete mRNA, a PCR approach called 5' RACE (Rapid Amplification of cDNA Ends) was used. Using this approach complete CDS of seven unique DELLA mRNAs (cDNAs), three unique *GID1* and three unique *SLY1* transcripts were determined.

3.2.1.1 Identification of DELLA protein family homologues in kiwifruit

The initial word search of the EST database using DELLA and GRAS terms, corresponding to the names of DELLA subfamily of the GRAS family of transcriptional regulators, of the database returned 15 ESTs. The tBLASTn searches with each entire *Arabidopsis* DELLA protein sequence, with the full C-terminal (GRAS) domains and with shorter highly conserved motifs within the GRAS domain generated 59 further hits. Examination of these sequences using alignment and

elimination of non *A. deliciosa* kiwifruit sequences yielded a final list of 8 individual EST clones: 115865, 78609, 49556, 113002, 227790, 101189, 98329 and 79743.

The EST cDNA clones 115865, 78609, 113002, 227790 and 79743 corresponded to full length mRNAs, however 49556, 98329 and 101189 were lacking the 5' portion. 5' RACE (Frohman et al., 1988) was employed to obtain the 5' portion missing from the CDS of 49556, 98329 and 101189 (see Material and Methods section 2.2.6). Amplification products were separated by agarose gel electrophoresis purified and cloned into pGEM-T easy vectors. The gel separation is shown in Figure 3.10. Once the recombinant plasmids were obtained, the DNA sequence of inserts was determined. Together with the 3' moiety of the CDS, this sequence resulted in obtaining complete CDSs of DELLA protein-encoded genes. From the obtained complete sequences it was determined that there are seven DELLA homologues encoded in the *A. deliciosa* genome (After RACE 101189 and 98329 were confirmed to be the same CDS).

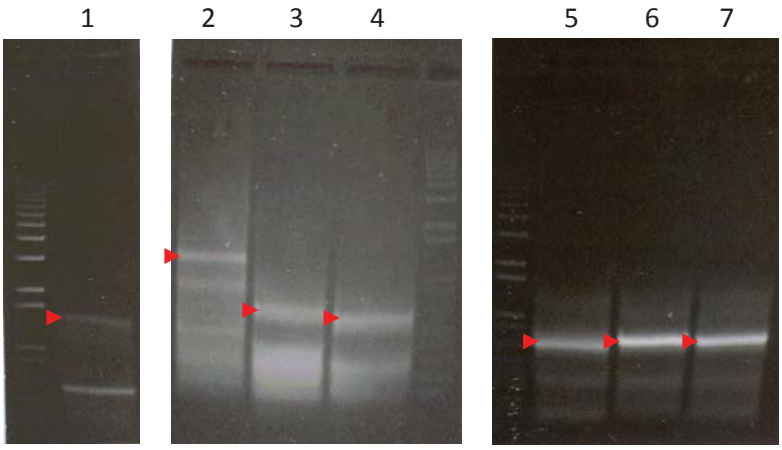

Figure 3.10. 5' RACE amplification products
5' RACE amplification of *A. deliciosa* ESTs in which the 5' portion of a complete cDNA was missing, as indicated after alignment of sequences, and expected sizes of missing portions could therefore estimated. Amplification was carried out from 5 µg of total RNA preparation made from *A. deliciosa* fruit cortex tissue. Products were separated by agarose gel electrophoresis and stained with SYBR safe. Bands that were isolated, cloned and sequenced are marked with a red arrow head.
Lanes:
1. 1.4 kb product generated from DELLA homologue ESTs 101189/ 98329 with GSP1 and 2 primer pair.
2. 1.4 kb product generated from DELLA homologue EST 49556 with GSP1 and 2 primer pair.
3. 0.5 kb product generated from SLY1 homologue ESTs 195089/ 91591 with GSP1 and 2 primer pair.
4. 0.5 kb product generated from SLY1 homologue EST 91591 with GSP1 and 2a primer pair.
5. 0.5 kb product generated from GID1 homologue EST 200355 with GSP1 and 2 primer pair.
6. 0.5 kb product generated from GID1 homologue ESTs 287619/ 17819 with GSP1 and 2 primer pair.
7. 0.5 kb product generated from GID1 homologue EST 287619, GSP1 and 2a primer pair.

To determine the relatedness of the seven DELLA protein family members, the amino acid sequences of these proteins were aligned. This showed that they fall into three distinct *AdDELLA* clades, two of which contained two DELLA proteins, and one contained three DELLA proteins. AdDELLA proteins within each clade are over 90% identical, consistent with the hexaploidy (2n=6x) observed in this plant (Testolin and Ferguson, 1997, Shi et al., 2010). The triplet may indicate a more recent duplication event (producing 49556 and 79743). Therefore, *A. deliciosa* appears to have three different DELLA proteins, each represented by duplicated genes (Figure 3.11 and Table 3.1).

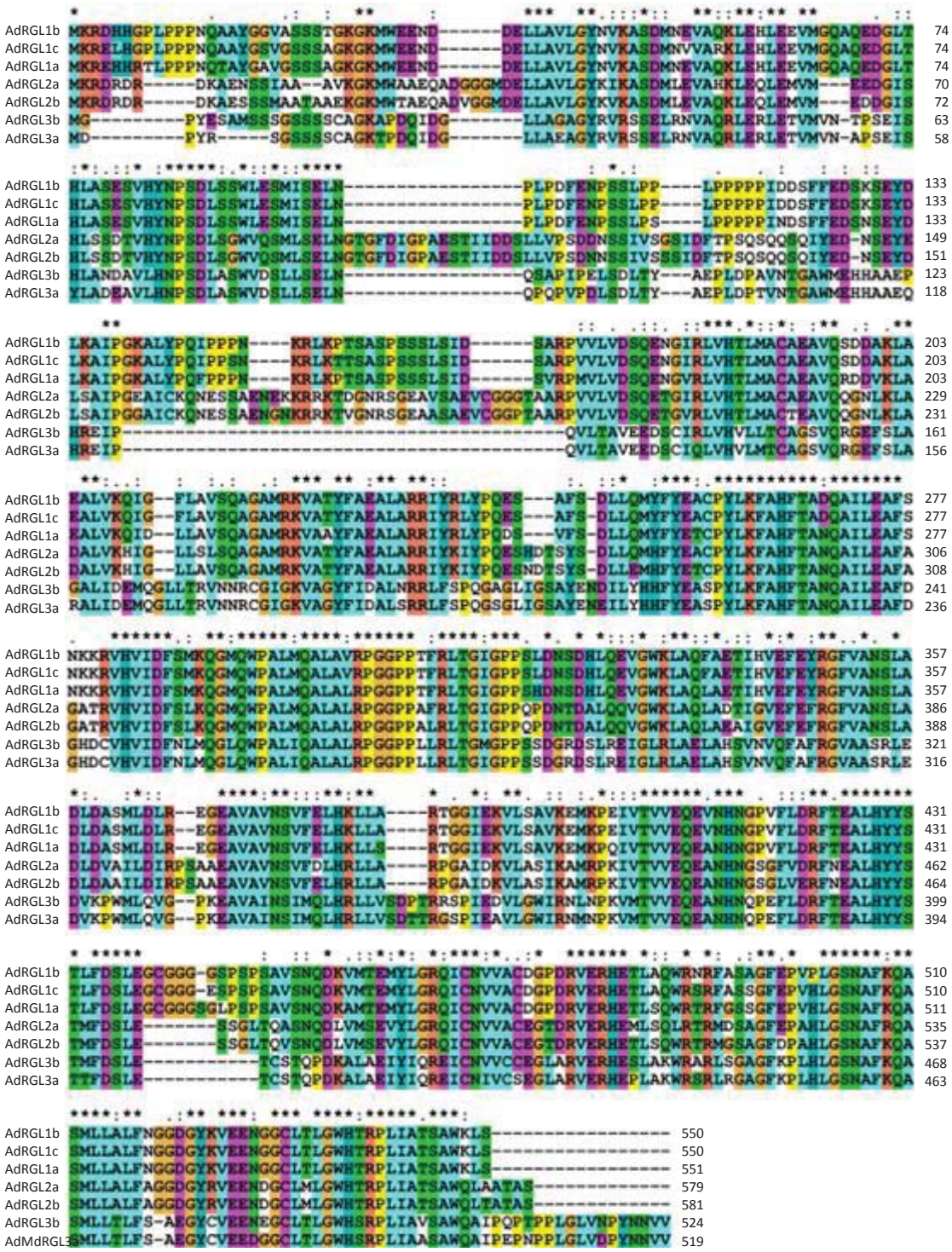

Figure 3.11. *A. deliciosa* DELLA amino acid sequence alignment
Alignment of the *A. deliciosa* DELLA homologue amino acid sequences as translated *in silico* from the full-length mRNA/ EST sequences. The alignment was obtained using the Clustal X2 algorithm (Larkin et al., 2007). Symbols: ***** identical; **:** strongly conserved; **.** weakly conserved.

Table 3.1. *A. deliciosa* DELLA homologue amino acid identity/distance table

	AdRGL1a	AdRGL1b	AdRGL1c	AdRGL2a	AdRGL2b	AdRGL3a	AdRGL3b
AdRGL1a		93[a]	93	68	69	51	51
AdRGL1b			98	68	69	50	50
AdRGL1c				68	68	50	50
AdRGL2a					93	49	50
AdRGL2b						49	50
AdRGL3a							93
AdRGL3b							

[a] Calculation of similarity between pairs of full length amino acid AdDELLA sequences. Produced and calculated in Vector NTi AlignX (Life Technologies) using the number of residue matches divided by the complete alignment length between the two sequences and given as a percentage.

Alignment of *A. deliciosa* DELLA proteins with DELLA protein sequences from a number of plants showed that the kiwifruit DELLAs group with different DELLA family members from other organisms. AdRGL1a, -1b, -1c (113002, 49556 and 79743) are most closely related to the GAI protein of *V. vinifera* (*VvGAI*). These three proteins also group with *A. thaliana* GAI and RGA, which are the most systemically-distributed DELLA proteins. Therefore, it could be concluded that these three *A. deliciosa* DELLA proteins are likely to be the homologues of the major DELLA proteins GAI and RGA. The apple MdRGL1 and pea PsCRY also sit within this clade. AdRGL2a and -2b (101189 and 227790) group in the other major dicotyledonous plant DELLA clade, with the apple (MdRGL2; section 3.1), tomato (SIGAI), pea (PsLA) and cotton (GhGAI) (Bassel et al., 2004, Liao et al., 2009, Weston et al., 2008). The three *Arabidopsis* RGLs also more loosely group to this clade. The remaining *Actinidia* DELLA proteins AdRGL3a and -3b (115865 and 78609) group most closely with the apple DELLA protein MdRGL3 as a separate branch from the dicots and appear closer to the cereal DELLA sequences. Therefore, AdRGL3a and -3b from *A. deliciosa* and one MdRGL3 from *M. domestica* perhaps represent a common branch in DELLA protein evolution.

This analysis shows that two pairs of *Actinidia* DELLA paralogues are closely related to two pairs from *M. domestica*. The *Actinidia* paralogue triplet, however, is most closely related to *V. vinifera* GAI. Therefore, we renamed the *A. deliciosa* genes in relation to the *M. domestica* nomenclature; 113002, 49556 and 79743 as *AdRGL1a*, *AdRGL1b* and *AdRGL1c*, respectively, 101189 and 227790 as *AdRGL2a* and *AdRG2b* respectively and 115865 and 78609 as *AdRGL3a* and *AdRGL3b*, respectively (Figures 3.11, 3.12 and 3.13 and Table 3.1). The GenBank accession numbers are listed in chapter 2, section 2.2.6.

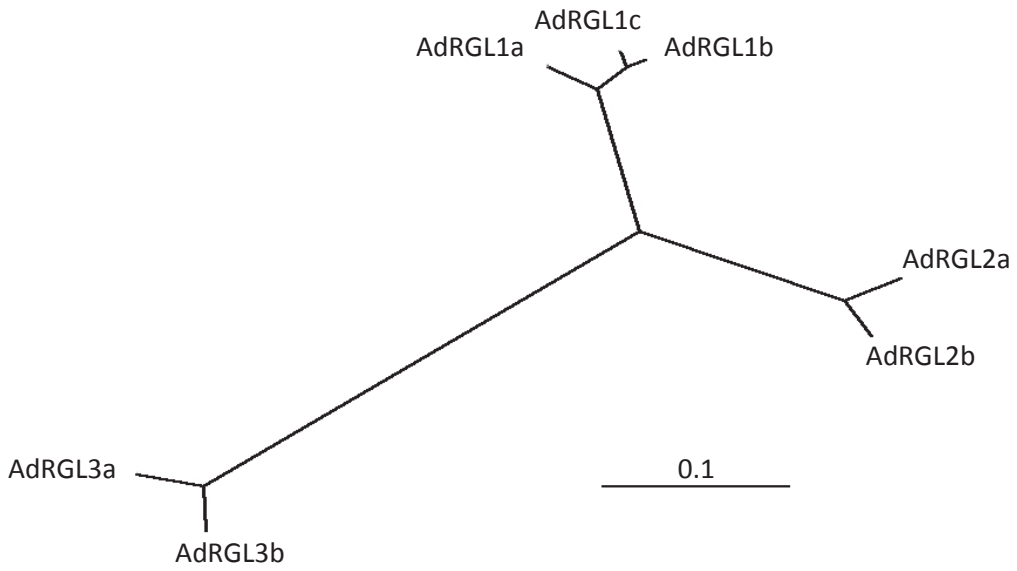

Figure 3.12. Unrooted tree view of *A. deliciosa* DELLA homologues
Produced from a ClustalX2 amino acid alignment (Larkin et al., 2007) of *in silico* translated full-length *A. deliciosa* DELLA homologue genomic sequence. Unrooted tree view produced in TreeView 1.6.6 (Page, 1996). Scale bar is 0.1 amino acid substitution per site.

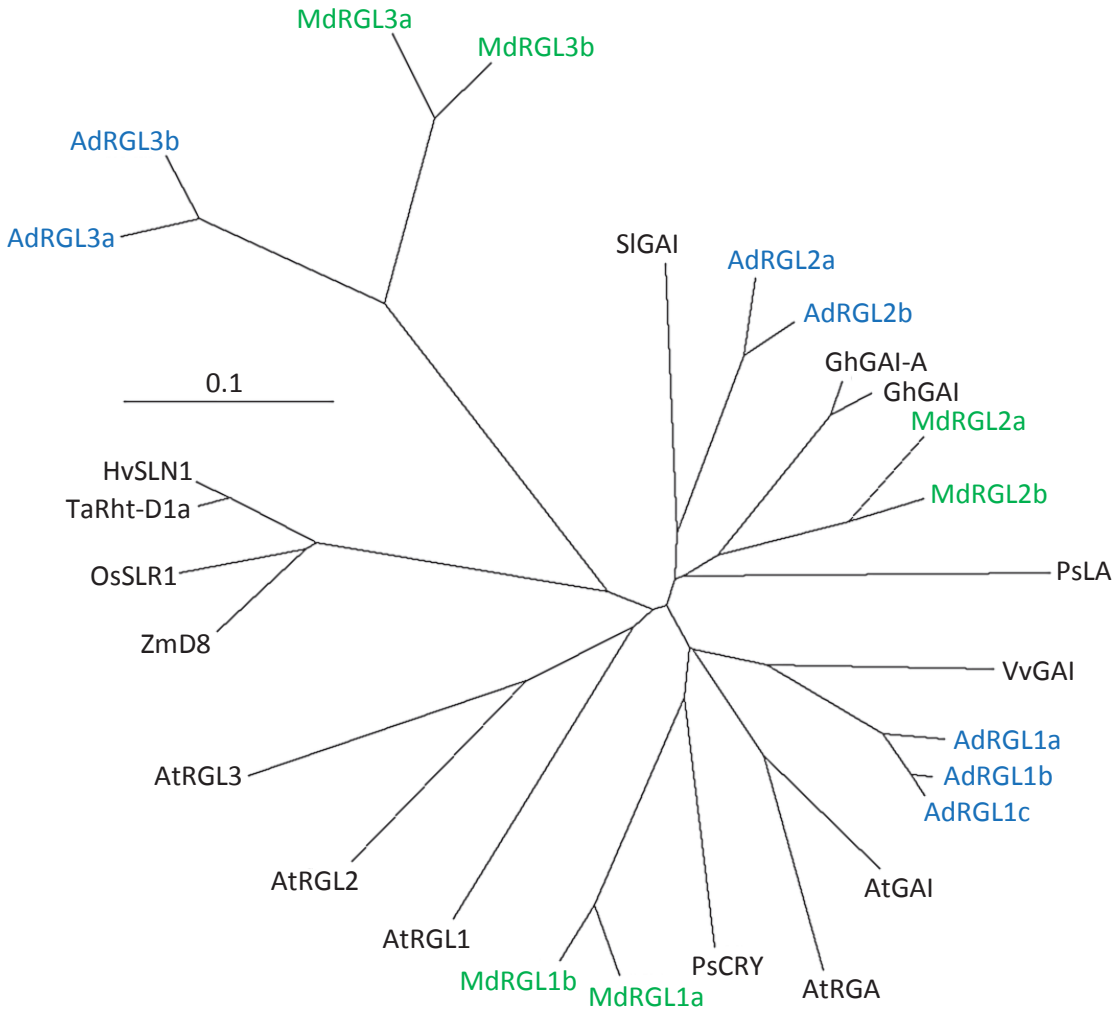

Figure 3.13. Unrooted tree view of DELLA homologues from various plants
Produced from a ClustalX2 amino acid alignment (Larkin et al., 2007) of *in silico* translated full-length DELLA homologue genomic or cDNA sequences. Unrooted tree view produced in TreeView 1.6.6 (Page, 1996). Scale bar is 0.1 amino acid substitution per site.

3.2.1.2 Identification of the *GID1* homologous sequences in kiwifruit

GID1 is the nuclear receptor for gibberellins. The cereals typically contain a single *GID1* protein, whereas dicotyledonous plants may contain multiple paralogues. *GID1* belongs to the carboxylesterase superfamily, but is enzymatically inactive. *GID1* homologues were identified in *A. deliciosa* EST database in order to establish the number of *GID1* genes in this plant and to compare the *A. deliciosa GID1* to homologues from other plants.

The initial word search of the Plant & Food Research EST database using *GID1* and *CXE* (Carboxylesterase superfamily) terms returned 46 ESTs. A tBLASTn search with rice GID1, *Arabidopsis* GID1a, -b and -c and barley GSE1 sequences yielded 18 further hits. Examination of these sequences using alignment and elimination of non *A. deliciosa* kiwifruit sequences yielded a final list of 5 sequences, EST numbers: 17819, 112858, 87170, 200355, and 287619.

The EST inserts were fully sequenced, revealing the full length CDS in 112858 and 87170, and the 5' end missing in 200355, 287619 and 17189. The remaining 5' portions of these three cDNAs (and therefore CDSs) were obtained by 5' RACE (Frohman et al., 1988) as described in 2.2.6. The complete cDNA sequences were obtained and designated 200355/4, 287619/17 and 287619/22. Alignment (Figure 3.14) showed that the two CDS 287619/17 and 287619/22 share 92 % homology and are more similar to each other than to 200355/4 which shares 78 % and 76% homology respectively to the other two CDS, indicating that they may represent a more recent duplication.

Alignment of three *A. deliciosa* GID1 protein sequences with homologues from other plants showed that 287619/22 and 287619/17 are most closely related to *V. vinifera* GID1, and are closely related to *A. thaliana* AtGID1a and AtGID1c and apple MdGID1a and MdGID1c. These two GID1 homologues were therefore renamed AdGID1a (287619/17) and AdGID1c (287619/22). The protein encoded by CDS 200355/4 is most closely related to SlGID1 from tomato and apple MdGID1b and these three form a group together with *A. thaliana* AtGID1b. The *Actinidia* GID1 homologue was therefore renamed AdGID1b (200355/4). GID1 proteins from the cereals form a separate cluster from those of dicotyledonous plants (Figure 3.15). The GenBank accession numbers of *AdGID1* CDSs are listed in chapter2, section 2.2.6.

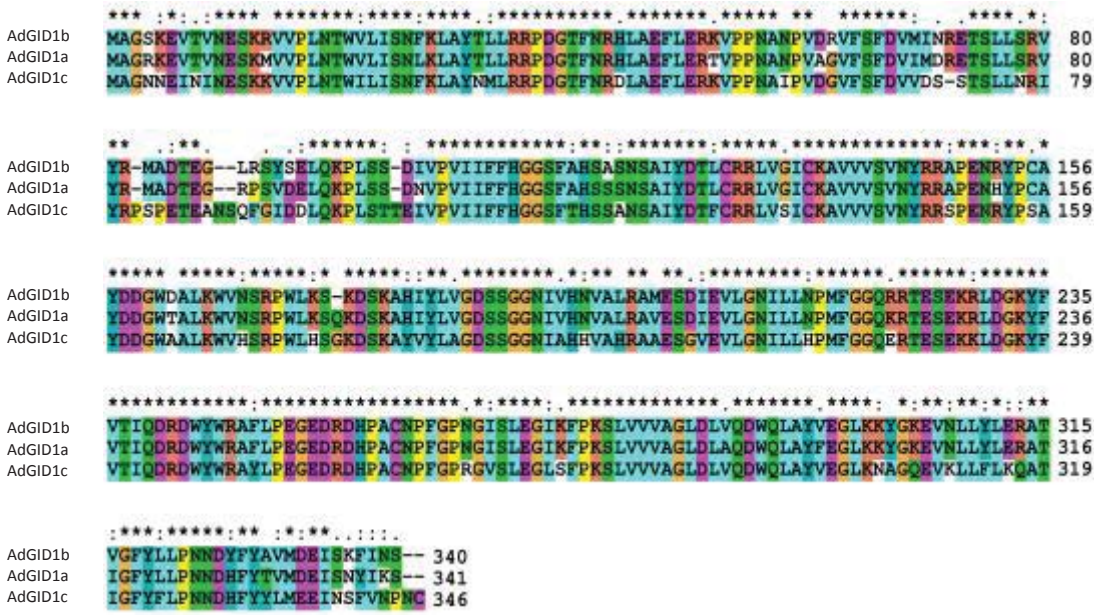

Figure 3.14. *A. deliciosa* GID1 amino acid sequence alignment
Alignment of the *A. deliciosa* GID1 homologue amino acid sequences as translated *in silico* from the full-length mRNA/ EST nucleotide sequences. The alignment was obtained using the Clustal X2 algorithm (Larkin et al., 2007). Symbols: ***** identical; **:** strongly conserved; **.** weakly conserved.

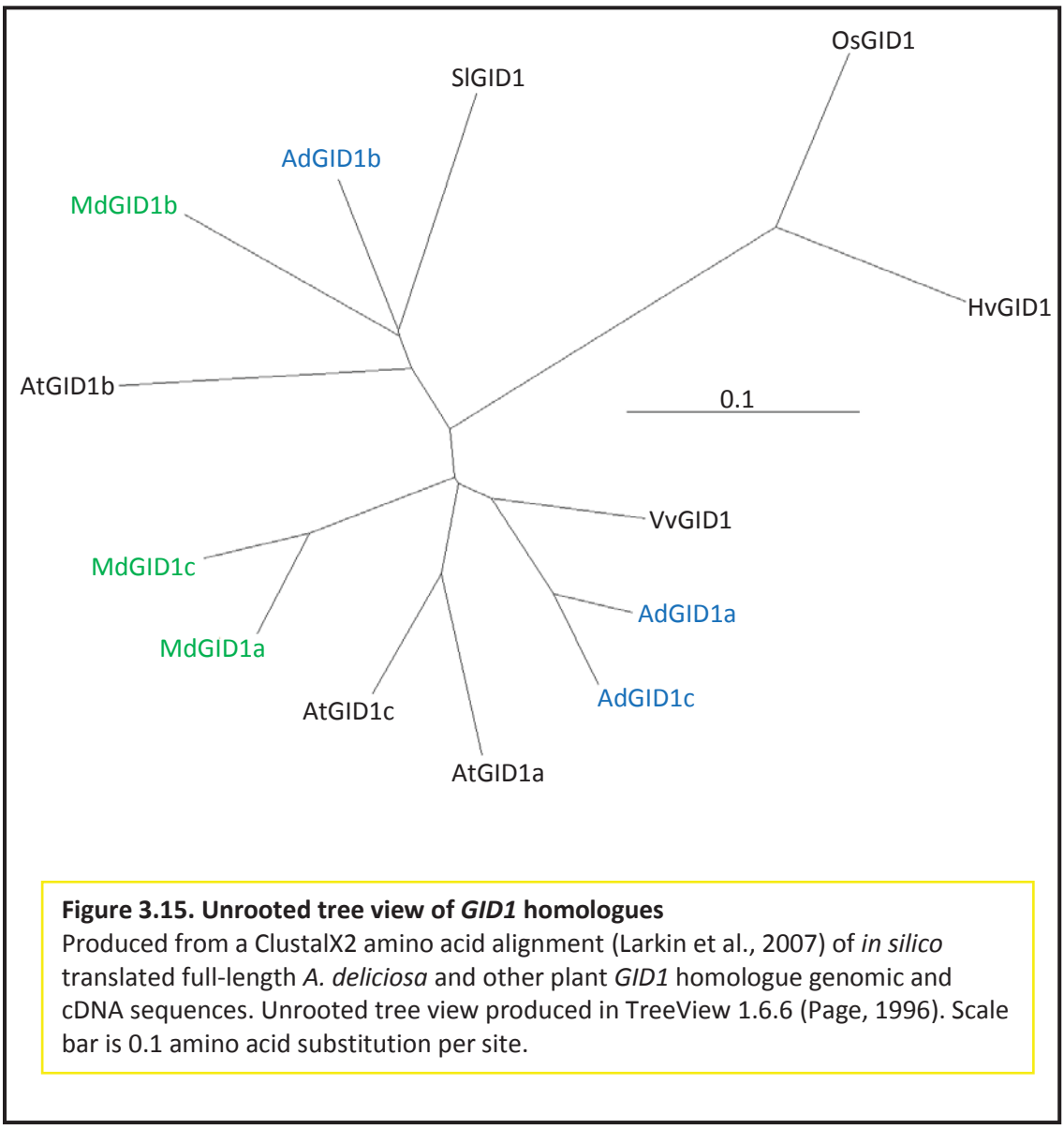

Figure 3.15. Unrooted tree view of *GID1* homologues
Produced from a ClustalX2 amino acid alignment (Larkin et al., 2007) of *in silico* translated full-length *A. deliciosa* and other plant *GID1* homologue genomic and cDNA sequences. Unrooted tree view produced in TreeView 1.6.6 (Page, 1996). Scale bar is 0.1 amino acid substitution per site.

3.2.1.3 Identification of *SLY1* homologous sequences in kiwifruit

The F-box proteins which target the E3 ubiquitin ligase to DELLA proteins are usually represented by one dominant protein in a genome. This is why it was not expected to identify a large number of *SLY1* homologues in *A. deliciosa*.

The initial word search using E3 ligase and SCF terms of the Plant & Food Research database returned 4337 ESTs, while F-box gave no hits. A tBLASTn search with rice GID2, *Arabidopsis* SLY1 and cotton FB2 amino acid sequences yielded 25 different hits. After examination of these sequences utilising alignment programmes and elimination of non-*A. deliciosa* sequences, a final list of three sequences was obtained, EST numbers: 91591, 195089 and 78262. The EST 78262 was full-length, whereas 91591 and 195089 lacked the 5' end of the open reading frame. As with the *DELLA* and *GID1* homologues, a 5' RACE (Frohman et al., 1988) experiment was employed to obtain the 5' portion of the CDS missing from the ESTs 91591 and 195089. Following sequencing of amplified 5' end of the cDNA and alignments, three complete *SLY1* CDS were obtained and designated *AdSLY1/7*, *AdSLY1/8* and *AdSLY1/12*. All three kiwifruit *SLY1* paralogues are highly conserved (85, 84 and 94 % identity for amino acid sequence). *A. deliciosa* has the highest number of the *SLY 1* homologues detected so far in a plant and this is consistent with the hexaploid nature of the *A. deliciosa* genome. As for AdDELLAs and AdGID1s, all *A. deliciosa* SLY1 paralogues cluster with the homologues from dicotyledonous plants (Figure 3.16 and 3.17), while the homologues from cereals (called GID2) cluster separately. The GenBank accession numbers of *Actinidia SLY1* homologues are listed in chapter 2, section 2.2.6.

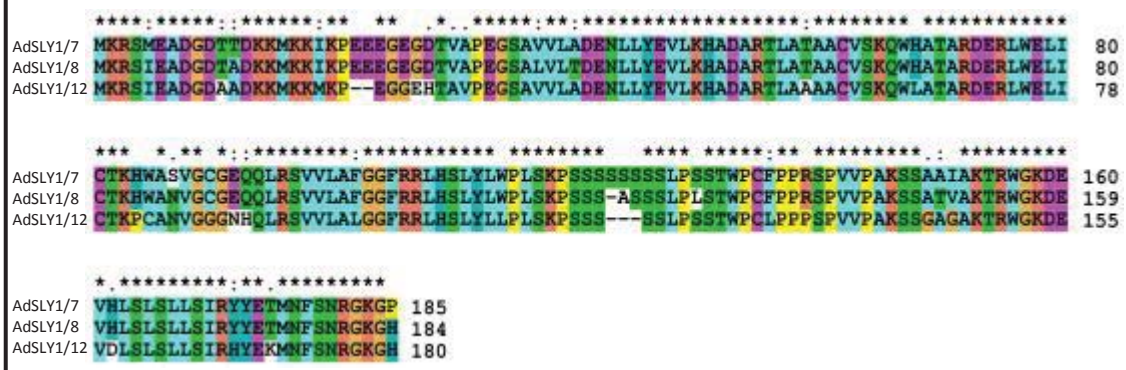

Figure 3.16. *A. deliciosa* SLY1/ GID2 amino acid sequence alignment
Alignment of the *A. deliciosa* SLY1/ GID2 homologue amino acid sequences as translated *in silico* from the full-length mRNA/ EST nucleotide sequences. The alignment was obtained using the Clustal X2 algorithm (Larkin et al., 2007). Symbols: ***** identical; **:** strongly conserved; **.** weakly conserved.

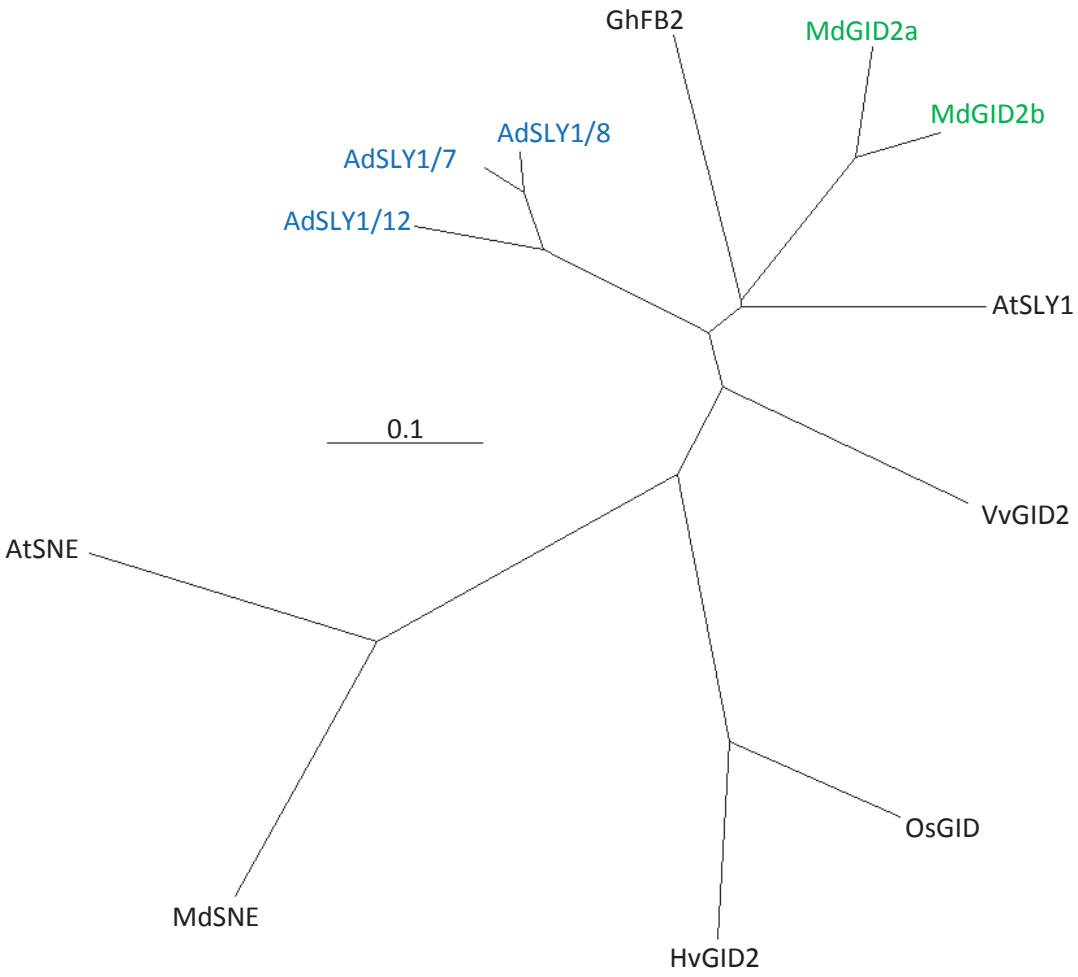

Figure 3.17. Unrooted tree view of SLY1 homologues
Produced from a ClustalX2 amino acid alignment (Larkin et al., 2007) of *in silico* translated full-length *A. deliciosa* and other plant SLY1/GID2 homologue genomic and cDNA sequences. Unrooted tree view produced in TreeView 1.6.6 (Page, 1996). Scale bar is 0.1 amino acid substitution per site.

3.2.2 Quantification of *A. deliciosa* genes encoding DELLA, *GID1* and *SLY1* homologues

In order to understand the expression patterns of *DELLA*, *GID1* and *SLY1* genes throughout the plant, quantification of the corresponding mRNAs was undertaken, using a quantitative PCR (qPCR) approach. This analysis also allowed comparison of the gene expression patterns of different clade members (e.g. *AdRGL1* vs. *AdRGL2* vs. *AdRGL3*), and to compare their expression patterns with the model organism *Arabidopsis thaliana* and a woody perennial, *Malus domestica*. Such a comparison may aid in proposing a particular role to a member that could be later confirmed through experimentation.

The tissues collected for analysis were dormant buds, breaking buds and shoot (vine) tips, female and male flower buds, stamens and styles from mature flowers, expanding leaves and mature leaves, fruit cortex and immature fruit. These tissues were chosen to examine expected places of variation of the amount of transcripts, based on the literature and their roles as repressors of growth and elongation. Of those, insufficient RNA was obtained from mature leaves, immature fruit and stamens. The mature leaf tissue did not yield sufficient mRNA. Immature fruit affected the RNA preparation adversely and this prevented sufficient purification. Similarly, the yield of RNA from the stamen tissue was too low.

RNA preparations without RT enzyme in reaction were used as negative controls, to detect residual genomic DNA or amplicon DNA contamination. Furthermore, reverse transcription with BMV RNA spike was used to examine inhibition of the RT reaction by potential impurities in the RNA sample. PCR amplification without RNA was used to examine handling contamination of preparations and primer-dimer formation. To monitor plate-to-plate qPCR machine run variability, identical RT sample was added to every qPCR plate. Melting curve profile was used to examine amplicon specificity.

3.2.2.1 Kiwifruit Reference gene homologous sequences

Reference genes for qPCR: *PP2A* (*SERINE/THREONINE-PROTEIN PHOSPHATASE 2A*), *UPL7* (*E3 UBIQUITIN-PROTEIN LIGASE 7*) and *ACT7* (*ACTIN7*) were chosen on the basis of findings in (Czechowski et al., 2005) that these are “housekeeping” genes, uniformly and constitutively expressed in all tissues of *Arabidopsis*. Multiple housekeeping genes were used in order to cover a broad range of expression: low (*UPL7*), mid (*PP2A*) and mid to high level (*ACT7*).

These reference genes were identified in the Plant and Food Research kiwifruit EST nr data base (Crowhurst et al., 1999-2011) by searching, using the BLASTn algorithm, for the kiwifruit orthologous sequences to *Arabidopsis* accessions At3g53090 (*UPL7*), At1g13320 (*PP2A*) and At5g09810 (*ACTIN 2/7*). Top hits, chosen for further work, were: EST 101815 for *PP2A*, EST 238886 for *UPL7* and EST 447680 for *ACT 2/7* (Appendix Figures 6.3, 6.4 and 6.5). Oligonucleotides designed based on these ESTs were used to amplify the reference genes, using both genomic DNA and mRNA as templates. Amplified products were cloned into pGEM-T easy vector for sequencing. Alignment against the *Arabidopsis* sequences was performed to map the intron and exon sequences. qPCR primers (Table. 2.2) were designed based on these findings and the primers used in (Czechowski et al., 2005).

3.2.2.2 Determining the primer amplification efficiencies

Amplification efficiency of primer pairs is the key to performing reliable quantitative PCR. Therefore, primer amplification efficiency was determined for each primer pair, using as templates recombinant plasmids containing each quantified CDS. Serial dilutions of plasmid templates were used to generate calibration curves and determine the crossing point for each primer pair. Crossing point values were plotted against the logarithm of the template concentration and the linear regression line was plotted to determine primer efficiencies (Table 3.2, Figures 3.18 and 3.19 and Appendix Figures 6.6, 6.7 and 6.8). Each primer pair that had an efficiency of amplification between 1.8 and 2 was deemed acceptable; if primers gave efficiencies outside of that range, new optimised primers were designed and tested (Nolan, 2006).

Table 3.2. Primer pair efficiencies

Target Amplicon	Primer pair[a]	Slope[b]	Efficiency[c]
***AdRGL1a* (113002)**	D5, 6	-3.514	1.92
***AdRGL1b* (49556)**	E1, 2	-3.661	1.87
***AdRGL1c* (79743)**	C11, 12	-3.474	1.94
***AdRGL2a* (101189)**	A3, 4	-3.625	1.88
***AdRGL2b* (227790)**	A11, 12	-3.849	1.81
***AdRGL3a* (115865)**	C2, 3	-3.436	1.95
***AdRGL3b* (78609)**	B5, 6	-3.414	1.96
***AdGID1b* (200355/4)**	E7, 8	-3.360	1.98
***AdGID1a* (287619/17)**	E11, 12	-3.378	1.97
***AdGID1c* (287619/22)**	F3, 4	-3.518	1.92
AdSLY1/7	F11, 12	-3.599	1.89
AdSLY1/8	G3, 4	-3.426	1.95
AdSLY1/12	F7, 8	-3.394	1.97
AdPP2A	G5, 6	-3.376	1.97
AdUPL7	G7, 8	-3.346	1.99
AdACT C	G9, 10	-3.795	1.83
AdACT N	G11, 12	-3.808	1.83
BMV	F, R	-3.464	1.94

[a] Primer sequences are listed in Table 2.2.
[b] The linear regression line slope is determined by plotting the logarithm of relative template concentration against the crossing point (Cp, quantitation cycle) values determined from each of the amplifications.
[c] Primer pair efficiencies were calculated from the linear regression line slope with the equation; efficiency=$10^{(-1/\text{Slope})}$.

A.

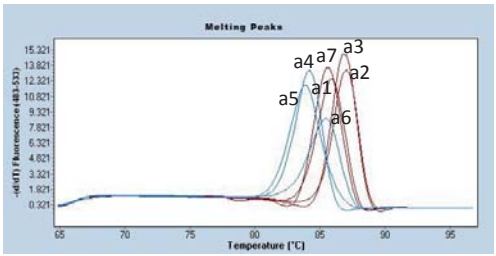

B.

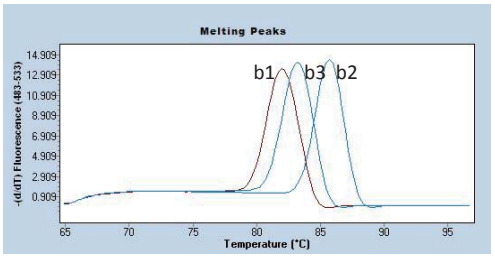

C.

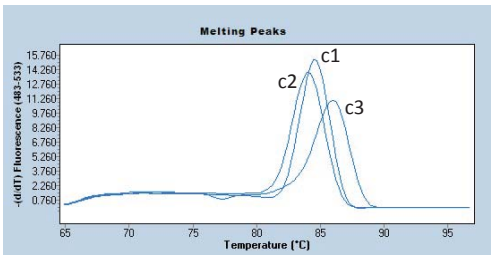

D.

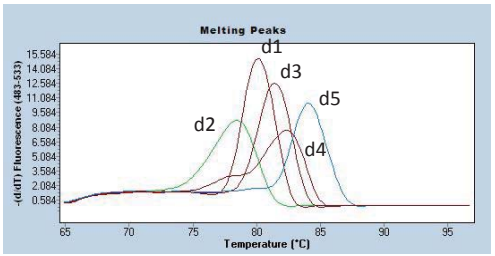

Figure 3.18. Amplicon Melting profiles
Following the completion of the amplification cycles of the qPCR melting curve for each reaction was determined, represented as -dFluorescence/dT (y axis) against temperature (x axis).
A, DELLA homologues; **a1,** *AdRGL1a* (113002); **a2,** *AdRGL1b* (49556); **a3,** *AdRGL1c* (79743); **a4,** *AtRGL2a* (101189); **a5,** *AdRGL2b* (227790); **a6,** *AdRGL3a* (115865); **a7,** *AdRGL3b* (78609).
B, *GID1* homologues; **b1,** *AdGID1a* (287619/17); **b2,** *AdGID1b* (200355/4); **b3,** *AdGID1c* (287619/22).
C, *SLY1* homologues; **c1,** *AdSLY1 /7*; **c2,** *AdSLY1 /8*; **c3,** *AdSLY1 /12.*
D, Reference genes; **d1,** BMV; **d2,** *AdPP2A*; **d3,** *AdUPL7*; **d4,** *AdACTIN* C; **d5,** *AdACTIN* N.

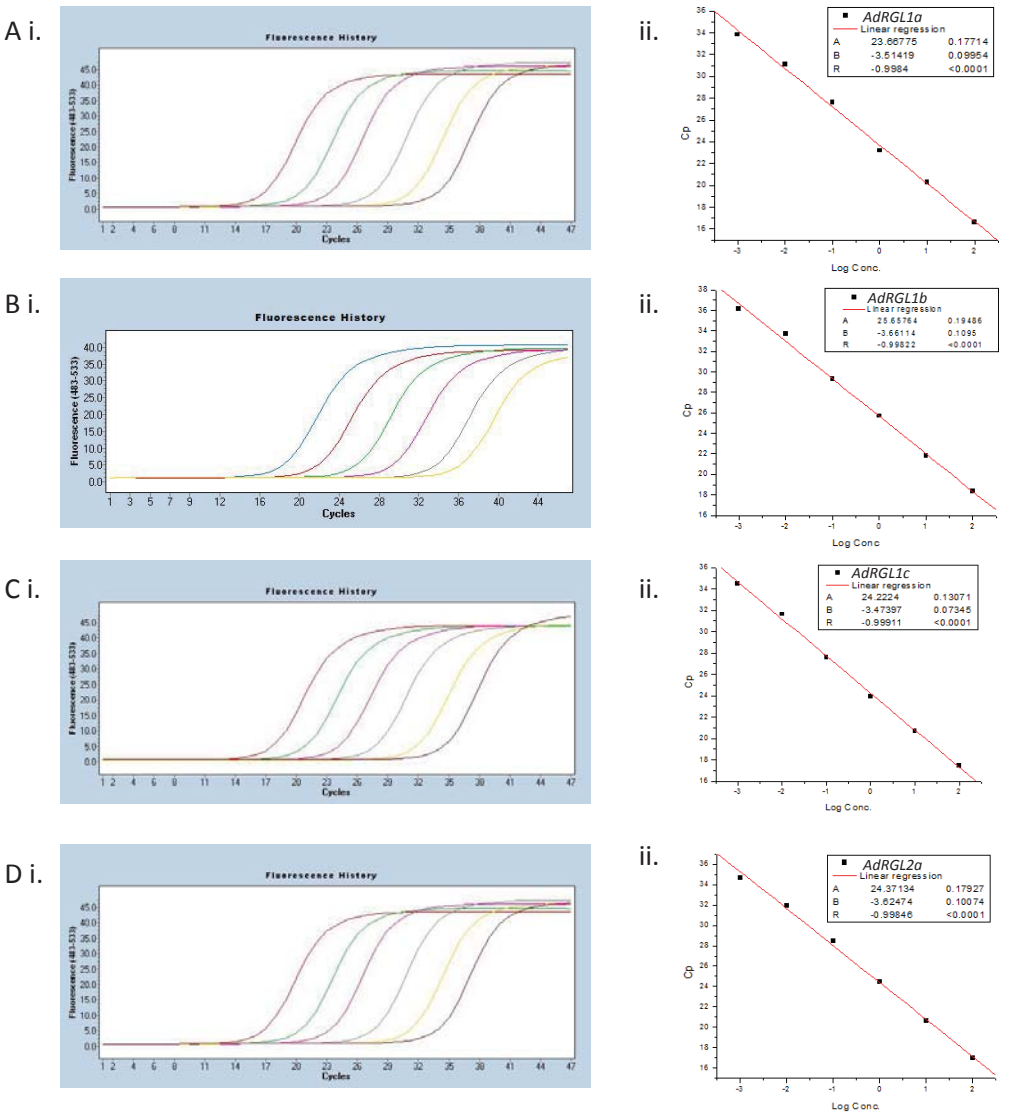

Figure 3.19. *A. deliciosa* DELLA homologue amplifications and standard curve linear regression plots

Determination of the PCR amplification efficiency for *AdDELLA* amplicon primer pairs. The amplification fluorescence threshold crossing point of the amplicon was plotted against the logarithm of the relative template concentrations. A linear regression line was fitted and the slope of the line determined in the Origin graphing application (OriginLab corp. USA). The efficiency of the amplification was calculated from the equation; efficiency $=10^{(-1/\text{Slope})}$.

A, *AdRGL1a*; **B,** *AdRGL1b*; **C,** *AdRGL1c*; **D,** *AdRGL2a*.

i, Graph of fluorescence vs. cycle of each of the six amplifications of a template dilution series; **ii,** Graph of crossing point versus Log of the relative target DNA concentration. **Inset**: B=Slope of the linear regression line with error, R= Fit of regression line with error, A=Crossing point on x axis (at 0) with error.

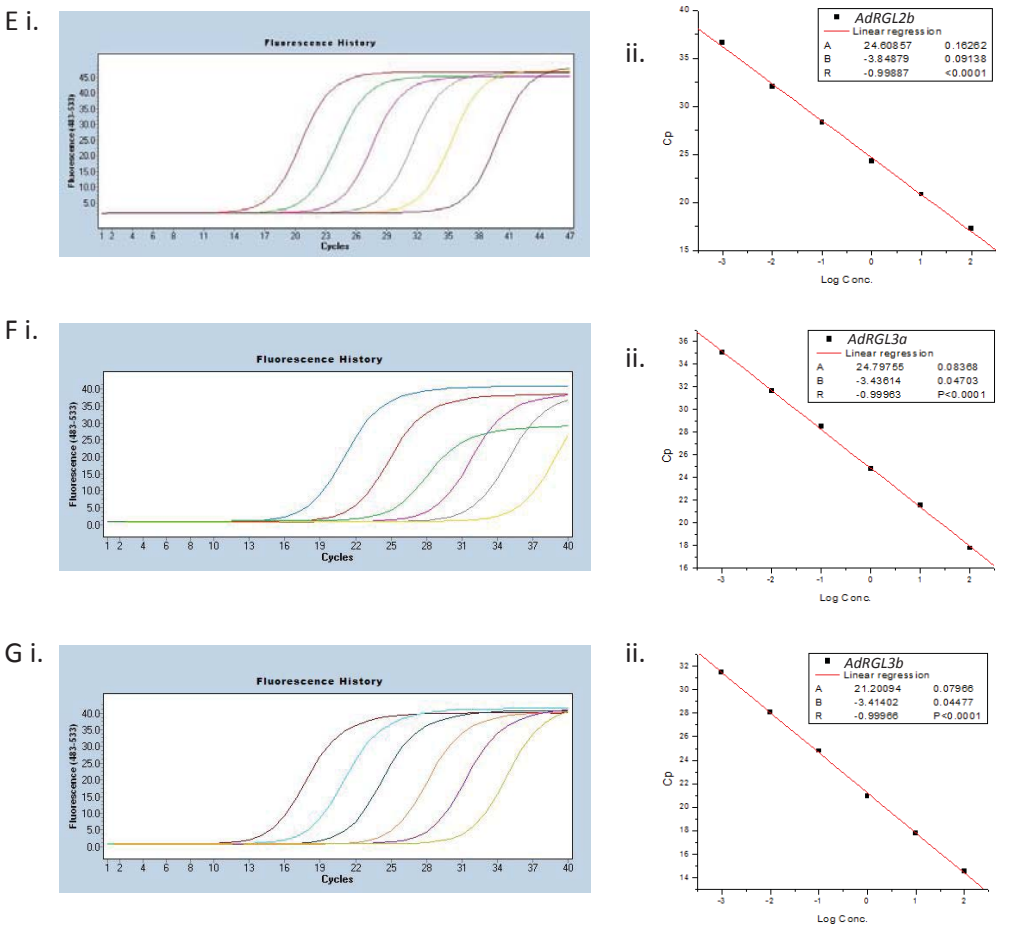

Figure 3.19. *A. deliciosa* DELLA homologue amplifications and standard curve linear regression plots

Determination of the PCR amplification efficiency for *AdDELLA* amplicon primer pairs. The amplification fluorescence threshold crossing point of the amplicon was plotted against the logarithm of the relative template concentrations. A linear regression line was fitted and the slope of the line determined in the Origin graphing application (OriginLab corp. USA). The efficiency of the amplification was calculated from the equation; efficiency $=10^{(-1/\text{Slope})}$.

E, *AdRGL2b*; **F,** *AdRGL3a*; **G,** *AdRGL3b*.

i. Graph of fluorescence vs. cycle of each of the six amplifications of a template dilution series.

ii. Graph of crossing point versus Log of the relative target DNA concentration. Inset: B=Slope of the linear regression line with error, R= Fit of regression line with error, A=Crossing point on x axis (at 0) with error.

3.2.2.4 qPCR results

qPCR amplification was carried out on all the target genes and the reference genes in technical triplicates for each biological replicate on a single 96 well plate. The normalisation and calculations of relative expression (compared to reference genes; Figures 3.20, 3.21, 3.22, 3.23, 3.24, and 3.25 and Tables 3.3 and Appendix Figures 6.9, 6.10, 6.11, 6.12 and Appendix Table 6.1) were performed using a web based software package, QPCR (Pabinger et al., 2009) and expressed as CNRCq (crossing point values of target genes normalised to the reference genes and plate-to-plate variation; for definitions and calculations, please refer to Appendix Table 6.1 footnotes). The QPCR programme was based upon the equations published in (Hellemans et al., 2007).

The transcript levels in two biological replicates of each sample were quite different for many of the tissues. The tissue samples were collected so that morphologically, they appeared to be at a similar developmental stage. However, given that the biological replicates were sampled on different days (up to 28 days apart), and from different plants, the results may indicate that the transcripts are different in these tissues and that, despite similar morphologies, tissues are, in fact, physiologically in different stages in those samples. For example, the breaking bud tissue undergoes a period of swift changes from dormancy to constant growth. In this state, a high flux in transcript levels of genes involved in development, including the core GA signalling genes, are expected. The pairs of data from the same tissue are presented in chronological order of harvest (left - first harvest, then right - second harvest, of the biological replicates) for each tissue type (Figures 3.20Ai, Bi, C1, 3.21A, 3.22A, 3.23A, and 3.24A).

The levels of each *AdDELLA* transcripts were, on the whole, higher in expanding leaves and shoot tips, at a mid-level in floral buds and at a yet lower level in the remaining tissues (Figures 3.20 to 3.22). This is in contrast to apple *DELLA* transcripts, which are generally the lowest in the growing shoots and expanding leaves. The amounts of the *AdDELLA* transcripts, however, do not necessarily indicate a strong repression of target genes by DELLA proteins, as the main point of DELLA activity regulation during signalling is post-translational: proteasome-dependent proteolysis, triggered by interaction by GID1-GA complex. Additional level of control is modulation of GA-dependent post-translational modifications.

The levels of *GID1* and *SLY1* homologues in expanding tissues that contained high levels of *AdDELLA* transcript (except *GID1* in expanding leaves 2) were also higher than in most other

tissues (Figures 3.23 and 3.24); this finding indicates that the level of GA signalling is very high in these tissues and that DELLA proteins in these tissues may be low or inactive. Quantification of AdDELLA proteins and their (as yet unknown) post-translational modifications will be required for a more complete assessment of DELLA activity in these tissues.

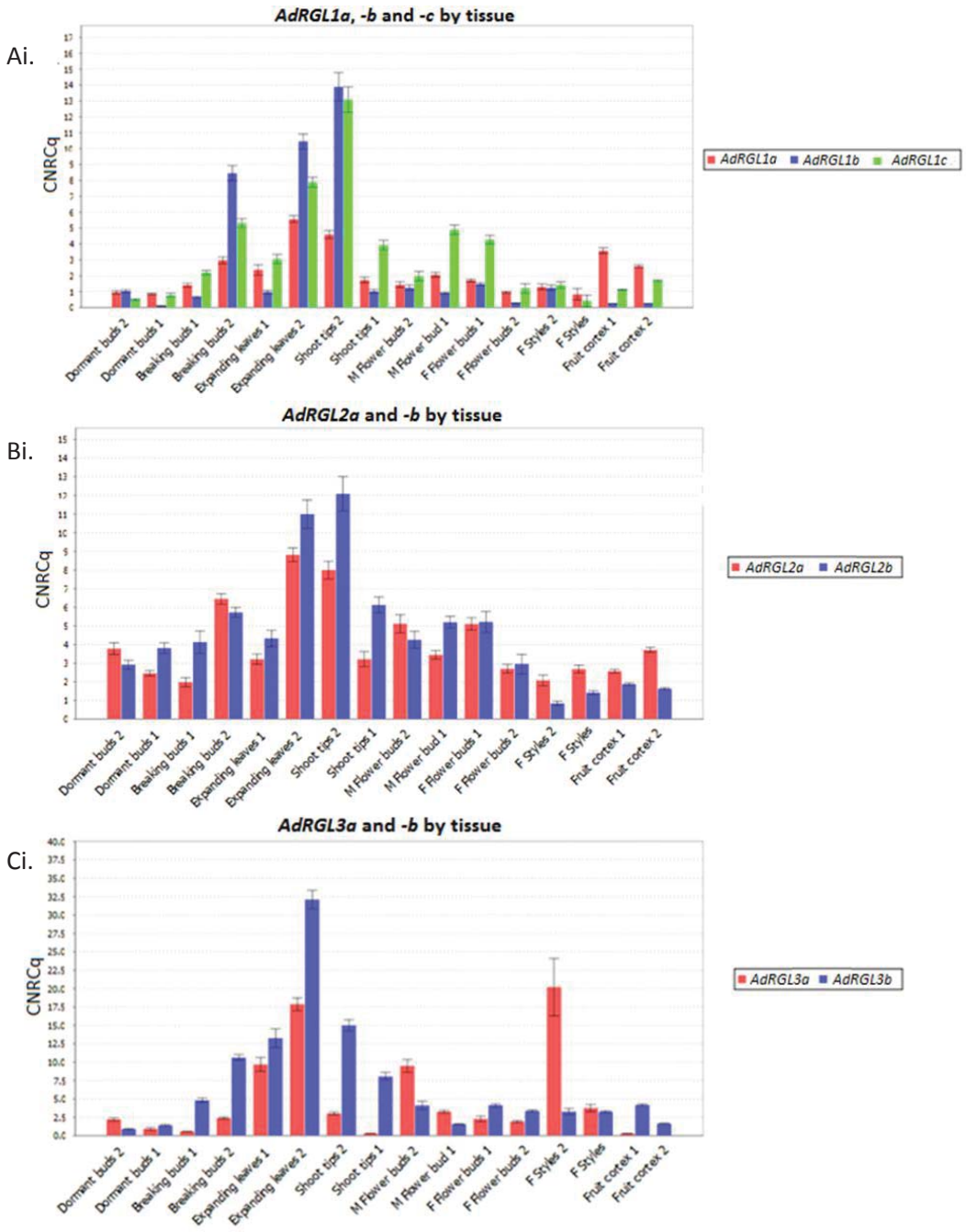

Figure 3.20. Relative expression (CNRCq) of the DELLA kiwifruit homologues by *AdRGL* group

Bar graphs representing the transcript expression levels of the *AdDELLAs* compared to the genorm (geometric averaging) of the reference genes (*AdPP2A*, *AdUPL7* and *AdACT2/7* -C). The quantitation cycle (crossing point) was determined by the AnalyzerMiner algorithm (Zhao and Fernald, 2005). The kiwifruit technical replicates were averaged and PCR efficiency was corrected for using the standard curve data. Genes were normalised against the reference genes and calibrated to account for inter-assay variability within the QPCR application. Standard error bars 1.0 (Pabinger et al., 2009). **A,** *AdRGL1*s; **B,** *AdRGL2*s; **C,** *AdRGL3*s; **i,** by tissue.

Aii.

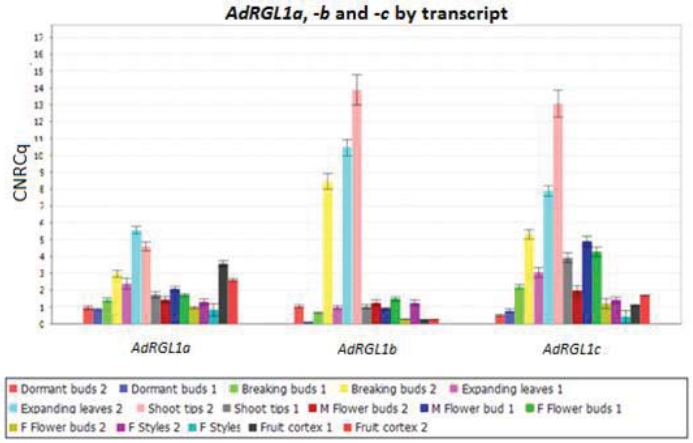

Bii.

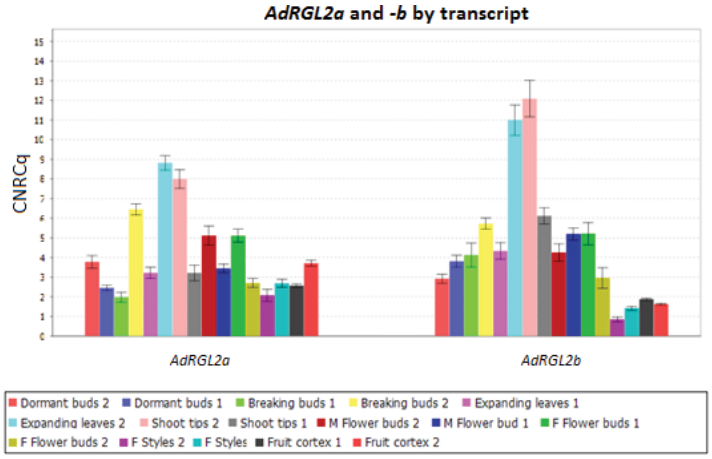

Cii.

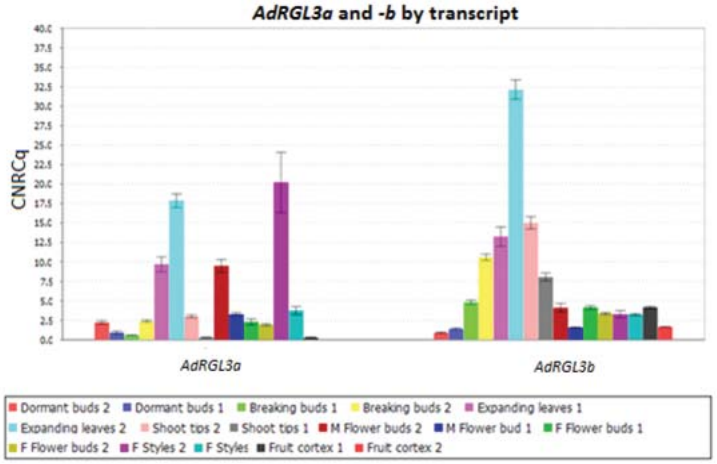

Figure 3.20. continued. Relative expression (CNRCq) of the DELLA kiwifruit homologues by *AdRGL* group
A, *AdRGL1*s; **B,** *AdRGL2*s; **C,** *AdRGL3*s; **ii,** by transcript.

A.

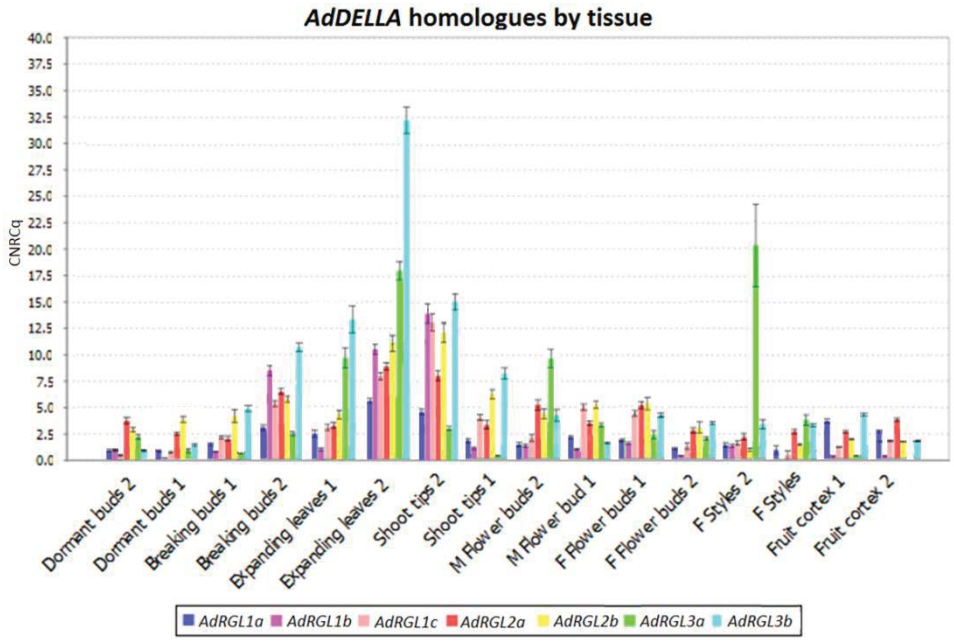

B.

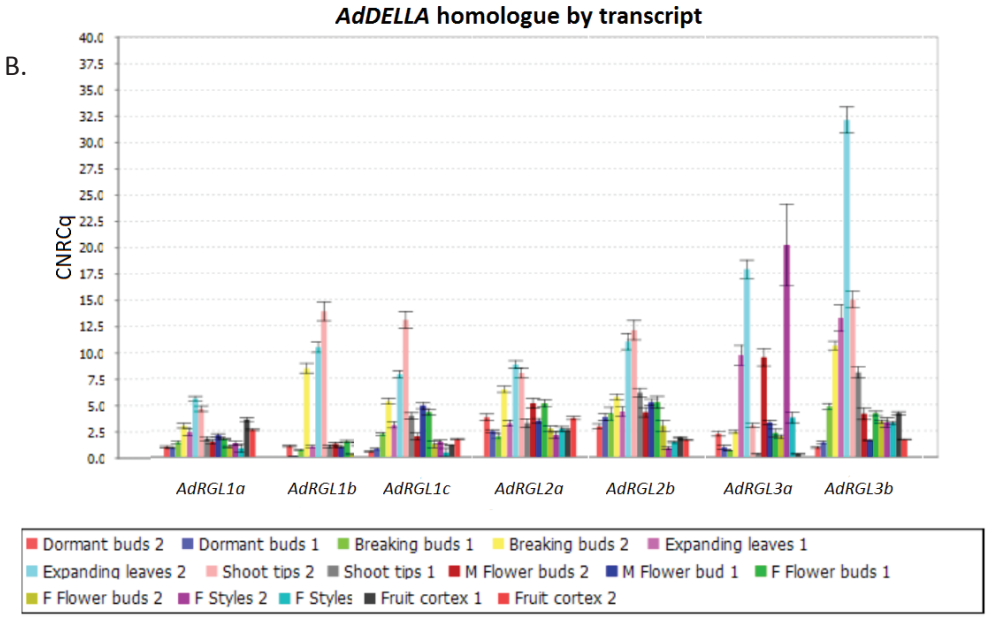

Figure 3.21. Relative expression (CNRCq) of the DELLA kiwifruit homologues by tissue and transcript

Bar graphs representing the transcript expression levels of all the *AdDELLAs* compared to the genorm (geometric averaging) of the reference genes (*AdPP2A*, *AdUPL7* and *AdACT2/7* -C). The quantitation cycle (crossing point) was determined by the AnalyzerMiner algorithm (Zhao and Fernald, 2005). The kiwifruit technical replicates were averaged and PCR efficiency was corrected for using the standard curve data. Genes were normalised against the reference genes and calibrated to account for inter-assay variability within the QPCR application. Standard error bars 1.0 (Pabinger et al., 2009).

A, by tissue; **B,** by transcript.

A.

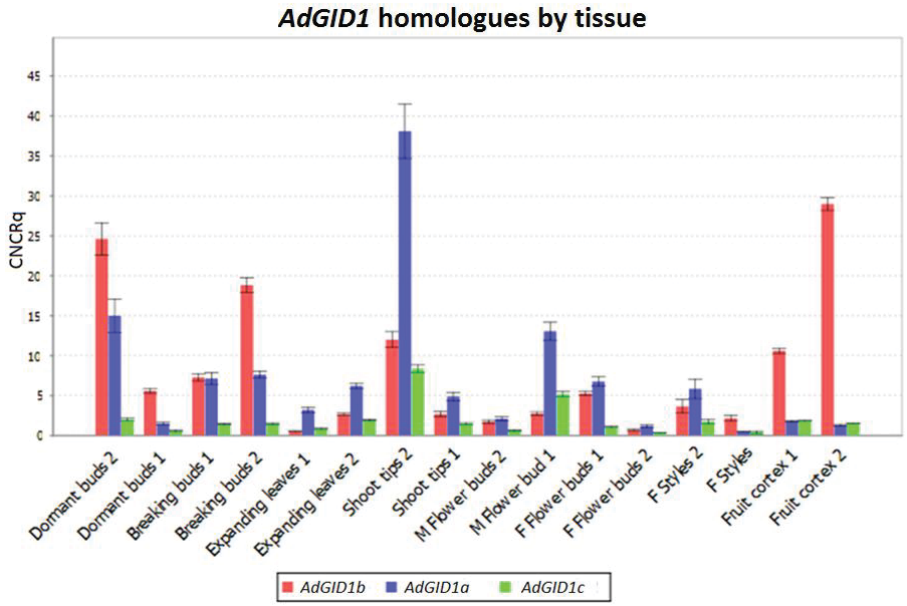

B.

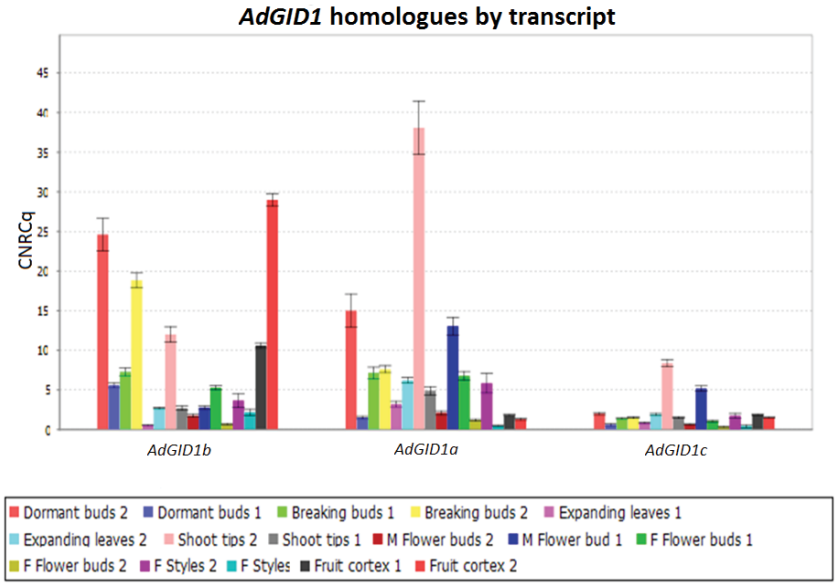

Figure 3.22. Relative expression (CNRCq) of *GID1* kiwifruit homologues, by tissue and transcript

Bar graphs representing the transcript expression levels of all the *AdGID1s* compared to the genorm (geometric averaging) of the reference genes (*AdPP2A*, *AdUPL7* and *AdACT2/7* -C). The quantitation cycle (crossing point) was determined by the AnalyzerMiner algorithm (Zhao and Fernald, 2005). The kiwifruit technical replicates were averaged and PCR efficiency was corrected for using the standard curve data. Genes were normalised against the reference genes and calibrated to account for inter-assay variability within the QPCR application. Standard error bars 1.0 (Pabinger et al., 2009).

A, by tissue; **B,** by transcript.

A.

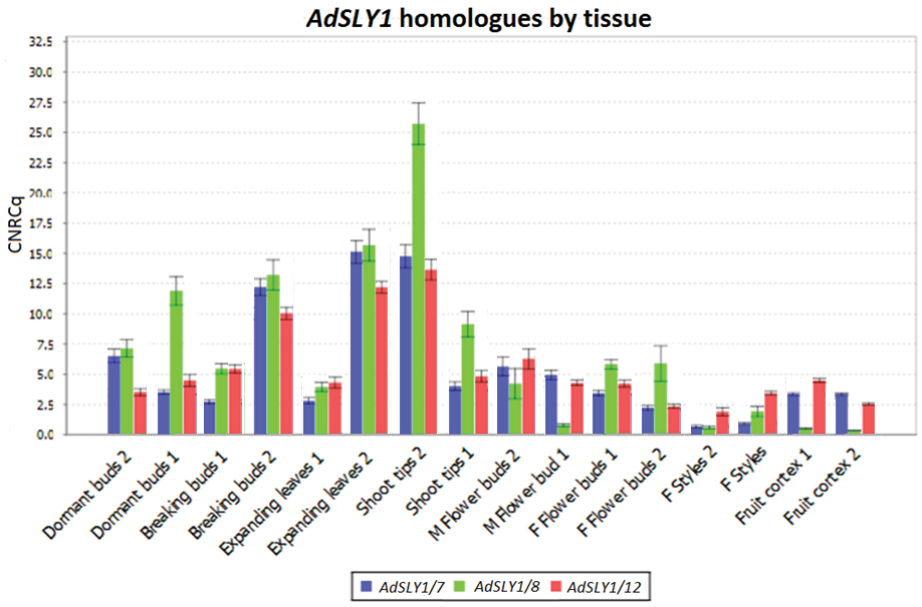

B.

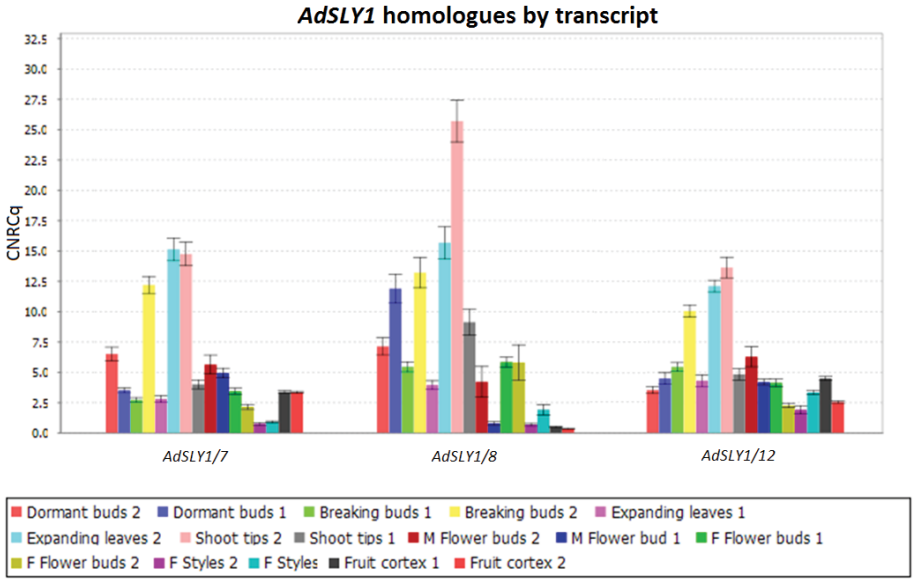

Figure 3.23. Relative expression (CNRCq) of *SLY1* kiwifruit homologues by tissue and transcript

Bar graphs representing the transcript expression levels of all the *AdSLY1s* compared to the genorm (geometric averaging) of the reference genes (*AdPP2A*, *AdUPL7* and *AdACT2/7* -C). The quantitation cycle (crossing point) was determined by the AnalyzerMiner algorithm (Zhao and Fernald, 2005). The kiwifruit technical replicates were averaged and PCR efficiency was corrected for using the standard curve data. Genes were normalised against the reference genes and calibrated to account for inter-assay variability within the QPCR application. Standard error bars 1.0 (Pabinger et al., 2009).

A, by tissue; **B,** by transcript.

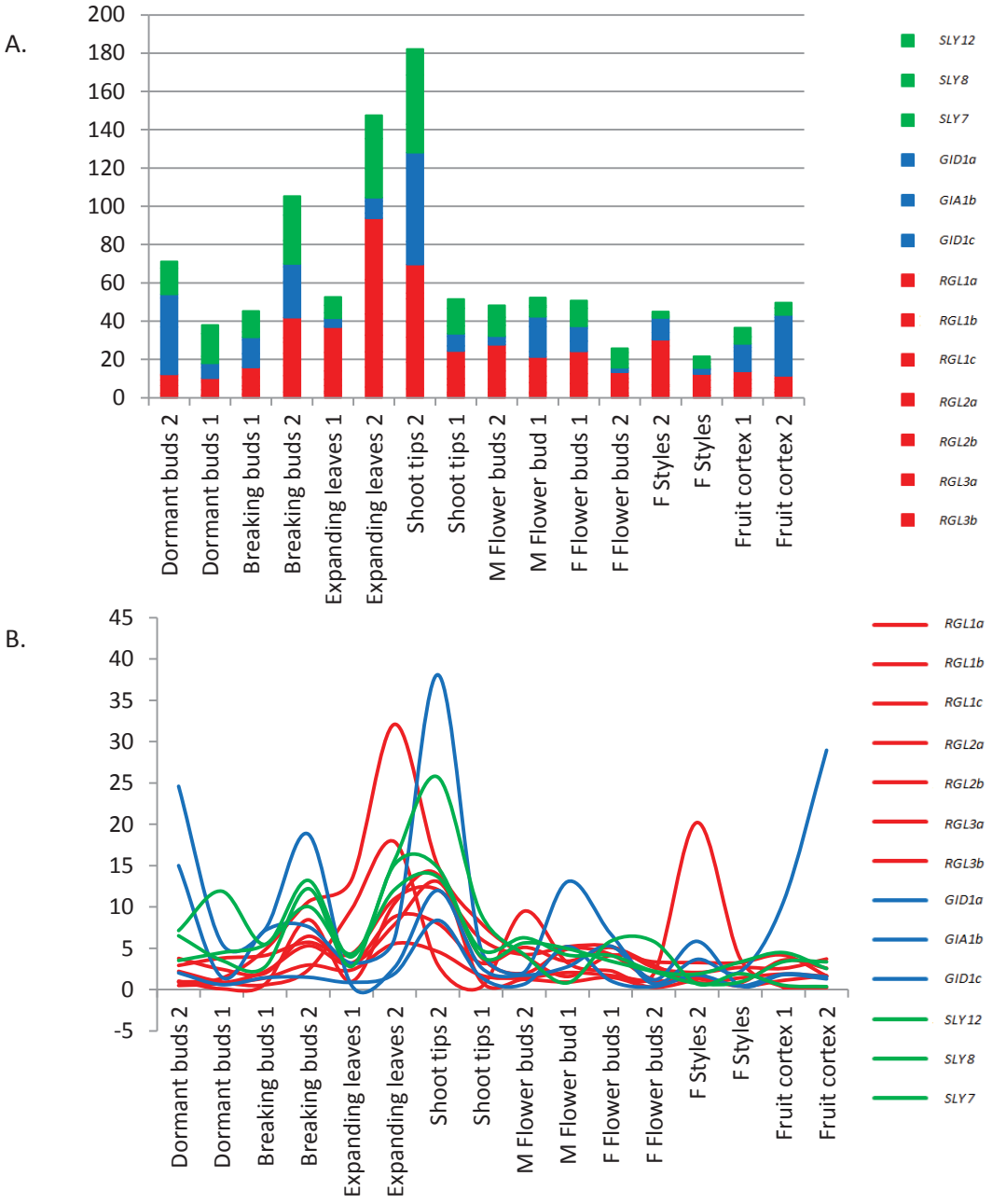

Figure 3.24. View of all target gene expression profiles
Relative transcript expression (CNRCq) of all the kiwifruit target genes compared to the genorm (geometric averaging) of the reference genes (*AdPP2A*, *AdUPL7* and *Ad*ACT2/7).
A, Additive bar graph; **B,** Individual overlapping line graph.
AdDELLA homologues, *AdGID1* homologues, *AdSLY1* homologues.

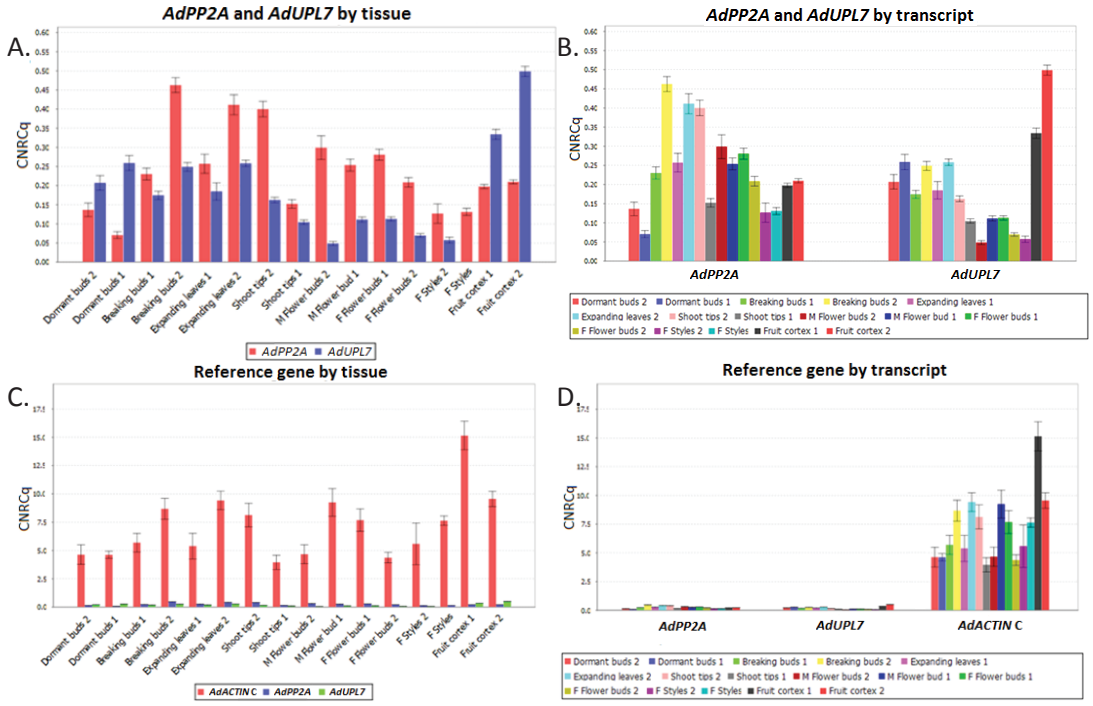

Figure 3.25. Relative expression of the individual kiwifruit reference genes
Bar graphs representing the transcript expression levels of the kiwifruit reference gene compared to the genorm (geometric averaging) of the reference genes (*AdPP2A*, *AdUPL7* and *AdACT2/7* -C). The quantitation cycle (crossing point) was determined by the AnalyzerMiner algorithm (Zhao and Fernald, 2005). The kiwifruit technical replicates were averaged and PCR efficiency was corrected for using the standard curve data. Genes were normalised against the reference genes and calibrated to account for inter-assay variability within the QPCR application (CNRCq) . Standard error bars 1.0 (Pabinger et al., 2009).
A, *AdPP2A* and *AdUPL7* by tissue; **B,** *AdPP2A* and *AdUPL7* by transcript; **C,** All by tissue; **D,** All by transcript.

Table 3.3. Reference gene Coefficient of variation (CV) and gene stability measure (M) values

	CV[a]	M[b]
***ACTIN* C**	77.33 %	0.7469
PP2A	41.27 %	0.9385
UPL7	47.08 %	0.9907
Mean	55.23 %	0.892

[a]Coefficient of variation of the normalised reference gene expression levels.
[b]M value (geNorm) represents the mean stability measure of the reference genes. The coefficient of variation (CV) percentage and the gene stability value (M) are a measure to gauge reference gene expression fluctuation. For stably expressed reference genes you expect CV < 25 % and M < 0.5. The CV and M values are calculated within the QPCR application (Pabinger et al., 2009). These reference genes would be considered outside the range of reference genes chosen for robust geometric normalisation (geNorm) of qPCR data.

Both *AdRGL2* group transcripts *(AdRGL2a* and *AdRGL2b*) show a less variable level of expression across all the tissues examined than *AdDELLA* transcripts of the other two clades. This may indicate that the *AdRGL2*'s act as basal repressors for the plant, an action *Arabidopsis* DELLA protein GAI has been proposed to perform, as underlying control over all-out development. However, the AdRGL2's do not group with the AtGAI, but rather with AtRGLs, which in *A. thaliana* have more variable expression levels than does *AtGAI* and are proposed to provide additional repression which is relieved during particular developmental events (Tyler et al., 2004). The *AdRGL1* group transcripts are in the same DELLA protein clade as *Arabidopsis AtRGA*/ *AtGAI*. Interestingly, these two DELLA genes do have an overall lower relative expression levels in comparison to other groups in most tissues. This is particularly the case with *AdRGL1a*, whose pattern of tissue-specific expression is similar to *AdRGL2a/b*. *AdRGL1b/c*, however, express highly in some tissues: *AdRGL1b* in breaking buds 2, expanding leaves 2 and shoot tips 1, and *AdRGL1c* in expanding leaves 1 and 2 and the styles 2. The *AdRGL3*'s show the highest levels of relative expression and greatest variation in relative levels.

Among the *AdGID1* transcripts, *AdGID1a* and *AdGID1c* expression pattern is very similar except that *AdGID1c* is at a relatively much lower expression level in all the tissues examined (Figures 3.22 and Appendix Figure 6.10). The expression pattern of *AdGID1b* is quite different and somewhat complementary to the *AdGID1 a/c* expression pattern. Of the *GID1* homologues no particular pattern in expression stands out in relation to vegetative or floral tissue dominance.

The *AdSLY1* homologues all have a similar expression profile and no particular CDS has dominant level of expression (Figures 3.23 and Appendix Figure 6.11). The *AdSLY1* homologue relative expression levels tended to be correlated with the *GID1* homologue expression levels.

Cumulative expression levels of genes encoding all three core GA signalling components were highest in breaking buds 2, expanding leaves 2 and shoot tips 2 (Figure 3.24); the expression levels in all other tissues were moderate. Overall, this means that the transcript amount is a resultant of complex regulatory networks and that each of the genes is expressed in all tested tissues, playing at least a minimal role in development of each organ.

Despite the widespread use of the chosen reference genes, in *Actinidia deliciosa* their expression was not as even across all tissues as expected, and therefore they are not ideal normalisation candidates (Figure 3.25, Appendix Figure 6.12 and Table3.3).

3.2.3 Immunogenic properties of *A. deliciosa* DELLA proteins

To examine the relationships between the kiwifruit DELLA (AdDELLA) proteins, and the *Arabidopsis* and *Malus* DELLA (MdDELLA) proteins, cross-reactivity of the kiwifruit DELLA proteins to monoclonal antibodies raised against conserved motifs, as well as against native DELLA proteins of *A. thaliana* and *M. domestica,* was analysed. Antibodies recognise the tertiary conformation of a protein and may therefore detect a commonality in 3-dimensional structure where the primary sequence analysis may not indicate one may exist (Tables 3.4 and 3.5) (Sun et al., 2010).

Table 3.4. Monoclonal antibody epitopes and antigens

Antibody designation [a]	Raised against / Specificity (epitope)[c]
BC9	At DELLAs / All At & Md DELLAs (DELL[A]VLGYKVR [b])
5E1	Peptide DELLAVLGYK / All At & Md DELLAs (DELL[A]VLGYKVR)
6C8	Peptide DELLAVLGYK / AtRGA1, AtRGL1,2, All Md (DELL[A]VLGYKVR)
AF2	AtDELLAs / GAI (N-terminal domain)
AD7	AtDELLAs / AtRGL's 1,2,3 (HYNPSDLxxW)
AB8	AtDELLAs / AtRGL1 (N-terminal domain)
BB7	AtDELLAs / AtRGL2 (N-terminal domain)
1C3	AtDELLAs / AtRGL3 (N-terminal domain)
D1F10	MdDELLAs / MdRGL1 (N-terminal domain)
A4C11	MdDELLAs / MdRGL2 (N-terminal domain)
A1B1	MdDELLAs / MdRGL3 (N-terminal domain)
G10	Peptide CPYLKFAHFTANQ / All At & Md DELLAs (C-terminal domain)
D9	R-tag peptide / Negative control

[a] A tabularised summary of the antigens or epitope of the suite mAbs. An alanine-scanning experiment involving the mAbs BC9, 5E1 and 6C8 was used to reveal the specific epitopes within the antigens. The remaining mAbs were screened by ELISA to confirm their specificity to *Arabidopsis* and Apple DELLA homologues.
[b] Residue olouring refers to the results of alanine scanning of the peptide to determine the contact residues. Black residue, no loss of binding; Green residue - 40% loss of binding; Red residue, 100% loss of binding when alanine substitution made.
[c] Coding sequences of antigens were amplified and cloned by C. Kirk into expression vectors; R tag peptide was designed by C. Kirk; antigens were expressed and purified by N. Frearson, X. Sun and C.Kirk; peptides were commercially produced by order; monoclonal antibodies were raised by W. Jones and D. Harvey and characterised by W. Jones, D. Harvey and D. Sheerin [This work; (Sheerin et al., 2011, Sun et al., 2010)].

Table 3.5. Monoclonal antibody-DELLA cross reactivity

DELLA	Monoclonal antibody designation[b]											
	BC9	5E1	6C8	AF2	AD7	AB8	BB7	1C3	D1F10	A4C11	A1B1	D9
AtRGA	+++[a]	+	+	-	-	-	-	-	-	-	-	-
AtGAI	+++	++	-	+++	-	-	-	-	-	-	-	-
AtRGL1	+++	++	-	-	+++	+++	-	-	-	+	-	-
AtRGL2	+++	++	+	-	+++	-	+++	-	-	-	-	-
AtRGL3	+++	+++	++	-	+++	-	-	+++	-	+++	-	-
MdRGL1	+++	+++	+++	-	+	-	-	-	+++	-	+	-
MdRGL2	+++	+++	+	-	+++	-	++	-	-	+++	-	-
MdRGL3	++	+++	+++	-	+++	-	-	+	-	-	+++	-

[a] **+++** strong recognition, **++** medium recognition, **+** weak recognition, **-** no recognition.

[b] Analyses of the monoclonal antibody cross reactivity toward *Arabidopsis* and Apple DELLA recombinant proteins based on ELISA results. Antigen-encoding sequences were amplified and vectors constructed by C. Kirk. *A. deliciosa* recombinant proteins were expressed and purified by C. Kirk; *A. thaliana* and *M. domestica* proteins for immunisations were expressed and purified by N. Frearson, X. Sun and C. Kirk; monoclonal antibodies were raised by W. Jones and D. Harvey and characterised by W. Jones, D. Harvey and D. Sheerin [This work; (Sun et al., 2010)].

The full-length DELLA homologue open reading frames from *A. deliciosa* were amplified by PCR from genomic DNA (the primers are listed in Table 2.2). The CDSs were cloned into expression vector pETM MBP R. The R stands for a novel peptide tag that is designed and constructed as part of this PhD thesis and used to produce high-affinity cognate R-tag-specific monoclonal antibody D9 [Section 2.2.3; (Sun et al., 2008)]. In this recombinant vector, an N-terminal His tag and maltose binding protein (MBP) tag are translationally fused to the full-length kiwifruit DELLA proteins, and expressed under control of the *lac* operator/T7 promoter in *E. coli*. The transcription of the fusion cassette was mediated by T7 RNA polymerase expressed from the *lac* promoter. The AdDELLA-MBP fusion proteins were affinity purified using immobilised amylose resin, and concentrated. The full length DELLA proteins readily degrade and form quasi-soluble microaggregates that could not be purified and separated by native PAGE (data not shown). Hence the purified AdDELLA-MBP fusion proteins were separated by denaturing acrylamide gel electrophoresis (SDS-PAGE) and western blotted in order to analyse their recognition by a battery of monoclonal antibodies against DELLA proteins (Figure 3.27). Only the C-terminal domain of the DELLA proteins is insoluble, whereas the N-terminaldomain is highly soluble and intrinsically unstructured along most of its length. Therefore, it is expected that the N-terminal domains, recognised by monoclonal antibodies, assume a native (unstructured) conformation after blotting to the membranes.. For the purpose of this analysis the N-terminal domains of purified AdDELLA proteins are therefore considered to be in a native conformation. Blotted AdDELLA proteins exposed to the monoclonal antibodies raised against *M. domestica* (mAbs D1F10, A4C11, and A1B1) and *A. thaliana* (mAbs BC9, AF2, AB8, BB7 and 1C3) mixtures of DELLA proteins (N-terminal domains), as well as antibodies raised against synthetic peptides with the consensus sequence of conserved DELLA protein motifs, two against the N-terminal DELLA motif DELLAVLGYK (mAbs 5E1 and 6C8) and one against the C-terminal motif CPYLKFAHFTANQ (mAb G10) (epitopes are given in Figure 3.26 and Table 3.4)(Sheerin et al., 2011, Sun et al., 2008, Sun et al., 2010).

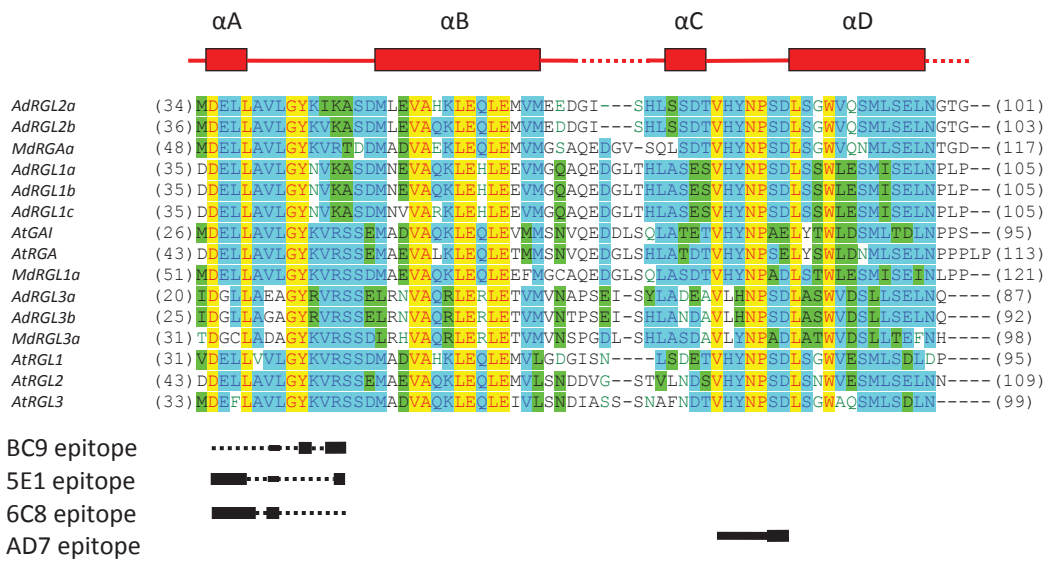

Figure 3.26. DELLA N-terminal domain conserved elements I and II alignment
Alignment of DELLA protein N-terminal domain conserved sequence elements. Known epitopes of the mAbs BC9, 5E1, 6C6 and AD7 are indicated below the alignment in **black lines**. Thickness of the bar indicates importance of the residue for mAb binding recognition (Sheerin et al., 2011, Sun, 2010).
A. deliciosa and *M. domestica* DELLA N-terminal domain amino acid sequences as translated *in silico* from the full-length mRNA/ EST sequences (sections 3.1.1 and 3.2.1). Other DELLA protein sequences were obtained from the NCBI database.
The secondary structures of AtGAI are represented with: **Red bars,** α-helicies; **solid lines,** loops; and **dotted lines,** disordered residues as presented in (Murase et al., 2008).
The alignment was made in the Clustal X2 algorithm (Larkin et al., 2007).
Epitopes of monoclonal antibodies were mapped by W. Jones, D. Harvey and D. Sheerin.

Recognition of apple and Arabidopsis DELLA proteins by monoclonal antibodies was compared to the pattern of recognition of the kiwifruit DELLA proteins (Tables 3.5 and 3.6 and Figure 3.27). The BC9 mAb detects all the *Arabidopsis* and *Malus* DELLA proteins strongly, with the exception to MdRGL3 where there is a small decrease in signal. In contrast, recognition of AdDELLAs is overall much weaker, with a complete lack of signal for AdRGL3a. 5E1 mAb also detects all the proteins, however it has a smaller response to the *Arabidopsis* DELLAs. In contrast, recognition of AdDELLA by 5E1 was relatively much stronger than that of BC9. 6C8 mAb does not recognise AtGAI and AtRGL1 but does detect all other proteins, including the AdDELLAs, to various degrees. The AdRGL3's and AtRGA/ AtGAI are more comparable in that they are detected in a similar pattern by this suite of mAbs, but are in distinct sequence-derived clades. These results do not fit particularly well with the sequence determined relationship clades. As the epitope of the antibodies corresponds to a short number of nearly sequential amino acids, the recognition emphasizes relationship focused on particular epitopes, rather than overall sequence.

The key epitope residues of mAbs 5E1 and 6C8 are D-E-L (of the hallmark DELLA motif). Western blotting of expressed kiwifruit DELLA proteins showed that these antibodies have the weakest detection of the AdRGL3a/ b, consistent with a change in the canonical DELLA motif to DGLLA, however they detect MdRGL3 which has a further altered motif DGCLA. Furthermore, mAb 6C8 does not detect AtGAI and AtRGL1 that have conserved DELLA motif and therefore contain all three residues of the 6C8 epitope. Based on all these observations, there does appear to be an unknown important sequence-independent component in the epitopes; perhaps the conformation of the protein backbone, rather than the presence of specific side chains.

AD7 does not detect AtRGA and AtGAI, and has poor detection of MdRGL1, but detects the other proteins strongly, including all AdRGL1s and AdRGL2s, with a low signal for AdRGL3s (Figure 3.27). The mAb AD7 epitope is within the VHYNP motif, which in the weakly-recognised AdRGL3a, b is less conserved than in AdRGL1a/ b/ c and AdRGL2a/ b. Based on the three-dimensional modelling using known structure of AtGAI as a template, two altered amino acids in AdRGL3a/ b have one change in the contact residue (YNPSD to HNPSD), whereas AdRGL2a, b changes are not in the contact residues, but rather in the residues that are likely to change the conformation of the protein in this area, and therefore mAb recognition. The 3D structure modelling was undertaken in Section 3.3 to investigate the influence of the changes in conserved motives of apple and kiwifruit DELLA proteins on conformation.

The mAbs AB8, BB7 and 1C3 show no cross reactivity to the AdDELLAs. These mAbs were screened for and chosen for their specificity to AtRGL1, AtRGL2 and AtRGL3 respectively. Their exact epitopes are undetermined.

The mAbs produced by immunisation with N-terminal domains of MdDELLA proteins (D1F10, A4C11 and A1B1) show some cross reactivity toward the AdDELLAs. However, they do not show congruency in their clade specificity between MdDELLAs and AdDELLAs. This finding suggests that dominant surface epitopes, which represent exposed portions of the N-terminal DELLA domains in three dimensions, do not follow the primary sequence-based relationships between apple and kiwifruit DELLA proteins. These are localised structural changes, however, and epitope recognition does not necessarily represent a broad structural picture.

In particular, mAb D1F10 (epitope unknown; within the N-terminal domain), which was produced with MdRGL1 as immunogen and screened for the same specificity, detects one of the AdRGL1a, but not AdRGL1b. The AdRGL1 interestingly lies in the same sequence clade as MdRGL1, however AdRGL1a is also detected by mAb A1B1, produced by immunisation and screening with MdRGL3. Furthermore, A1B1 detects weakly one AdDELLA in each primary-sequence-derived clade. mAb A4C11, produced by immunisation with MdRGL2 N-terminal domain, showed good cross reactivity toward AtRGL3 and to a much lesser degree to AtRGL1, however it detects all but 2 of the AdDELLAs.

mAb G10 epitope lies in the highly conserved C-terminal motif CPYLKFAHFTANQ of the DELLA proteins. However, it detects only AdRGL3 a and b with medium strength (Figure 3.27 and Table 3.6).

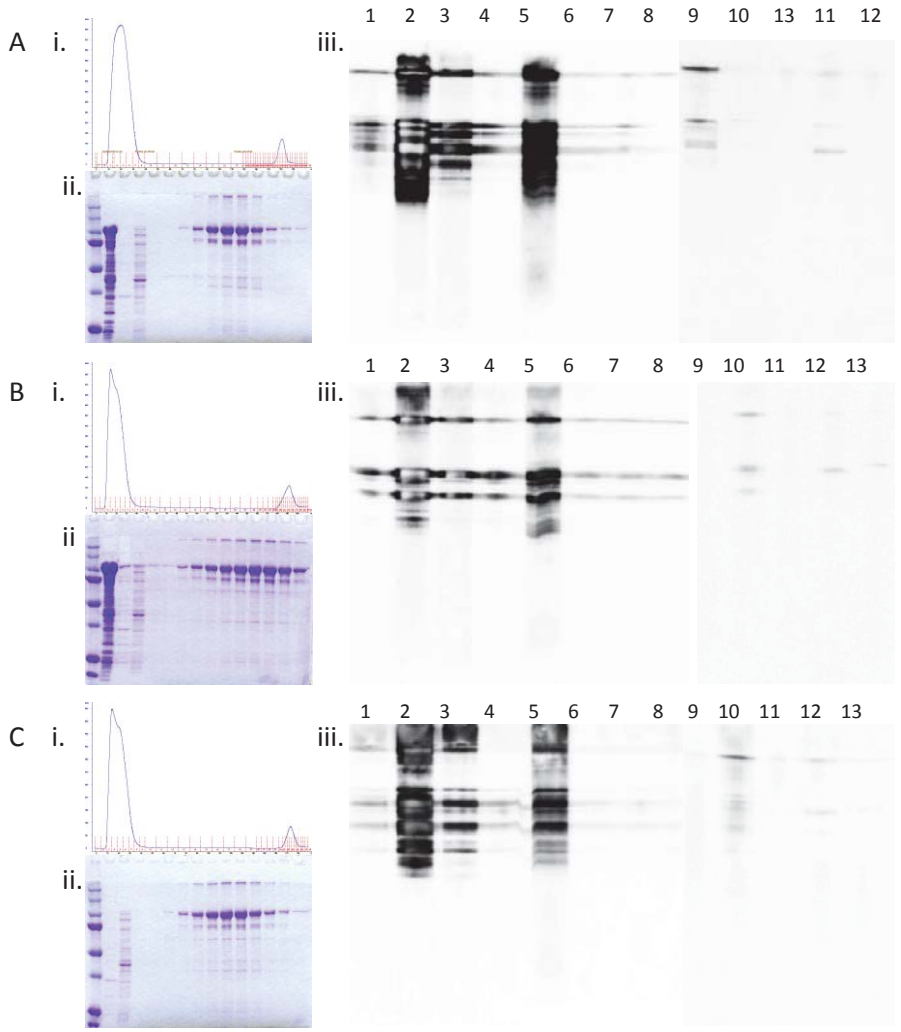

Figure 3.27. Kiwifruit recombinant DELLA protein purification and antibody immunogenicity

Purification and immunoblot analysis of recombinant *A. deliciosa* DELLA homologue proteins. *E. coli* containing an *A. deliciosa* DELLA construct as His-MBP translational fusions were expressed. The whole cell lysate was centrifuged and the soluble fraction was loaded onto an amylose resin column. Elution of column bound protein was made by the addition of 10 mM maltose to the extraction buffer. Fractions were collected while monitoring protein levels by absorbance of light at 280 nm. Confirmation on the purification of a protein of the expected molecular weight was done with PAGE and staining with Coomassie brilliant blue R. 10 µg of the recombinant protein was separated by 10 % SDS-PAGE and probed with 1 µg/ mL mAb.

A, AdRGL1a; **B,** AdRGL1b; **C,** AdRGL1c.

i, UV Absorbance trace (mAu against Volume); **ii,** Comassie stained acrylamide gel of purification fractions; **iii,** Western blot lanes: **1,** BC9; **2,** 5E1; **3,** 6C8; **4,** AF2; **5,** AD7; **6,** AB8; **7,** BB7; **8,** 1C3; **9,** D1F10; **10,** A4C11; **11,** A1B1; **12,** G10; **13,** D9.

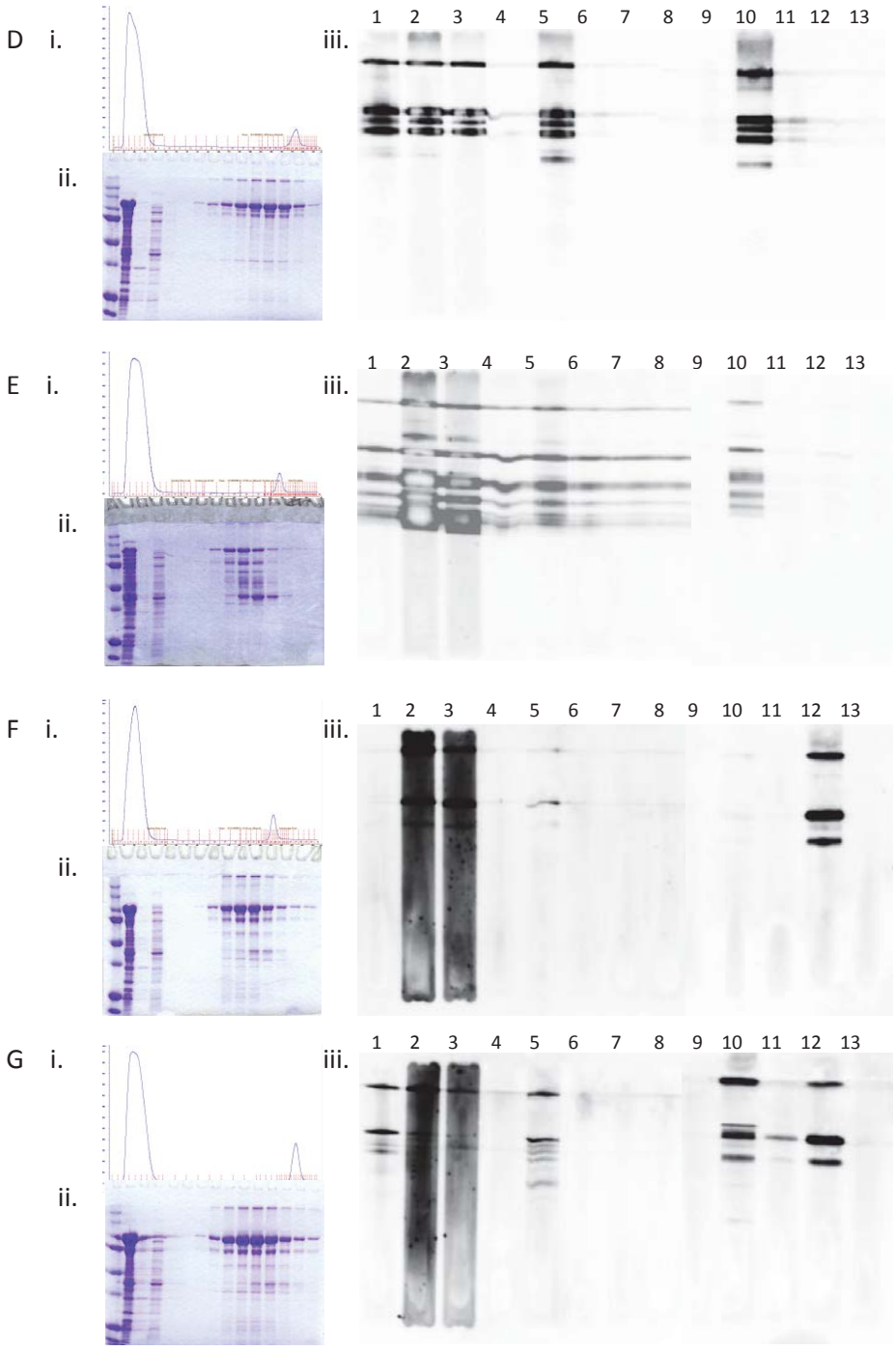

Figure 3.27 (*continued*). Kiwifruit recombinant DELLA protein purification and antibody immunogenicity
D, AdRGL2a; **E,** AdRGL2b; **F,** AdRGL3a; **G,** AdRGL3b.
i, UV Absorbance trace (mAu against Volume); **ii,** Coomassie stained acrylamide gel of purification fractions; **iii,** Western blot lanes: **1,** BC9; **2,** 5E1; **3,** 6C8; **4,** AF2; **5,** AD7; **6,** AB8; **7,** BB7; **8,** 1C3; **9,** D1F10; **10,** A4C11; **11,** A1B1; **12,** G10; **13,** D9.

Table 3.6. Cross reactivity of the anti-DELLA monoclonal antibodies to *A. deliciosa* recombinant DELLA proteins

KF DELLA	Monoclonal antibody designation[b]												
	BC9	5E1	6C8	AF2	AD7	AB8	BB7	1C3	D1F10	A4C11	A1B1	G10	D9
AdRGL1a	+[a]	+++	++	+	+++	-	-	-	+	-	+	-	-
AdRGL1b	+	+++	++	+	+++	-	-	-	-	+	-	-	-
AdRGL1c	+	+++	++	+	+++	-	-	-	-	+	-	+	-
AdRGL2a	++	++	++	-	++	-	-	-	-	++	+	-	-
AdRGL2b	++	+++	+++	+	++	-	-	-	-	+	-	-	-
AdRGL3a	-	++	++	-	+	-	-	-	-	-	-	++	-
AdRGL3b	+	++	+	-	+	-	-	-	-	++	+	++	-

[a] **+++,** strong recognition; **++,** medium recognition; **+,** weak recognition; **-,** no recognition.
[b] Analysis of the *A. deliciosa* recombinant proteins western blot results (Figure 3.27), presented in tabulated form.

3.3 Modelling N-terminal domains of the kiwifruit and apple DELLA proteins

3.3.1 Modelling of kiwifruit N terminal domain

Using the automated mode of SWISS-MODEL; http://swissmodel.expasy.org/workspace/ (Arnold et al., 2006) the N-terminal *Actinidia* DELLA proteins sequences were structurally modelled on the existing *Arabidopsis* GAI N-terminal structure template 2zsiB from (Murase et al., 2008). This structure is GAI N-terminal domain in its folded form, within the quaternary complex with GID1a/ GA_3, and corresponds to amino acids 11 to 113, lacking the N-terminal 10 amino acids and highly disordered S/T/V region downstream of the two conserved N-terminal domains (template structures 2zsiA and -B). As it was shown that the N-terminal domains of DELLA proteins are disordered in unbound form, the conformational switch occurs upon binding to GID1a/GA_3 (Murase et al., 2008, Sheerin et al., 2011, Sun et al., 2010). This conformational switch is likely to induce a further conformational change in the C-terminal GRAS domain, enabling interaction with the F-box protein, SLY1.

The modelled *Actinidia* structures appear to be of good quality (Appendix Table 6.2). There are no significant differences in the N-terminal DELLA modelled structures from the template. The kiwifruit α-helix B does not extend as far C-terminally as the template's α-helix B. However, the residues involved in the GID1 interaction are not in this region [according to the Murase et al (2008) structure]. The α-helix C also shows a little variation among kiwifruit DELLA proteins, some being a little longer but again this does not involve the residues expected to be interacting with GID1. The main difference is seen in the B-C loop region, which is not conserved between DELLA orthologues, and the amino acids in this region play no role in the contact with GID1 (Figure 3.28). The mAbs used in this thesis with known epitopes (BC9, 5E1, 6C8 and AD7) bind either the DELLA motif corresponding to the α-helix A (5E1, 6C8), the immediately adjacent sequence VLGYKVR corresponding to the loop connecting α-helices A and B (BC9), or YNPSD sequence of the VHYNPS motif corresponding to the loop between α-helices C and D (AD7). Using DELL-binding mAb 6C8 and competition assays, it was shown previously that, although the α-helix A contains contact residues for the AtGAI-AtGID1/GA interaction, these residues are not essential for AtGID1 interaction; the residues essential for interaction lay later in the extended motif, corresponding to A-B loop, as shown by the BC9 antibody competition experiments (Sheerin et al., 2011). The TVHYNPSD motif (α-helix C and

C-D loop), was shown to be essential for the AtGAI-AtGID1/ GA interaction by competition with the YNPSD-specific mAb BC9.

A.

B.

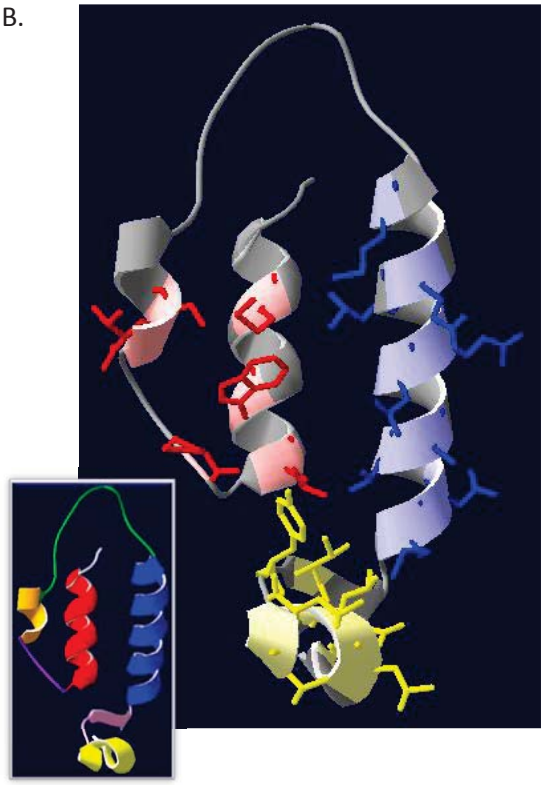

C.

Figure 3.28. SWISS-MODEL Alignment, Overlapping ribbon structures and highlight of residues involved in GID1 association

The N-terminal domains of the *Actinidia* DELLA orthologues were modelled on the *Arabidopsis* GAI coordinates from PDB 2zsiB as a template. The modelled structures show no significant alterations from the template, except in the non-conserved B-C loop region. This region is not thought to play a role in DELLA-GID1 protein-protein interaction.

A, The modelled amino acid sequence alignment; **B,** AdRGL1a ribbon representation and underlying Cα backbone. The AtGID1-interacting surface of the DELLA proteins is facing towards the reader. The side chains from the amino acid residues involved in the AtGID1A interaction reported in Murase *et al* (2008) are included on the backbone and are highlighted on the ribbon model; **B (insert),** Ribbon model KEY: A α-helix (at the N-terminal), B α-helix, C α-helix, D α-helix (at the C-terminal). Between the helices are loops; A-B loop, B-C loop, C-D loop; **C,** Overlapping ribbon representations of all the modelled structures, coloured as shown in sequence A.

3.3.2 Modelling of apple N terminal domain

The N-terminal domains of the apple DELLA proteins were modelled on the *Arabidopsis* GAI template 2zsiB (Arnold et al., 2006, Murase et al., 2008) using the same approach as done for the kiwifruit DELLAs. In contrast to the modelled kiwifruit N-terminal DELLA sequences, the modelled apple sequences showed larger deviations from the template (please refer to previous section 3.3.1 for *Actinidia* models). Specifically, in the modelled MdRGL2a structure there is no α-helix C, and the MdRGL2b predicted structure has an incomplete α-helix C. In addition to this, the MdRGL2b also has no structure predicted for the amino acids of the AB loop (Note: this can't be seen in the figure presented). In contrast to MdRGL2, MdRGL3b is modelled to have a longer C α-helix than AtGAI. All the *Malus* DELLA modelled structures have a shorter α-helix B (truncated at the C-terminal end) with the MdRGL1a/b having the shortest helix (Figure. 3.29). The observation of shortened helices would be predicted to alter the MdGID1 interaction as residues in the α-helix C, specifically Thr^{62} (of TVHYNP domain), is involved in the GID1 interaction surface and is likely to be essential for interaction, based on competition studies (Murase et al., 2008, Sheerin et al., 2011). The residue is modelled pointing away relative to the GAI equivalent. If no rigid α-helix is formed and the structure is still a random coil, the loop may assume a number of different conformations, however the interaction with GID1/GA is likely to be less prominent than in DELLAs that contain expected helical conformation and correct residue orientation.

A.

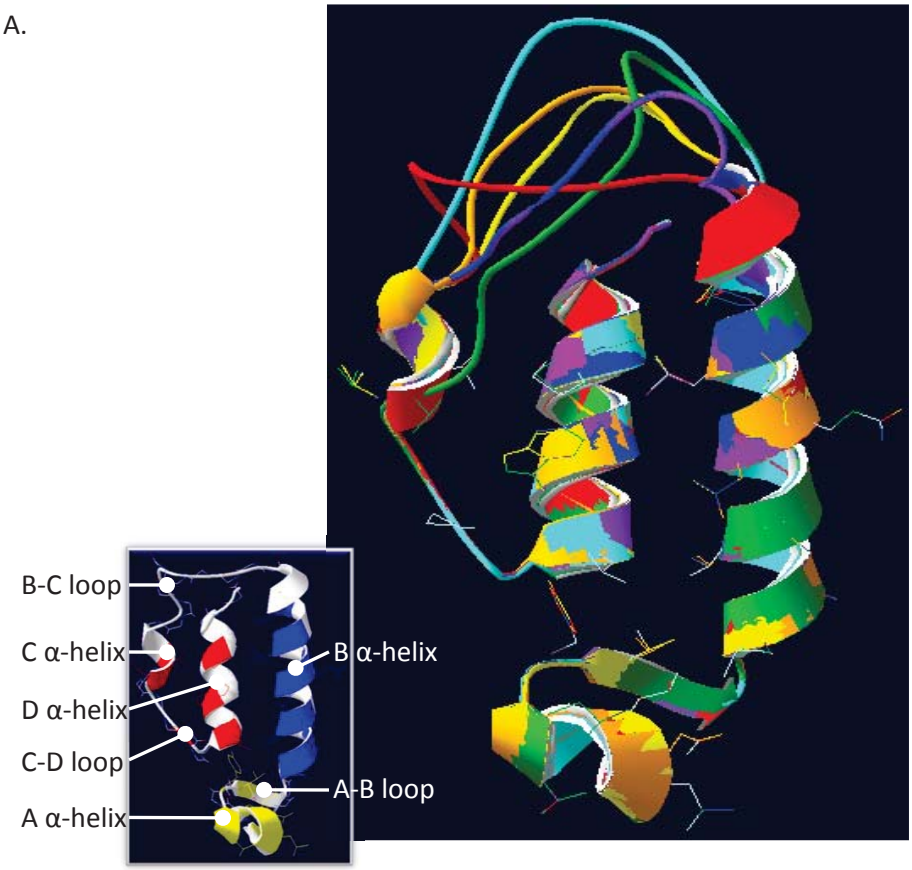

B.

Figure 3.29. SWISS-MODEL alignment overlapping ribbon representation of *Malus* N-terminal DELLA sequences

The N-terminal domains of the *Malus* DELLA orthologues were modelled on the *Arabidopsis* GAI coordinates from PDB file 2zsiB as a template.

A, Overlapping ribbon representations of the structurally modelled apple DELLA proteins and side chains of residues involved in GID1-interacting interface (Murase et al., 2008).

KEY: AtGAI, MdRGL1a, MdRGL1b, MdRGL2a, MdRGL2b, MdRGL3a, MdRGL3b.

A insert, named helices and loop regions on the AtGAI ribbon model of the GAI structure, 2zsiB. Residues involved in the GID1 interaction are coloured, in the DELLA motif, in the LExLE motif and in the TVHYNP motif; **B,** sequence alignment, with the residues involved in GID1 binding highlighted.

3.4 Summary of identification and expression analyses

The *A. deliciosa* core components of the GA signalling pathway have been identified and partially characterised: the repressor DELLA proteins, the GA receptor proteins (GID1) and the F-box SCF proteasome components (SLY1). We identified seven DELLA, three *GID1* and three *SLY1* family genes. The seven DELLA amino acid sequences clustered into three clades and the corresponding genes were named based on these findings as *AdRGL1* (*a*, *b*, *c*), *AdRGL2* (*a*, *b*) and *AdRGL3* (*a*, *b*). The amino acid comparisons showed that the members within each clade were 93 % similar, whereas the similarity between the clades was 70 % (AdRGL1 to AdRGL2) and 50 % similar (AdRGL1 to AdRGL3 and AdRGL2 to AdRGL3). The three GID1 homologues were 76 % and 92 % similar on pairing. The three SLY1 homologues were 85 % and 94 % similar. In each homologue grouping there were pairs of more closely related homologues than the third member and likewise, this was seen with the DELLA homologues - two clades were more closely related than the third clade. The three homologues and groupings most likely represent the genome duplication events of *A. deliciosa* as a hexaploid plant, and indicate two separate ploidisation events, with one duplication (2n) occurring more recently than the first.

Apple contains three pairs of DELLA homologues that have >93% identity, consistent with the evidence of genome hybridisation in Maloideae. Most probable parental lineages are derived from Spiraeoideae subfamily (Evans and Campbell, 2002).

Transcription analyses by quantitative PCR showed that the patterns of expression between the apple and kiwifruit *DELLA* genes is very different, hence the regulation of expression and/or transcript turnover between these two woody perennials must be different. The kiwifruit analysis included biological replicates, which demonstrated very large differences in *AdDELLA* transcript levels between separately collected, but morphologically identical tissues. This is particularly pronounced in breaking buds, expanding leaves and shoot tips. This variation shows that otherwise morphologically identical developing tissues are in dynamic flux.

The DELLA-specific mAb recognition experiment confirmed the broad nature of epitope conservation in *A. deliciosa* DELLA homologues, which were isolated based on sequence homology. However examining this similarity at a finer level of sequence determined clade

structure to antibody recognition pattern did not yield consistent data. The mAbs BC9 and 5E1 identified in ELISA screening experiments to detect all apple and *Arabidopsis* DELLA proteins also detected all the *A. deliciosa* DELLA proteins (with the exception of AdRGL3a by BC9). However, mAbs specific for particular DELLA homologues did not detect only those DELLAs with in the same clade, for example mAb A1B1, isolated for detection of MdRGL3, detected one *A. deliciosa* DELLA from each clade. This protein represented the members in the more distant DELLA clade; however considerable homology is obviously still present. This mAb result likely indicates the generally more restricted structural nature of an epitope compared to whole sequence relatedness.

The N-terminals of the DELLA proteins were modelled on the AtGAI template (Murase et al., 2008). This template is from the solved quaternary structure of the AtGID1(GA)-DELLA complex co-crystals. The kiwifruit N-terminal DELLA protein models deviated little from the AtGAI template and did not appear to have significant differences. The apple proteins did however show differences. There were alterations in the lengths of the B and C α-helices, and it is postulated that this could change the GID1 interaction. This was most strongly represented in the MdRGL2's, which were predicted to either not form a C α helix or have a shortened helix relative to other DELLA homologues. This helix and C-D loop region are the TVHYNP motif amino acid residues. This is interesting, as the formation of these helices in otherwise intrinsically disordered conformation of the N-terminal DELLA domains, are important for the interaction of the GA-liganded GID1 (Murase et al., 2008, Sheerin et al., 2011) and indicates that the MdRGL2's may have a different interaction mode with GID1 in comparison to other DELLA proteins. Furthermore, the mAb AD7, has its epitope mapped to the VHYNP residues and only detects the AtRGLs and does not detect AtGAI and AtRGA. It was also found to detect the MdDELLAs with high affinity (though less so the MdRGL1s) (Table 3.5). This indicates the structures are different between AtGAI and the AtRGLs and MdRGLs in this area. It has been reported that in *A. thaliana* each AtDELLA interacts with each AtGID (Nakajima et al., 2006). However, this may be different in the case of MdDELLA and MdGID1s, where sequence and conformational differences may confer some level of specificity in MdGID1-MdDELLA pairing.

4. Immunopurification and localisation

In order to understand how DELLA proteins repress growth and development it is important to identify proteins with which they interact. These interacting proteins are likely to be immediately upstream or downstream of DELLA proteins in the network of cell-signalling. Even though DELLA proteins regulate gene expression, there is no experimental evidence for direct binding of DELLA proteins at promoter regions of genes they regulate; furthermore, DELLA proteins contain no known DNA-binding motifs (Xi et al., 2010, Zentella et al., 2007). Therefore, DELLA proteins regulate transcription through modification of other proteins' functions. To date a family of transcription factors containing a bHLH domain, in subfamily 15, (including *PIF3, PIF4*, *PIL2, PIL5*, *SPT* and *ALC*) have been discovered that can be prevented from activating transcription through DELLA protein interaction (de Lucas et al., 2008, Feng et al., 2008). To mediate the inhibitory effect on these proteins DELLAs bind the bHLH domain and block this domain's interaction with DNA, thereby preventing activation of the promoter and preventing expression of the genes whose products promote growth and development.

Besides direct interaction, posttranslational modifications of DELLA proteins, phosphorylation and O-glycosylation, have been proposed to have a role in modulation of their function. However, the O-glycosylation of DELLA proteins has not yet been demonstrated directly (Swain et al., 2001, Tseng et al., 2001). The DELLA proteins are phospho-proteins, but phosphorylation sites of DELLA proteins have not been mapped to the primary sequence and there are contradictory reports on the role(s) of phosphorylation in DELLA turnover and regulatory functions (Gomi et al., 2004, Hussain et al., 2005, Hussain et al., 2007, Itoh et al., 2005a, Sasaki et al., 2003).

AtRGL2 is the key DELLA protein in *A. thaliana* that controls flower development and germination; this activity very likely involves interaction with a number of transcription factors and is likely controlled by upstream and downstream regulators of GA- and other signalling pathways that were shown to act on DELLA proteins. Although some proteins interacting with the DELLAs have been identified, the number is neither large nor diverse, mostly confined to a family of bHLH transcription factors and to core GA-signalling proteins, GA receptor GID1 and F-box protein SLY1/ GID2 (Arnaud et al., 2010, de Lucas et al., 2008, Feng et al., 2008, Gallego-Bartolome et al., 2010, Hou et al., 2010, Zhang et al., 2011). Identification of additional

interaction partners, e.g. potential kinases or other proteins that convey environmental and hormonal cues to DELLA-dependent targets, and characterisation of post-translational modifications would give a more complete picture of the way by which DELLA activity is regulated. To be able to isolate interacting proteins and determine post-translational modifications, microgram amounts of AtRGL2 have to be isolated from plant inflorescence tissue. This should be achieved without over-expression, which to date has led to some controversial results, in particularly with respect to phosphorylation (Hussain et al., 2007, Hussain et al., 2005). Two methodologies were used; an indirect precipitation of AtRGL2 tagged fusion expressed from the native *RGL2* promoter, containing a tag developed during this work, and a direct precipitation of the wild type AtRGL2 protein from plant extract using AtRGL2-specific monoclonal antibodies. Given that the transgene expression is driven by the *RGL2* promoter, the over-expression of *AtRGL2* which could lead to artefacts due to over-saturation of the system that typically results in changed plant phenotype consistent with aberrant DELLA protein regulation (Fleck and Harberd, 2002, Wen and Chang, 2002), is expected to be prevented.

4.1 A novel peptide tag for detection and purification of proteins

A limited number of tags are available for purification and immunodetection. To widen the assortment of tags available to researchers, a novel peptide tag was identified. Furthermore, a cognate high-affinity monoclonal antibody against this tag was produced, mAb D9, in order to allow identification and affinity purification of proteins into which this tag was engineered (Jones et al., 2007). This new tag freed the group from intellectual property issues and gives essentially an unlimited amount of antibody to work with. mAb D9 is a high affinity antibody with an affinity constant (K_D) of 1.3 X 10^{-10} M, comparatively higher than a Qiagen anti-His mAb with a K_D of 1 X 10^{-9} M but lower than an AbCam rabbit monoclonal anti-cMyc with a K_D of 3.8 X 10^{-12} M. The sequence of the R tag, PDQYEYKYP, was chosen so that it does not have a match in plants, animals or bacteria (in the existing protein sequence databases). Because of some similarity of this peptide to a sequence from a rabies virus protein, the tag was named the “R tag”. Expression vectors containing the R-tag were constructed (Jones et al., 2007, Sun et al., 2008).

A transgene expression construct was made with *Arabidopsis RGL2* and a translationally in-frame modified tandem affinity purification (TAP) tag fusion. Tandem tag fusions improve the capture and reduce background of non-specific binding proteins in affinity purification (pull-down or immunoprecipitation) experiments. The original TAP tag is composed of two parts: a calmodulin-binding domain (CBD) and two repeats of the protein A domain that binds to the constant (Fc) region of the IgG immunoglobulin heavy chain (Rigaut et al., 1999, Rohila et al., 2004). Given that monoclonal antibodies were planned to be used to detect and precipitate DELLA proteins, the protein A part of the tag would interfere in many of the experiments by binding to the antibodies non-specifically. To overcome this problem, a novel twin tag was constructed by replacing the protein A domains of the original TAP tag with the R peptide (PDQYEYKYP), allowing utilisation of the high-affinity R-specific mAb D9, and was named TAPR tag (Jones et al., 2007) (Figure 4.1). The TAPR tag is designed so that the first purification step is carried out using immobilised mAb D9, chemically attached to the column matrix. Any bound fusion protein complexes are released by a site specific rTEV protease cleavage at the specific target sequence (ENLYFQG) which is engineered between the R tag and the CBD. In the second step, the eluted fusion is further purified using a calmodulin column. The CBD of the TAP tag binds calmodulin only in the presence of Ca^{++} ions. Bound proteins are eluted using the Ca^{++} chelator EGTA, which acts by removing Ca^{++}, the binding cofactor, from the buffer. Elution of bound proteins in both steps is carried out under the pH and salt concentrations equivalent to those used in binding. These mild conditions are intended to minimise the disassociation of proteins that may be interacting with the DELLA protein, avoiding harsh conditions, such as low or high pH, with may cause dissociation of any interaction trying to be captured. To identify affinity-purified proteins, the eluted proteins from the second purification step are separated by SDS-PAGE and identified by mass spectroscopy.

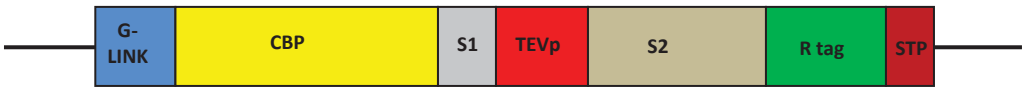

Figure 4.1. Tandem Affinity Purification R (TAPR) tag layout
A recombinant fusion peptide was designed and constructed to facilitate purification by protocols that include immunoprecipitation.
G-LINK, glycine linker (GGGS); **CBP,** calmodulin binding protein; **S1,** spacer 1; **TEVp,** tobacco etch virus protease site; **S2,** spacer2; **R tag,** peptide tag recognised by mAb D9; **STP,** stop codons.

4.1.1 Testing TAPR, the novel TAP tag

A trial experiment was performed to test the TAPR tag in *E. coli*. A recombinant construct expressing a TAPR-tagged, MBP fusion-*RGL2* N-terminal domain (MBP-*nRGL2*-TAPR) fusion protein was subjected to the two-step purification protocol described above. Following transformation and selection of *E. coli* carrying the construct, the expression was carried out as stated in chapter 2, methods section. In the trial *E. coli* expression experiment both steps of purification were successful (Figure. 4.2). Due to the high expression of the tagged protein, the anti-R mAb D9 column capacity was exceeded, hence some MBP-*nRGL2*-TAPR is visible in the flow-through and washing lanes (Figure 4.2Bi, lanes 2-8). However, this would not be considered as a likely problem *in planta*, where low levels of expression are expected, given that the transgenic cassette designed for the affinity-purification experiment contains native *RGL2* plant promoter driving the expression of the tagged protein. The elution by rTEV protease cleavage was also tested (Figure 4.2Bi, lane 9). This experiment showed that a protein slightly smaller than the MBP-RGL2n-TAPR tag was released, consistent with the cleavage between the CBD and R tags. The cloning vector also encodes a second rTEV cleavage site, between the MBP and RGL2n. Two bands that correspond to MBP and RGL2n-CBD were expected products from the cleavage at the two rTEV sites, and they were detected by SDS-PAGE (Figure 4.2; Bi, line 9). The presence of both the cleavage products, MBP (44 kDa) and RGL2n-CBD (24 kDa), and the entire product MBP-RGL2 n-CBD (68 KDa) shows that the rTEV recognition site between the MBP and RGL2n-CBD (encoded by the vector) was only partially cleaved by the rTEV protease. The eluate from the rTEV cleavage was purified further on the calmodulin column (Figure 4.2Bii, lane 6). The 68 kDa and 24 kDa proteins bound to this column, whereas the 44 KDa protein did not. This is consistent with the large (68 kDa) band corresponding to MBP-RGL2n-CBD and the small 24 kDa band to RGL2n-CBD, whereas the 44 kDa non-binding band corresponds to the vector-encoded MBP protein. Since the rTEV site between the MBP and RGL2n is not the site in the TAPR tag and is not present in the transgenic plant construct, this site is not relevant for plant transformation. Therefore, all the components of the TAPR tag were functional (Figure 4.2).

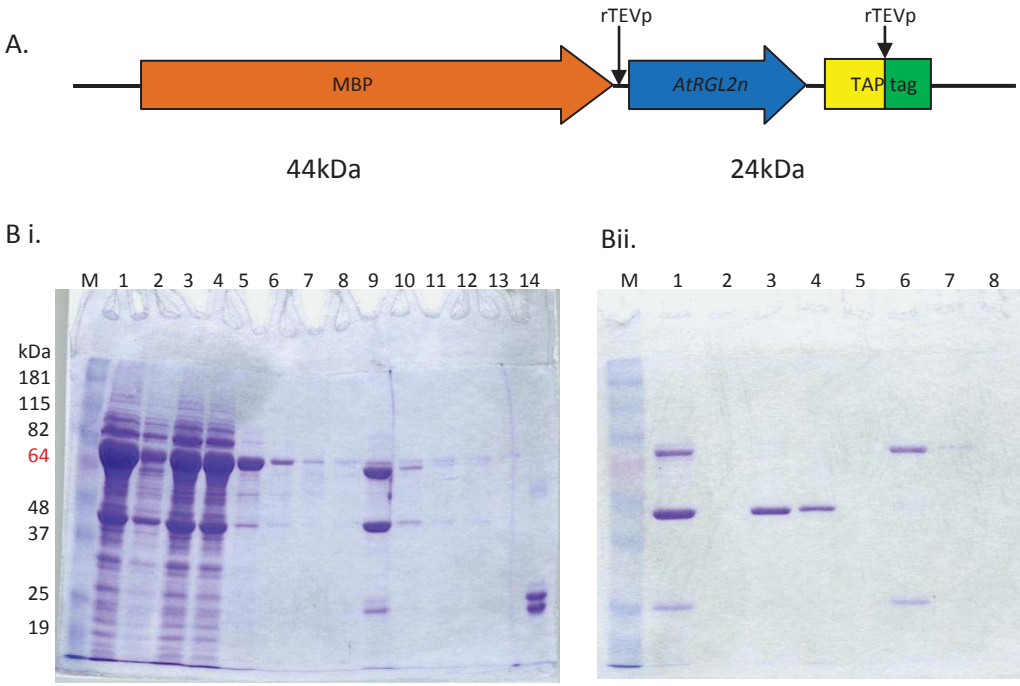

Figure 4.2. TAPR tag bacterial recombinant expression and purification test experiment

A, Recombinant expression construct *RGL2n*-TAPR, in pETM-MBP R backbone (pPMB 0380).

B i, and **B ii,** Expression and purification of the MBP-RGL2n-TAPR protein fusion, monitored by SDS-PAGE and protein staining with Coomassie R250.

B i, Purification of the MBP-RGL2n-TAPR on the mAb D9 (anti-R) column.

Lanes: **1,** protein extract of *E. coli* expressing MBP-RGL2n-TAPR; **2, 3** & **4,** non-bound column flow-through; **5, 6, 7 & 8,** column washes; **9, 10, 11** & **12,** proteins released by rTEV protease incubation over-night at 4 °C; **13,** Strip wash (0.2 M Glycine, pH 2.5); **14,** rTEV protease.

B ii, Purification of MBP-RGL2n-TAPR on a calmodulin column.

Lanes: **1,** The rTEV-protease-released recombinant protein (Bi, lane 9) loaded onto the calmodulin column; **2,** calmodulin column void volume; **3, 4** and **5,** calmodulin column wash fractions; **6, 7** & **8,** eluate from the calmodulin column (2 mM EGTA); **9,** column regeneration wash.

rTEVp, TEV protease cleavage site; **M,** Marker; **kDa,** molecular weight in kiloDaltons.

4.2 Transgene TAPR tag cassettes and genetic backgrounds

Three constructs were made for *in planta* expression; two *Arabidopsis RGL2*-TAPR tag constructs (one with the TAPR tag N-terminal, and one C-terminal to the RGL2 protein) and one GUS reporter construct, the *E. coli* β-D-glucuronidase (*GusA*/*uidA*) gene (*UidA*-TAPR tag). All constructs were under the *Arabidopsis RGL2* native promoter and terminator sequences. The vector used to construct the transgenic constructs was pGREEN II-0229 (Hellens et al., 2000), containing *BAR* marker for selection of the transgenic construct transfer to the plant by treatment with phosphinothricin (Appendix Figure 6.1 and Figure 4.3).

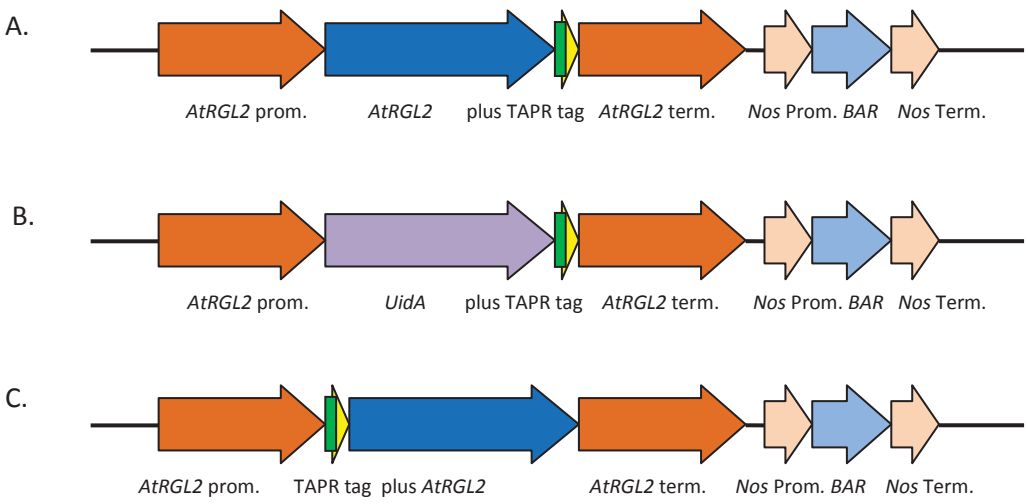

Figure 4.3. Schematic diagrams of transgenic cassettes cloned into plant transformation vectors
Transgenic cassettes were cloned into pGREEN II-0229 plasmid backbone for plant transformation.
A, *AtRGL2-TAPR* cassette (plasmid constructs in pGREEN II-0229 are pPMB 0387 and pPMB 0402, which differ only in one vector backbone restriction site (SmaI).
B, *UidA-TAPR* cassette (plasmid construct in pGREEN II-0229 is pPMB 0389).
C, *TAPR-AtRGL2* cassette (plasmid construct in pGREEN II-0229 is pPMB 0433).
Prom, promoter sequence; **term,** terminator sequence; ***AtRGL2,*** *Arabidopsis thaliana* gene encoding DELLA protein RGL2 (AtRGL2); ***Nos,*** Nopaline synthase promoter and terminator sequences; ***UidA,*** gene encoding reporter protein Gus; ***BAR,*** gene encoding phosphinothricin resistance.

Plants of two different genetic backgrounds were transformed with the transgene constructs: i. *ga1-3* (GA biosynthetic mutant that contains increased amounts of all DELLA proteins) and ii. *Δquad* (where four of the five DELLA-encoding genes, *gai*, *rga*, *rgl1* and *rgl2*, are null mutants). The different genetic backgrounds offer several advantages. The *ga1-3* genotype with its very low GA levels means there is no signal to target the DELLA proteins for destruction and hence the *ga1-3* plants over-accumulate DELLA proteins. The amount of RGL2-TAPR is expected to be elevated in this background, as well as its interacting proteins that are involved in gene regulation. The *Δquad* plants have to utilise the transgene-encoded AtRGL2 for repressive function, as other DELLAs are absent [*AtRGL3*, the only DELLA gene in the *Δquad* plants, is expressed as comparatively very low amount and does not appear to be functional, judging from the reported *Δquad* phenotype (Cao et al., 2005, Cheng et al., 2004)]. The absence of other DELLA proteins from these genetic backgrounds decreases competition for binding for the same interacting partners and increases the likelihood of detecting interacting proteins by pull-down of the RGL2-TAPR fusion. By observing the transgenic plant phenotypes in the DELLA-deficient genetic background, it is possible to confirm that the transgenic *AtRGL2-TAPR* construct is functional.

All constructs were transformed into the *Arabidopsis* seeds using the floral dip method and transformed plants selected for under glufosinate treatment (to select for integration of the *BAR* selective marker from the transgenic cassette) as described in the methods section. The glufosinate resistant plants were obtained for transgenic cassettes: *AtRGL2-TAPR* (pPMB 0402); *TAPR-AtRGL2* (pPMB 0433); and *UidA-TAPR* (pPMB 0389) and examined further by PCR using two pairs of primers, one pair that amplifies the *RGL2-TAPR* cassette or *UidA-TAPR* cassette and one that amplifies the *BAR* gene (phosphinothricin resistance marker). Transgenic plants were obtained for *AtRGL2-TAPR* and *TAPR-AtRGL2* in *Δquad* background, *AtRGL2-TAPR* in *ga1-3* background and the control/reporter transgene *UidA-TAPR* in *ga1-3* background (data not shown). Two independent plant transformation lines were analysed from each construct.

4.2.1 Reporter gene visualisation of AtRGL2 promoter driven expression

To determine the pattern of *A. thaliana* RGL2 promoter-driven expression, inflorescences from transgenic plants containing the reporter *UidA*-TAPR fusion were stained for activity of GUS (product of *UidA* gene). This fusion was controlled by the native *AtRGL2* promoter and terminator sequences; the *UidA* coding sequence was constructed in such a way that it

accurately replaced the *AtRGL2* CDS in the transgenic cassette. The expression of *RGL2* was monitored histologically by the GUS assay. Young inflorescence flowers showed strong expression of GUS from the *AtRGL2* promoter that lessened as they matured (Figure 4.4). Expression of GUS was the lowest in petals and moderate in sepals and stamens. Higher expression levels were seen in older stamens (anther and filament). This is consistent with AtRGL2 expression before floral expansion and then again after the pedicels and filaments have completed their GA-driven elongation. The highest GUS levels were seen in the styles. With the age, GUS expression focused to the stigma. Significant levels were also seen at the style/pedicel boundary. This GUS staining indicates where the *AtRGL2* promoter is active. However, the amount of AtRGL2 protein, like other DELLA proteins, is also regulated at posttranscriptional level, by GA-dependent degradation through Ubiquitin-proteasome pathway. Therefore, the synthesis of *AtRGL2* RNA does not necessarily ensure that the AtRGL2 protein is present in a given tissue. An interesting note was that the TAPR tag on the *UidA* construct was readily detectable in western blots of transgenic tissues with the anti-R tag mAb D9, but this epitope could not be detected in AtRGL2 fusions containing either the N-terminal or C-terminal TAPR tag, in the transgenes TAPR-AtRGL2 and AtRGL2-TAPR respectively (data not shown). This is a very important observation, suggesting that not the transcription, but rather the protein turnover and/ or modification have major contribution to *AtRGL2* regulation *in planta*.

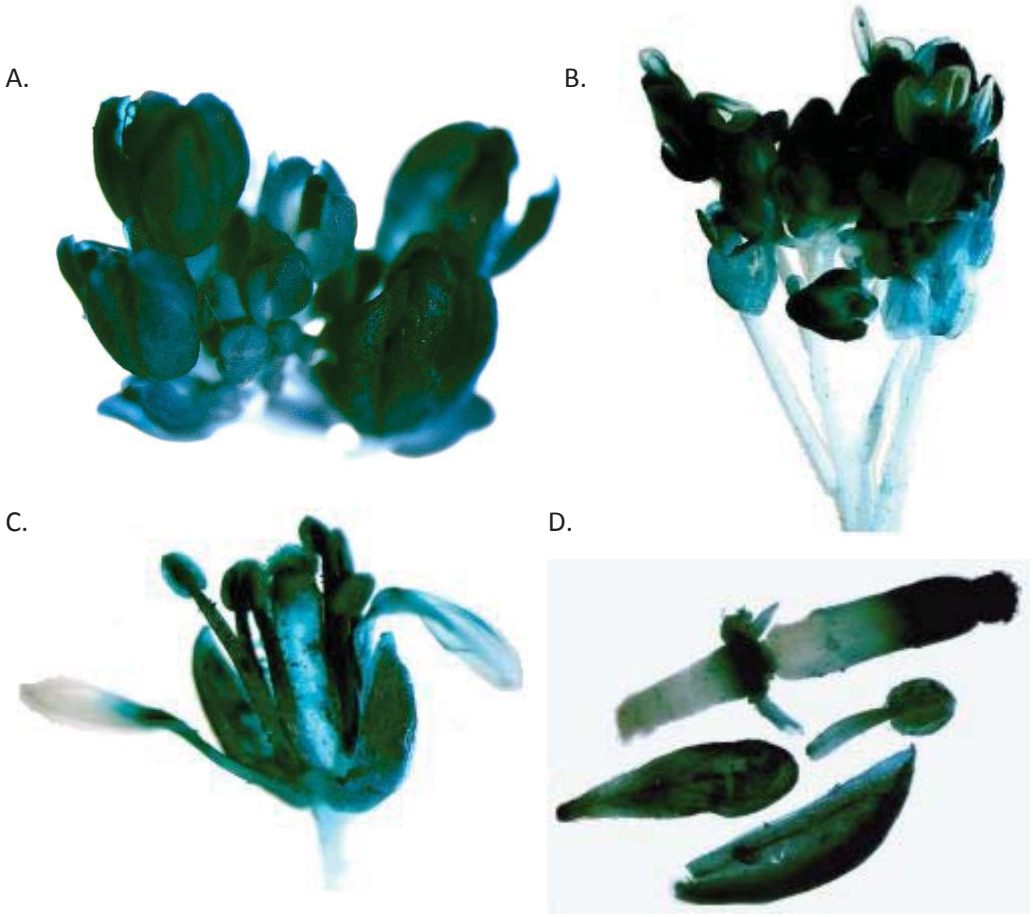

Figure 4.4. GUS staining of p*RGL2-UidA*-TAP (pPMB 0389) transgenic plant inflorescence
An inflorescence was stained for GUS activity as described in section 2.2.14.
A, Young inflorescence, before flower opening.
B, Older inflorescence.
C, Flower (some petals and sepals were removed to open it up for viewing).
D, Flower parts; (clockwise from the top) style, stamen, sepal and petal.

4.2.2 Analysis of transgenes expressing AtRGL2 fusions to TAPR tag

Western blots on protein extracts from inflorescences of these transgenic plants detected both transgene products *TAPR-AtRGL2* in the *ga1-3* background (Figure 4.5) and *AtRGL2-TAPR* in *Δquad* background (Figure 4.6), using the anti-DELLA mAb BC9. The TAPR-tagged proteins were distinguishable from the wild-type AtRGL2 in the *ga1-3* background through their increased size (by ~8 kDa). However, the R-tag epitope (part of the TAPR tag) was not detected in any of the transgenic plants using the anti-R tag mAb D9 (Figures 4.5 and 4.6). This may be due to a lower affinity of the anti-R-tag mAb antibody D9 compared to the anti-DELLA mAb BC9, the former not being able to detect the fusion protein which is present in the cells in a very low amount. It should be mentioned here that the amount of DELLA proteins produced in the host cell is very low, and that all published work has been done with highly over-expressed transgenic construct. Alternatively, proteolytic cleavage of the R peptide within the tag could have eliminated the epitope in the construct. The R tag is at the very terminus of the protein (either the very N- or very C- terminus, depending on the recombinant product in question). However, this is unlikely as the transgenic product had the expected shift in size on electrophoresis. Other possible explanations would be a conformational change of the epitope that rendered the R-tag unrecognisable by the antibody, or folding of the fusion in such a way that the R-epitope is not accessible to mAb D9, or plant-specific post-translational modification has changed the epitope. Given that the R-tag expressed in *E. coli* has been recognised both in the native and denatured forms, as shown above (Figure 4.2), this effect of protein folding is hard to rationalise, therefore the post-translational modification or marginal exopeptidase cleavage specific to plants are the most likely explanations of the lack of recognition by the R-tag specific antibodies. However, given that DELLA proteins are expressed at a very low level, even in *ga1*-3 plants, the explanation for lack of the R-tag detection due to insufficiently high affinity of the D9 antibodies cannot be ruled out. Interestingly, mAb D9 detects the R-tag epitope in the Gus reporter transgene that has an identical cassette (including promoter and terminator) as the AtRGL2-expressing transgenes (data not shown). This indeed suggests that AtRGL2-specific event (degradation or modification) eliminates the mAb D9 epitope.

The expression of functional AtRGL2 under control of the AtRGL2 promoter from the *RGL2-TAPR* (pPMB 0402) transgene (Figure 4.3 C) was not quantified, but based on the GUS reporter construct the promoter demonstrated the expected expression pattern (Figure 4.4).

Furthermore, production of functional AtRGL2-TAPR protein fusion was phenotypically confirmed by rescue of the *Δquad* phenotype. The transgenic plants had a phenotype of the wild-type *A. thaliana*, in contrast to the parent *Δquad* plants which exhibit a more slender phenotype (data not shown).

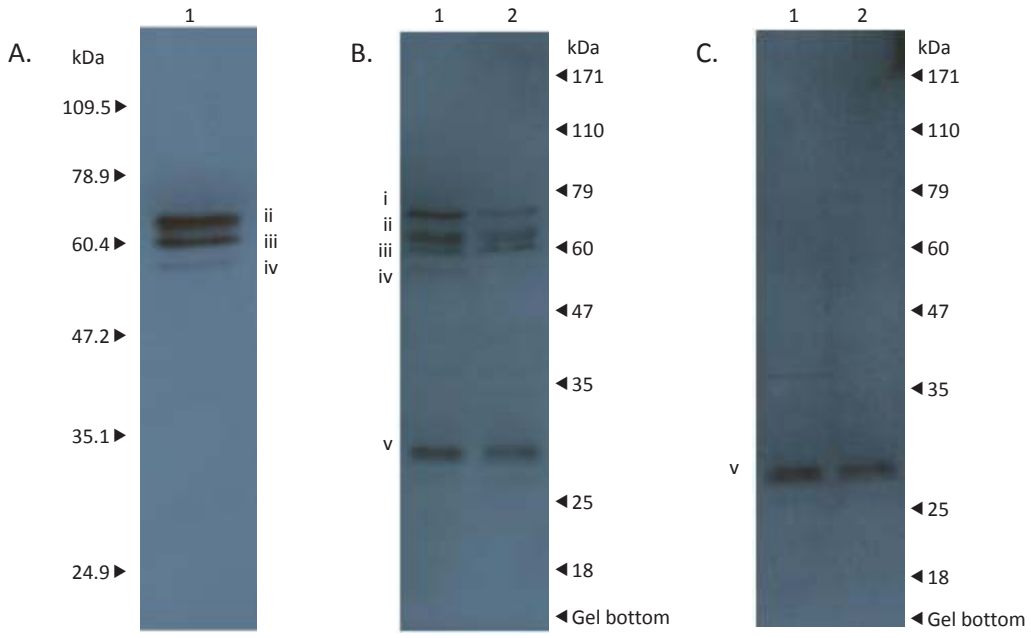

Figure 4.5. Western blot of non-transgenic *ga1-3* and transgenic plants carrying *AtRGL2-TAPR* tag cassette in *ga1-3* genetic background

DELLA-enriched protein extracts after immunoprecipitation with anti-DELLA mAb BC9, probed with either anti-DELLA mAb BC9 or anti-R-tag mAb D9.

A, Western blot of non-transgenic *ga1-3* inflorescence protein extract. Lane **1**, inflorescence extract.

B, Western blot of *ga1-3*::*AtRGL2-TAPR* inflorescence protein. Lanes **1** and **2**, inflorescence protein extract probed with anti-DELLA mAb BC9.

C, Western blot of *ga1-3*::*AtRGL2-TAPR* inflorescence protein. Lanes **1** and **2**, inflorescence protein extract probed with anti-R-tag mAb D9.

M, molecular weight marker; **kDa** kiloDaltons. **B** and **C**: Lanes **1,** and **2,** correspond to two different transgenic plant lines

Bands detected (from top to bottom): **i,** AtRGL2-TAPR; **ii,** AtRGA (calculated MW=64.0 kDa); **iii,** RGL2 (calculated MW=60.5 kDa); **iv,** GAI (calculated MW=58.8 kDa); **v,** Possibly light chain of the anti-mouse mAb used in immunoprecipitation.

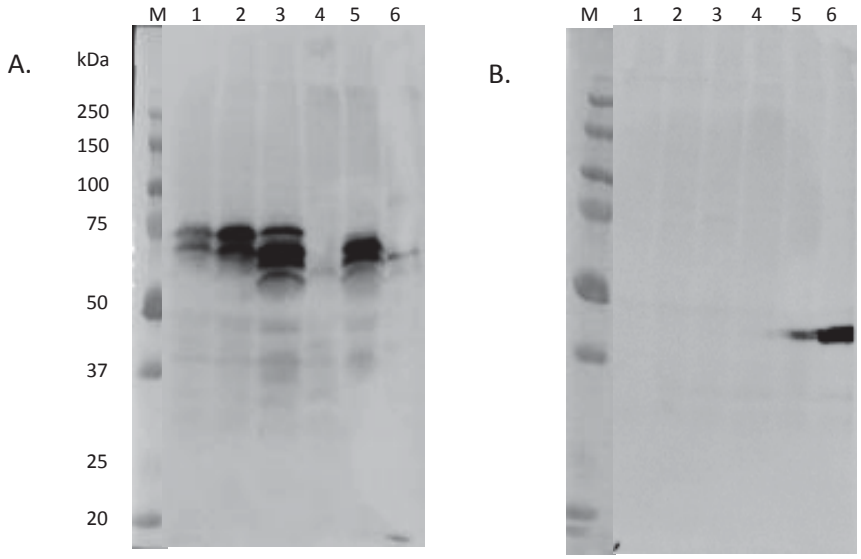

Figure 4.6. Western blot of *Δquad* ::*TAPR-AtRGL2* transgenic plant protein extracts
A, Western blot of inflorescence total cell protein extract, probed with anti-DELLA mAb BC9.
B, Western blot of inflorescence total cell protein extract probing with anti-R-tag mAb D9.
Lanes contain inflorescence total cell extract from: **1** and **2**, *Δquad::TAPR-AtRGL2* transgenes, plants 1 and 2, respectively; **3,** *Δquad::AtRGL2-TAPR* transgenic plant; **4,** *Δquad* parent plant; **5,** *ga1-3* non-transgenic plant; **6,** *Δquad* parent plant inflorescence total cell protein extract, spiked with AtRGL2n-TAPR recombinant protein expressed in *E. coli* (see Figure 4.2).
M, molecular weight marker; **kDa,** kiloDaltons.

4.2.3 Affinity purification (pull-down) of the RGL2-TAP tag fusion using anti-R tag mAb D9

The western blots for detection of the R tag were done on a very small amount of total plant extract. Given that the amount of DELLA proteins in the cell, when expressed from their own promoters, is extremely low, the lack of detection by the R tag-specific mAb D9 could be attributed to a very low concentration of the protein, coupled with relatively lower affinity of D9 mAb to the R tag in comparison to mAb BC9 whose affinity for DELLA proteins is extremely high (Jones et al., 2007). On the other hand, detection and affinity purification of the R-tagged protein in *E. coli* showed that the D9 affinity purification is very effective. This is why the *A. thaliana* extract preparation was up-scaled and the D9 affinity purification of the TAP-tagged fusions from the transgenes was undertaken.

A scaled-up extract (2.7 mL) was prepared from inflorescence (0.9 g) of p*RGL2-RGL2*-TAP (pPMB 0402) transgenic plants (in both *Δquad* and *ga1-3* backgrounds) and also from non-transgenic *ga1-3* plants (as a negative control in the experiment). To purify proteins by R tag pull down (immunoaffinity chromatography), each of the extracts was loaded onto an anti-R tag mAb D9 column. Following elimination of non-bound proteins by extensive washing, the column was loaded with rTEV protease to release the bound proteins. To avoid potential losses in the further steps of purification, the eluates were not subjected to the further calmodulin-binding purification step. To determine whether mAb D9 affinity purification resulted in an enrichment of RGL2-TAPR tag, proteins in the eluate were separated by SDS PAGE and analysed by western blotting using DELLA-specific high affinity mAb BC9 (Figure 4.7). An extract of non-transgenic *ga1-3* plants was taken through the same procedure in parallel as a negative control, to compare the enrichment of AtRGL2 in the absence of TAPR tag. The western blotting using DELLA-specific mAb BC9 showed specific enrichment of the AtRGL2-TAPR tag fusion, whereas in the control *ga1-3* extract no AtRGL2 or other DELLA proteins were detected, showing that in the absence of the tag AtRGL2 was washed off the column (Figure 4.7). This proves that the D9 antibody was binding the R-tag in the TAPR-tagged AtRGL2 fusion. However, when the eluate was resolved by SDS-PAGE and proteins were stained by unspecific protein staining, a large number of the background bands were obtained. There were as many proteins present in the eluates from the *ga1-3*::*AtRGL2-TAPR* transgene as in the eluate from the *ga1-3* control, and no detectable differences in the banding pattern were seen when both samples were run side-by-side. To identify the AtRGL2-TAPR fusion in the eluate by mass

spectroscopy, protein bands that corresponded to the BC9 (anti-DELLA)-detected protein bands in the western blot of the *ga1-3*::*AtRGL2-TAPR* eluate were excised. The gel fragments were sent for mass spectrometry analysis to identify the proteins (See section 4.3).

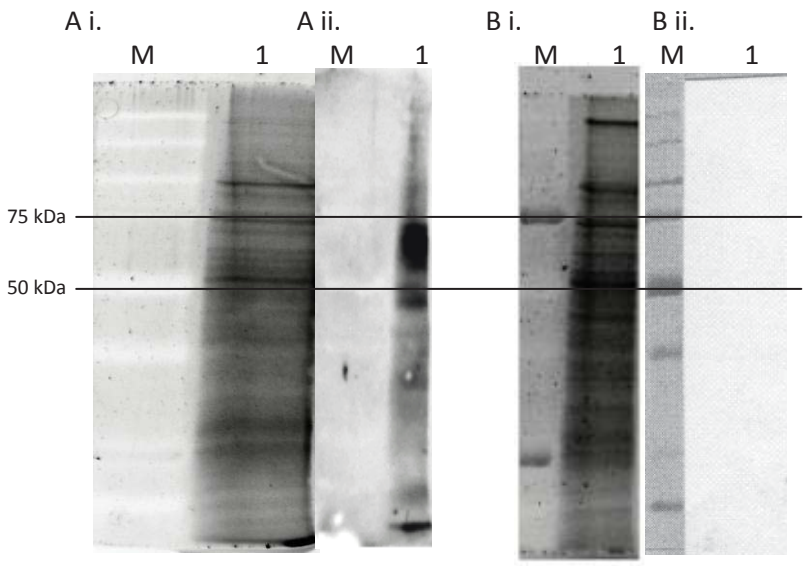

Figure 4.7. Post anti-R tag mAb D9 Immunopurification column
Proteins were immunopurified from inflorescence extract of transgenic plants *ga1-3::AtRGL2-TAPR* using R-tag-specific mAb D9. Parent plant *ga1-3* was subjected to the same protocol and has served as a control. The antibody was covalently linked to the column matrix; after binding and washing steps, proteins were eluted using rTEV site-specific protease cleavage of AtRGL2-CBD moiety of the fusion away from the C-terminal R-tag. Eluted proteins were separated by SDS-PAGE and either stained or analysed by western blotting.
A, *ga1-3::AtRGL2-TAPR*; **B,** *ga1-3* parent plant;
A i and B i, Sypro-ruby stained eluted proteins**;**
A ii and B ii, Western blot of eluted proteins probed with anti-DELLA mAb BC9.
kDa, kiloDaltons; **M**, molecular weight markers; **1**, eluate.

4.2.4 Immunoprecipitation of AtRGL2 from plant extracts using DELLA-specific mAb BC9

A low recovery of AtRGL2-TAPR fusion, using the R-tag affinity purification, warranted a change of strategy for purification of AtRGL2 from the plant extract. Very high affinity of the DELLA-specific mAb BC9 was a logical next choice for affinity purification of AtRGL2 and other AtDELLA proteins from *A. thaliana* tissues. An initial experiment to determine the *Arabidopsis* DELLA protein affinity purification using mAb BC9 was performed with inflorescences from the *ga1-3* mutant, which contains elevated levels of AtDELLA proteins.

Proteins were extracted from inflorescences of the *ga1-3* mutant and incubated over-night with anti-DELLA mAb BC9-conjugated paramagnetic beads as described in sections 2.2.13 and 2.2.16. Following the binding and washing steps, the beads were heat-denatured and subjected to SDS-PAGE and western blot analyses. The Coomassie staining did not reveal clear DELLA protein bands, and therefore their amount was below the limits of detection by this staining method (50 to 100ng). However, the western blot showed that the AtDELLA proteins were successfully immunoprecipitated. They were clearly concentrated when comparing eluate from the BC9 beads to the crude extract before affinity purification (Figure 4.8).

Four out of five DELLA proteins, RGA, RGL2, GAI and RGL1, can be detected in the plant extract using BC9 (AtRGL3 is present at extremely low level in comparison to other AtDELLAs) (Sheerin, 2010). Following immunoprecipitation of the DELLA proteins from plant extracts, boiling of the beads eluted not only DELLA proteins, but also the Light (25kDa) and Heavy (50kDa) chains of the monoclonal antibody, despite their covalent bond attachment to the beads. The heavy chain, which migrates at the similar level in the SDS-PAGE as the AtDELLA proteins do, interfered with detection of DELLAs in western blotting. The eluted heavy chain was detected by the goat anti-mouse IgG (Fc) secondary peroxidise-labelled antibody, interfering with detection of AtDELLAs by western blotting. In following experiments, the secondary antibody was switched to an anti-mouse IgG (Fab) which detects the light chain of a mAb (25 kDa). Despite the large amount of the heavy chain in the eluate that was threatening to interfere with mass spectroscopy, DELLA proteins were successfully separated from the IgG heavy chain by using low-density PAGE (Figure 4.8). A gel slab corresponding to the DELLA protein bands detected by western blotting that does not overlap with the antibody heavy chain, was excised and sent for mass spectrometry analysis to characterise the eluted proteins (See section 4.3).

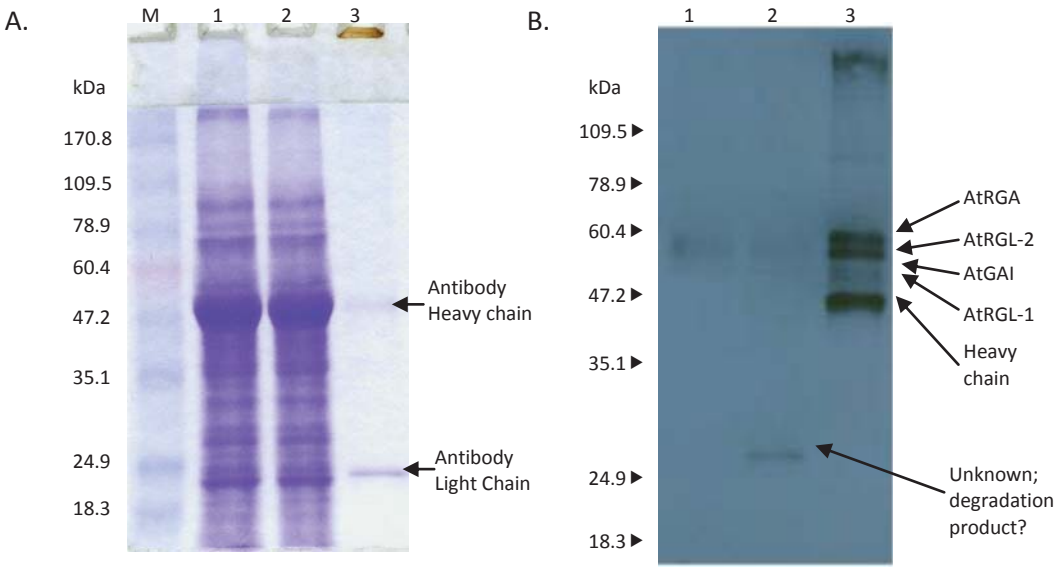

Figure 4.8. Direct immunoprecipitation of DELLA proteins with mAb BC9
Immunoprecipitation using beads conjugated with "universal" anti-DELLA mAb BC9. **A,** Bound proteins were detected by Coomassie blue R staining; **B,** western blotting with anti-DELLA mAb BC9.
Lanes: **1,** total extract (before binding); **2,** supernatant (after bead incubation); **3,** eluate (proteins eluted from the beads by heating SDS-containing buffer at 100 °C).
M, molecular weight markers; **kDa,** kiloDaltons.

4.2.5 Immunoprecipitation with AtRGL2-specific antibody BB7

The BC9 antibody recognises all AtDELLA proteins; in order to isolate only AtRGL2, an AtRGL2-specific monoclonal antibody, BB7, which does not recognise other DELLA proteins, was used for immunoaffinity purification (immunoprecipitation) from the plant extract. BB7-AtRGL2 complex was captured using anti-mouse IgG antibody immobilized by covalent attachment to magnetic beads. Protein extracts from inflorescences of *ga1-3*, that have an elevated amount of DELLA proteins relative to wild-type *A. thaliana* and *Δglobal*, a mutant expressing no DELLA proteins were subjected to immunoprecipitation. Western blot of proteins eluted from the anti-mouse IgG magnetic beads, probed with anti-DELLA mAb BC9, showed that AtRGL2 was immunoprecipitated successfully from *ga1-3* plants and no DELLA proteins are detectable in *Δglobal* plants. A slab from the deep purple-stained gel that corresponds to the AtRGL2 band(s) in western blot were excised and sent for mass spectrometry analysis (See section 4.3). There was no detectable difference in the band pattern of deep purple stained gels between the *ga1-3* and *Δglobal* lane protein bands, consistent with a low level of DELLA protein recovery and high level of background. The level of background appears higher in the control *Δglobal* lane (Figure 4.9).

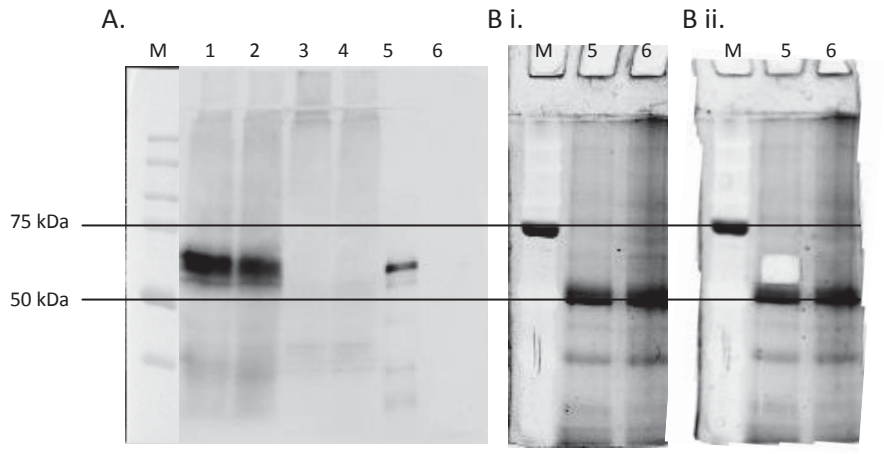

Figure 4.9. Immunoprecipitation using *AtRGL2*-specific mAb BB7 from *ga1-3* and *Δglobal* inflorescence protein extracts
Immunoprecipitation of proteins from *A. thaliana* inflorescence cell extracts with AtRGL2-specific mAb BB7 and anti-mouse IgG magnetic beads. Eluted proteins were separated by SDS-PAGE. Western blot was probed with anti-DELLA mAb BC9.
A, Anti-DELLA mAb BC9 western blot.
B i, Deep purple protein stained gel (before excision of protein bands).
B ii, Deep purple protein stained, after excising protein bands.
Lanes: **1,** *ga1-3* protein extract before immunoprecipitation; **2,** *ga1-3* plant protein extract, unbound fraction; **3,** *Δglobal* protein extract before immunoprecipitation; **4,** *Δglobal* plant protein extract, unbound fraction after immunoprecipitation; **5,** *ga1-3* eluate from the IgG magnetic beads; **6,** *Δglobal* eluate from IgG magnetic beads.
M, molecular weight markers; **kDa,** kiloDaltons.

4.2.6 Two-Dimensional separation of BB7 immunoprecipitation products

The immunoprecipitated RGL2 bands could not be identified by general protein staining (sypro ruby) above the background by simple SDS-PAGE. To overcome this problem, the BB7-immunoprecipitated proteins were analysed by a method that has much higher resolution, two-dimensional protein polyacrylamide gel electrophoresis. The proteins are separated in the first dimension by isoelectric focusing (IEF), which separates native proteins on their overall charge (isoelectric point). This is followed by separation in a second dimension, by SDS-PAGE, which separates denatured proteins by size. Separating the immunoprecipitated proteins using IEF would also separate AtRGL2 from antibody light and heavy chain fragments that have interfered with analysis when using a single dimension SDS-PAGE only. *A thaliana ga1-3* inflorescence protein extract was subjected to immunoprecipitation with the AtRGL2-specific mAb BB7, followed by first dimension separation of the eluted proteins by IEF on a pH 3 to 6 gradient gel and second dimension separation by SDS-PAGE. Sypro-ruby protein stain and western blotting, probing with anti-DELLA mAb BC9, were used to examine the immunoprecipitated proteins (Figure 4.10). The western blot of two-dimensional gels, probed with anti-DELLA mAb BC9 detected an AtRGL2 spot, clearly separated from the antibody heavy and light chain fragments. AtRGL2 has a theoretical PI of 4.82 and size of 60.4 kDa and this matches its position as detected on the blot. However, the AtRGL2 could still not be detected in the eluate using the sypro-ruby protein staining alone. Sypro-ruby has a limit of detection of 1 to 10 ng, therefore the amount of recovered AtRGL2 must be below 1 ng.

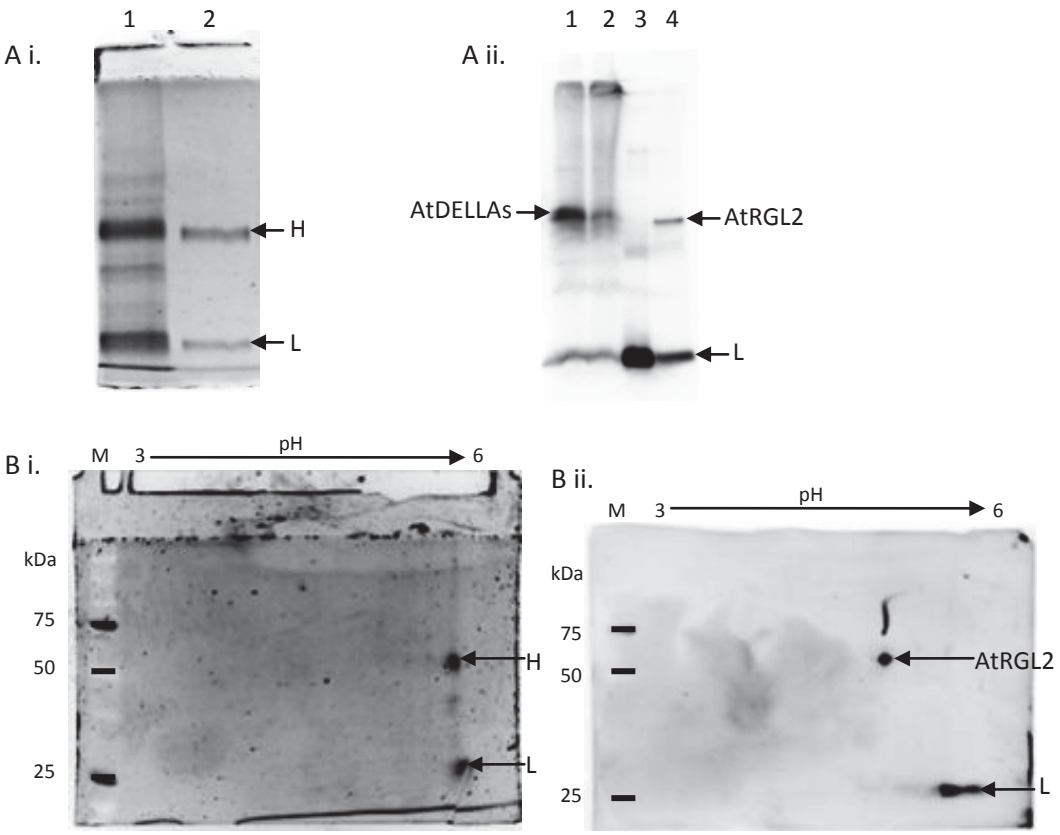

Figure 4.10. Immunoprecipitation of AtRGL2 using BB7 and analysis by two-dimensional PAGE

Proteins from *ga1-3 A. thaliana* total cell extract were immunoprecipitated using mAb BB7 and anti-mouse IgG magnetic beads and analysed by one- and two-dimensional PAGE.

Ai, Sypro ruby stained one-dimensional SDS-PAGE gel. Lanes: **1,** mAb-immunoprecipitated proteins; **2,** antibody light and heavy chain proteins.

Aii, Western blot monitoring the immunoprecipitation, probed with anti-DELLA mAb BC9. Lanes: **1,** plant extract before immunoprecipitation; **2,** proteins remaining in the extract after immunoprecipitation; **3,** mAb BB7; **4,** immunoprecipitated proteins in the eluate.

Bi, Sypro ruby stained protein gel following separation in two dimensions; IEF (horizontal) and denaturing (vertical) PAGE.

Bii, Western blot of an identical two-dimensional gel as shown in Bi; probed with anti-DELLA mAb BC9.

H, Heavy and; **L,** Light antibody chains; **kDa,** kiloDaltons; **M**, molecular weight marker; **pH**, the pH range of the IEF gel electrophoresis.

4.2.7 Separation of total protein extract by native-denaturing 2D electrophoresis and determination of DELLA-protein complex size

An alternative to specific co-immunoprecipitation is to separate out complexes directly from the mass of the proteome by two-dimensional PAGE. To identify protein complexes that contain DELLA proteins, instead of isoelectric focusing in the first dimension, native-blue PAGE was used which preserves protein complexes and allows migration based on protein size. The samples (total inflorescence protein extract from A. thaliana ga1-3::AtRGL2-TAPR transgenic plants) were pre-stained with Coomassie G-250, a non-specific protein dye that is negatively charged, allowing an extremely broad-range size-resolution of proteins (between sizes of 20 and 2,000 KDa)(Wittig et al., 2006). The proteins that migrate in complexes in the first (native) dimension were separated by size using SDS-PAGE (denaturing electrophoresis) in the second direction. Western blotting with anti-DELLA mAb BC9 was used for detection of DELLA proteins after the two-dimensional native-denatured electrophoresis of the crude lysate (Figure 4.11). A dominant DELLA signal was detected in the gel position that indicates a main complex of approximately 140-160 kDa; only a faint band was detected at intervals indicating a much smaller proportion of larger complexes, up to 600 kDa in size. The main three protein bands detected by mAb BC9 (RGA, RGL2 and GAI) were also detected at the position that corresponds to a monomer size. Possible composition of the 140 kDa complex could be a hetero- or homo-dimer of the DELLA proteins, each protein approximately 60 kDa. A comparatively faint ladder of bands of a much higher molecular weight is detected, in the range ~280 to 600 KDa. In the *ga1-3* background, in the absence of GA, it is hard to expect that the full GID1-DELLA-SCF-E3 complex is formed. In absence of GA, complexes of DELLA proteins with their target transcription factors (e.g. PIF3, PIF4 etc.) are expected to be dominant, hence the complexes detected in this work reflect the types of complexes that DELLA proteins belong to in their function of repressors of growth.

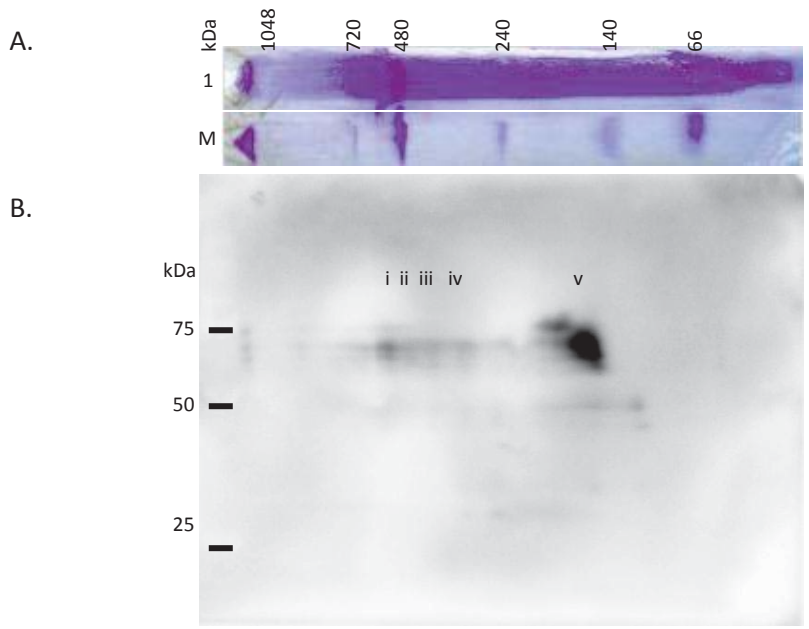

Figure 4.11. Two-dimensional separation of protein complexes and western blot
Total cell protein extract from inflorescences of *ga1-3::AtRGL2-TAPR* transgenic plants were separated by size in two dimensions. First dimensional separation was by blue native electrophoresis and the second by denaturing SDS-PAGE.
A, First dimension, blue native electrophoresis (BNE).
B, Western blot after the second dimension (denaturing) PAGE separation. The blot was probed with the anti-DELLA mAb BC9. Bands detected correspond to: **i – iv**, a ladder of bands between ~600 and ~280 kDa; **v**, ~140 kDa
M, molecular weight markers; **kDa,** kiloDaltons.

4.3 Mass Spectrometry

Mass spectrometry was used to identify proteins that were immunoaffinity purified using antibodies against AtDELLAs and also AtRGL2 specifically in sections 4.2.3, 4.2.4 and 4.2.5. Given that proteins from SDS-PAGE gel slab in the range expected for DELLAs (50-70 kDa) were analysed, only DELLAs and the interacting proteins matching that size range could be identified. A summary of identified peptides from all four mass spectrometry analyses are presented in Table 4.1. The highly-significant matches that were represented in the results several polypeptides (E-12 to E-06) correspond to highly abundant proteins in the total cell extracts, such as RuBisCo, ATP synthase, HSP70, chaperonins and tubulin. The only common hits between the four analyses were these highly abundant proteins. A dozen or so possibly interesting proteins were also identified, among them Serine/Threonine kinases, transcription factors, proteins involved in gene silencing, and factors involved in protein-protein interactions and RNA editing, as well as a ring-finger protein that is involved in protein ubiquitination and turnover. These hits are consistent with being possible targets for DELLA protein repressor activity and forming complexes with AtRGL2, which served as bait in immunoprecipitations. Further experiments are required in order to validate whether the identified hits are interaction partners rather than non-specific proteins. A DELLA peptide hit in the mass spectrometry data was expected, however it was not detected. Two main reasons for not detecting DELLA proteins by mass spectroscopy are: i. overall low amount; ii. post-translational modifications, which prevent correct identification of proteolytic peptides using mass spectroscopy fingerprinting. DELLA proteins contain multiple Ser and Thr residues which have been reported to be phosphorylated (Gubler et al., 2002, Hussain et al., 2007, Itoh et al., 2005a). Furthermore, O-acetylation of multiple Ser and Thr residues in these proteins has been speculated (Jacobsen et al., 1996). The AtDELLA proteins were detected by western blot experiments in a parallel control lane that was ran concurrently with the lane from which the proteins were extracted for mass spectroscopy, confirming that the analysed proteins should have been enriched for through immunoaffinity chromatography with anti-DELLA monoclonal antibodies. Evidence to confirm a genuine interaction may come from further refinement of pull-down experiments or with more sensitive methods, such as yeast-two-hybrid system or bimolecular fluorescence complementation (BiFC) experiments using recombinant proteins *in vitro*.

Table 4.1. Mass Spectrometry results

Peptides[a]	MW[b]	Protein[c]	Accession No.[d]	P (pro)[e]	Score XC[f]	% TIC[g]
K.EGIQEQLER.F R.ADEISNIIR.E R.PAINVGISVSR.V R.LIESPAPGIISR.R R.FLLQEKV R.EAYPGDVFYLHSR.L K.TLTAEAESFLK.E R.EVTIVNTGTVLQVGDGIAR.I R.SVYEPLQTGLIAIDSM*IPIGR.G R.IFNVLGEPVDNLGPVDTR.T R.IFNVLGEPVDNLGPVDTR.T	(α) 55 (ß) 63	ATPase subunits α & ß	5881679 5881701	4.16E-12 8.05E-07	88.25 10.22	7.97 0.94
K.WSPELAAA#EVWK.E K.EITFNFPTIDKLDGQE.-	52	RuBisCo	5881702	6.15E-10	30.25	2.03
Not given	49	ß Tubulin 1	4105696	1.38E-06	20.15	0.67
R.IINEPTAAALSYGM*TNK.E K.VQSIVAEIFGK.S	72	Mitochondrial Heat shock protein 70; ATP binding.	15242459	8.74E-12	20.25	NG
R.AIELPNAM*ENAGAALIR.E R.GYISPQFVTNPEK.L K.LLAEFENAR.V R.NVVLDEFGSPK.V K.ELFETDSVYDSEK.L K.LADLVGVTLGPK.G K.VVAAGANPVLITR.G K.SAENNLYVVEGM*QFDR.G	62	Chaperonin 60α & ß; ATP binding / protein binding	15226314 15222729	2.03E-09 1.29E-06	50.22 30.20	NG
R.VINALANPIDGR.G R.LIESPAPGIISR.R	55	Chloroplast ATP synthase CF1α	7525018	3.85E-03	18.14	NG
K.LEGIGKEM*NMKVK.R	55	Serine/ Threonine kinase (AGC family); NAF domain.	15215664	8.86E-02	8.12	NG
R.DGFEPNVFTYNVLLK.A	74	Pentatricopeptide repeat-containing (PPR) protein. Unknown function	15229026	1.27E-03	10.12	NG

Peptides[a]	MW[b]	Protein[c]	Accession No.[d]	P (pro)[e]	Score XC[f]	% TIC[g]
K.SDVYSFGILLLELLTAKR.P	86	Serine/threonine kinase	30685668	1.00E+00	10.11	NG
R.F]HDKADSLLHC#LPGCLTVNVM*R.A	47	Unknown function; Armadillo (ARM) repeat,C2 domain	26451199	1.00E+00	10.13	25.63
K.VNQIGSVTESIEAVK.M	47	Bifunctional; Transcriptional activator/ Enolase 2	15227987	2.26E-04	10.17	4.72
R.N]ILEDM*PCVSTR.D	35	Ninja family protein AFP4/ TMAC2. Unknown function, ABES elements	18396086	5.30E-02	10.13	3.82
R.LNHSKIDGKSV.E	55	BRIZ1; RRM domain, Zinc fingers RING type and ubiquitin-hydrolase domain	42569859	1.00E+00	10.10	14.15
SQGAANS	49	TCP family 18/ BRC1. Non-canonical bHLH structure, R domain	186510200	NG	NG	NG
SQTIS(OxH)	40	2A6; 2-oxoglutarate dioxygenase (Ethylene)	599622	NG	NG	NG
NVIFKK HLNGTVLQ HRLGLLT(OxM)YDQFLSRK	82	CPSF100; mRNA cleavage, poly Adenylation and gene silencing	15237845	NG	NG	NG
SGAFITI DGVVKNLTR	48	RNA binding protein, S1-like domain/ Tex	15982885	NG	NG	NG
GGVEGIQ KSGQHIN HVVPLTE GGVEGIQYI	65	Jasmonate inducible protein (putative); Lectin domain	12321345	NG	NG	NG
SQSIKKVD	68	PUMILIO 12; RNA binding 3'UTR	22327888	NG	NG	NG
SSPTGS(OxH) SKGFEIRR	55	OTU-like cysteine protease, UBA domain	18401397	NG	NG	NG
SSSASKPFSKK EESIK AIDYIYSFGMV(OxH)R	44	Unknown function; FRIDIGA-Like protein	93007384	NG	NG	NG

Peptides[a]	MW[b]	Protein[c]	Accession No.[d]	P (pro)[e]	Score XC[f]	% TIC[g]
ELAATR LLKLEEAGLTISAASR RRLRHGFSELNSSFDR	31	Unknown function; ARM repeat family protein	30688260	NG	NG	NG
(OxM)AQKNKFEK LASGIF	89	R gene (TIR class)	30696524	NG	NG	NG
S.LLSDSFRQVISSVDLFQTR.S	47	F-box/ kelch repeat-protein	15227579	18	10.2	16.21
R.DLNIEWSHSEE.H	52	Phloem protein 2-like A3; AIG1 domain	15225799	4.1	10.1	17.33
L.TDEVLAFAR.N	48	BSD domain-containing protein; BSD domain	18391195	16.2	16.2	10.91

[a] peptide sequence obtained from mass.
[b] protein molecular weight (kDa).
[c] & [d] BLAST search of NCBI Arabidopsis Genbank database with peptide to find protein hit and accession number.
[e] Protein probability value.
[f] Seaquest score.
[g] Indication of the relative amount of the peptide's presence in the protein mix.
[e], [f], [g] are three of the evaluation metrics used to determine the peptide hit relevance and balanced to judge the significance.
NG- Not Given

4.4 Immunolocalisation experiments

Localisation of DELLA proteins to specific cells has to date only been done using over-expressed GFP fusions in roots and in etiolated plants (Silverstone et al., 2001, Wen and Chang, 2002). Localisation of DELLA RNA into regions in tissues has been done using Northern assays (Chandler et al., 2002). However, RNA is not a good indicator of DELLA protein localisation because the key regulatory step in this family of proteins is protein degradation and turnover (Dill et al., 2001, Silverstone et al., 2001). A battery of monoclonal DELLA-specific antibodies produced within the research group is a unique resource that provided an opportunity to monitor DELLA proteins, in specific cell types within the inflorescence and other developing tissues. DELLA proteins have been detected using these antibodies by western blotting [section 4.3 (Sheerin, 2010, Sun et al., 2008)]. However, this method can only analyse the whole tissues, and it cannot be used to detect the exact cells within a tissue in which DELLAs are localised. There is a lack of published data about DELLA protein distribution and this can be attributed to the low amount of DELLA proteins, even in the tissues where they are most abundant and also through a lack of specific monoclonal antibodies that could be used to detect these proteins without detecting non-specific "background". To attempt detection of specific inflorescence cell containing DELLA proteins, immunohistological methods were employed. As in the previous sections, *ga1-3* mutant plants were used in order to maximise chance of success, because of the higher amount of DELLA proteins in this GA-deficient mutant compared to the wild-type plants. Also, like in the immunoprecipitation experiments, a null (*Δglobal*), or nearly null (*Δquad*) DELLA genetic background (which were negative in western blotting) was used as a negative control.

To prepare the samples for immunolocalisation and microscopy, plant inflorescences were fixed, embedded and sectioned according to the protocol laid out in sections 2.2.21 and 2.2.22. As a low amount of DELLA proteins was expected (based on the western blotting data), three different fixatives were used in order to find best conditions for immunodetection: 2% formaldehyde with high glutaraldehyde (2.5%) and low glutaraldehyde (0.1%) in PBS and FAA (50 % ethanol, 10 % glacial acetic acid, 5 % formaldehyde). Embedding was done in LR white for the light and electron microscopy. Embedding in paraplast wax, following fixation in FAA, was also done for light microscopy. For light microscopy immunodetection, experiments using primary antibodies (either DELLA-specific BC9 or AtRGL2-specific BB7), were used in conjunction with secondary antibodies conjugated to alexa fluorophors 594 or 488.

Numerous attempts were made to detect DELLA proteins in the inflorescence, the organ that is easy to collect and store and contains relatively higher amount of DELLAs than any other organ (as determined by western blotting, this study). Even though some signal was obtained in these experiments, no conclusive data were obtained. There was no significant overall increase of staining signal in *ga1-3* sections relative to the *Δquad* sections. Overall, the signal was weak and no difference was observed between the AtRGL2-specific antibody and the control (irrelevant antibody) when the fluorescently labelled cells were investigated by light microscopy (Figure 4.12).

A.

B.

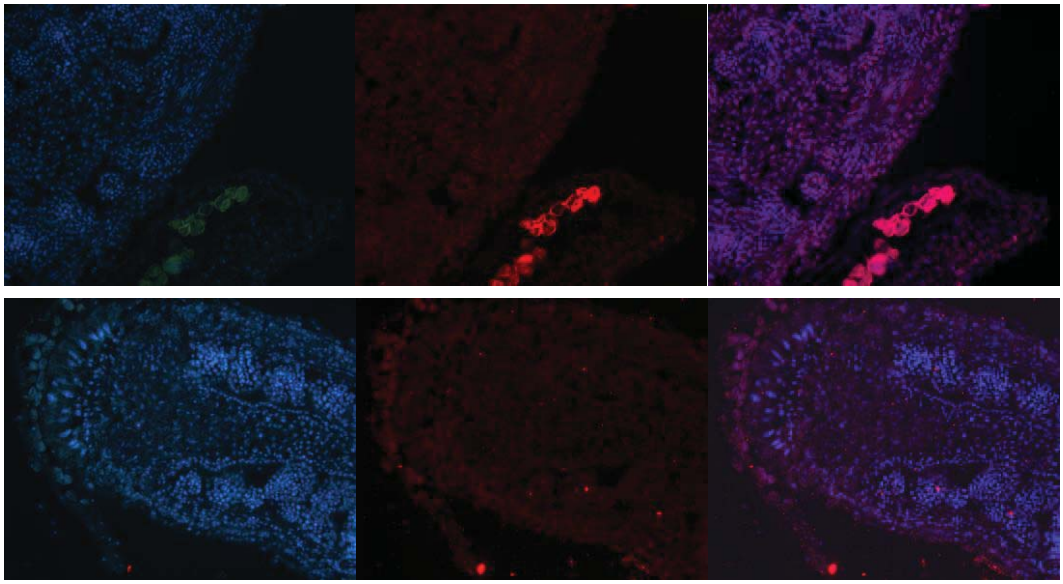

Figure 4.12. Immunohistological localisation of AtRGL2 in A. thaliana gai-3 styles
The tissue sections were fixed and probed with: **A,** AtRGL2-specific mAb BB7;
B, negative control mAb D9
Panels (left to right); DAPI nuclear stain, mAb –anti-mouse IgG Alexa 594, Merge.
400X magnification.
Note: Auto-fluorescence from pollen grains was very strong.

To increase the sensitivity of DELLA localisation and to eliminate non-specific auto fluorescence, sections were cut and probed for electron microscopy. This experiment utilises the primary antibodies as the previous immunolocalisation technique but with gold-conjugated secondary antibody. Nucleus-localised staining was observed in transmission electron micrograph when DELLA-specific antibody BC9 was used, but not when an unrelated (negative control) antibody was used (Figure 4. 13). This is consistent with DELLA-GFP fusion protein experiments where fluorescence is seen to be localised to root nuclei (Fleck and Harberd, 2002, Itoh et al., 2002, Silverstone et al., 2001).

Numerous experiments were undertaken in which fixing, blotting, binding and detection dyes were varied for light microscopy; however the detection could not be improved. It appears, then, that the lack of data on histological localisation of DELLA proteins is caused by the low abundance of these proteins, which could not have been overcome by using high-affinity monoclonal antibodies.

A.

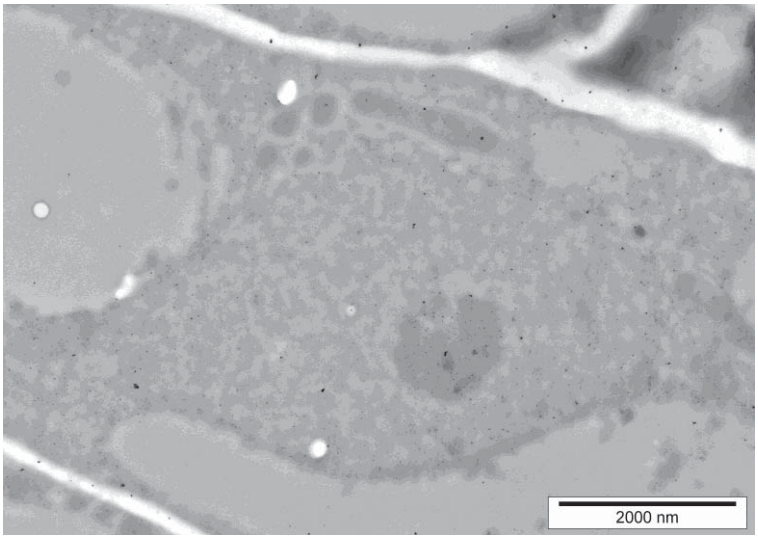

B.

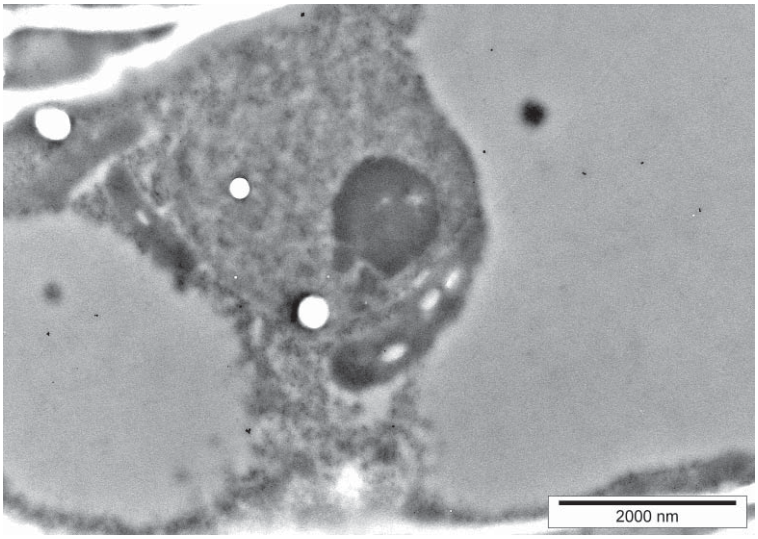

Figure 4.13. AtRGL2-specific immunogold-labelled transmission electron micrograph
Tissue sections of *ga1-3 A. thaliana* plants were probed with: **A**, anti-AtRGL2 mAb BB7 or **B,** negative control mAb D9; both sections were incubated with immunogold-labelled secondary antibody.

4.5 Summary of Immunopurification and localisation

A monoclonal antibody, D9, was produced against a novel peptide sequence called the R-tag. A tandem purification fusion tag was modified to incorporate this novel immunogenic peptide to produce a high-affinity purification and tracking tag named TAPR, to use with expression of recombinant proteins in plants. The TAPR tag was shown to function when produced in *E. coli* and was used for affinity purification of tagged proteins from *E. coli* extracts. However, when used in transgenic plant constructs, the expressed proteins were not able to be detected in western blots of these transgenic plants using the R-tag epitope, although the recombinant protein as a whole could be visualised using DELLA-specific antibodies. The increased molecular weight of the product over the wild-type proteins after SDS-PAGE and western blot indicates that some portion of the R-tag was part of the fusion and was successfully used to affinity-purify AtRGL2-TAPR fusion from a whole cell protein extract using monoclonal antibody D9 anti-R columns.

The AtRGL2-TAPR affinity-purification (pull-down) and immunoprecipitation experiments with anti-DELLA mAb BC9 and anti-RGL2 mAb BB7 were all analysed by mass spectroscopy in order to identify potential novel RGL2-interacting proteins. The plant extracts were derived from the plants that have no GA signalling (*ga1-3* plant background) and therefore they focus on isolating interacting proteins involved in regulatory or suppressor functions of RGL2 on the target genes. The results from the mass spectrometry analysis of these immunoprecipitation experiments are combined and shown in Table 4.1. The table represents the 'best' hits after a set of evaluation metrics was used to sort the data (pers. com, Dr Dave Greenwood). Although the DELLA proteins themselves were not detected, some of the identified proteins (after the major cell componentry proteins are removed) are considered interesting and would be worth investigating further. They are discussed in section 5.3.3.

The transgenic *RGL2-TAPR* plants were also used to investigate the size of RGL2-containing complex in the absence of GA signalling (*ga1-3* plant background) using 2D-PAGE and detection using mAb BC9, which detects all *A. thaliana* DELLA proteins (Figure 4.11). A major complex incorporating DELLA proteins was detected at ~160 kDa in size and a much smaller complement of complexes were detected as a ladder of increasing size, up to 600 kDa, showing that DELLA proteins act as a complex that must include other proteins.

Transgenic plants expressing the GUS reporter under the control of the *AtRGL2* promoter and terminator sequences were constructed to confirm the correct expression of the RGL2 transgenes under the native promoter. The pattern of reporter expression seen was consistent with the growth/ expansion state of the organ developmental process. With the various inflorescence organ tissue areas undergoing and then ceasing expansion, GUS activity was detected in young tissue prior to and then again after expansion had taken place (Figure 4.4). This indicates a level of control at the promoter that is inversely correlated with the (expected) places of GA location/ activity. This pattern was not necessarily expected, as the point of control on DELLAs is thought to be predominantly post-translational (degradation on GA-signalling), and DELLA transcript may well be present where the protein would be degraded in order to compensate for the loss of protein.

Immunolocalisation experiments were performed, utilising light and electron microscopy with fluorescently-labelled and gold-labelled secondary antibodies respectively, on inflorescence tissue. Non-specific binding and auto-fluorescence were problematic and despite a number of attempts were not solved to yield consistent results in the light microscopy sections. However, they indicated nuclear-localised expression. The TEM results offered better images and indicated localisation in the nucleolus of the nucleus (Figure 4.13). However, unsuccessful definitive repetition and non-specific background confound a conclusion.

5. Discussion

5.1 Identifying the gibberellin signalling components

Apple and kiwifruit are horticulturally important crops for New Zealand. Apple is a small deciduous tree that after a juvenile phase will fruit for 50 or more years. Many apple cultivars are biennial bearers, with alternating light and heavy cropping, and this is undesirable, though it can be evened out through orchard management (GA inhibitors and thinning fruit buds) and also through selective breeding. Kiwifruit is a perennial plant that grows using twining vines in a two year seasonal cycle. At the start of a cycle dormant shoot buds break. Some grow through to the end of the season, while others terminate shortly after the break, wither, and die off. Floral buds form on the canes in the leaf axils but remain dormant through winter before breaking in the next season. These apple and kiwifruit developmental processes are regulated, in part, by the phytohormone gibberellin. The defined tissues with alternating growth and fruiting and the fact that they are economically important make apple and kiwifruit interesting plants to study.

The orthologous core components of the gibberellin signalling response were sought in apple and kiwifruit. They are the gene expression regulator DELLA protein family, the nuclear gibberellin receptor GID1 protein family, and the DELLA-specific F-box protein SLY1 (or GID2) protein family which mediates DELLA degradation upon the GA signal.

5.1.1 Database mining and sequence comparisons

The Plant and Food Research and Rosaceae data bases were mined and several candidates identified by the highly conserved elements within their sequences. Following further examination, sequencing to complete the mRNAs and elimination of redundancies, a final group of CDS was identified. In apple six *DELLA* orthologues, three *GID1* orthologues and two *SLY1*/ *GID2* orthologues; in kiwifruit seven DELLA orthologues, three *GID1* orthologues and three *SLY1*/ *GID2* orthologues were identified.

The clusters of similarities matched the known genome structures of the *Malus* and *Actinidia* stock in each case. For both the apple and the kiwifruit, two of the three groups (Ad/MdRGL1s and Ad/MdRGL2s) were distinctly closer to each other than the remaining third group

(Ad/MdRGL3s). They also clustered into separate clades when aligned with other plant DELLAs. This may help in analysing possible variations of functions, where a subgroup has a more (or less) dominant role in a particular developmental process. This analysis also identified a DELLA sub-family and appears to be the common denominator in both kiwifruit and apple, distinct from all other identified DELLAs. These are Ad/MdRGL3s, which cluster together, but are distant to all other DELLAs of dicotyledonous plants. Furthermore, the Ad/MdRGL3 branch was closer to the cereal DELLAs than to DELLAs of other dicotyledonous plants. The majority of the other dicotyledonous DELLA proteins are divided into two clades; kiwifruit and apple RGL1s belong to the same clade, and align with the "systemic" *A. thaliana* DELLAs GAI and RGA and also with one of two pea DELLA proteins, PsCRY. The other dicotyledonous clade contains the Md/AdRGL2s and also group with the second pea DELLA protein, PsLA. Interestingly the *Arabidopsis* RGLs are separate from these two main clades.

Expression studies of apple and kiwifruit DELLAs did not show a striking tissue-specificity of expression, however. The expression analysis also showed differences in both overall and specific *DELLA* transcript level between apple and kiwifruit DELLA sub-groups. These findings point to diversity in regulation of expression for *DELLA* genes in the kiwifruit and apple.

5.1.2 Tertiary structure probing

Following the primary sequence analysis, the tertiary structure of the kiwifruit DELLA proteins was modelled using the N-terminal tertiary structure of *A. thaliana* DELLA protein AtGAI. Furthermore, the conformation of the kiwifruit proteins was probed through cross-reactivity with a suite of monoclonal antibodies against N-terminal DELLA protein domain epitopes, some of which recognise different conformations of conserved DELLA protein motifs, again with the intension of seeing if patterns would emerge that would help in role/function analysis. Although the site of antibody interaction may represent a very small portion of the overall conformation, some are specifically targeted to conserved and functionally important regions of the protein eg. DELLA and TVHYNP motifs. Other antibodies with unknown epitope could still provide valuable information as epitopes are generally on the outside surface of proteins and would still show if a particular conformation existed, with the strength of the interaction indicating small variations in the broader conformation. Further work, such as nested deletion analysis followed by alanine scanning mutagenesis around the predicted epitope sequence would have to be done if the specific antibody contact residues are to be determined.

This analysis was broadly congruent with the primary sequence analysis, but also produced some interesting results. The clade with the wider separation from the other apple and kiwifruit DELLA sequence clades, containing the Md and AdRGL3a/ b pairs, did have (on the whole) a slightly different detection profile from other DELLAs, but this was not consistent for all different antibodies in the suite. For example, one of the monoclonal antibodies detected only one kiwifruit protein from each clade. The main conclusion would be that the substantial similarities between all *M. domestica* and *A. deliciosa* DELLA proteins dominated the detection process, with many antibodies detecting multiple DELLAs. The small differences in the mAb affinities for the various DELLA homologues could not be identified with this method without substantial optimisation. ELISA methodology would be a second method to investigate conformational differences. However, this too would be compromised as the full length DELLA proteins were not very soluble and therefore construction of truncated N-domain proteins would be required for analysis by ELISA.

5.2 Expression analysis of genes in apple and kiwifruit

The tissue-specific expression patterns of *MdDELLAs* and *AdDELLAs*, *AdGID1s* and *AdSLYs* was examined using quantitative PCR. The qPCR in the kiwifruit was carefully controlled, in accordance with the state-of-the-art standards. Furthermore, it was extensive in that it analysed all identified homologues (13 genes). This was a highly controlled experiment, normalised and calibrated with three reference genes and internal control. All of the genes studied were transcriptionally active in each and every tissue.

For apple the DELLA transcript relative levels were highest in the arrested tissues; the spur-type shoots and vegetative and floral buds. This is consistent with the paradigm that DELLA proteins mediate the restraint in tissues which are in a developmental pause; DELLA proteins have a dominant physiological role in those tissues and are expected to be present at this high level relative to that in expanding tissue. However, given that the key regulatory points for DELLA protein activity are at the level of protein turnover, the transcript doesn't need to be low in the expanding tissue in order to remove DELLA activity in growth/expansion restraint. This is supported by the findings presented in this thesis, showing that, for the kiwifruit, the relative *DELLA* transcript levels were highest in assayed somatic tissues of expanding leaves

and active shoot tips, followed by the breaking floral buds. On the whole, the relative DELLA transcript levels were lowest in the least active or dormant tissues. Concomitant with high relative levels of DELLA transcripts were high relative levels of transcripts encoding GA receptor *GID1* and the DELLA-specific F-box protein *SLY1*/ *GID2* orthologues. Bearing in mind that the relationship between transcript levels and protein levels is not linear nor equal across protein/transcript families (Foss et al., 2011) the high transcript level does not infer a high protein level. A high level of *A. deliciosa DELLA, GID* and *SLY* transcripts may have an advantage, in that it gives a maximal possible range of DELLA activity as well as an immediate response to a changing environment, signalled either by the GA or other upstream influences modulated by other hormones, pathogens or other stresses. The mechanisms of these other influences are not understood and they all may act at post-transcriptional and translational level. This is consistent with findings that, in general, *DELLA* transcripts are relatively much higher than *DELLA* proteins, implying multiple levels of post-transcriptional control. Overall, a high relative level of the *DELLA* transcript in comparison to generally very low protein level implies a fast turnover, and also a high dynamic range, allowing a broad scope for modulation of DELLA activity.

The apple *MdRGL3* was more highly expressed than either *MdRGL1* or *MdRGL2* in the recently arrested spur-type shoots, and may suggest a dominant role in initiating and maintaining developmental arrest of meristematic tissue. *Arabidopsis*, a short-lived annual, has no comparative tissues and developmental situation and specific sampling of the meristem during the vegetative-to-floral transition has not been reported. *Arabidopsis AtRGA* and *AtGAI* are the predominant repressors in the vegetative growth phase, overlaid by modulatory roles of the *AtRGL*s during the reproductive growth phase. In the (arrested tissues of) floral and vegetative buds in apple, each DELLA is at a similar relative expression level, none assuming a dominant role. However, the difference of the *DELLA* transcript levels between these two arrested tissues is large. This may indicate that in apple DELLAs have assumed a dominant repressive role in the vegetative buds and are less important in the floral buds and that floral tissue may have a DELLA-independent system in operation as well. In the actively expanding tissues of shoots and leaves the *MdRGL2* transcript is lower than either *MdRGL1* or *MdRGL3*. This may indicate the *MdRGL2* has an important role in these tissues, and its transcription is strongly repressed in order to enable the expansion to proceed. After the period of vernalisation, the seeds show a slight increase in expression between three and eight weeks post-germination. However, the relative levels are still low and comparable to expanding tissues. This is in

contrast to *Arabidopsis* that maintains high relative levels of the DELLA transcripts during germination (Foster et al., 2007, Lee et al., 2002b, Tyler et al., 2004).

The kiwifruit *AdRGL1*'s have the lowest relative expression levels of all *AdDELLA*s in all tissues and may have a basal repressor role. The kiwifruit *RGL1*s do group with the *Arabidopsis GAI*/*RGA* orthologues, whose transcription levels are also more even throughout the plant in comparison to the *AtRGL*s, which are tissue specific (Tyler et al., 2004). The *AdRGL2*'s show the least variable expression in various tissues among all *DELLA* genes, but their expression is much higher overall than that of *AdRGL1's*. This may indicate a role as the main repressor control in all tissue types, as it is with *AtRGA* in *Arabidopsis*. Where the other *AdDELLA*s are more highly expressed, they might be expected to add to the versatility and range of regulation available to the plant, or to take a more dominant role, such as in expanding leaves and styles. However, AtRGA-like kiwifruit DELLA proteins (AdRGL2s) do not group with *GAI*/*RGA* in the primary sequence alignment. The *AdRGL3*'s show the highest inducible expression and the largest variation across the tissues. This pattern of expression indicates mostly tissue-specific regulatory roles, during particular developmental processes. The expression of *AdRGL3*'s in styles of female flowers was particularly high.

The level of variation of the kiwifruit and apple *DELLA*s is smaller than their *Arabidopsis* counterparts. In *Arabidopsis AtRGL2* expression had a ~500 fold difference between 12 h seed and 33 day rosette leaf, apple *MdRGL3* showed a ~60 fold difference between spur-type arrested shoot and 8 day seed, while kiwifruit *AdRGL3b* showed a ~20 fold difference in expanding leaves relative to the male flower buds. Also, in contrast to *Arabidopsis*, the apple and kiwifruit DELLA transcripts were all found to be expressed in all analysed tissues. In contrast to *Arabidopsis*, where the *AtRGA* and *AtGAI* transcripts were clearly more highly and evenly expressed in comparison to the *AtRGLs* (Tyler et al., 2004),in apple and kiwifruit, despite *AdRGL1s* and *AdRGL2s* being more even than *AdRGL3s,* all transcripts showed some level of tissue regulation (Figures 3.8 and 3.27b).

On the whole, the *Arabidopsis*, apple and kiwifruit sequence relatedness did not correlate with the relatedness of expression patterns (Figure 3.14). The apple and kiwifruit RGL1's belong to the AtGAI/AtRGA clade, the apple and kiwifruit RGL2's formed a clade together as did the apple and kiwifruit RGL3's in a separate clade, and each of these two clades grouped with various other DELLA homologues. The curious point to this is that the *A. thaliana* RGLs were clustered together and apart from the apple, kiwifruit and other DELLA protein homologues.

This may be an indication of the very different life cycles of the plants, perennial versus annual, and is also an indication of heritage, such as with the cereal DELLA homologues clustered together but in a separate clade.

The observation of the apple and kiwifruit RGL3's clustering with the cereal DELLA proteins and the finding that these DELLA proteins also have a disrupted DELLA motif leads to further speculation of distinct clade functions. Cereal plants have a single DELLA gene (single per genome ploidy) that carries out all developmental functions which in the dicotyledonous plants are mediated by multiple DELLA proteins. It is possible that the cereal plants have evolved other GRAS family members to fulfil some of the DELLA protein functions. For example, rice genome encodes GRAS proteins that are closely related to DELLAs, and could be functionally categorised as DELLA proteins OsSLRL1 and 2; however these homologues completely lack the DELLA motif. They are speculated to maintain a basal level of growth restraint in specific tissues at points in development despite of the presence of GA in these tissues (Itoh et al., 2005b, Liu et al., 2007). With respect to the DELLA proteins from dicotyledonous plants, disrupted DELLA motifs are less responsive to GA-induced degradation (Boss and Thomas, 2002, Silverstone et al., 2001). On this basis it can be speculated that the *RGL3*'s in apple and kiwifruit, whose DELLA motifs partially diverged from the consensus, could have a basal role rather than the *RGL1*'s. Overall, transcriptional analyses in this thesis provide a range of observations that formulated multiple hypotheses on the roles of DELLA proteins in apple and kiwifruit. These hypotheses can be tested in the future by construction of knock-down and over-expression plants for each of the RGL groups in apple and kiwifruit.

Analysis of the kiwifruit GA receptor (*AdGID1s*) expression showed that the two closely related kiwifruit *AdGID1a* and *AtGID1c* share a very similar expression pattern, though *AdGID1c* orthologue has an overall much lower relative level. The third member, *AdGID1b,* which is an outlier in the AdGID1 family, also shows different and somewhat complementary pattern of expression in comparison to AdGID1a and AdGID1c. Based on the structural modelling of the kiwifruit DELLAs presented in this thesis, and findings in *Arabidopsis* (Nakajima et al., 2006), it could be hypothesised that all the AdGID1 proteins could potentially interact with all the AdDELLA homologues. Further to this, the simple presence of a GID1 homologue was found to be the critical factor for maintaining near-wild-type phenotype, with only a minor phenotypic modulation dependent on the particular paralogue present (Griffiths et al., 2006). Similar redundancy is observed for DELLA proteins (Gallego-Bartolome et al., 2010). A final point is

that DELLA proteins of one plant are able to function analogously in another plant, indicating a very high conservation of function [section 3.3; (Foster et al., 2007)].

All kiwifruit orthologues of the DELLA-specific F-box protein-encoding genes *SLY1*/ *GID2* have a comparable relative expression level pattern with no notable exceptions. Their patterns correlate more closely to AdDELLAs than to the AdGIDs. The transcriptional analysis of the core GA signalling genes in the kiwifruit showed both the co-regulation and differential regulation, which are likely to govern the abundance of transcripts in analysed tissues.

5.3 Isolation of DELLA proteins and interactions

A central role of DELLA proteins in plant development implies multiple interactions with other proteins and multiple post-translational modifications. Due to a relative ease of protein purification and large body of accumulate knowledge about the cell signalling in the model plant *A. thaliana*, DELLA proteins in this thesis were sought for in this system. Separation of the proteins in the crude plant extractions was carried out to isolate the DELLA proteins from the confounding complex mix. The aim of these experiments in isolating the DELLA protein(s) was to find any post-translational modifications if they were present and co-isolate interacting proteins. These would be determined and identified through mass spectrometry.

5.3.1 Detection of GA-independent DELLA-containing complexes

To determine the size of complexes that include DELLA proteins, 2D electrophoresis was performed, combining the blue native electrophoresis (BNE) in the first and SDS-PAGE in the second dimension. In each dimension in this method separation is on size (kDa), first separating the native proteins and protein complexes, and second, denaturing, which breaks up the complexes and identifies individual proteins (Figure 4.11). The DELLA proteins were detected after the BNE/ SDS-PAGE by western blotting and indicated possible protein complexes. The main complex detected had an approximate size of 160 kDa. In addition, a ladder of larger-size complexes was detected, up to 600 kDa. As the plant genetic background for this experiment was *ga1-3* and the plant therefore almost completely lacking in GA, it is not expected that the detected DELLA complexes contain the cell machinery for DELLA degradation e.g. the proteins: GID1, SLY1, and CUL, SKP and RBX components of the 26S proteasome. Instead, it is thought that these complexes represent the 'repressome' by which DELLA protein action is filtered. That is, these are the proteins that DELLAs bind in the developing inflorescences and are likely preventing them from performing their role such as

activating genes for floral organ expansion and flowering. The 160 kDa main complex detected is larger than a predicted DELLA dimer (~120 kDa); hence it likely contains at least one additional protein. Given that it is isolated from the inflorescence extract in the absence of GA, this 160 kDa complex may represent the most abundant DELLA "repressome" complex in *A. thaliana* inflorescences that include a primary target protein of DELLAs. The ladder of larger complexes (up to 600 kDa) most likely represent further secondary interactions or less common interactions, more fleeting and more variable interactions by comparison with the 160 kDa complex. The 160 kDa complex may also represent a core repressome unit, for example a DELLA duplex (~120 kDa) plus an additional (scaffolding/ repressor) protein (unknown, ~40 kDa), and the laddering may represents the recruited proteins being bound and prevented from performing their role. If so, the larger complexes could include additional proteins that bind the core complex under different circumstances, in different floral organs or are more loosely bound.

5.3.2 Immunoprecipitation and mass spectrometry

Affinity separation experiments were carried out with the aim to identify DELLA-interacting proteins in *A. thaliana* inflorescence. Direct immunoprecipitations (IP) were carried out with mAb BC9 that recognises all *A. thaliana* DELLAs, and mAb BB7 with a specific affinity for AtRGL2. In addition, indirect IP experiments using the anti-R-tag-specific antibody D9 was used, which acts on recombinant TAPR-tagged AtRGL2 transgene-encoded fusion proteins (the tag was developed within this thesis work). The experiments demonstrated an ability to enrich the DELLA proteins from inflorescence protein extracts, however no DELLA proteins were identified in the immunoprecipitated samples using mass spectrometry, despite the strong detection and enrichment as detected by the western blotting. DELLA proteins have large numbers of Ser and Thr residues and are reportedly phosphorylated on those residues. Together with potential O-acetylation, these modifications alter the detection of DELLAs by mass spectrometry and must be taken into account. The mass spectrometry data is screened for significant hits through several evaluation metrics and believed to represent good quality data. Furthermore, as seen in the results of western blots on slices of gel or of duplicate loadings of the IP samples, the presence of DELLA proteins was confirmed.

The data from the four experiments had very few identical hits, but those were matching the highly abundant proteins in plant cells, including RuBisCo, tubulin and ATP synthase subunits, that represent the background. Besides these hits, several hits that could be involved in DELLA

modification (protein kinases), repressor function (putative transcription factors) were identified. These hits were not repeated in more than one of four experiments analysed by mass spectrometry. This could be due to different methods/ antibodies/ genotypes used in the four immunoprecipitation experiments, but could also indicate the fleeting and variable nature of the DELLA interactions or a very low amount of both DELLAs and the co-immunoprecipitated proteins in the samples, placing them at the margin of detectability. The hits that are candidates for DELLA-interacting proteins included protein kinases, Zinc finger containing, and bHLH domain containing proteins. There were also proteins involved in other hormones' signalling pathways, in developmental processes such as germination and floral induction and others of unknown function. However, some cannot be explained due to insufficiency of published data, or are otherwise hard to rationalise. All require further experimental evidence of an interaction, through experiments such as yeast-two-hybrid system or the reverse co-immunoprecipitation experiment. Potential of identified hits for a role in DELLA repressor function or modulation is discussed below.

- Ser/Thr kinase AGC family with NAF domain protein: The NAF domain is a protein-protein interaction domain of Ca^{++}-regulated kinases. The AGC is a family of kinases that are important regulators of growth, development and defence (Bögre et al., 2003, Hirt et al., 2011).
- PPR-containing protein, of no known function. The PPR (pentatricopeptide repeat) structure is not solved, but is predicted to fold in a helix-turn-helix structure. PPR proteins are a very large family of proteins and have been demonstrated to bind nucleic acids and are involved in gene regulation (translation), especially RNA processing and stability. They are usually mitochondria and chloroplast targeted (Prikryl et al., 2011). DELLA proteins have been demonstrated to bind at the bHLH domain/ structure of the target proteins (Feng et al., 2008).
- A Ser/ Thr/ Tyr protein kinase with α-β-α sandwich fold possibly involved in response to stress. Not sufficient information to examine, however DELLAs are phosphoproteins (Fu et al., 2004)
- ARM/ β-catenin repeat and C2 domain protein. Armadillo repeats are probably protein-protein interaction domains. The C2 domain is an eight-stranded β-sandwich. Most C2 domain proteins are signal transducers, Ca^{++}-dependent and membrane-targeted.
- *LOS2* (*LOW EXPRESSION OF OSMOTICALLY RESPONSIVE GENES 2*) is an enolase 2/ bifunctional transcriptional activator involved in response to salt stress, ABA, cold and

light. Enolases are enzymes that catalyse a reversible dehydration reaction in the glycolytic or glucogenesis pathways (Lee et al., 2002a). This function fits with the known role DELLAs play in modulating growth in response to stress (Achard et al., 2006).

- *AFP4* (*ABI BINDING PROTEIN 4*) is a ninja family protein (a.k.a. TMAC2). *AFP4* is a negative regulator of ABA and salt stress responses, and could play a role in controlling root elongation, floral initiation and starch degradation. It contains ABA response elements (ABREs) and promotes ABI5 degradation, a bZIP Transcription factor, by binding to it. *ABI5* is induced by ABA and arrests growth during stress (Lopez-Molina et al., 2003). A scenario could be envisaged in which the DELLA action prevents AFP4 promoting AB15 degradation and thus promotes continued growth restraint.
- *BRIZ1* (*BRAP2 RING ZnF UBP DOMAIN CONTAINING PROTEIN 1*). This protein has a RING zinc finger protein-protein (C3HC4 type) domain and a UBP zinc finger ubiquitin hydrolase domain. The BRAP2 domain binds the nuclear localisation signal (NLS) domain. BRIZ1 heterodimerises with BRIZ2 to form an E3 ligase complex required in seed germination and post germination growth (Hsia and Callis, 2010). It could be speculated that the DELLA proteins, by interacting with BRIZ1 in the inflorescence, may be holding the E3 complex apart, and holding off activation of E3 ligase, to allow time for development of the seed cells while they are being defined in the ovules, and preventing premature germination.
- *TCP18* (named for a family of proteins derived from the first members described TB1, CYC and PCF, this is number 18; also called *BRC1*). *TCP18* is a transcription factor that has a non-canonical helix-loop-helix (bHLH) structure. Family members are known to regulate organ morphogenesis in plant development. *TCP18* has been specifically implicated in delaying axillary bud development and outgrowth and therefore works with the auxin-induced control of apical dominance (Aguilar-Martínez et al., 2007). Its role in the axillary structures such as the flower is less clear. While auxin maintains apical dominance, and cytokinin promotes outgrowth, GA also has a role promoting differentiation and is therefore low in meristematic tissues such as axillary meristems. *LATERAL SUPRESSOR* (*LS*) is a VHIID/GRAS protein of the same family as the DELLA proteins and promotes lateral stem formation and it may also have a role as a negative regulator of GA signalling (Shimizu-Sato and Mori, 2001). In this regulatory circle, DELLA proteins may therefore be binding TCP18 to allow the outgrowth from axillary meristems and help maintain the meristem tissue by preventing the GA-promoted differentiation.
- *2A6* (*1-AMINOCYCLOPROPANE-1-CARBOXYLATE OXIDASE HOMOLOG* 5) is a putative 2-oxoglutarate/ FeII-dependent dioxygenase, likely involved in ethylene biosynthesis.

Ethylene and GA both contribute to elongation and differentiation in certain developmental processes such as flower opening and germination, however ethylene is also thought to increase DELLA stability under stress conditions (Achard et al., 2003, Chiwocha et al., 2005). Interaction of DELLAs with 2A6 in the inflorescences may be acting to prevent ethylene biosynthesis and thereby delaying the development and opening of the flowers.

- *CPSF100* (*CLEAVAGE AND POYADENYLATION SPECIFICITY FACTOR 2,100 kDa SUBUNIT*) is involved in poly-adenylation of transcripts. CPS100 forms a complex in *Arabidopsis* with four other CPSFs and acts in post-transcriptional gene silencing in the embryo and during seed germination. CFS100 complex interacts with the flowering time regulator FY (Herr et al., 2006). FY also interacts with FCA (in the autonomous flowering pathway). The FCA/FY complex promotes reproductive development by down-regulation of FLC floral repressor (Simpson et al., 2003). If the DELLA protein interaction interrupts the CPSF complex and prevents silencing of this complex's targets it will be assisting the FLC repression of floral development.
- An unknown RNA binding protein. It has S1 and S1_tex RNA-binding domains.
- T8L23.4 is a putative and uncharacterised protein with a jacalin-like lectin domain that can bind O-linked GlcNAc sugars. DELLA proteins may be post-translationally modified with O-linked GlcNAc moieties, however this has not been directly demonstrated (Jacobsen and Olszewski, 1993).
- *APUM12* (*ARABIOPSIS PUMILO 12*) is a Pumilo family protein, which is defined by the PUF domains. The Pumilo proteins bind 3'UTR of mRNAs and are involved in post-transcriptional RNA metabolism, however their targets are unknown in *Arabidopsis* (Abbasi et al., 2011). A DELLA protein that binds PUMILO 12 could be blocking its activity, in turn increasing the amount of transcripts and the translation efficiency of Pumilo targets.
- 2OTU-like cysteine type protease contains a UBA-ubiquitin associated-domain. Although in the absence of GA (this protein is isolated from the *ga1-3* mutant), the UBA domain proteins may act by limiting the ubiquitin chain length on a protein targeted for the 26S proteasome (Mueller and Feigon, 2002). The DELLA proteins in this case would be contributing to the instability of another ubiquitinated protein.
- Unknown protein, similar to *FRIDIGA*. *FRIDIGA* is involved in flowering time regulation in the vernalisation pathway; it accelerates flowering after a cold period. It interacts with *FLOWERING LOCUS C* (*FLC*). FLC interacts with and negatively regulates *SUPRESSOR OF OVEREXPRESSION OF CONSTANS 1* (*SOC1*) which promotes flowering through *LEAFY* (*LFY*).

SOC1 also integrates the GA-dependent and autonomous flowering pathways. FLC is part of a protein complex and may be a target of multiple intersecting pathways (Johanson et al., 2000, Moon et al., 2003, Helliwell et al., 2006). It is not clear how the DELLA interaction with a FRIDIGA-like protein aids in the repression of FLC.

- ARM/ β-catenin-like repeat protein of unknown function. The ARM repeats are likely a protein-protein interaction domain. There is no commonality between the diverse proteins that have ARM repeats that has enabled a biological familial function to be discerned. Poor characterisation therefore makes it impossible to speculate on its potential role in a putative complex with DELLA.
- TIR-class disease resistance protein contains the TIR domain that mediates protein-protein interactions between Toll-like receptors and signal transduction components and is located in the membrane. It is not immediately clear how a nuclear-located DELLA protein would interact with a membrane protein. However, the closest match to another protein is *CIP7* (*COP1-INTERACTING PROTEIN 7*), a nuclear protein and a positive regulator of light-regulated genes. The CIP7 protein is a match for only one of the two peptides identified by mass spectrometry; the second peptide had no match, hence the reliability of this hit is questionable, however if correct, it could be involved in the cross-talk between the light and GA pathways mediated through E3 ubiquitin ligase COP1 that targets transcription factors such as HY5 and CIP7 for degradation (Alabadi et al., 2008). The HY5 transcription factor has been demonstrated to interact with DELLA proteins; DELLAs may be involved indirectly in the turnover of transcription factors such as HY5 or CIP7.
- F-box/ Kelch repeat protein of unknown function; kelch repeats are a β-sheet structure and are found in a diverse group of proteins.
- *PP2-A3* (*PHLOEM PROTEIN 2-LIKE A3*). *PHLOEM PROTEIN 2* is a very common protein in the phloem, but not well understood. It has RNA-binding and lectin (carbohydrate-binding) activities and responds to nitrate levels and bacteria. *PP2-A3* contains an AIG1 (avrRpt2-induced gene 1) domain involved in the plant response to bacteria (Dinant et al., 2003). DELLA proteins are involved in the stress responses (Achard et al., 2006), and GA and DELLAs are involved in the balance between the SA and JA pathways (Navarro et al., 2008). DELLAs bind a repressor of the JA pathway and therefore promote the JA response to necrotrophic pathogens, while the presence of GA modulates the SA response to biotrophic pathogens (Hou et al., 2010).

- BSD domain containing protein of unknown function. The BSD domain is associated with basal transcription factors and probably involved in chromatin association. The structure is predicted to be three bundled alpha helices (Doerks et al., 2002).

Of the 20 proteins discussed here there are some common themes: six are transcription factors or signal transducing proteins, four are RNA binding/ processing proteins, four are stress response related and two each are involved in disease resistance and ubiquitination. There are two Ser/ Thr kinases, two proteins containing ARM repeats and two bHLH domain containing proteins. Based on their predicted functions, all these proteins are potential candidates for targets or accessories involved in DELLA-mediated repressor functions or could be proteins involved in regulatory modifications of DELLAs independent of GA signal.

5.4 Immunolocalisation of DELLA proteins in *A. thaliana*

Although the expression of DELLA genes has been monitored using transcriptional reporter fusions and *in situ* RNA hybridisation, the histological investigation of DELLA proteins' distribution in plant tissues and within the cells has only been studied using over-expressed translational fusion to green fluorescent protein, which could only be monitored in roots due to natural fluorescence of chlorophyll in above ground structures (Lee et al., 2002b, Silverstone et al., 2001). DELLA proteins have not to date been detected using direct immunohistological approach using specific antibodies. Given that a suite of monoclonal DELLA-specific antibodies developed at Plant and Food Research have high affinity for DELLA proteins (Sun et al., 2010), this was an excellent opportunity to investigate whether detection of DELLA proteins without over-expression would be possible. This investigation acknowledged that western blotting (Chapter 3.1.2 and (Sheerin, 2010)) and reports by others (Willige et al., 2007) indicated low abundance of DELLA proteins, yet the antibody suite in hand gave the impetus for attempt to localise DELLA proteins by immunohistology. This work was also motivated by the crucial role of intrinsic DELLA protein turnover in regulation of GA signalling.

The tissues were chosen over time points to cover large development courses or tissues that have been seen in other plants to express relatively higher levels of DELLA mRNA than other tissues. For example, samples were taken from vegetative buds starting from the stage of dormancy to the stage after growth initiation, from floral buds starting with the stage of

dormancy and throughout their development into floral organs. A number of species, tissues, antibodies and fixation/staining conditions were trialled, with only marginal success (Figures 4.12 and 4.13). Results from inflorescence tissue are presented.

From the light microscopy of a style, the auto florescence was high and tended to obscure the signal (Figure 4.12). However, although the results are not particularly definitive, they do on balance of likelihood, confirm the protein is localised predominantly in the nucleus. DELLAs appeared to be present in all the cell nuclei of the style prior to elongation. No further sub-cellular location conclusion could be made. Therefore, in order to overcome the auto fluorescence, and to examine the cells with greater magnification, electron microscopy was undertaken.

Coming to a definitive conclusion from immunolocalisation experiments utilising electron microscopy suffered from similar problems as with the light microscopy technique, both being limited due to the very low signal, which brought up the non-specific background binding. However, the nucleolus of the nucleus did contain patches of dense signal, much more so than the singular spots of non-specific signal scattered elsewhere (Figure 4.13). In support of this conclusion, some of the mass spectrometry hits, CPSF100, APUM12 and 2A6, are also reported to be located in the nucleolus. The nucleolus has been proposed as a protein sequestration region within the nucleus to prevent interaction with binding targets (Audas et al., 2012).

The exhaustive immunolocalisation experiments that were undertaken in this work showed that the amount of natively expressed DELLA proteins *in situ*, even in tissues where they are most abundant, is too low for reproducible detection by immunohistological approach. In addition, it is possible that the antibody epitopes are altered and/or destroyed in the fixation process or were blocked through their interaction with interacting molecules.

Interestingly, the GUS reporter gene expressed from the native *AtRGL2* promoter gave very strong signal in the light microscope, in contrast to the transgenic *AtRGL2* CDS under the native *AtRGL2* for which the antibody detection was difficult to achieve (Figure 4.4) As GA-deficient mutants were used in the immunohistological experiments, this implies attrition of DELLA proteins due to other signals, aside from GA. Indeed, a proteasome inhibitor was required in the protein extracts isolated from *A. thaliana* in order to preserve DELLA proteins beyond 30 min after breaking the plant cells. This suggests that unknown pathway(s) of DELLA proteasome-dependent degradation operate, in addition to the GA-triggered pathway.

5.5 Future directions

Comparing the amount of DELLA transcript with the amount of protein in various tissues appears to vary in different species. Work in barley indicated DELLA presence in the expanding basal portion of the leaves nearest the culm where GA would also be expected at its highest (Chandler et al., 2002). The kiwifruit work in this thesis also shows a higher relative transcript level in active expanding tissues. However, the apple work indicates higher relative levels in the less actively expanding and arrested tissues [Section 3.1.3; (Foster et al., 2007)]. Another reported contradictory finding is that the transcript levels of the phenotypically observed dominant repressor of seed germination *AtRGL2* in *Arabidopsis* is lower than the transcript levels of the "systemic" DELLA, *AtRGA* (Tyler et al., 2004). These observed 'discrepancies' are undoubtedly manifestations of complex regulation much beyond a simple interpretation of the current paradigm that DELLA and GA are in equilibrium. Rather, the DELLA transcript and protein levels appear to be a result of complex species-specific regulatory mechanisms that act at multiple levels; expression, transcript turnover, translation, and protein modification and turnover. Experimentation to determine and compare all these layers of regulation, from transcript level, transcript turnover, translation efficiency, protein modification and protein turnover in a particular tissue at a particular developmental stage is required to understand the overall DELLA activity regulation. Additional experimental samples over consecutive years would improve the biological replicate data and could confirm whether or not there is a sharp mean transcript level at a developmental stage, however if a complex regulatory situation exists a broad range could exist. In summary, a comprehensive effort must be invested in order to obtain all 'variables' required to understand the relationship between the amount of transcript and the penultimate pattern of DELLA activity.

The DELLAs have been reported to be constitutively phosphorylated and there is conflicting evidence on what this is actually signalling (Fu et al., 2004, Gubler et al., 2002, Itoh et al., 2005a). This controversy in the interpretation of phosphorylation data is likely due to oversimplification; a large number of Ser and Thr residues in DELLA proteins in conjunction with the key role of these proteins - that of processing a number of environmental and developmental cues, in addition to the GA signal - sets the stage for complex phosphorylation patterns obtained by action of multiple kinases. This is the case with, for example, cell-cycle regulating proteins such as CDC25 (Frazer and Young, 2012, Zeng and Piwnica-Worms, 1999). One facet of phosphorylation is modulation of DELLA-protein-marking for proteasome-

mediated degradation. In that respect, *Arabidopsis* and rice, which have distinctly different sets of phosphorylation target residues (Ser/Thr and Tyr) in their N-terminal regulatory region, have distinct phosphorylation patterns that may have opposing effect on susceptibility of the corresponding DELLAs to degradation. There is no direct evidence for O-glycosylation of DELLAs, however, a putative O-glycosyl transferase, SPY, has a large impact on GA signalling pathway and also on many cellular processes. It would be useful to dissect the post-translational modifications found on the DELLA proteins in tissues, cell types and at developmental stages in order to understand the functional significance of each state by relating it to the levels and modifications of DELLAs in the tissue from which they were extracted.

Some twenty DELLA-co-immunoprecipitated proteins were isolated during this thesis experimental work from the model plant *A. thaliana* inflorescence tissue in the absence of GA. Characteristics of these proteins are consistent with potential roles as DELLA targets, accessories or GA-independent post-translation modification enzymes. To confirm their identities, further up-scaling of immunoprecipitations is required. Furthermore, the confirmation of their interactions with DELLAs is necessary, by the yeast two- or three-hybrid system in the first instance and by other available/appropriate methods. For the confirmed interactions reverse pull-down experiments, using the interacting protein as bait, are required as an ultimate confirmation of interaction. For those confirmed interactions, construction of knock-down and transgenic (over-expression) *A. thaliana* lines would point to the function of the interacting proteins in inflorescence and general plant development. Moreover, up-scaling of the immunoprecipitation will likely yield new interaction candidates; analysis of the current and new candidates will begin to decode the complex developmental networks that have DELLAs at their key nodes.

Detection, in this thesis, of several high-molecular-weight complexes that include DELLAs is worth pursuing - again through up-scaling and identification of the components. The components of these complexes, if identified, may reveal the DELLA 'repressome', in this case in the inflorescence. This approach can be used in other tissues, to determine whether the composition of the 'repressome' varies in different organs and tissues.

Given the profound effect of DELLAs on plant development, it is likely that DELLAs interact with an array of different proteins. Identification of the complete complement of these DELLA-

interacting proteins is required in order to understand the upstream regulation and downstream regulatory roles and targets of DELLA proteins.

5.6 Concluding remarks

By identifying core gibberellin signalling genes and proteins in two woody perennial plants (chapter 3), this thesis has broadened the knowledge base on GA signalling 'hardware'. Transcriptional analysis highlighted redundancies of the core GA signalling components and indicated an analysis of proteins, rather than transcripts, was required in order to gain the knowledge required, for example, to use these proteins in plant breeding programmes.

Surprisingly, amino acid sequence alignments showed that one of the DELLA clades from each of apple and kiwifruit orthologues (the Md- or Ad-RGL3s) are more similar to DELLA proteins from monocotyledonous plants. This is interesting, as no other dicotyledonous DELLA proteins analysed to date show this mode of clustering.

The most intriguing finding from the protein-protein interaction analysis (chapter 4) is the discovery in *A. thaliana* of several large complexes that include DELLA protein AtRGL2 in the inflorescence, in the absence of GA. Under these conditions DELLA proteins are expected to be interacting with transcriptional regulators, resulting in growth-repressing functions. The mass spectography analysis of four AtRGL2 pull-down experiments has identified candidate proteins that may be included in the complexes. These proteins may be used to initiate further studies that may begin to resolve the current stalemate in the understanding of DELLA regulatory mechanisms.

6. Appendix

A.

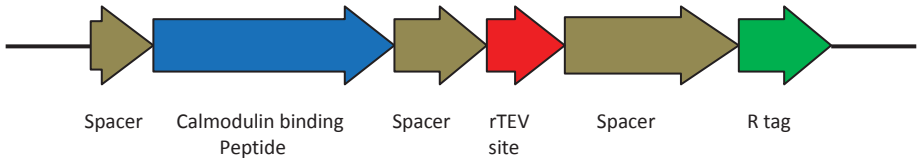

B.

```
  1   GTCGACGGTG GAGGTTCAAT GGAATCTAGT AGATGGTTGA GTAATTTTAT
 51   TGCTGTTTCA GCTGCAAATA GATTCAAGAA AATTTCTTCA AGTGGTGCTC
101   TTGATTATGA TATTCCTACT ACAGCTTCTG AGAATCTTTA CTTCCAAGGA
151   AATAACAATA ACAATAACAA TAACAATAAC GGTGGAGGTG GATCAGGTGG
201   AGGTGGATCT CCTGATCAAT ATGAATACAA GTATCCATAA CTCGAG
```

Figure 6.1. Modified TAP tag incorporating R tag
A, Schematic diagram of TAP tag construct showing the 3 components of the tag separated by spacer regions. The Rab tag epitope is used for high affinity purification of a recombinant tagged protein by the anti-rab tag mAb D9 immobilised on a substrate. Bound proteins are released after non-specific proteins are washed away by digestion with the site specific Tobacco Etch virus (rTEV) protease. A second purification step can be made using the Calmodulin binding peptide affinity for (immobilised) calmodulin. After non-specific proteins are washed away the bound proteins may be eluted by the addition of EGTA to remove Ca^{++} ions from the buffer solution which is an essential co-factor for calmodulin binding.
B, Blue bases Calmodulin binding peptide CDS; **Red** bases rTEV protease site CDS; **Green** bases R-tag CDS.

A.

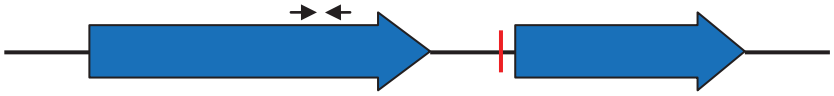

B.

```
   1   GTAAAATACC AACTAATTCT CGTTCGATTC CGGCGAACAT TCTATTTTAC
  51   CAACATCGGT TTTTTCAGTA GTGATACTGT TTTTGTTCCC GATGTCTAAC
 101   ATAGTTTCTC CCTTCAGTGG TTCCTCACGA ACTACGTCTG ACGTTGGCAA
 151   GCAAGCGGGA GGTACTAGCG ATGAGAAGCT CATTGAGTCG CTGTTCTCTG
 201   AAAAGGCTGT GAAAGAGATA GCTGCCGAGT GTAAACTCGG ATGTTATAAC
 251   TATCTGAAGT CTAATGAACC CCGCAACTAT ATAGACCTGG TGCCAAAGTC
 301   ACACGTATCT GCTTGGCTCT CATGGGCTAC ATCCAAGTAT GATAAAGGAG
 351   AGTTACCTTC CAGGGGATTC ATGAACGTTC CACGCATCGT TTGTTTTCTC
 401   GTTCGTACCA CAGATAGCGC AGAGTCCGGT TCTATAACCG TGAGCCTGTG
 451   CGATTCTGGT AAGGCTGCTC GTGCTGGAGT ACTCGAAGCC ATTGATAATC
 501   AGGAGGCCAC AATTCAGTTG TCGGCTTTAC CTGCTTTGAT AGCTTTGACG
 551   CCTAGCTATG ATTGTCCGAT GGAAGTCATC GGCGGTGATA GCGGTAGGAA
 601   TCGATGTTTT GGGATAGCAA CCCAACTTAG CGGTGTGGTG GGGACAACAG
 651   GTTCCGTTGC AGTTACTCAT GCGTATTGGC AAGCTAATTT CAAAGCGAAG
 701   CCCAACAACT ATAAGTTGCA TGGTCCCGCT ACAATTATGG TAATGCCATT
 751   TGACAGACTG AGACAACTCG ATAAGAAAAG CCTCAAAAAT TATATTAGAG
 801   GTATTTCTAA CCAGTCTGTG GATCATGGGT ATCTTCTCGG AAGACCGTTA
 851   CAATCTGTTG ATCAGGTTGC CCAGGAAGAT TTGTTAGTTG AGGAATCCGA
 901   GTCTCCTTCC GCTCTCGGCA GAGGTGTGAA GGATAGTAAG TCTGTATCCG
 951   CGTCATCTGT CGCTGGACTT CCTGTGTCCA GTCCTACGCT TAGAATTAAA
1001   TAGGTAAATC CGGTCTAACA AGCTCGGTCC ATTTCGTAGA GTTAAGCAAG
1051   CTGGGGAGAC CCCCGACAGC CGTTTGGATC AGCGCTCGCG TCTCGTTTGG
1101   GTTCAATTCC CTTACCTTAC AACGGCGTGT TGAGATAGGT CCTCGGGGGA
1151   GGTTATCCAT GTTTGTGGAT ATTCTATGTT GTGTGTCTGA GTTATTATTA
1201   AAAAAAAAAA AAAAAGATCT ATGTCCTAAT TCAGCGTATT AATAATGTCG
1251   ACTTCAGGAA CTGGTAAGAT GACTCGCGCG CAGCGTCGTG CTGCCGCTCG
1301   CAGAAATCGT TGGACCGCTA GGGTCCAACC AGTAATTGTC GAACCACTCG
1351   CTGCTGGCCA AGGCAAGGCC ATTAAAGCGA TTGCAGGATA CAGCATATCA
1401   AAGTGGGAGG CGTCTTCGGA CGCGATTACA GCGAAAGCCA CCAATGCCAT
1451   GAGTATCACT CTGCCCCATG AGCTCTCTTC TGAAAAGAAT AAGGAGCTTA
1501   AGGTCGGCAG GGTGCTGCTT TGGTTGGGAC TTCTTCCTAG CGTTGCTGGG
1551   AGGATTAAGG CTTGTGTTGC TGAGAAACAG GCACAGGCCG AGGCTGCTTT
1601   TCAAGTAGCC TTGGCGGTTG CAGACTCCTC GAAAGAGGTG GTCGCGGCCA
1651   TGTATACGGA CGCCTTTCGA GGGGCGACTC TGGGGGATTT GCTTAATCTC
1701   CAGATTTATC TGTATGCATC TGAAGCAGTG CCTGCTAAGG CGGTCGTTGT
1751   ACATCTAGAA GTTGAGCACG TAAGGCCTAC GTTCGATGAC TTCTTCACCC
1801   CGGTTTATAG GTAGTGCCCC TGCTCGGAGA GCCCCTGACT GGGTTAAAGT
1851   CACAGGCCCC TTGTCTCAGG TAGAGACCCT GTCCAGGTAG GACACTTTGG
1901   CTAAGGTTAA AAGCTTGTTG AATCAGTACA ATAACTGATA GTCGTGGTTG
1951   ACACGCAGAC CTCTTACAAG AGTGTCTAGG TGCCTTTGAG AGTTACTCTT
2001   TGCTCTCTTC GGAAGAACCC TTAGGGGTTC GTGCATGGGC TTGCATAGCA
2051   AGTCTTAGAA TGCGGGTACC GTACAGTGTT GAAAAACACT GTAAATCTCT
2101   AAAAGAGACC A
```

Figure 6.2. Brome mosaic virus RNA3
The BMV RNA sequence when spiked into the plant mRNA preparations was used as an internal control for reverse transcription efficiency.
A, Schematic representation of the BMV *RNA3* and location of important sites.
B, **Blue** bases start and stop codons for the two CDS within the RNA; **Red** bases poly-A sequence used in RT priming poly T strategy; **Green** bases are to forward and reverse qPCR priming sites.

A.

```
   1   ATGGCCATGG TCGATGAGCC TCTGTATCCC ATCGCGGTTC TGATAGATGA
  51   GCTCAAGAAT GAAGACATTC AGCTGAGACT GAACTCGATC CGGCGTCTCT
 101   CTACCATCGC TCGCGCCCTC GGAGAGGAGA GGACCCGGAA GGAGTTGATC
 151   CCGTTCCTGA GCGAAAACAA CGATGACGAT GATGAAGTGC TCCTCGCAAT
 201   GGCCGAAGAA TTGGGGGTTT TTGTTCCGTA TGTAGGAGGG GTCGAGCACG
 251   CAAATGTGCT GCTTCCTCCG TTGGAGACTC TTTGCACGGT TGAAGAGACT
 301   TGTGTGAGGG ATAAAGCTGT GGAGTCATTG TGTAGGATTG GGGCTCAGAT
 351   GAGGGAGCAG GACTTGGTCG ATTCATTTAT TCCTCTGGTG AAGAGACTGG
 401   CTGCTGGAGA ATGGTTTACA GCTCGAGTTT CCTCTTGTGG ATTATTTCAT
 451   ATTGCTTACC CAAGTGCCCC AGAGGCATTA AAGACTGAGC TACGGACAAT
 501   ATATAGCCAA CTGTGTCAAG ATGACATGCC CATGGTGAGG AGAGCTGCTG
 551   CAACAAACCT GGGGAAATTT GCTGCTACTG TTGAAGCTGC TCATATGAAG
 601   ACTGACATCA TGTCAATGTT TGAGGATCTG ACACAAGATG ATCAAGATTC
 651   TGTTCGGTTA TTGGCGGTTG AGGGTTGTGC AGCTCTTGGG AAGCTGCTGG
 701   ATCCCCAAGA TTGTGTAGCA CATATCCTGC CCGTTATTGT TAATTTCTCT
 751   CAGGATAAAT CTTGGCGTGT TCGTTACATG GTTGCAAATC AATTATACGA
 801   GCTTTGTGAA GCAGTCGGCC CAGAATCTAC CAGAACAGAC TTGGTTCCTG
 851   CATACGTTCG ACTTCTTCGG GACAATGAGG CTGAAGTACG TATCGCCGCT
 901   GCGGGAAAAG TAACTAAGTT TTGTCGAATT TTGAGTCCAG AGCTTGCAAT
 951   TCAGCATATC CTTCCTTGTG TGAAGGAACT ATCCTCCGAT TCATCCCAGC
1001   ATGTACGTTC TGCTTTGGCA TCAGTTATAA TGGGAATGGC GCCAGTTCTA
1051   GGAAAGGATG CGACAATAGA GCAGCTTTTG CCGATCTTCC TTTCTCTTCT
1101   GAAAGATGAG TTCCCTGATG TCCGACTGAA TATCATCAGC AAGCTCGATC
1151   AAGTGAATCA GGTCATTGGA ATTGATCTGC TTTCCCAGTC CCTGCTGCCA
1201   GCAATTGTTG AACTTGCAGA GGACAGACAC TGGAGAGTTC GGCTTGCAAT
1251   AATAGAATAC ATACCGTTAT TGGCAAGTCA GTTGGGTGTA GGGTTTTTTG
1301   ATGACAAACT CGGTGCTCTT TGCATGCAAT GGTTAAATGA TAAGGTTTAC
1351   TCCATTCGAG ATGCTGCAGC TAACAATGTG AAGCGCCTTG CAGAAGAATT
1401   TGGTCCAGAA TGGGCAATGC AGCACATAAT TCCACAGGTA TTGGACATGA
1451   TTAGCAGCCC ACATTATCTG TACCGTATGA CCATACTACA CTCGATCTCT
1501   CTTCTTGCTC CTGTTATGGG CTCAGAAATT ACATGTTCCA AACTTCTGCC
1551   TGTAGTCGTT ACTGCATCAA AAGACAGGGT ACCTAACATC AAGTTCAATG
1601   TGGCAAAGGT GTTGCAGTCT CTTATTCCTA TAGTTGACCA GTCTGTGGTA
1651   GAGCAGACGA TCCGACCCTG TTTGGTTGAG CTAAGCGAGG ATCCCGATGT
1701   TGATGTAAGG TTCTTTGCCA GCCAAGCATT GCAGGCAATT GATCAAGTCA
1751   TGATGTCTAG CTAG
```

Figure 6.3. *A. deliciosa* PROTEIN PHOSPHATASE 2A REGULATORY SUBUNIT A3 (*PP2A*) coding sequence

A, This kiwifruit *PP2A* homologue sequence was determined to be the closest match through BLAST searching in the *Actinidia* database using the *Arabidopsis* sequence At1g13320.

qPCR primer pair annealing sites are highlighted with **green** bases.

A.

```
1      ATGGCCGATG CTGAGGATAT TCAGCCTCTT GTCTGTGACA ATGGAACTGG
51     AATGGTGAAG GCTGGGTTTG CTGGTGATGA TGCTCCCCGG GCAGTGTTTC
101    CCAGTATTGT TGGTCGGCCC AGGCACACAG GTGTCATGGT TGGGATGGGC
151    CAGAAGGATG CTTATGTAGG TGATGAGGCC CAATCCAAAA GAGGTATTCT
201    TACCTTAAAG TATCCTATTG AACACGGTAT TGTCAGCAAC TGGGATGACA
251    TGGAAAAGAT CTGGCATCAT ACATTCTACA ATGAGCTTCG TGTTGCTCCA
301    GAAGAGCACC CTGTGCTGCT TACAGAGGCA CCACTCAACC CTAAGGCCAA
351    CAGAGAGAAG ATGACACAAA TTATGTTTGA AACTTTCAAT GTTCCTGCCA
401    TGTATGTTGC CATTCAGGCC GTTCTCTCTC TATATGCCAG TGGCCGTACA
451    ACTGGTATTG TGCTGGATTC CGGTGATGGT GTGAGTCACA CGGTCCCCAT
501    CTATGAGGGA TATGCTCTTC CTCATGCTAT CCTCCGTCTC GACCTTGCTG
551    GCCGTGATCT AACAGATGCC CTCATGAAGA TCCTTACCGA GAGAGGATAC
601    ATGTTCACCA CCACGGCCGA ACGGGAAATT GTCCGTGATG TGAAGGAAAA
651    ACTTGCATAC GTCGCACTTG ACTATGAGCA GGAGCTGGAG ACTGCAAAGA
701    GCAGCTCCTC AGTTGAGAAG AACTATGAGC TACCCGATGG TCAGGTTATC
751    ACAATTGGAG CTGAGAGATT CCGTTGCCCA GAAGTTCTCT TCCAGCCATC
801    TTTGATTGGA ATGGAAGCTG CAGGAATCCA TGAGACTACC TACAATTCTA
851    TCATGAAATG TGATGTTGAT ATCAGGAAAG ATCTATATGG CAACATTGTG
901    CTCAGTGGTG GTTCAACTAT GTTCCCTGGT ATCGCAGACC GCATGAGTAA
951    GGAAATTACT GCTCTTGCTC CCAGCAGCAT GAAAATCAAG GTTGTGGCTC
1001   CACCTGAGAG GAAATACAGC GTCTGGATTG GAGGATCTAT CCTCGCATCC
1051   CTCAGCACCT TTCAACAGAT GTGGATTTCG AAGGGTGAAT ATGACGAATC
1101   TGGTCCGTCC ATCGTCCACA GGAAGTGCTT CTGA
```

Figure 6.4. *A. deliciosa ACTIN 2* (formally 7) (*ACT2/7*) coding sequence
A,This kiwifruit *ACT2* sequence was determined to be the closest match through BLAST searching in the *Actinidia* database using the *Arabidopsis* sequence At3g18780.
5' and 3' qPCR primer pair annealing sites are highlighted with **green** bases.

A.

```
   1    ATGGATTTAT CAAGCACGGA AGCTTATTTC TTTATGCTTG TTCATTCTTG
  51    GAGAGTGTGA TAACTCCCAC CGAGCAGGTC AAGATGTTGT TCCTCTTACG
 101    GCTCTGGCAA TGCGGTTTGC TGTTGTCTTG ACTGATCTGA AGAGTTGGAA
 151    AAGCATTACA GATGATAATC TTCAGGATGC AGAAACAGCA ATGAAGGATT
 201    TGGTTCAGTT CATGGGAAGT AAAAGAAGTG GACTGTACAA TCATGTTAGA
 251    ATATACATTA AAAAATTAGG TGCTCGGATA AACTGTTCTG GCTCGACAGA
 301    TGATAGATTC TTGATTACTG CAAGTGCACT GACTTTAGCT TTACGGCCTA
 351    TTCATATTGC AAATTTAAAT GACCCTGACC ACTTGGATGG GCATTATGCT
 401    ACTGAGCAGT ACTGCGTGCT TGTACTGACA ATCCCTTGGC TTACTCAACG
 451    TCTACCAGCA GCACTCTTAC CTGCTCTGCA GCACAAGTCT ATCTTATCAC
 501    CTTGCTTCAG GACACTACTG GTGATGGCAG ATCCTGAAAG AGAAAATCTT
 551    AAAGGAGATT TCAGAGGTGG ATCAGGGGAA AGTTGTCTCT CATTCCAAGG
 601    AGATGCCGCA AGTTGGTTGG CTTCTTGCAA ATGTTCTATG CCTTGCATCT
 651    GTGAGTGATA ACAATTATGG GATTCCTGGA AAGTTCATTC AAGGCCTGGA
 701    CTATGCTTCC TATATCCATG CTGTTACCAT CCTTTCAGAG AACTTTATAA
 751    ATTGGTTGGA GAATTCTGGA TGGCTAAGAA AGGAGAGCCA AGAGTCTGAG
 801    ATTCATTCTG AAACTTCTGC AGAGTCTATT GATACCCAGT TGTTTGGGAC
 851    GCTGACAACT TGTGAGTCCT TGAAGATGTC ATACATTGAC TTTTATAAGC
 901    CTGTTTATCA GCAGTGGCAT CTTATGAAGC TATTATCCTT GGAGAAAGAA
 951    ACTTTTGTTC ACCGGGTTGA TAATCCCCCG CCAAACAATC TGGAATCACT
1001    TGGGAAGTGT GATCTGCTTG ATGTTGCATA TTATTATTCT TACATGCTAA
1051    GAATATTTTC AGTACTGAAT CCCGTGGTTG GGTCTTTATC TGTACTCAAC
1101    GTGCTGTCTT TTACCCCTGG ATTTCTGGTC AATCTATGGC TAGCCCTGGA
1151    AAGATCCACG TTTCCAGGAA AAAGTCATAA TGCGGAGGAT AATTTTCTTT
1201    CTGGCAATAA AACTTTTGGA AACAAGAATG ATGGGGTTAC TGAGAGAAAG
1251    CAAAAAGTGG TATCGAAGGA TGGAGCCAAT AAATGGGCTG TTGCACTCCA
1301    TAAAATCACT GGTAAATCTG ATGTTGATTA TACAGCATCA ACAGAGGTTC
1351    AACCTAGTCA TAACCAGGTT TATGAAGGTT CTTCTGATGT ATGGGACATA
1401    GAGCCTTTGA GGCATGGTCC AGAAGGTTTA TCAAAAGATN ACTTCTTGCC
1451    TACTACATCT ATTCAGTGCC TCCTATTCAC ATCTGCTGCT AGTTCTTGAT
1501    GACATAGAGT TCTATGAAAA ACAGGTTCCT TTCACATTGG AGCAGCAACG
1551    ACGAATCGTA TCGGTGCTTA ATACATTGGT GTATAATGCC TTGTCCCATG
1601    GTATTAGTCA ACAGAACATA CCTCTTATGG ATGCTGCAAT CCGATGCCTA
1651    CATCTGTTGT ATGAAAGGGA TTGCAGGCAC CAGTTTTGCC CCCCTGCTTT
1701    GTGGCTTTCA CCTGCTAAAA AGAATCGACC AACAATTGCA GTAGCTACTA
1751    GGACTCGTGA AGTTTTATCA GCTACTATAA GATCAGATGA TGCTTTGACC
1801    CTTCCAAAAA TGGGTTCTGT CATCACTACT ACCCCACATG TCTTCCCATT
1851    TGAGGAAAGG GTTGAAATGT TCAGAGAATT TATCAACACG GACAAAGCAT
1901    CTCGAAGAAT GGCTGGAGAA GTGCTTGGAC CCGGTTCACG ATCAGTCGAG
1951    ATAGTAATCC GTCGTGGTCA TATAGTCGAA GATGGTTTTC AACAGTTAAA
2001    TTCCCTTGGG TCAAGGTTGA AATCTAACAT CCATGTCTCA TTTGTTAGTG
2051    AATCTGGCCT TCCAGAGGCT GGTCTAGACT ATGGTGGGTT ATCTAAGGAG
2101    TTTTTGACTG ATATATCAAA AGCAGCCTTT TCCCCTGCGT ATGGGCTATT
2151    CTCTCAGACT TTAACTTCAG ACAGACTTCT AATTCCTAAT ACAGCTGCCA
2201    GATTTATAGA GAATGGTATC CAGATGATTG AGTTTCTTGG AAGAGTTGTT
2251    GGAAAAGCTC TTTATGAAGG AATATTGCTA GATTATTCCT TTTCACATGT
2301    TTTTGTACAA AAGTTGTTAG GCCGCTATAG CTTTCTCGAC GAACTATCTA
2351    CACTTGATCC TGAGCTCTAC AGGAATCTCA TGTATGTTAA GCATTATGAT
2401    GGTGATGTCA AAGAACTCTG TCTCGATTTC ACAGTTACAG AAGAAGCACT
2451    TGGGAAAAGG CATATTATTG AACTTAAACC AGGTGGCAAG GATGTGTACG
2501    TGACAAATGA GAACAAGTTA CAGTATGTTC ATGCAATTGC AGACTATAAA
2551    CTTAATCGAC AGATATTGCC TTTGTCAAAT GCATTCTATA GAGGGTTGAC
2601    AGATCTAATT GCCCCATCGT GGTTGAAGTT GTTCAATGCT AGTGAGTTTA
```

```
2651   ATCAGTTGCT TTCAGGTGGG AAACATGACA TTGATGTTAC CGATTTAAGA
2701   AACAACACGC GTTACACTGG TGGTTATACC GAAGGAAGTC GGGCAATTAA
2751   AATCTTTTGG GAGGTAATCA CAGGATTTGA ACCAAAAGAG CGATGTATGC
2801   TTCTTAAGTT TGTAACAAGT TGTTCTCGAG CTCCTTTGCT TGGATTCAAG
2851   TACTTGCAGC CAACCTTTAC CATTCACAAG GTTGCATGTG ATGTGCCACT
2901   CTGGGCAACA TTTAGTGGAC AGGATGTGGA TCGGCTTCCA TCAGCTTCTA
2951   CATGCTACAA TACTCTCAAG CTTCCAACGT ATAAACGGAC AGGCACTATG
3001   AGATCCAAGC TTCTATATGC TATCAATTCT AATGCAGGAT TTGAACTTTC
3051   ATAA
```

Figure 6.5. ***A. deliciosa HECT DOMAIN CONTAINING UBIQUITIN LIGASE 7*** **(*UPL7*) coding sequence**
A, This kiwifruit UPL7 homologue sequence was determined to be the closest match through BLAST searching in the *Actinidia* database using the *Arabidopsis* sequence At3g53090.
qPCR primer pair annealing sites are highlighted with **green** bases.

A i. ii.

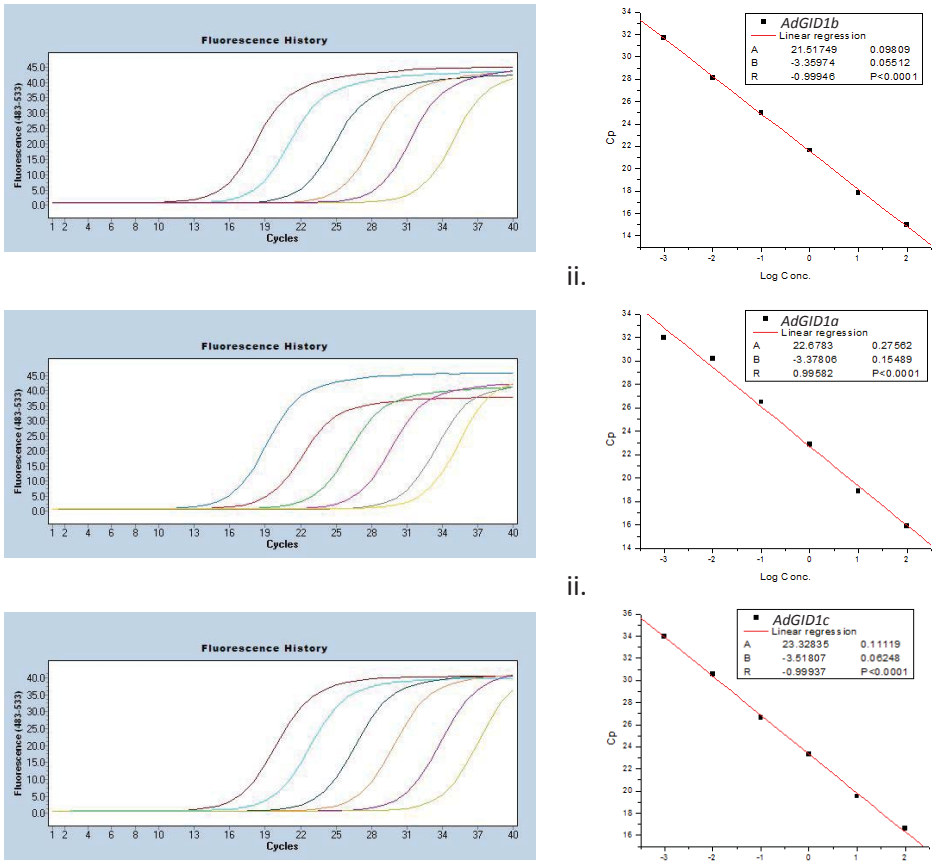

Figure 6.6. *A. deliciosa GID1* homologue amplifications and standard curve linear regression plots

Determination of the PCR amplification efficiency for *AdGID1* amplicon primer pairs. The amplification fluorescence threshold crossing point of the amplicon was plotted against the logarithm of the relative template concentrations. A linear regression line was fitted and the slope of the line determined in the Origin graphing application (OriginLab corp. USA). The efficiency of the amplification was calculated from the equation; efficiency $=10^{(-1/\text{Slope})}$.

A, *AdGID1b*; **B,** *AdGID1a*; **C,** *AdGID1c*.

i, Graph of fluorescence vs. cycle of each of the six amplifications of a template dilution series; **ii,** Graph of crossing point versus Log of the relative target DNA concentration. **Inset**: B=Slope of the linear regression line with error, R= Fit of regression line with error, A=Crossing point on x axis (at 0) with error.

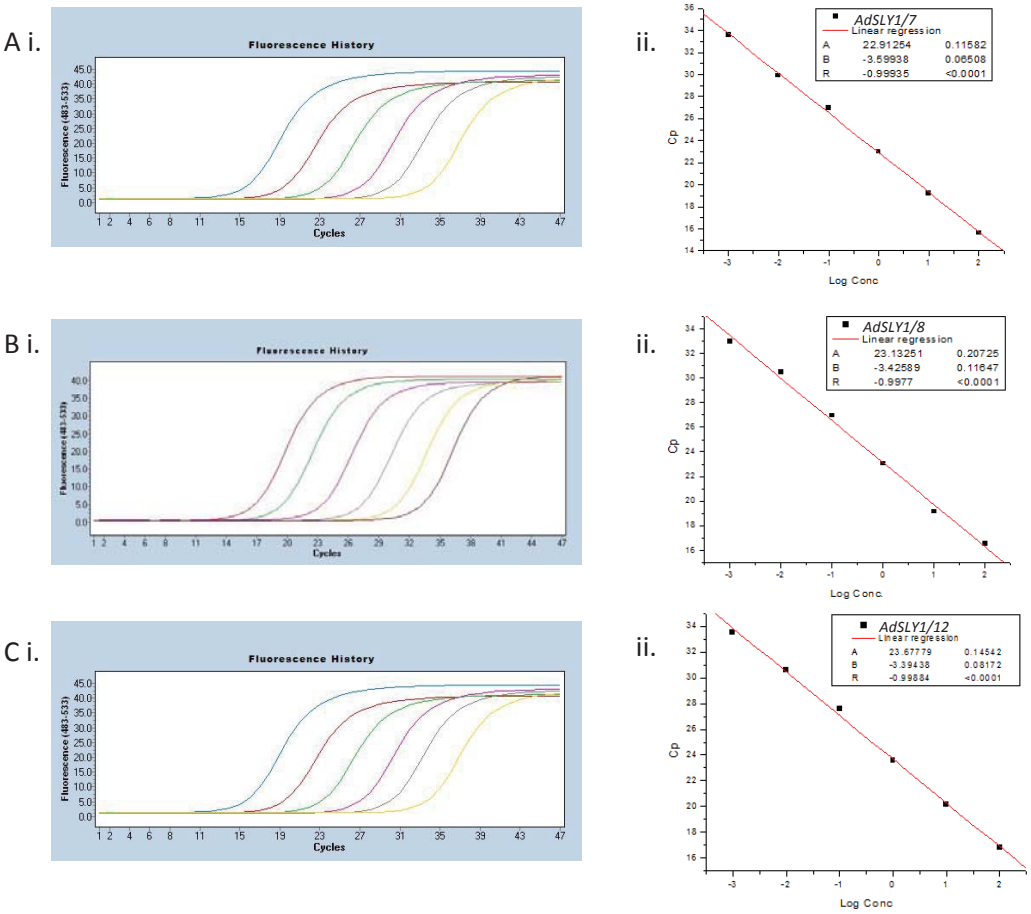

Figure 6.7. *A. deliciosa SLY1* homologue amplifications and standard curve linear regression plots

Determination of the efficiency of PCR amplification of *AdSLY1* homologue amplicon primer pairs by standard curve. PCR amplifications were made from a dilution series of template concentrations. The amplification fluorescence threshold crossing point of the amplicon was plotted against the logarithm of the relative template concentrations. A linear regression line was drawn and the slope of the line determined in the Origin graphing application (OriginLab corp. USA). The efficiency of the amplification was calculated from the equation; efficiency $=10^{(-1/\text{Slope})}$.

A, *AdSLY1/7*; **B,** *AdSLY1/8*; **C,** *AdSLY1/12*.

i, Graph of fluorescence vs. cycle of each of the six amplifications of a template dilution series; **ii,** Graph of crossing point versus Log of the relative target DNA concentration. **Inset**: B=Slope of the linear regression line with error, R= Fit of regression line with error, A=Crossing point on x axis (at 0) with error.

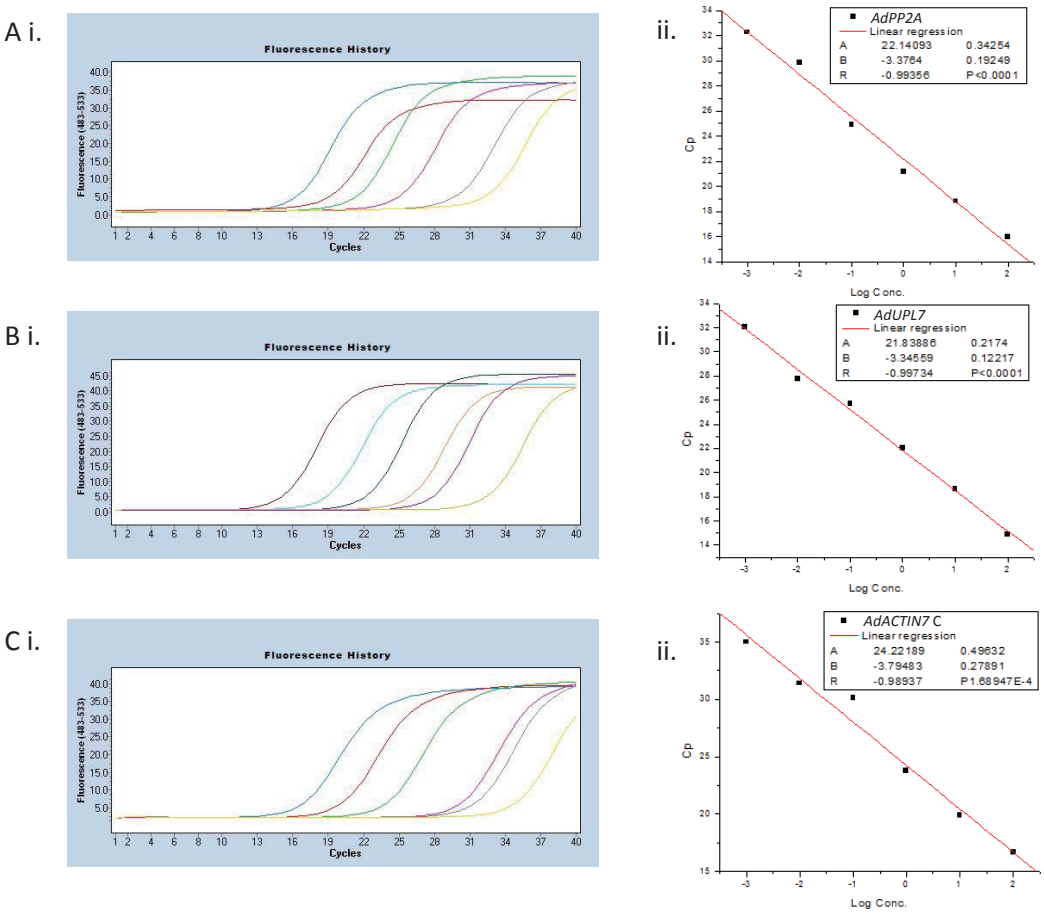

Figure 6.8. *A. deliciosa* reference gene homologue amplifications and standard curve linear regression plots

Determination of the efficiency of PCR amplification of the *Actinidia* reference gene homologues amplicon primer pairs by standard curve. PCR amplifications were made from a dilution series of template concentrations. The amplification fluorescence threshold crossing point of the amplicon was plotted against the logarithm of the relative template concentrations. A linear regression line was drawn and the slope of the line determined in the Origin graphing application (OriginLab corp. USA). The efficiency of the amplification was calculated from the equation; efficiency $=10^{(-1/\text{Slope})}$.

A, *AdPP2A*; **B,** *AdUPL7*; **C,** *AdACTIN C*.

i, Graph of fluorescence vs. cycle of each of the six amplifications of a template dilution series; **ii,** Graph of crossing point versus Log of the relative target DNA concentration. **Inset**: B=Slope of the linear regression line with error, R= Fit of regression line with error, A=Crossing point on x axis (at 0) with error.

D i.

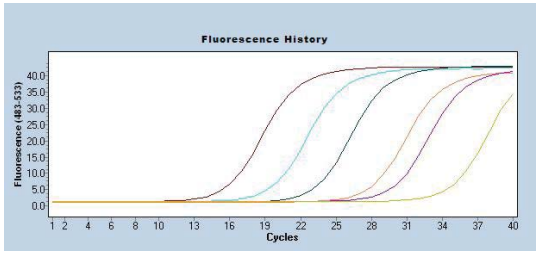

ii.

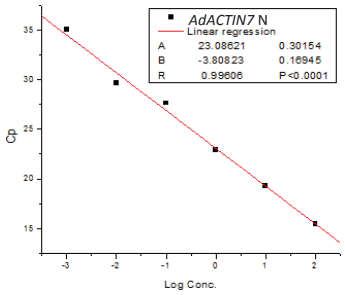

E ii.

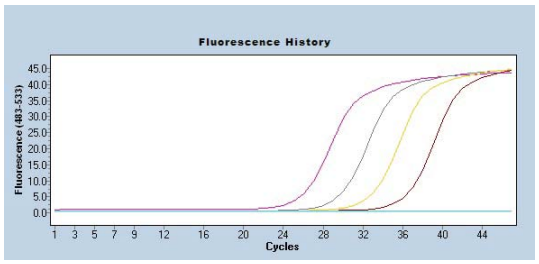

ii.

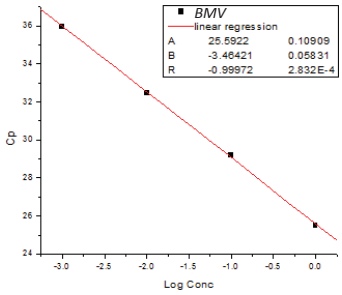

Figure 6.8 (*continued*). *A. deliciosa* reference gene homologue amplifications and standard curve linear regression plots

Determination of the efficiency of PCR amplification of the *Actinidia* reference gene homologue amplicon primer pairs by standard curve. PCR amplifications were made from a dilution series of template concentrations. The amplification fluorescence threshold crossing point of the amplicon was plotted against the logarithm of the relative template concentrations. A linear regression line was drawn and the slope of the line determined in the Origin graphing application (OriginLab corp. USA). The efficiency of the amplification was calculated from the equation; efficiency $=10^{(-1/\text{Slope})}$.

D, *AdACTIN* N; **E,** BMV.

i. Graph of fluorescence vs. cycle of each of the six amplifications of a template dilution series.

ii. Graph of crossing point versus Log of the relative target DNA concentration. Inset: B=Slope of the linear regression line with error, R= Fit of regression line with error, A=Crossing point on x axis (at 0) with error.

Table 6.1. Calculation of relative expression levels

RNA from[a]	Target[b]	avg Cq[c]	SE avg Cq	CV	rel Cq[d]	SE rel Cq	NRCq[e]	SE NRCq	CNRCq[f]	SE CNRCq
Breaking buds 1	113002 (AdRGL1a)	26.059	0.061	0.235	17.020	0.730	2.304	0.121	1.409	0.121
Breaking buds 2	113002 (AdRGL1a)	24.303	0.075	0.310	53.533	3.386	2.975	0.215	2.975	0.215
Dormant buds 1	113002 (AdRGL1a)	33.053	0.016	0.049	0.177	0.002	1.945	0.049	0.853	0.049
Dormant buds 2	113002 (AdRGL1a)	26.289	0.048	0.184	14.649	0.510	1.886	0.094	0.958	0.094
Expanding leaves 1	113002 (AdRGL1a)	23.703	0.089	0.375	79.210	5.758	3.741	0.326	2.376	0.326
Expanding leaves 2	113002 (AdRGL1a)	24.877	0.002	0.008	36.801	0.723	5.558	0.211	5.558	0.211
F Flower buds 1	113002 (AdRGL1a)	26.901	0.010	0.037	9.824	0.138	2.746	0.083	1.715	0.083
F Flower buds 2	113002 (AdRGL1a)	30.069	0.037	0.123	1.242	0.030	2.430	0.070	0.969	0.070
F Styles	113002 (AdRGL1a)	35.697	0.663	1.857	0.032	0.014	0.834	0.363	0.834	0.363
F Styles 2	113002 (AdRGL1a)	24.312	0.022	0.091	53.214	1.384	3.775	0.182	1.297	0.182
Fruit cortex 1	113002 (AdRGL1a)	26.417	0.059	0.223	13.472	0.551	3.572	0.177	3.572	0.177
Fruit cortex 2	113002 (AdRGL1a)	27.288	0.019	0.071	7.631	0.183	2.594	0.085	2.594	0.085
M Flower bud 1	113002 (AdRGL1a)	26.530	0.052	0.197	12.511	0.461	3.232	0.151	2.066	0.151
M Flower buds 2	113002 (AdRGL1a)	27.229	0.070	0.256	7.930	0.371	3.520	0.191	1.436	0.191
Shoot tips 1	113002 (AdRGL1a)	27.039	0.051	0.187	8.976	0.316	4.363	0.179	1.736	0.179
Shoot tips 2	113002 (AdRGL1a)	23.934	0.029	0.123	68.136	2.038	5.684	0.257	4.594	0.257
Breaking buds 1	49556 (AdRGL1b)	29.483	0.025	0.086	7.989	0.160	1.082	0.039	0.662	0.039
Breaking buds 2	49556 (AdRGL1b)	24.788	0.048	0.193	152.154	6.446	8.455	0.466	8.455	0.466
Dormant buds 1	49556 (AdRGL1b)	38.985	0.020	0.051	0.021	0.001	0.226	0.008	0.099	0.008
Dormant buds 2	49556 (AdRGL1b)	28.402	0.028	0.100	15.746	0.381	2.027	0.088	1.030	0.088
Expanding leaves 1	49556 (AdRGL1b)	27.246	0.076	0.281	32.534	1.700	1.537	0.109	0.976	0.109
Expanding leaves 2	49556 (AdRGL1b)	26.043	0.030	0.116	69.218	2.185	10.455	0.474	10.455	0.474
F Flower buds 1	49556 (AdRGL1b)	29.385	0.047	0.159	8.494	0.271	2.374	0.099	1.483	0.099
F Flower buds 2	49556 (AdRGL1b)	34.449	0.002	0.006	0.354	0.004	0.692	0.014	0.276	0.014
F Styles	49556 (AdRGL1b)	No Amp[†]								
F Styles 2	49556 (AdRGL1b)	26.535	0.020	0.076	50.832	1.350	3.606	0.175	1.239	0.175
Fruit cortex 1	49556 (AdRGL1b)	32.950	0.000	0.000	0.907	0.003	0.240	0.007	0.240	0.007
Fruit cortex 2	49556 (AdRGL1b)	33.289	0.060	0.179	0.733	0.027	0.249	0.011	0.249	0.011
M Flower bud 1	49556 (AdRGL1b)	30.061	0.045	0.151	5.559	0.168	1.436	0.060	0.918	0.060
M Flower buds 2	49556 (AdRGL1b)	29.723	0.075	0.253	6.872	0.334	3.050	0.170	1.244	0.170
Shoot tips 1	49556 (AdRGL1b)	30.143	0.069	0.229	5.280	0.248	2.566	0.132	1.021	0.132
Shoot tips 2	49556 (AdRGL1b)	24.305	0.037	0.153	205.904	8.108	17.177	0.893	13.884	0.893

RNA from[a]	Target[b]	avg Cq[c]	SE avg Cq	CV	rel Cq[d]	SE rel Cq	NRCq[e]	SE NRCq	CNRCq[f]	SE CNRCq
Breaking buds 1	79743 (AdRGL1c)	26.133	0.026	0.099	26.545	0.568	3.594	0.133	2.198	0.133
Breaking buds 2	79743 (AdRGL1c)	24.191	0.025	0.102	95.605	3.534	5.313	0.272	5.313	0.272
Dormant buds 1	79743 (AdRGL1c)	33.876	0.092	0.271	0.160	0.010	1.759	0.113	0.772	0.113
Dormant buds 2	79743 (AdRGL1c)	28.022	0.069	0.245	7.632	0.351	0.983	0.057	0.499	0.057
Expanding leaves 1	79743 (AdRGL1c)	24.097	0.041	0.170	101.722	3.325	4.805	0.279	3.051	0.279
Expanding leaves 2	79743 (AdRGL1c)	25.107	0.023	0.093	52.240	1.146	7.890	0.309	7.890	0.309
F Flower buds 1	79743 (AdRGL1c)	26.256	0.040	0.153	24.472	0.717	6.840	0.271	4.273	0.271
F Flower buds 2	79743 (AdRGL1c)	30.448	0.154	0.505	1.540	0.156	3.012	0.309	1.201	0.309
F Styles	79743 (AdRGL1c)	37.361	1.335	3.573	0.016	0.014	0.425	0.375	0.425	0.375
F Styles 2	79743 (AdRGL1c)	24.945	0.025	0.101	58.123	1.347	4.123	0.192	1.417	0.192
Fruit cortex 1	79743 (AdRGL1c)	28.920	0.032	0.112	4.220	0.093	1.119	0.040	1.119	0.040
Fruit cortex 2	79743 (AdRGL1c)	28.673	0.013	0.044	4.967	0.071	1.688	0.045	1.688	0.045
M Flower bud 1	79743 (AdRGL1c)	25.965	0.035	0.133	29.643	0.785	7.659	0.300	4.894	0.300
M Flower buds 2	79743 (AdRGL1c)	27.481	0.081	0.294	10.907	0.591	4.841	0.294	1.974	0.294
Shoot tips 1	79743 (AdRGL1c)	26.541	0.028	0.107	20.271	0.449	9.852	0.302	3.921	0.302
Shoot tips 2	79743 (AdRGL1c)	23.119	0.045	0.195	193.866	7.039	16.173	0.804	13.072	0.804
Breaking buds 1	101189 (AdRGL2a)	23.952	0.108	0.450	23.939	1.686	3.241	0.248	1.982	0.248
Breaking buds 2	101189 (AdRGL2a)	21.461	0.007	0.034	116.123	3.048	6.453	0.284	6.453	0.284
Dormant buds 1	101189 (AdRGL2a)	30.023	0.024	0.080	0.510	0.008	5.604	0.147	2.457	0.147
Dormant buds 2	101189 (AdRGL2a)	22.562	0.013	0.057	57.778	1.359	7.439	0.320	3.778	0.320
Expanding leaves 1	101189 (AdRGL2a)	21.587	0.015	0.070	107.185	2.913	5.063	0.279	3.215	0.279
Expanding leaves 2	101189 (AdRGL2a)	22.546	0.023	0.103	58.371	1.549	8.816	0.370	8.816	0.370
F Flower buds 1	101189 (AdRGL2a)	23.637	0.039	0.166	29.232	0.905	8.171	0.334	5.104	0.334
F Flower buds 2	101189 (AdRGL2a)	27.005	0.046	0.172	3.458	0.104	6.764	0.231	2.697	0.231
F Styles	101189 (AdRGL2a)	32.571	0.111	0.341	0.102	0.007	2.686	0.216	2.686	0.216
F Styles 2	101189 (AdRGL2a)	21.951	0.025	0.115	85.126	2.466	6.038	0.301	2.075	0.301
Fruit cortex 1	101189 (AdRGL2a)	25.379	0.026	0.104	9.693	0.201	2.570	0.089	2.570	0.089
Fruit cortex 2	101189 (AdRGL2a)	25.192	0.047	0.186	10.913	0.354	3.709	0.147	3.709	0.147
M Flower bud 1	101189 (AdRGL2a)	24.168	0.036	0.149	20.883	0.588	5.395	0.218	3.448	0.218
M Flower buds 2	101189 (AdRGL2a)	23.691	0.032	0.133	28.254	0.763	12.540	0.481	5.115	0.481
Shoot tips 1	101189 (AdRGL2a)	24.528	0.066	0.271	16.625	0.745	8.080	0.400	3.216	0.400
Shoot tips 2	101189 (AdRGL2a)	21.427	0.034	0.159	118.618	4.010	9.895	0.474	7.998	0.474

RNA from[a]	Target[b]	avg Cq[c]	SE avg Cq	CV	rel Cq[d]	SE rel Cq	NRCq[e]	SE NRCq	CNRCq[f]	SE CNRCq
Breaking buds 1	227790 (AdRGL2b)	22.220	0.138	0.622	49.840	4.205	6.748	0.605	4.127	0.605
Breaking buds 2	227790 (AdRGL2b)	21.008	0.045	0.214	103.073	3.371	5.728	0.276	5.728	0.276
Dormant buds 1	227790 (AdRGL2b)	29.133	0.045	0.155	0.791	0.021	8.684	0.298	3.808	0.298
Dormant buds 2	227790 (AdRGL2b)	22.400	0.017	0.078	44.741	0.827	5.760	0.233	2.925	0.233
Expanding leaves 1	227790 (AdRGL2b)	20.445	0.058	0.285	144.416	5.814	6.821	0.427	4.332	0.427
Expanding leaves 2	227790 (AdRGL2b)	21.588	0.099	0.460	72.811	4.512	10.997	0.770	10.997	0.770
F Flower buds 1	227790 (AdRGL2b)	23.075	0.101	0.440	29.862	1.861	8.347	0.566	5.214	0.566
F Flower buds 2	227790 (AdRGL2b)	26.518	0.114	0.431	3.793	0.261	7.419	0.523	2.958	0.523
F Styles	227790 (AdRGL2b)	33.616	0.095	0.284	0.054	0.003	1.424	0.098	1.424	0.098
F Styles 2	227790 (AdRGL2b)	22.821	0.043	0.188	34.770	1.020	2.466	0.123	0.848	0.123
Fruit cortex 1	227790 (AdRGL2b)	25.475	0.014	0.055	7.086	0.082	1.879	0.057	1.879	0.057
Fruit cortex 2	227790 (AdRGL2b)	26.126	0.025	0.096	4.797	0.078	1.630	0.046	1.630	0.046
M Flower bud 1	227790 (AdRGL2b)	22.987	0.035	0.153	31.481	0.795	8.134	0.312	5.198	0.312
M Flower buds 2	227790 (AdRGL2b)	23.474	0.051	0.219	23.511	0.782	10.435	0.449	4.256	0.449
Shoot tips 1	227790 (AdRGL2b)	22.978	0.017	0.076	31.654	0.549	15.385	0.421	6.123	0.421
Shoot tips 2	227790 (AdRGL2b)	20.085	0.079	0.393	179.226	9.257	14.952	0.924	12.085	0.924
Breaking buds 1	115865 (AdRGL3a)	29.957	0.020	0.066	7.047	0.113	0.954	0.033	0.584	0.033
Breaking buds 2	115865 (AdRGL3a)	27.345	0.061	0.222	42.908	1.930	2.384	0.136	2.384	0.136
Dormant buds 1	115865 (AdRGL3a)	35.174	0.119	0.338	0.191	0.016	2.098	0.178	0.920	0.178
Dormant buds 2	115865 (AdRGL3a)	27.683	0.052	0.186	33.959	1.314	4.372	0.231	2.220	0.231
Expanding leaves 1	115865 (AdRGL3a)	24.424	0.042	0.172	323.380	12.296	15.274	0.935	9.701	0.935
Expanding leaves 2	115865 (AdRGL3a)	25.876	0.043	0.166	118.444	4.269	17.890	0.868	17.890	0.868
F Flower buds 1	115865 (AdRGL3a)	29.059	0.138	0.476	13.117	1.263	3.666	0.366	2.290	0.366
F Flower buds 2	115865 (AdRGL3a)	31.472	0.041	0.131	2.473	0.071	4.838	0.159	1.929	0.159
F Styles	115865 (AdRGL3a)	35.603	0.182	0.511	0.142	0.018	3.757	0.496	3.757	0.496
F Styles 2	115865 (AdRGL3a)	23.063	0.064	0.277	828.868	43.663	58.796	3.906	20.208	3.906
Fruit cortex 1	115865 (AdRGL3a)	32.662	0.078	0.238	1.086	0.058	0.288	0.017	0.288	0.017
Fruit cortex 2	115865 (AdRGL3a)	No Amp[†]								
M Flower bud 1	115865 (AdRGL3a)	28.466	0.027	0.097	19.765	0.452	5.107	0.188	3.263	0.188
M Flower buds 2	115865 (AdRGL3a)	27.054	0.023	0.086	52.458	1.221	23.283	0.835	9.496	0.835
Shoot tips 1	115865 (AdRGL3a)	32.115	0.038	0.118	1.585	0.042	0.770	0.026	0.307	0.026
Shoot tips 2	115865 (AdRGL3a)	27.283	0.046	0.169	44.776	1.602	3.735	0.184	3.019	0.184

RNA from[a]	Target[b]	avg Cq[c]	SE avg Cq	CV	rel Cq[d]	SE rel Cq	NRCq[e]	SE NRCq	CNRCq[f]	SE CNRCq
Breaking buds 1	78609 (AdRGL3b)	22.552	0.024	0.105	58.147	1.099	7.872	0.281	4.815	0.281
Breaking buds 2	78609 (AdRGL3b)	20.793	0.006	0.030	191.085	2.608	10.618	0.402	10.618	0.402
Dormant buds 1	78609 (AdRGL3b)	30.393	0.035	0.115	0.289	0.007	3.172	0.102	1.391	0.102
Dormant buds 2	78609 (AdRGL3b)	24.671	0.065	0.264	13.870	0.618	1.786	0.102	0.907	0.102
Expanding leaves 1	78609 (AdRGL3b)	19.554	0.036	0.182	441.816	16.200	20.869	1.260	13.254	1.260
Expanding leaves 2	78609 (AdRGL3b)	20.635	0.024	0.117	212.597	4.469	32.111	1.243	32.111	1.243
F Flower buds 1	78609 (AdRGL3b)	23.876	0.022	0.091	23.735	0.394	6.634	0.208	4.144	0.208
F Flower buds 2	78609 (AdRGL3b)	26.396	0.012	0.047	4.317	0.040	8.445	0.155	3.367	0.155
F Styles	78609 (AdRGL3b)	31.650	0.020	0.064	0.123	0.002	3.266	0.129	3.266	0.129
F Styles 2	78609 (AdRGL3b)	21.312	0.025	0.118	134.461	2.811	9.538	0.435	3.278	0.435
Fruit cortex 1	78609 (AdRGL3b)	24.482	0.025	0.100	15.752	0.282	4.177	0.139	4.177	0.139
Fruit cortex 2	78609 (AdRGL3b)	26.219	0.016	0.062	4.864	0.057	1.653	0.042	1.653	0.042
M Flower bud 1	78609 (AdRGL3b)	25.212	0.002	0.009	9.617	0.056	2.485	0.073	1.588	0.073
M Flower buds 2	78609 (AdRGL3b)	23.939	0.069	0.289	22.753	1.081	10.098	0.553	4.119	0.553
Shoot tips 1	78609 (AdRGL3b)	23.045	0.018	0.076	41.650	0.626	20.243	0.525	8.057	0.525
Shoot tips 2	78609 (AdRGL3b)	20.568	0.031	0.151	222.541	5.536	18.565	0.782	15.005	0.782
Breaking buds 1	200355/4	24.009	0.032	0.133	87.986	2.282	11.912	0.474	7.286	0.474
Breaking buds 2	200355/4	22.041	0.008	0.037	338.827	11.369	18.828	0.917	18.828	0.917
Dormant buds 1	200355/4	30.322	0.015	0.050	1.163	0.012	12.772	0.299	5.601	0.299
Dormant buds 2	200355/4	21.888	0.016	0.074	376.460	8.084	48.470	2.030	24.614	2.030
Expanding leaves 1	200355/4	26.295	0.054	0.205	18.361	0.698	0.867	0.053	0.551	0.053
Expanding leaves 2	200355/4	26.335	0.039	0.147	17.868	0.500	2.699	0.116	2.699	0.116
F Flower buds 1	200355/4	25.567	0.019	0.074	30.244	0.504	8.454	0.266	5.281	0.266
F Flower buds 2	200355/4	30.693	0.071	0.230	0.902	0.044	1.764	0.090	0.703	0.090
F Styles	200355/4	34.182	0.242	0.707	0.083	0.014	2.183	0.371	2.183	0.371
F Styles 2	200355/4	23.226	0.092	0.394	150.494	10.369	10.675	0.853	3.669	0.853
Fruit cortex 1	200355/4	25.158	0.008	0.033	40.029	0.511	10.614	0.326	10.614	0.326
Fruit cortex 2	200355/4	24.055	0.010	0.041	85.261	1.305	28.977	0.792	28.977	0.792
M Flower bud 1	200355/4	26.429	0.048	0.182	16.759	0.573	4.330	0.194	2.767	0.194
M Flower buds 2	200355/4	27.233	0.050	0.182	9.656	0.335	4.286	0.189	1.748	0.189
Shoot tips 1	200355/4	26.691	0.052	0.196	14.006	0.515	6.807	0.289	2.709	0.289
Shoot tips 2	200355/4	22.979	0.071	0.309	178.167	10.139	14.863	0.985	12.013	0.985

RNA from[a]	Target[b]	avg Cq[c]	SE avg Cq	CV	rel Cq[d]	SE rel Cq	NRCq[e]	SE NRCq	CNRCq[f]	SE CNRCq
Breaking buds 1	287619/17	24.977	0.053	0.212	86.433	4.645	11.702	0.721	7.157	0.721
Breaking buds 2	287619/17	24.301	0.012	0.049	137.172	6.108	7.622	0.433	7.622	0.433
Dormant buds 1	287619/17	33.187	0.059	0.176	0.316	0.013	3.464	0.160	1.519	0.160
Dormant buds 2	287619/17	23.548	0.056	0.238	229.557	14.164	29.556	2.111	15.009	2.111
Expanding leaves 1	287619/17	24.657	0.039	0.157	107.568	5.308	5.081	0.350	3.227	0.350
Expanding leaves 2	287619/17	26.060	0.039	0.150	41.211	1.752	6.225	0.333	6.225	0.333
F Flower buds 1	287619/17	26.150	0.046	0.177	38.761	1.761	10.834	0.571	6.768	0.571
F Flower buds 2	287619/17	30.870	0.059	0.192	1.539	0.063	3.010	0.131	1.200	0.131
F Styles	287619/17	37.339	0.054	0.143	0.018	0.001	0.488	0.031	0.488	0.031
F Styles 2	287619/17	23.482	0.050	0.213	240.220	14.303	17.040	1.227	5.857	1.227
Fruit cortex 1	287619/17	28.687	0.058	0.201	6.840	0.294	1.814	0.093	1.814	0.093
Fruit cortex 2	287619/17	29.523	0.128	0.432	3.862	0.348	1.313	0.122	1.313	0.122
M Flower bud 1	287619/17	25.106	0.036	0.143	79.133	3.639	20.445	1.111	13.065	1.111
M Flower buds 2	287619/17	27.902	0.046	0.163	11.699	0.445	5.193	0.243	2.118	0.243
Shoot tips 1	287619/17	26.771	0.034	0.127	25.353	0.938	12.322	0.525	4.904	0.525
Shoot tips 2	287619/17	22.232	0.042	0.190	564.745	35.761	47.113	3.386	38.079	3.386
Breaking buds 1	287619/22	27.449	0.012	0.043	17.233	0.237	2.333	0.077	1.427	0.077
Breaking buds 2	287619/22	26.790	0.073	0.272	26.897	1.470	1.495	0.097	1.495	0.097
Dormant buds 1	287619/22	34.742	0.135	0.388	0.125	0.011	1.372	0.129	0.602	0.129
Dormant buds 2	287619/22	26.583	0.014	0.053	30.932	0.510	3.983	0.158	2.022	0.158
Expanding leaves 1	287619/22	26.678	0.040	0.150	28.999	0.874	1.370	0.078	0.870	0.078
Expanding leaves 2	287619/22	27.890	0.063	0.228	12.791	0.563	1.932	0.106	1.932	0.106
F Flower buds 1	287619/22	28.978	0.070	0.243	6.136	0.295	1.715	0.094	1.071	0.094
F Flower buds 2	287619/22	32.826	0.081	0.246	0.456	0.025	0.892	0.051	0.356	0.051
F Styles	287619/22	37.768	0.547	1.448	0.016	0.006	0.429	0.160	0.429	0.160
F Styles 2	287619/22	25.334	0.049	0.195	71.898	2.689	5.100	0.281	1.753	0.281
Fruit cortex 1	287619/22	28.770	0.019	0.065	7.060	0.105	1.872	0.059	1.872	0.059
Fruit cortex 2	287619/22	29.435	0.024	0.082	4.506	0.078	1.531	0.044	1.531	0.044
M Flower bud 1	287619/22	26.557	0.031	0.118	31.479	0.790	8.133	0.311	5.197	0.311
M Flower buds 2	287619/22	29.744	0.053	0.177	3.657	0.132	1.623	0.073	0.662	0.073
Shoot tips 1	287619/22	28.621	0.021	0.073	7.809	0.127	3.795	0.101	1.510	0.101
Shoot tips 2	287619/22	24.523	0.028	0.114	124.328	3.326	10.372	0.448	8.383	0.448

RNA from[a]	Target[b]	avg Cq[c]	SE avg Cq	CV	rel Cq[d]	SE rel Cq	NRCq[e]	SE NRCq	CNRCq[f]	SE CNRCq
Breaking buds 1	SLY 7	25.057	0.034	0.135	33.080	0.834	4.479	0.176	2.739	0.176
Breaking buds 2	SLY 7	22.075	0.062	0.282	219.696	9.757	12.208	0.693	12.208	0.693
Dormant buds 1	SLY 7	31.057	0.016	0.052	0.733	0.008	8.051	0.189	3.531	0.189
Dormant buds 2	SLY 7	23.321	0.027	0.117	99.576	2.447	12.821	0.558	6.511	0.558
Expanding leaves 1	SLY 7	23.421	0.049	0.210	93.485	3.336	4.416	0.264	2.804	0.264
Expanding leaves 2	SLY 7	23.311	0.078	0.336	100.229	5.278	15.139	0.937	15.139	0.937
F Flower buds 1	SLY 7	25.872	0.052	0.199	19.719	0.682	5.511	0.241	3.443	0.241
F Flower buds 2	SLY 7	28.967	0.052	0.178	2.764	0.091	5.408	0.198	2.156	0.198
F Styles	SLY 7	35.863	0.109	0.304	0.035	0.002	0.917	0.073	0.917	0.073
F Styles 2	SLY 7	25.171	0.041	0.164	30.763	0.899	2.182	0.109	0.750	0.109
Fruit cortex 1	SLY 7	26.561	0.009	0.033	12.732	0.236	3.376	0.113	3.376	0.113
Fruit cortex 2	SLY 7	26.962	0.005	0.017	9.869	0.090	3.354	0.082	3.354	0.082
M Flower bud 1	SLY 7	25.212	0.063	0.251	29.976	1.266	7.745	0.397	4.949	0.397
M Flower buds 2	SLY 7	25.151	0.075	0.300	31.158	1.547	13.829	0.783	5.640	0.783
Shoot tips 1	SLY 7	25.791	0.043	0.166	20.762	0.613	10.091	0.366	4.016	0.366
Shoot tips 2	SLY 7	22.081	0.055	0.249	218.809	8.854	18.254	0.964	14.754	0.964
Breaking buds 1	SLY 8	24.927	0.035	0.140	65.925	2.322	8.925	0.414	5.459	0.414
Breaking buds 2	SLY 8	23.008	0.120	0.522	237.758	20.759	13.212	1.244	13.212	1.244
Dormant buds 1	SLY 8	29.840	0.058	0.193	2.471	0.096	27.132	1.199	11.899	1.199
Dormant buds 2	SLY 8	24.173	0.029	0.120	109.181	3.854	14.057	0.708	7.139	0.708
Expanding leaves 1	SLY 8	23.892	0.006	0.025	131.731	4.078	6.222	0.355	3.952	0.355
Expanding leaves 2	SLY 8	24.249	0.108	0.444	103.759	8.055	15.672	1.319	15.672	1.319
F Flower buds 1	SLY 8	25.941	0.036	0.140	33.482	1.098	9.358	0.395	5.846	0.395
F Flower buds 2	SLY 8	28.189	0.146	0.517	7.453	0.732	14.580	1.452	5.813	1.452
F Styles	SLY 8	35.116	0.317	0.904	0.073	0.015	1.923	0.415	1.923	0.415
F Styles 2	SLY 8	26.196	0.037	0.143	28.243	0.922	2.003	0.104	0.689	0.104
Fruit cortex 1	SLY 8	30.202	0.117	0.388	1.941	0.152	0.515	0.043	0.515	0.043
Fruit cortex 2	SLY 8	31.120	0.070	0.223	1.051	0.049	0.357	0.018	0.357	0.018
M Flower bud 1	SLY 8	28.831	0.138	0.480	4.852	0.451	1.254	0.122	0.801	0.122
M Flower buds 2	SLY 8	26.482	0.175	0.662	23.324	2.773	10.352	1.263	4.222	1.263
Shoot tips 1	SLY 8	25.427	0.050	0.195	47.222	1.941	22.951	1.061	9.134	1.061
Shoot tips 2	SLY 8	22.302	0.030	0.134	381.200	16.150	31.801	1.727	25.703	1.727

RNA from[a]	Target[b]	avg Cq[c]	SE avg Cq	CV	rel Cq[d]	SE rel Cq	NRCq[e]	SE NRCq	CNRCq[f]	SE CNRCq
Breaking buds 1	SLY 12	21.496	0.026	0.121	65.716	1.748	8.897	0.358	5.442	0.358
Breaking buds 2	SLY 12	20.002	0.037	0.185	180.974	6.379	10.056	0.502	10.056	0.502
Dormant buds 1	SLY 12	27.770	0.060	0.214	0.933	0.038	10.244	0.466	4.493	0.466
Dormant buds 2	SLY 12	21.782	0.005	0.024	54.120	1.045	6.968	0.284	3.539	0.284
Expanding leaves 1	SLY 12	20.340	0.066	0.323	143.871	7.261	6.796	0.473	4.316	0.473
Expanding leaves 2	SLY 12	21.203	0.011	0.053	80.177	1.778	12.110	0.477	12.110	0.477
F Flower buds 1	SLY 12	22.999	0.047	0.206	23.710	0.840	6.627	0.294	4.140	0.294
F Flower buds 2	SLY 12	26.102	0.034	0.129	2.893	0.068	5.660	0.160	2.257	0.160
F Styles	SLY 12	30.716	0.044	0.142	0.127	0.004	3.349	0.161	3.349	0.161
F Styles 2	SLY 12	21.238	0.063	0.297	78.268	3.719	5.552	0.347	1.908	0.347
Fruit cortex 1	SLY 12	23.494	0.023	0.096	16.956	0.346	4.496	0.156	4.496	0.156
Fruit cortex 2	SLY 12	24.695	0.021	0.084	7.510	0.128	2.552	0.072	2.552	0.072
M Flower bud 1	SLY 12	22.894	0.016	0.068	25.459	0.475	6.578	0.226	4.203	0.226
M Flower buds 2	SLY 12	22.437	0.062	0.278	34.718	1.582	15.409	0.818	6.285	0.818
Shoot tips 1	SLY 12	22.922	0.040	0.174	24.987	0.775	12.144	0.456	4.833	0.456
Shoot tips 2	SLY 12	19.838	0.040	0.202	202.306	7.509	16.877	0.849	13.641	0.849
Breaking buds 1	PP2A	20.659	0.039	0.187	2.780	0.080	0.376	0.016	0.230	0.016
Breaking buds 2	PP2A	19.077	0.008	0.042	8.324	0.192	0.463	0.019	0.463	0.019
Dormant buds 1	PP2A	28.226	0.041	0.145	0.015	0.001	0.161	0.009	0.071	0.009
Dormant buds 2	PP2A	21.071	0.079	0.373	2.089	0.115	0.269	0.018	0.137	0.018
Expanding leaves 1	PP2A	19.034	0.044	0.232	8.572	0.326	0.405	0.025	0.257	0.025
Expanding leaves 2	PP2A	20.689	0.077	0.374	2.722	0.149	0.411	0.026	0.411	0.026
F Flower buds 1	PP2A	21.448	0.025	0.114	1.608	0.029	0.450	0.014	0.281	0.014
F Flower buds 2	PP2A	24.037	0.017	0.071	0.267	0.005	0.523	0.013	0.209	0.013
F Styles	PP2A	29.792	0.038	0.128	0.005	0.000	0.131	0.009	0.131	0.009
F Styles 2	PP2A	19.754	0.065	0.327	5.206	0.286	0.369	0.025	0.127	0.025
Fruit cortex 1	PP2A	22.558	0.007	0.030	0.745	0.004	0.198	0.006	0.198	0.006
Fruit cortex 2	PP2A	22.830	0.003	0.013	0.617	0.006	0.210	0.005	0.210	0.005
M Flower bud 1	PP2A	21.513	0.037	0.174	1.537	0.041	0.397	0.016	0.254	0.016
M Flower buds 2	PP2A	21.409	0.046	0.214	1.652	0.053	0.733	0.031	0.299	0.031
Shoot tips 1	PP2A	22.478	0.030	0.133	0.788	0.016	0.383	0.011	0.152	0.011
Shoot tips 2	PP2A	19.566	0.019	0.096	5.931	0.135	0.495	0.020	0.400	0.020

RNA from[a]	Target[b]	avg Cq[c]	SE avg Cq	CV	rel Cq[d]	SE rel Cq	NRCq[e]	SE NRCq	CNRCq[f]	SE CNRCq
Breaking buds 1	UPL7	24.146	0.030	0.123	2.108	0.044	0.285	0.011	0.175	0.011
Breaking buds 2	UPL7	23.052	0.042	0.183	4.482	0.139	0.249	0.012	0.249	0.012
Dormant buds 1	UPL7	29.470	0.023	0.077	0.054	0.001	0.590	0.020	0.259	0.020
Dormant buds 2	UPL7	23.556	0.042	0.178	3.167	0.095	0.408	0.019	0.207	0.019
Expanding leaves 1	UPL7	22.590	0.087	0.385	6.160	0.377	0.291	0.023	0.185	0.023
Expanding leaves 2	UPL7	24.450	0.009	0.037	1.710	0.012	0.258	0.009	0.258	0.009
F Flower buds 1	UPL7	25.860	0.022	0.084	0.647	0.010	0.181	0.006	0.113	0.006
F Flower buds 2	UPL7	28.735	0.015	0.051	0.089	0.002	0.175	0.004	0.070	0.004
F Styles	UPL7	No amp[†]								
F Styles 2	UPL7	23.988	0.035	0.144	2.351	0.058	0.167	0.008	0.057	0.008
Fruit cortex 1	UPL7	24.893	0.041	0.164	1.260	0.035	0.334	0.013	0.334	0.013
Fruit cortex 2	UPL7	24.672	0.018	0.073	1.467	0.019	0.499	0.013	0.499	0.013
M Flower bud 1	UPL7	25.803	0.037	0.145	0.673	0.017	0.174	0.007	0.111	0.007
M Flower buds 2	UPL7	27.138	0.045	0.164	0.268	0.009	0.119	0.005	0.049	0.005
Shoot tips 1	UPL7	26.123	0.007	0.029	0.540	0.004	0.262	0.006	0.104	0.006
Shoot tips 2	UPL7	23.953	0.021	0.090	2.409	0.039	0.201	0.008	0.162	0.008
Breaking buds 1	ACTIN C	19.206	0.025	0.128	68.768	5.729	9.310	0.825	5.695	0.825
Breaking buds 2	ACTIN C	17.802	0.019	0.106	156.199	15.402	8.680	0.909	8.680	0.909
Dormant buds 1	ACTIN C	26.516	0.038	0.145	0.959	0.022	10.526	0.323	4.616	0.323
Dormant buds 2	ACTIN C	19.155	0.051	0.264	70.834	6.217	9.120	0.865	4.631	0.865
Expanding leaves 1	ACTIN C	17.562	0.125	0.713	179.715	22.372	8.489	1.132	5.391	1.132
Expanding leaves 2	ACTIN C	19.373	0.011	0.055	62.361	5.015	9.419	0.817	9.419	0.817
F Flower buds 1	ACTIN C	19.970	0.037	0.183	43.997	3.364	12.298	0.996	7.682	0.996
F Flower buds 2	ACTIN C	23.497	0.036	0.154	5.598	0.221	10.950	0.467	4.366	0.467
F Styles	ACTIN C	28.569	0.054	0.189	0.289	0.011	7.636	0.413	7.636	0.413
F Styles 2	ACTIN C	17.148	0.006	0.033	228.955	24.144	16.241	1.835	5.582	1.835
Fruit cortex 1	ACTIN C	19.523	0.012	0.060	57.129	4.500	15.148	1.266	15.148	1.266
Fruit cortex 2	ACTIN C	20.735	0.023	0.109	28.128	1.858	9.560	0.668	9.560	0.668
M Flower bud 1	ACTIN C	19.557	0.014	0.072	56.014	4.398	14.472	1.211	9.248	1.211
M Flower buds 2	ACTIN C	20.883	0.044	0.210	25.793	1.755	11.448	0.839	4.669	0.839
Shoot tips 1	ACTIN C	21.278	0.018	0.084	20.483	1.219	9.955	0.629	3.962	0.629
Shoot tips 2	ACTIN C	18.245	0.053	0.292	120.536	11.816	10.056	1.043	8.127	1.043

[a] Tissue from which mRNA was extracted. [b]Gene amplicon target. [c]avg Cq, average of the crossing points for the technical triplicate quantitation cycles. [d]rel Cq, relative expression levels of the transcript, with the efficiency of PCR amplification taken into account. [e]NCRq, normalised relative quantities calculated to the geNorm of the reference genes. [f]CNCRq, calibrated normalised relative quantities (normalised relative quantities calibrated for inter-run plate variability).
SE, Standard error, the standard error values are propagated through the analysis. **CV,** coefficient of variation of the replicates. The qPCR data was tabulated in the order (from left to right) that the data manipulation was performed. All the values are calculated within the QPCR application (Pabinger et al., 2009).The Highlighted column was graphed. [†]No amplification in the wells for this transcript in this tissue.

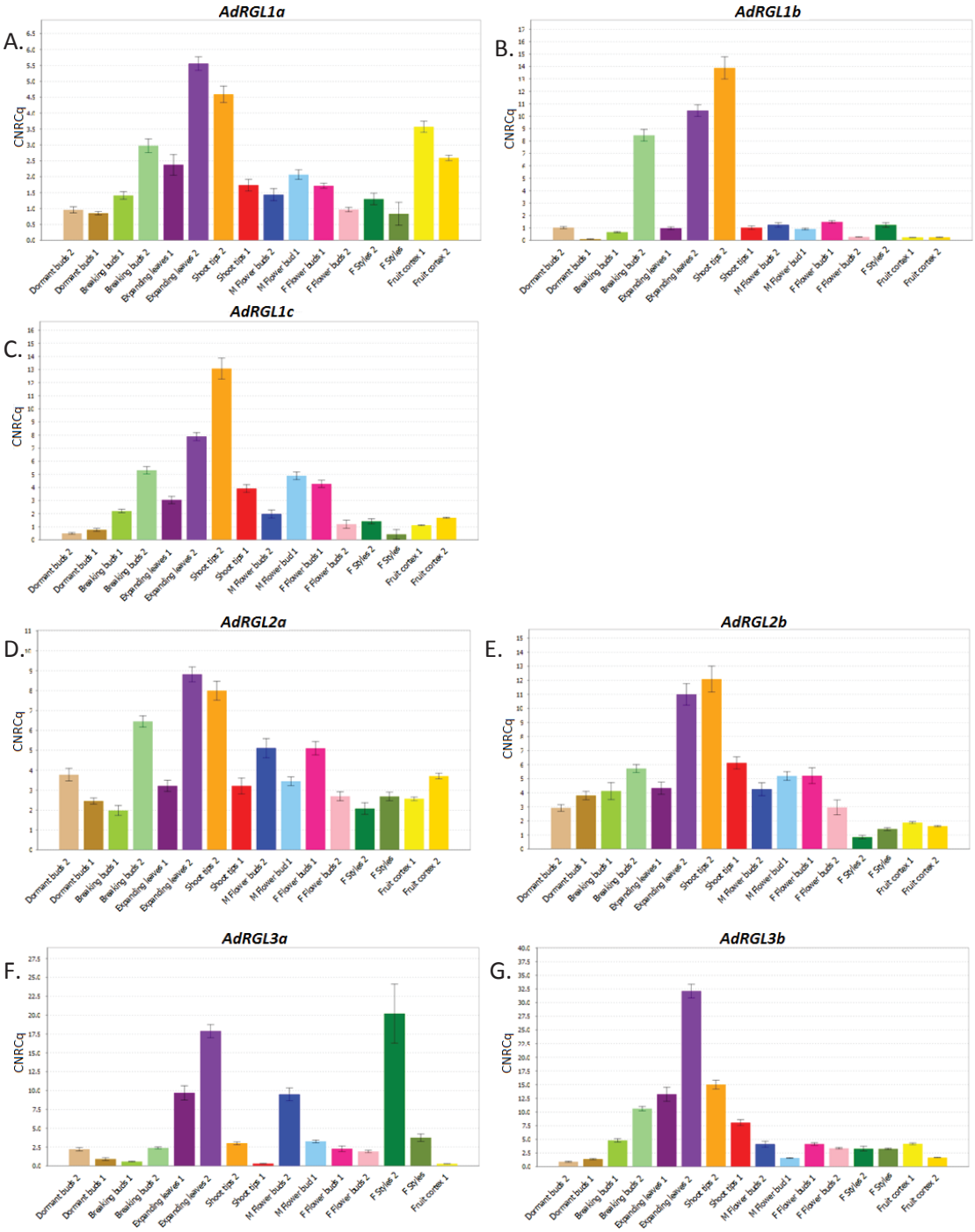

Figure 6.9. Relative expression (CNRCq) of the DELLA kiwifruit homologues
Bar graphs representing the transcript expression levels of the kiwifruit DELLA homologues compared to the genorm (geometric averaging) of the reference genes (*PP2A*, *UPL7* and *ACT2/7* -C). The quantitation cycle (crossing point) was determined by the AnalyzerMiner algorithm (Zhao and Fernald, 2005). The kiwifruit technical replicates were averaged and PCR efficiency was corrected for using the standard curve data. Genes were normalised against the reference genes and calibrated to account for inter-assay variability within the QPCR application. Standard error bars 1.0 (Pabinger et al., 2009).
A, *AtRGL1a*; **B,** *AtRGL1b*; **C.** *AtRGL1c*; **D,** *AtRGL2a*; **E,** *AtRGL2b*; **F,** *AtRGL3a*; **G,** *AtRGL3b*.

A.

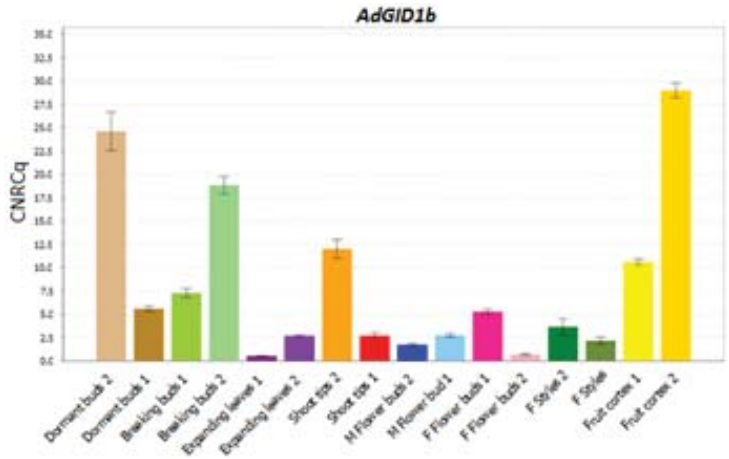

B.

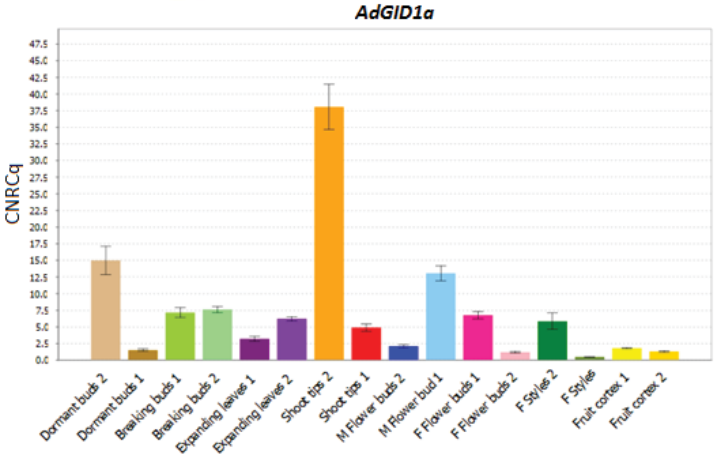

C.

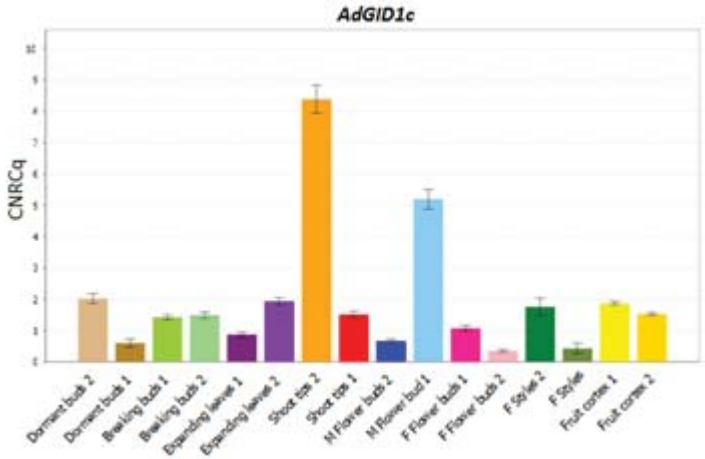

Figure 6.10. Relative expression (CNRCq) of the *GID1* kiwifruit homologues
Bar graphs representing the transcript expression levels of the *AdGID1s* compared to the genorm (geometric averaging) of the reference genes (*AdPP2A*, *AdUPL7* and *AdACT2/7* -C). The quantitation cycle (crossing point) was determined by the AnalyzerMiner algorithm (Zhao and Fernald, 2005). The kiwifruit technical replicates were averaged and PCR efficiency was corrected for using the standard curve data. Genes were normalised against the reference genes and calibrated to account for inter-assay variability within the QPCR application. Standard error bars 1.0 (Pabinger et al., 2009).
A, *AdGID1b*; **B,** *AdGID1a;* **C,** *AdGID1c*.

A.

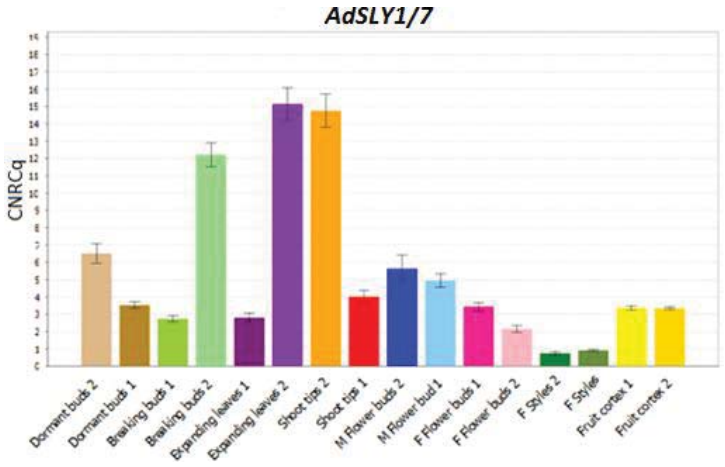

B.

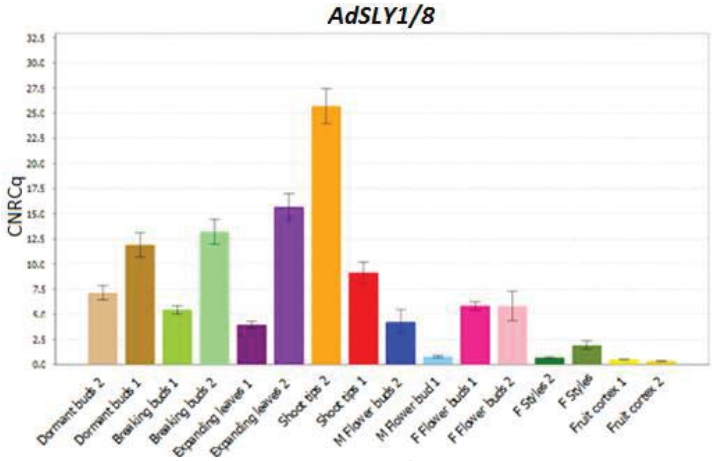

C.

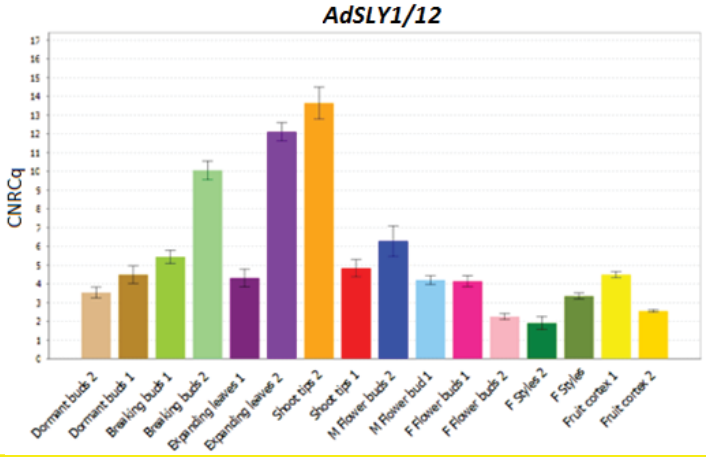

Figure 6.11. Relative expression (CNRCq) *SLY1/ GID2* kiwifruit homologues
Bar graphs representing the transcript expression levels of the *AdSLY1s* compared to the genorm (geometric averaging) of the reference genes (*AdPP2A*, *AdUPL7* and *AdACT2/7* -C). The quantitation cycle (crossing point) was determined by the AnalyzerMiner algorithm (Zhao and Fernald, 2005). The kiwifruit technical replicates were averaged and PCR efficiency was corrected for using the standard curve data. Genes were normalised against the reference genes and calibrated to account for inter-assay variability within the QPCR application. Standard error bars 1.0 (Pabinger et al., 2009).
A, *AdSLY1/7;* **B,** *AdSLY1/8;* **C,** *AdSLY1/12.*

A.

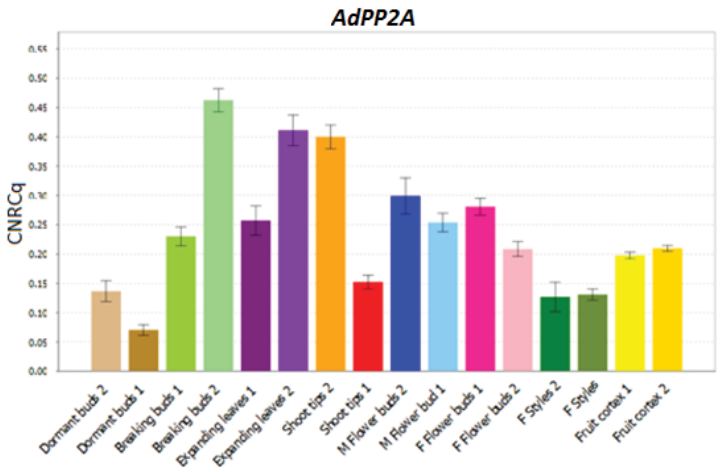

B.

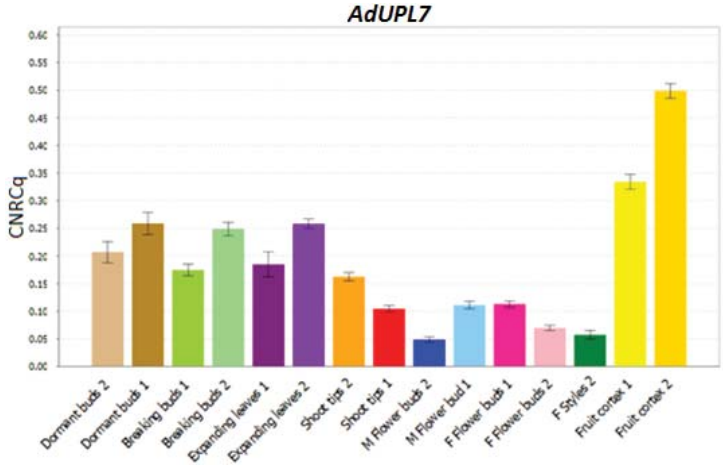

C.

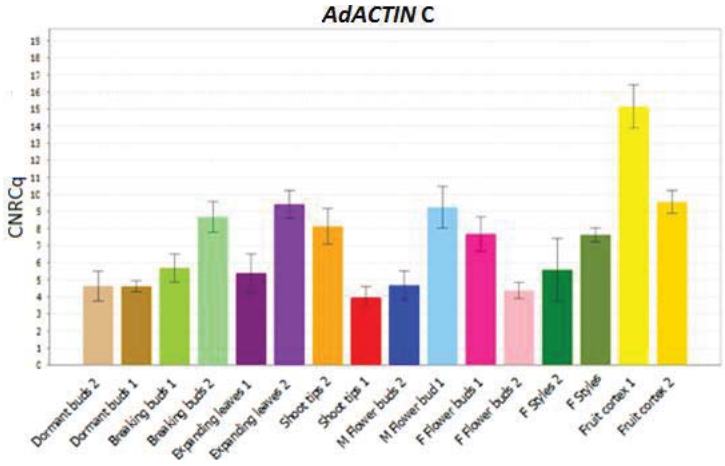

Figure 6.12. Relative expression of the individual kiwifruit reference genes
Bar graphs representing the transcript expression levels of the kiwifruit reference gene compared to the genorm (geometric averaging) of the reference genes (*AdPP2A*, *AdUPL7* and *AdACT2/7* -C). The quantitation cycle (crossing point) was determined by the AnalyzerMiner algorithm (Zhao and Fernald, 2005). The kiwifruit technical replicates were averaged and PCR efficiency was corrected for using the standard curve data. Genes were normalised against the reference genes and calibrated to account for inter-assay variability within the QPCR application (CNRCq) . Standard error bars 1.0 (Pabinger et al., 2009).
A, *AdPP2A*, **B,** *AdUPL7*, **C,** *AdACTIN2/7* C-terminal.

Table 6.2. Reliability of DELLA modelling

DELLA	QMEAN Z-Score[a]	QMEAN4 Score[b]	Sequence Identity (%)[c]
AdRGL1a	-0.108	0.754	53.7
AdRGL1b	-0.108	0.754	53.7
AdRGL1c	-0.312	0.720	52.2
AdRGL2a	-0.601	0.668	57.8
AdRGL2b	-0.274	0.721	60.9
AdRGL3a	-0.227	0.729	50.0
AdRGL3b	-0.294	0.718	48.5
AtGAI	-0.314	0.720	89.5

[a]QMEAN Z-score and [b]QMEAN4-score give an indication of the reliability or quality of the model. The QMEAN Z-score estimates the 'degree of nativeness' for a quality measure from comparisons of X-ray crystallography solved structures. The smaller the score, the better the reliability. The QMEAN4 score evaluates the model on the combination of four structural descriptors of the amino acid placements and gives a score on the model in the range 0 to 1. A higher score is better (Benkert et al., 2011).
[c]Sequence identity by alignment to the structural template , 2zsiB.
Note that the template model, 2zsiB, is amino acid residues 26 to 92 excluding the b-c loop (amino acids 61 to 67). AtGAI tabled here is the N-terminal amino acids 11 to 113 inclusive, modelled on the 2zsi template and is the amino acid sequence used in the crystallised recombinant protein.

7. Papers

Foster, T., Kirk, C. A., Jones, W. T., Allan, A. C., Espley, R., Karunairetnam, S. & Rakonjac, J. (2007). Characterisation of the DELLA subfamily in Apple (*Malus* x *domestica* Borkh.). *Tree Genetics and Genomes,* **3**: 187-197.

Jones, W. T., Harvey, D., Kirk, C., Rakonjac, J., Sun, X., Frearson, N. & Al-Samarrai, T. A. (2007). A Novel Peptide tag for Detection and Purification of Recombinant Expressed Proteins. *Protein Expression and Purification,* **53**: 404-410.

Sun, X., Frearson, N., Kirk, C., Jones, W. T., Harvey, D., Rakonjac, J., Foster, T. & Al-Samarrai, T. (2008). An *E. coli* Expression System optimized for DELLA Proteins. *Protein Expression and Purification,* **58**: 168-174.

Sun, X. L., Jones, W. T., Harvey, D., Edwards, P. J. B., Pascal, S. M., Kirk, C., Considine, T., Sheerin, D. J., Rakonjac, J., Oldfield, C. J., Xue, B., Dunker, A. K. & Uversky, V. N. (2010). N-terminal Domains of DELLA Proteins Are Intrinsically Unstructured in the Absence of Interaction with GID1/Gibberellic Acid Receptors. *Journal of Biological Chemistry,* **285**: 11557-11571.

Sheerin, D. J., Buchanan, J., Kirk, C., Harvey, D., Sun, X., Spagnuolo, J., Li, S., Liu, T., Woods, V. A., Foster, T., Jones, W. T. & Rakonjac, J. (2011). Inter- and Intra-Molecular Interactions of *Arabidopsis thaliana* DELLA protein RGL1. *Biochemical Journal,* **435**: 629-639.

8. References

ABBASI, F., ONODERA, H., TOKI, S., TANAKA, H. & KOMATSU, S. 2004. *OsCDPKI3*, a Calcium-dependent protein Kinase gene from Rice, is Induced by Cold and Gibberellin in Rice leaf Sheath. *Plant Molecular Biology,* 55**,** 541-552.

ABBASI, N., PARK, Y.-I. & CHOI, S.-B. 2011. Pumilio Puf domain RNA-binding proteins in *Arabidopsis*. *Plant Signaling & Behavior,* 6**,** 364-368.

ACHARD, P., CHENG, H., DE GRAUWE, L., DECAT, J., SCHOUTTETEN, H., MORITZ, T., VAN DER STRAETEN, D., PENG, J. R. & HARBERD, N. P. 2006. Integration of Plant Responses to Environmentally Activated Phytohormonal Signals. *Science,* 311**,** 91-94.

ACHARD, P., HERR, A., BAULCOMBE, D. C. & HARBERD, N. P. 2004. Modulation of Floral Development by a Gibberellin-regulated MicroRNA. *Development,* 131**,** 3357-3365.

ACHARD, P., RENOU, J. P., BERTHOME, R., HARBERD, N. P. & GENSCHIK, P. 2008. Plant DELLAs Restrain growth and Promote survival of adversity by Reducing the levels of Reactive Oxygen Species. *Current Biology,* 18**,** 656-660.

ACHARD, P., VRIEZEN, W. H., VAN DER STRAETEN, D. & HARBERD, N. P. 2003. Ethylene Regulates *Arabidopsis* Development via the Modulation of DELLA protein Growth Repressor Function. *Plant Cell,* 15**,** 2816-2825.

AGUILAR-MARTÍNEZ, J. A., POZA-CARRIÓN, C. & CUBAS, P. 2007. *Arabidopsis* BRANCHED1 Acts as an Integrator of Branching Signals within Axillary Buds. *The Plant Cell Online,* 19**,** 458-472.

AIT-ALI, T., RANDS, C. & HARBERD, N. P. 2003. Flexible control of plant Architecture and Yield via Switchable expression of *Arabidopsis gai*. *Plant Biotechnology Journal,* 1**,** 337-343.

ALABADI, D., GALLEGO-BARTOLOME, J., ORLANDO, L., GARCIA-CARCEL, L., RUBIO, V., MARTINEZ, C., FRIGERIO, M., IGLESIAS-PEDRAZ, J. M., ESPINOSA, A., DENG, X. W. & BLAZQUEZ, M. A. 2008. Gibberellins modulate Light signaling pathways to Prevent *Arabidopsis* seedling De-etiolation in Darkness. *The Plant Journal,* 53**,** 324-335.

ALABADI, D., GIL, J., BLAZQUEZ, M. A. & GARCIA-MARTINEZ, J. L. 2004. Gibberellins Repress Photomorphogenesis in Darkness. *Plant Physiology,* 134**,** 1050-1057.

ALEMAN, L., KITAMURA, J., ABDEL-MAGEED, H., LEE, J., SUN, Y., NAKAJIMA, M., UEGUCHI-TANAKA, M., MATSUOKA, M. & ALLEN, R. D. 2008. Functional analysis of Cotton orthologs of GA Signal transduction factors *GID1* and *SLR1*. *Plant Molecular Biology,* 68**,** 1-16.

ALTSCHUL, S. F., GISH, W., MILLER, W., MYERS, E. W. & LIPMAN, D. J. 1990. Basic Search Alignment Tool. *Journal of Molecular Biology,* 215**,** 403-410.

ALVEY, L. & HARBERD, N. P. 2005. DELLA proteins: Integrators of Multiple Plant Growth Regulatory Inputs? *Physiologia Plantarum,* 123**,** 153-160.

AMADOR, V., MONTE, E., GARCIA-MARTINEZ, J. L. & PRAT, S. 2001. Gibberellins signal nuclear import of *PHOR1*, a Photoperiod-responsive protein with homology to *Drosophila ARMADILLO*. *Cell,* 106**,** 343-354.

ANTEROLA, A. & SHANLE, E. 2008. Genomic insights in Moss Gibberellin Biosynthesis. *Bryologist,* 111**,** 218-230.

ARIIZUMI, T., LAWRENCE, P. K. & STEBER, C. M. 2011. The Role of Two F-Box Proteins, SLEEPY1 and SNEEZY, in Arabidopsis Gibberellin Signaling. *Plant Physiology,* 155**,** 765-775.

ARIIZUMI, T. & STEBER, C. M. 2007. Seed Germination of GA-Insensitive *sleepy1* Mutants Does Not require RGL2 protein Disappearance in *Arabidopsis*. *Plant Cell,* 19**,** 791-804.

ARNAUD, N., GIRIN, T., SOREFAN, K., FUENTES, S., WOOD, T. A., LAWRENSON, T., SABLOWSKI, R. & OSTERGAARD, L. 2010. Gibberellins Control Fruit Patterning in *Arabidopsis thaliana*. *Genes & Development,* 24**,** 2127-2132.

ARNOLD, K., BORDOLI, L., KOPP, J. & SCHWEDE, T. 2006. The SWISS-MODEL Workspace: A web-based environment for Protein Structure Homology Modelling. *Bioinformatics,* 22**,** 195-201.

ASSMANN, S. M. 2005. G Proteins Go Green: A Plant G Protein Signaling FAQ Sheet. *Science,* 310**,** 71.

AUDAS, TIMOTHY E., JACOB, MATHIEU D. & LEE, S. 2012. Immobilization of Proteins in the Nucleolus by Ribosomal Intergenic Spacer Noncoding RNA. *Molecular Cell,* 45**,** 147-157.

AYA, K., UEGUCHI-TANAKA, M., KONDO, M., HAMADA, K., YANO, K., NISHIMURA, M. & MATSUOKA, M. 2009. Gibberellin Modulates Anther Development in Rice via the Transcriptional Regulation of *GAMYB*. *Plant Cell,* 21**,** 1453-1472.

BALTIMORE, D. 1970. Viral RNA-dependent DNA Polymerase: RNA-dependent DNA Polymerase in Virions of RNA Tumour Viruses. *Nature,* 226**,** 1209-1211.

BASSEL, G. W., MULLEN, R. T. & BEWLEY, J. D. 2008. *procera* is a Putative DELLA mutant in Tomato (*Solanum lycopersicum*): Effects on the Seed and Vegetative Plant. *Journal of Experimental Botany,* 59**,** 585-593.

BASSEL, G. W., ZIELINSKA, E., MULLEN, R. T. & BEWLEY, J. D. 2004. Down-Regulation of DELLA Genes Is Not Essential for Germination of Tomato, Soybean, and *Arabidopsis* Seeds. *Plant Physiol.,* 136**,** 2782-2789.

BENKERT, P., BIASINI, M. & SCHWEDE, T. 2011. Toward the Estimation of the Absolute Quality of individual protein Structure Models. *Bioinformatics,* 27**,** 343-350.

BERENDZEN, K., SEARLE, I., RAVENSCROFT, D., KONCZ, C., BATSCHAUER, A., GEORGE, C., SOMSSICH, I. E. & ÜLKER, B. 2005. A Rapid and Versatile combined DNA/RNA Extraction protocol and its application to the Analysis of a Novel DNA Marker set Polymorphic between *Arabidopsis thaliana* ecotypes Col-0 and Landsberg *erecta*. *Plant Methods,* 1**,** 4-19.

BISHOPP, A., MAHONEN, A. P. & HELARIUTTA, Y. 2006. Signs of Change: Hormone Receptors that Regulate Plant Development. *Development,* 133**,** 1857.

BÖGRE, L., OKRÉSZ, L., HENRIQUES, R. & ANTHONY, R. G. 2003. Growth signalling pathways in *Arabidopsis* and the AGC protein kinases. *Trends in Plant Science,* 8**,** 424-431.

BOLLE, C. 2004. The Role of GRAS proteins in Plant Signal Transduction and Development. *Planta,* 218**,** 683-692.

BOSS, P. K. & THOMAS, M. R. 2002. Association of Dwarfism and Floral Induction with a Grape `green revolution' Mutation. *Nature,* 416**,** 847-850.

BOTTO, J. F., IBARRA, S. & JONES, A. M. 2009. The Heterotrimeric G protein Complex Modulates Light Sensitivity in *Arabidopsis thaliana* Seed Germination. *Photochemistry and Photobiology,* 85**,** 949-954.

BRENNER, W. G., ROMANOV, G. A., KOLLMER, I., BURKLE, L. & SCHMULLING, T. 2005. Immediate-early and Delayed Cytokinin Response genes of *Arabidopsis thaliana* Identified by Genome-wide Expression Profiling reveal Novel Cytokinin-sensitive processes and suggest Cytokinin action through Transcriptional Cascades. *The Plant Journal,* 44**,** 314-333.

BUSOV, V., MEILAN, R., PEARCE, D. W., ROOD, S. B., MA, C., TSCHAPLINSKI, T. J. & STRAUSS, S. H. 2006. Transgenic Modification of *gai* or *rgl1* causes Dwarfing and Alters Gibberellins, Root growth, and Metabolite profiles in *Populus*. *Planta,* 224**,** 288-299.

CAO, D., CHENG, H., WU, W., SOO, H. M. & PENG, J. 2006. Gibberellin Mobilizes Distinct DELLA-Dependent Transcriptomes to Regulate Seed Germination and Floral Development in *Arabidopsis*. *Plant Physiol.,* 142**,** 509-525.

CAO, D., HUSSAIN, A., CHENG, H. & PENG, J. 2005. Loss of function of four DELLA genes leads to Light- and Gibberellin-Independent Seed Germination in *Arabidopsis*. *Planta,* 223**,** 105-113.

CARRERA, E., RUIZ-RIVERO, O., PERES, L. E. P., ATARES, A. & GARCIA-MARTINEZ, J. L. 2012. Characterization of the procera Tomato Mutant Shows Novel Functions of the SlDELLA Protein in the Control of Flower Morphology, Cell Division and Expansion, and the Auxin-Signaling Pathway during Fruit-Set and Development. *Plant Physiology,* 160**,** 1581-1596.

CASSANI, E., BERTOLINI, E., BADONE, F. C., LANDONI, M., GAVINA, D., SIRIZZOTTI, A. & PILU, R. 2009. Characterization of the first Dominant Dwarf Maize mutant carrying a Single Amino acid Insertion in the VHYNP domain of the *dwarf8* Gene. *Molecular Breeding,* 24**,** 375-385.

CHANDLER, P. M., MARION-POLL, A., ELLIS, M. & GUBLER, F. 2002. Mutants at the *SLENDER1* Locus of Barley cv Himalaya. Molecular and Physiological Characterization. *Plant Physiol.,* 129**,** 181-190.

CHEN, J.-G., WILLARD, F. S., HUANG, J., LIANG, J. & AL, E. 2003. A Seven-Transmembrane RGS Protein That Modulates Plant Cell Proliferation. *Science,* 301**,** 1728.

CHEN, K. & AN, Y.-Q. C. 2006. Transcriptional Responses to Gibberellin and Abscisic Acid in Barley Aleurone. *Journal of Integrative Plant Biology,* 48**,** 591-612.

CHEN, K. G., TIAN, S. L., YANDELL, B. S., KAEPPLER, S. M. & AN, Y. Q. C. 2010. Loss-of-function of DELLA protein *SLN1* activates GA Signaling in Barley Aleurone. *Acta Physiologiae Plantarum,* 32**,** 789-800.

CHENG, H., QIN, L. J., LEE, S. C., FU, X. D., RICHARDS, D. E., CAO, D. N., LUO, D., HARBERD, N. P. & PENG, J. R. 2004. Gibberellin Regulates *Arabidopsis* Floral Development via Suppression of DELLA protein Function. *Development,* 131**,** 1055-1064.

CHENG, H., SONG, S. S., XIAO, L. T., SOO, H. M., CHENG, Z. W., XIE, D. X. & PENG, J. R. 2009. Gibberellin Acts through Jasmonate to Control the Expression of *MYB21*, *MYB24*, and *MYB57* to Promote Stamen Filament Growth in *Arabidopsis*. *Plos Genetics,* 5.

CHHUN, T., AYA, K., ASANO, K., YAMAMOTO, E., MORINAKA, Y., WATANABE, M., KITANO, H., ASHIKARI, M., MATSUOKA, M. & UEGUCHI-TANAKA, M. 2007. Gibberellin Regulates Pollen Viability and Pollen Tube Growth in Rice. *Plant Cell,* 19**,** 3876-3888.

CHIWOCHA, S. D. S., CUTLER, A. J., ABRAMS, S. R., AMBROSE, S. J., YANG, J., ROSS, A. R. S. & KERMODE, A. R. 2005. The *etr1-2* mutation in *Arabidopsis thaliana* affects the Abscisic acid, Auxin, Cytokinin and Gibberellin Metabolic pathways during Maintenance of Seed Dormancy, Moist-chilling and Germination. *Plant Journal,* 42**,** 35-48.

CLOUGH, S. J. & BENT, A. F. 1998. Floral Dip: A simplified Method for *Agrobacterium*-mediated Transformation of *Arabidopsis thaliana*. *The Plant Journal,* 16**,** 735-743.

COLUCCI, G., APONE, F., ALYESHMERNI, N., CHALMERS, D. & CHRISPEELS, M. J. 2002. *GCR1*, the putative *Arabidopsis* G protein-Coupled Receptor gene is Cell Cycle-regulated, and its Over-expression Abolishes Seed Dormancy and Shortens Time to Flowering. *Proceedings of the National Academy of Sciences of the United States of America,* 99**,** 4736-4741.

CROWHURST, R. N., DAVY, M. D. & DENG, C. H. 1999-2011. BioPipe and BioView - Automated cDNA Sequence Annotation Pipeline and Viewer System. *The Plant and Food Research Institute of New Zealand Limited,* Not Published.

CZECHOWSKI, T., STITT, M., ALTMANN, T., UDVARDI, M. K. & SCHEIBLE, W.-R. 2005. Genome-Wide Identification and Testing of Superior Reference Genes for Transcript Normalization in *Arabidopsis*. *Plant Physiology,* 139**,** 5-17.

DAI, C. & XUE, H. W. 2010. Rice *EARLY FLOWERING 1*, a CKI, Phosphorylates DELLA protein *SLR1* to Negatively Regulate Gibberellin Signalling. *Embo Journal,* 29**,** 1916-1927.

DAVIERE, J. M., DE LUCAS, M. & PRAT, S. 2008. Transcriptional Factor Interaction: A central step in DELLA Function. *Current Opinion in Genetics & Development,* 18**,** 295-303.

DE GRAUWE, L., CHAERLE, L., DUGARDEYN, J., DECAT, J., RIEU, I., VRIEZEN, W. H., MORITZ, T., BEEMSTER, G. T. S., PHILLIPS, A. L., HARBERD, N. P., HEDDEN, P. & VAN DER STRAETEN, D. 2008. Reduced Gibberellin Response Affects Ethylene Biosynthesis and

Responsiveness in the *Arabidopsis gai eto2-1* Double Mutant. *New Phytologist,* 177**,** 128-141.

DE LUCAS, M., DAVIERE, J.-M., RODRIGUEZ-FALCON, M., PONTIN, M., IGLESIAS-PEDRAZ, J. M., LORRAIN, S., FANKHAUSER, C., BLAZQUEZ, M. A., TITARENKO, E. & PRAT, S. 2008. A Molecular Framework for Light and Gibberellin Control of Cell Elongation. *Nature,* 451**,** 480-484.

DILL, A., JUNG, H. S. & SUN, T. P. 2001. The DELLA Motif is Essential for Gibberellin-Induced Degradation of *RGA*. *Proceedings of the National Academy of Sciences of the United States of America,* 98**,** 14162-14167.

DILL, A. & SUN, T. P. 2001. Synergistic Derepression of Gibberellin Signaling by Removing *RGA* and *GAI* Function in *Arabidopsis thaliana*. *Genetics,* 159**,** 777-785.

DILL, A., THOMAS, S. G., HU, J. H., STEBER, C. M. & SUN, T. P. 2004. The *Arabidopsis* F-box protein *SLEEPY1* targets Gibberellin Signaling Repressors for Gibberellin-induced Degradation. *Plant Cell,* 16**,** 1392-1405.

DINANT, S., CLARK, A. M., ZHU, Y., VILAINE, F., PALAUQUI, J.-C., KUSIAK, C. & THOMPSON, G. A. 2003. Diversity of the Superfamily of Phloem Lectins (Phloem Protein 2) in Angiosperms. *Plant Physiology,* 131**,** 114-128.

DJAKOVIC-PETROVIC, T., DE WIT, M., VOESENEK, L. & PIERIK, R. 2007. DELLA protein Function in Growth Responses to Canopy Signals. *Plant Journal,* 51**,** 117-126.

DOERKS, T., HUBER, S., BUCHNER, E. & BORK, P. 2002. BSD: a novel domain in transcription factors and synapse-associated proteins. *Trends in Biochemical Sciences,* 27**,** 168-170.

DRUART, N., JOHANSSON, A., BABA, K., SCHRADER, J., SJODIN, A., BHALERAO, R. R., RESMAN, L., TRYGG, J., MORITZ, T. & BHALERAO, R. P. 2007. Environmental and Hormonal Regulation of the Activity-Dormancy Cycle in the Cambial Meristem involves Stage-specific Modulation of Transcriptional and Metabolic Networks. *Plant Journal,* 50**,** 557-573.

ERIKSSON, S., BOHLENIUS, H., MORITZ, T. & NILSSON, O. 2006. GA_4 Is the Active Gibberellin in the Regulation of *LEAFY* Transcription and *Arabidopsis* Floral Initiation. *Plant Cell,* 18**,** 2172-2181.

EVANS, R. C. & CAMPBELL, C. S. 2002. The origin of the apple subfamily (Maloideae; Rosaceae) is clarified by DNA sequence data from duplicated GBSSI genes. *American Journal of Botany,* 89**,** 1478-1484.

FENG, S., MARTINEZ, C., GUSMAROLI, G., WANG, Y., ZHOU, J., WANG, F., CHEN, L., YU, L., IGLESIAS-PEDRAZ, J. M., KIRCHER, S., SCHAFER, E., FU, X., FAN, L.-M. & DENG, X. W. 2008. Coordinated Regulation of *Arabidopsis thaliana* Development by Light and Gibberellins. *Nature,* 451**,** 475-479.

FILARDO, F. F. & SWAIN, S. M. 2003. *SPY*ing on GA Signaling and Plant Development. *Journal of Plant Growth Regulation,* 22**,** 163-175.

FLECK, B. & HARBERD, N. P. 2002. Evidence that the *Arabidopsis* Nuclear Gibberellin Signalling protein GAI is Not Destabilised by Gibberellin. *Plant Journal,* 32**,** 935-947.

FLEET, C. M. & SUN, T. P. 2005. A DELLAcate Balance: The role of Gibberellin in Plant Morphogenesis. *Current Opinion in Plant Biology,* 8**,** 77-85.

FLEISHON, S., SHANI, E., ORI, N. & WEISS, D. 2011. Negative Reciprocal Interactions between Gibberellin and Cytokinin in Tomato. *New Phytologist,* 190**,** 609-617.

FOSS, E. J., RADULOVIC, D., SHAFFER, S. A., GOODLETT, D. R., KRUGLYAK, L. & BEDALOV, A. 2011. Genetic Variation Shapes Protein Networks Mainly through Non-transcriptional Mechanisms. *PLoS Biol,* 9**,** e1001144.

FOSTER, T., JOHNSTON, R. & SELEZNYOVA, A. 2003. A Morphological and Quantitative Characterization of Early Floral Development in Apple (*Malus × domestica* Borkh.). *Annals of Botany,* 92**,** 199-206.

FOSTER, T., KIRK, C. A., JONES, W. T., ALLAN, A. C., ESPLEY, R., KARUNAIRETNAM, S. & RAKONJAC, J. 2007. Characterisation of the DELLA subfamily in Apple (*Malus* x *domestica* Borkh.). *Tree Genetics and Genomes,* 3**,** 187-197.

FRAZER, C. & YOUNG, P. 2012. Carboxy-terminal phosphorylation sites in Cdc25 contribute to enforcement of the DNA damage and replication checkpoints in fission yeast. *Current Genetics,* 58**,** 217-234.

FRIDBORG, I., KUUSK, S., MORITZ, T. & SUNDBERG, E. 1999. The *Arabidopsis* Dwarf Mutant *shi* Exhibits Reduced Gibberellin Responses Conferred by Over-expression of a New Putative Zinc Finger Protein. *Plant Cell,* 11**,** 1019-1032.

FRIDBORG, I., KUUSK, S., ROBERTSON, M. & SUNDBERG, E. 2001. The *Arabidopsis* protein *SHI* Represses Gibberellin Responses in *Arabidopsis* and Barley. *Plant Physiology,* 127**,** 937-948.

FROHMAN, M. A., DUSH, M. K. & MARTIN, G. R. 1988. Rapid Production of Full-length cDNAs from Rare Transcripts: Amplification using a Single Gene-specific Oligonucleotide Primer. *Proceedings of the National Academy of Sciences,* 85**,** 8998-9002.

FU, X. D. & HARBERD, N. P. 2003. Auxin Promotes *Arabidopsis* Root Growth by Modulating Gibberellin Response. *Nature,* 421**,** 740-743.

FU, X. D., RICHARDS, D. E., AIT-ALI, T., HYNES, L. W., OUGHAM, H., PENG, J. R. & HARBERD, N. P. 2002. Gibberellin-mediated Proteasome-dependent Degradation of the Barley DELLA protein *SLN1* Repressor. *Plant Cell,* 14**,** 3191-3200.

FU, X. D., RICHARDS, D. E., FLECK, B., XIE, D. X., BURTON, N. & HARBERD, N. P. 2004. The *Arabidopsis* mutant *sleepy1*$^{(gar2\text{-}1)}$ protein Promotes Plant Growth by Increasing the Affinity of the SCF^{SLY1} E3 Ubiquitin Ligase for DELLA protein Substrates. *Plant Cell,* 16**,** 1406-1418.

FU, X. D., SUDHAKAR, D., PENG, J. R., RICHARDS, D. E., CHRISTOU, P. & HARBERD, N. P. 2001. Expression of *Arabidopsis* GAI in Transgenic Rice Represses multiple Gibberellin Responses. *Plant Cell,* 13**,** 1791-1802.

FUJISAWA, Y., KATO, H. & IWASAKI, Y. 2001. Structure and Function of Heterotrimeric G proteins in Plants. *Plant and Cell Physiology,* 42**,** 789-794.

FULFORD, R. M. 1965. The Morphogenesis of Apple Buds: I. The Activity of the Apical Meristem. *Annals of Botany,* 29**,** 167-180.

FULFORD, R. M. 1966. The Morphogenesis of Apple Buds: III. The Inception of Flowers. *Annals of Botany,* 30**,** 207-219.

GALLEGO-BARTOLOME, J., MINGUET, E. G., MARIN, J. A., PRAT, S., BLAZQUEZ, M. A. & ALABADI, D. 2010. Transcriptional Diversification and Functional Conservation between DELLA Proteins in *Arabidopsis*. *Molecular Biology and Evolution,* 27**,** 1247-1256.

GAZZARRINI, S. & MCCOURT, P. 2003. Cross-talk in Plant Hormone Signalling: What *Arabidopsis* Mutants are Telling Us. *Annals of Botany,* 91**,** 605-612.

GILROY, S. & JONES, R. L. 1994. Perception of Gibberellin and Abscisic Acid at the External Face of the Plasma Membrane of Barley (*Hordeum vulgare* L.) Aleurone Protoplasts. *Plant Physiology,* 104**,** 1185-1192.

GLEAVE, A. P. 1992a. A Versatile Binary Vector System with a T-DNA Organisational Structure Conducive to Efficient Integration of Cloned DNA into the Plant Genome. *Plant Molecular Biology,* 20**,** 1203-1207.

GLEAVE, A. P. 1992b. A versatile binary vector system with a T-DNA organisational structure conducive to efficient integration of cloned DNA into the plant genome. *Plant Molecular Biology,* 20**,** 1203-1207.

GOCAL, G. F. W., POOLE, A. T., GUBLER, F., WATTS, R. J., BLUNDELL, C. & KING, R. W. 1999. Long-day Up-Regulation of a *GAMYB* gene during *Lolium temulentum* Inflorescence Formation. *Plant Physiology,* 119**,** 1271-1278.

GOCAL, G. F. W., SHELDON, C. C., GUBLER, F., MORITZ, T., BAGNALL, D. J., MACMILLAN, C. P., LI, S. F., PARISH, R. W., DENNIS, E. S., WEIGEL, D. & KING, R. W. 2001. *GAMYB*-like genes, Flowering, and Gibberellin Signaling in *Arabidopsis*. *Plant Physiology,* 127**,** 1682-1693.

GOMEZ-CADENAS, A., VERHEY, S. D., HOLAPPA, L. D., SHEN, Q., HO, T.-H. D. & WALKER-SIMMONS, M. K. 1999. An Abscisic acid-induced Protein kinase, *PKABA1*, Mediates Abscisic acid-Suppressed gene expression in Barley Aleurone Layers. *PNAS,* 96**,** 1767-1772.

GOMEZ-CADENAS, A., ZENTELLA, R., WALKER-SIMMONS, M. K. & HO, T. H. D. 2001. Gibberellin/ Abscisic acid Antagonism in Barley Aleurone Cells: Site of action of the protein kinase *PKABA1* in relation to Gibberellin Signalling Molecules. *Plant Cell,* 13**,** 667-679.

GOMI, K. & MATSUOKA, M. 2003. Gibberellin Signalling Pathway. *Current Opinion in Plant Biology,* 6**,** 489-493.

GOMI, K., SASAKI, A., ITOH, H., UEGUCHI-TANAKA, M., ASHIKARI, M., KITANO, H. & MATSUOKA, M. 2004. GID2, an F-box subunit of the SCF E3 complex, specifically Interacts with Phosphorylated SLR1 protein and Regulates the Gibberellin-dependent Degradation of SLR1 in Rice. *Plant Journal,* 37**,** 626-634.

GOU, J. Q., STRAUSS, S. H., TSAI, C. J., FANG, K., CHEN, Y. R., JIANG, X. N. & BUSOV, V. B. 2010. Gibberellins Regulate Lateral Root Formation in *Populus* through Interactions with Auxin and Other Hormones. *Plant Cell,* 22**,** 623-639.

GREENBOIM-WAINBERG, Y., MAYMON, I., BOROCHOV, R., ALVAREZ, J., OLSZEWSKI, N., ORI, N., ESHED, Y. & WEISS, D. 2005. Cross talk between Gibberellin and Cytokinin: The *Arabidopsis* GA response inhibitor *SPINDLY* plays a Positive role in Cytokinin Signalling. *Plant Cell,* 17**,** 92-102.

GRIFFITHS, J., MURASE, K., RIEU, I., ZENTELLA, R., ZHANG, Z. L., POWERS, S. J., GONG, F., PHILLIPS, A. L., HEDDEN, P., SUN, T. P. & THOMAS, S. G. 2006. Genetic Characterization and Functional Analysis of the *GID1* Gibberellin Receptors in *Arabidopsis*. *Plant Cell,* 18**,** 3399.

GUBLER, F., CHANDLER, P. M., WHITE, R. G., LLEWELLYN, D. J. & JACOBSEN, J. V. 2002. Gibberellin Signaling in Barley Aleurone Cells. Control of *SLN1* and *GAMYB* Expression. *Plant Physiology,* 129**,** 191-200.

GUBLER, F., KALLA, R., ROBERTS, J. K. & JACOBSEN, J. V. 1995. Gibberellin-Regulated Expression of a *myb* gene in Barley Aleurone Cells: Evidence for Myb Transactivation of a High-pl α-Amylase Gene Promoter. *Plant Cell,* 7**,** 1879-1891.

GUBLER, F., RAVENTOS, D., KEYS, M., WATTS, R., MUNDY, J. & JACOBSEN, J. V. 1999. Target Genes and Regulatory Domains of the *GAMYB* Transcriptional Activator in Cereal Aleurone. *The Plant Journal,* 17**,** 1-9.

HAN, Y., ZHENG, D., VIMOLMANGKANG, S., KHAN, M. A., BEEVER, J. E. & KORBAN, S. S. 2011. Integration of physical and genetic maps in apple confirms whole-genome and segmental duplications in the apple genome. *Journal of Experimental Botany*.

HANAHAN, D., JESSEE, J. & BLOOM, F. R. 1991. Plasmid Transformation of *Escherichia coli* and other Bacteria. *In:* JEFFREY, H. M. (ed.) *Methods in Enzymology.* Academic Press.

HARTWECK, L. M., SCOTT, C. L. & OLSZEWSKI, N. E. 2002. Two *O*-Linked N-Acetylglucosamine Transferase Genes of *Arabidopsis thaliana* L. Heynh. Have Overlapping Functions Necessary for Gamete and Seed Development. *Genetics,* 161**,** 1279-1291.

HAYASHI, K., HORIE, K., HIWATASHI, Y., KAWAIDE, H., YAMAGUCHI, S., HANADA, A., NAKASHIMA, T., NAKAJIMA, M., MANDER, L. N., YAMANE, H., HASEBE, M. & NOZAKI, H. 2010. Endogenous Diterpenes Derived from ent-Kaurene, a Common Gibberellin Precursor, Regulate Protonema Differentiation of the Moss Physcomitrella patens. *Plant Physiology,* 153**,** 1085-1097.

HAYWOOD, V., YU, T. S., HUANG, N. C. & LUCAS, W. J. 2005. Phloem Long-distance Trafficking of *GIBBERELLIC ACID-INSENSITIVE* RNA Regulates Leaf Development. *Plant Journal,* 42**,** 49-68.

HEDDEN, P. & PHILLIPS, A. L. 2000. Gibberellin Metabolism: New Insights Revealed by the Genes. *Trends in Plant Science,* 5**,** 523-530.

HELLEMANS, J., MORTIER, G., DE, P., SPELEMAN, F. & VANDESOMPELE, J. 2007. qBase Relative Quantification Framework and Software for Management and Automated Analysis of Real-Time Quantitative PCR Data. *Genome Biol,* 8**,** R19.

HELLENS, R. P., EDWARDS, E. A., LEYLAND, N. R., BEAN, S. & MULLINEAUX, P. M. 2000. pGreen: A Versatile and Flexible Binary Ti vector for *Agrobacterium*-mediated Plant Transformation. *Plant Molecular Biology,* 42**,** 819-832.

HELLIWELL, C. A., WOOD, C. C., ROBERTSON, M., JAMES PEACOCK, W. & DENNIS, E. S. 2006. The *Arabidopsis* FLC protein interacts directly in vivo with SOC1 and FT chromatin and is part of a high-molecular-weight protein complex. *The Plant Journal,* 46**,** 183-192.

HENIKOFF, S., HENIKOFF, J. G., ALFORD, W. J. & PIETROKOVSKI, S. 1995. Automated Construction and Graphical Presentation of Protein Blocks from Unaligned Sequences. *Gene,* 163**,** GC17-GC26.

HEO, J. O., CHANG, K. S., KIM, I. A., LEE, M. H., LEE, S. A., SONG, S. K., LEE, M. M. & LIM, J. 2011. Funneling of Gibberellin Signaling by the GRAS transcription Regulator *SCARECROW-LIKE 3* in the *Arabidopsis* Root. *Proceedings of the National Academy of Sciences of the United States of America,* 108**,** 2166-2171.

HERR, A. J., MOLNÀR, A., JONES, A. & BAULCOMBE, D. C. 2006. Defective RNA processing enhances RNA silencing and influences flowering of *Arabidopsis*. *Proceedings of the National Academy of Sciences,* 103**,** 14994-15001.

HIRANO, K., ASANO, K., TSUJI, H., KAWAMURA, M., MORI, H., KITANO, H., UEGUCHI-TANAKA, M. & MATSUOKA, M. 2010. Characterization of the Molecular Mechanism Underlying Gibberellin Perception Complex Formation in Rice. *Plant Cell,* 22**,** 2680-2696.

HIRANO, K., AYA, K., HOBO, T., SAKAKIBARA, H., KOJIMA, M., SHIM, R. A., HASEGAWA, Y., UEGUCHI-TANAKA, M. & MATSUOKA, M. 2008. Comprehensive Transcriptome Analysis of Phytohormone Biosynthesis and Signaling Genes in Microspore/Pollen and Tapetum of Rice. *Plant and Cell Physiology,* 49**,** 1429-1450.

HIRANO, K., UEGUCHI-TANAKA, M., NAKAJIMA, M., ASANO, K., SAKAKIBARA, H., KOJIMA, M., NISHIYAMA, T., TANAHASHI, T., HASEBE, M., AHIKARI, M., KITANO, H. & MATSUOKA, M. 2007. Evolution of *GID1*-Dependent Gibberellin Signaling Pathway in Plants. *Plant and Cell Physiology,* 48**,** S60.

HIRT, H., GARCIA, A. V. & OELMÜLLER, R. 2011. AGC kinases in plant development and defense. *Plant Signaling & Behavior,* 6**,** 1030-1033.

HOOLEY, R., BEALE, M. H. & SMITH, S. J. 1991. Gibberellin Perception at the Plasma Membrane of *Avena fatua* Aleurone Protoplasts. *Planta,* 183**,** 274-280.

HOOLEY, R., BEALE, M. H., SMITH, S. J., WALKER, R. P., RUSHTON, P. J., WHITFORD, P. N. & LAZARUS, C. M. 1992. Gibberellin Perception and the *Avena fatua* Aleurone: Do our Molecular keys fit the correct Locks? *Biochemical Society Transactions,* 20**,** 85-9.

HOU, X., HU, W.-W., SHEN, L., LEE, L. Y. C., TAO, Z., HAN, J.-H. & YU, H. 2008. Global Identification of DELLA Target Genes during *Arabidopsis* Flower Development. *Plant Physiol.,* 147**,** 1126-1142.

HOU, X., LEE, L. Y. C., XIA, K., YAN, Y. & YU, H. 2010. DELLAs Modulate Jasmonate Signaling via Competitive Binding to JAZs. *Developmental Cell,* 19**,** 884-894.

HSIA, M. M. & CALLIS, J. 2010. BRIZ1 and BRIZ2 Proteins Form a Heteromeric E3 Ligase Complex Required for Seed Germination and Post-germination Growth in *Arabidopsis thaliana*. *Journal of Biological Chemistry,* 285**,** 37070-37081.

HU, J. H., MITCHUM, M. G., BARNABY, N., AYELE, B. T., OGAWA, M., NAM, E., LAI, W. C., HANADA, A., ALONSO, J. M., ECKER, J. R., SWAIN, S. M., YAMAGUCHI, S., KAMIYA, Y. &

SUN, T. P. 2008. Potential Sites of Bioactive Gibberellin Production during Reproductive Growth in *Arabidopsis*. *Plant Cell,* 20**,** 320-336.

HUANG, N. C. & YU, T. S. 2009. The Sequences of *Arabidopsis GA-INSENSITIVE* RNA Constitute the Motifs that are necessary and sufficient for RNA Long-distance Trafficking. *Plant Journal,* 59**,** 921-929.

HUQ, E. 2006. Degradation of Negative Regulators: A common theme in Hormone and Light Signalling Networks? *Trends in Plant Science,* 11**,** 4.

HUSSAIN, A., CAO, D., CHENG, H., WEN, Z. & PENG, J. 2005. Identification of the Conserved Serine/ Threonine Residues important for Gibberellin-sensitivity of *Arabidopsis* RGL2 Protein. *The Plant Journal,* 44**,** 88-99.

HUSSAIN, A., CAO, D. & PENG, J. 2007. Identification of Conserved Tyrosine Residues important for Gibberellin Sensitivity of *Arabidopsis* RGL2 Protein. *Planta,* 226**,** 475-483.

IKEDA, A., UEGUCHI-TANAKA, M., SONODA, Y., KITANO, H., KOSHIOKA, M., FUTSUHARA, Y., MATSUOKA, M. & YAMAGUCHI, J. 2001. *slender rice*, a Constitutive Gibberellin Response Mutant, is caused by a Null Mutation of the *SLR1* gene, an Ortholog of the Height-regulating gene *GAI* / *RGA* / *RHT* / *D8*. *Plant Cell,* 13**,** 999-1010.

ISABEL-LAMONEDA, I., DIAZ, I., MARTINEZ, M., MENA, M. & CARBONERO, P. 2003. *SAD*: a new DOF protein from Barley that Activates Transcription of a cathepsin B-like thiol protease gene in the Aleurone of Germinating Seeds. *The Plant Journal,* 33**,** 329-340.

ISKANDAR, H., SIMPSON, R., CASU, R., BONNETT, G., MACLEAN, D. & MANNERS, J. 2004. Comparison of Reference Genes for Quantitative Real-Time Polymerase Chain Reaction Analysis of Gene Expression in Sugarcane. *Plant Molecular Biology Reporter,* 22**,** 325-337.

ITOH, H., MATSUOKA, M. & STEBER, C. M. 2003. A Role for the Ubiquitin-26S-Proteasome pathway in Gibberellin Signaling. *Trends in Plant Science,* 8**,** 492-497.

ITOH, H., SASAKI, A., UEGUCHI-TANAKA, M., ISHIYAMA, K., KOBAYASHI, M., HASEGAWA, Y., MINAMI, E., ASHIKARI, M. & MATSUOKA, M. 2005a. Dissection of the Phosphorylation of Rice DELLA Protein, SLENDER RICE1. *Plant Cell Physiol.,* 46**,** 1392-1399.

ITOH, H., SHIMADA, A., UEGUCHI-TANAKA, M., KAMIYA, N., HASEGAWA, Y., ASHIKARI, M. & MATSUOKA, M. 2005b. Overexpression of a GRAS protein lacking the DELLA Domain confers altered Gibberellin Responses in Rice. *The Plant Journal,* 44**,** 669-679.

ITOH, H., UEGUCHI-TANAKA, M., SATO, Y., ASHIKARI, M. & MATSUOKA, M. 2002. The Gibberellin Signalling pathway is Regulated by the Appearance and Disappearance of SLENDER RICE1 in Nuclei. *Plant Cell,* 14**,** 57-70.

IUCHI, S., SUZUKI, H., KIM, Y.-C., IUCHI, A., KUROMORI, T., UEGUCHI-TANAKA, M., ASAMI, T., YAMAGUCHI, I., MATSUOKA, M., KOBAYASHI, M. & NAKAJIMA, M. 2007. Multiple loss-of-function of *Arabidopsis* Gibberellin Receptor *AtGID1*s completely shuts down a Gibberellin Signal. *The Plant Journal,* 50**,** 958-966.

JACOBSEN, S. E., BINKOWSKI, K. A. & OLSZEWSKI, N. E. 1996. *SPINDLY*, a Tetratricopeptide Repeat protein involved in Gibberellin Signal Transduction in *Arabidopsis*. *Proceedings of the National Academy of Sciences of the United States of America,* 93**,** 9292-9296.

JACOBSEN, S. E. & OLSZEWSKI, N. E. 1993. Mutations at the *SPINDLY* Locus of *Arabidopsis* Alter Gibberellin Signal Transduction. *Plant Cell,* 5**,** 887-896.

JASINSKI, S., TATTERSALL, A., PIAZZA, P., HAY, A., MARTINEZ-GARCIA, J. F., SCHMITZ, G., THERES, K., MCCORMICK, S. & TSIANTIS, M. 2008. PROCERA encodes a DELLA protein that Mediates Control of Dissected Leaf form in Tomato. *Plant Journal,* 56**,** 603-612.

JIANG, C., GAO, X., LIAO, L., HARBERD, N. P. & FU, X. 2007. Phosphate Starvation Root Architecture and Anthocyanin Accumulation Responses are Modulated by the Gibberellin-DELLA Signaling Pathway in *Arabidopsis*. *Plant Physiol.,* 145**,** 1460-1470.

JOHANSON, U., WEST, J., LISTER, C., MICHAELS, S., AMASINO, R. & DEAN, C. 2000. Molecular Analysis of *FRIGIDA*, a Major Determinant of Natural Variation in *Arabidopsis* Flowering Time. *Science,* 290**,** 344-347.

JONES, W. T., HARVEY, D., KIRK, C., RAKONJAC, J., SUN, X., FREARSON, N. & SAMARRAI, T. A. 2007. A Novel Peptide tag for Detection and Purification of Recombinant Expressed Proteins. *Protein Expression and Purification,* 53**,** 404-410.

JOSEFSSON, L.-G. & RASK, L. 1997. Cloning of a Putative G Protein Coupled Receptor from *Arabidopsis thaliana*. *European Journal of Biochemistry,* 249**,** 415-420.

JUNG, S., STATON, M., LEE, T., BLENDA, A., SVANCARA, R., ABBOTT, A. & MAIN, D. 2008. GDR (Genome Database for Rosaceae): integrated web-database for Rosaceae genomics and genetics data. *Nucleic Acids Research,* 36**,** D1034-D1040.

KANEKO, M., ITOH, H., INUKAI, Y., SAKAMOTO, T., UEGUCHI-TANAKA, M., ASHIKARI, M. & MATSUOKA, M. 2003. Where do Gibberellin Biosynthesis and Gibberellin Signaling Occur in Rice Plants? *Plant Journal,* 35**,** 104-115.

KING, K. E., MORITZ, T. & HARBERD, N. P. 2001. Gibberellins are Not Required for normal Stem Growth in *Arabidopsis thaliana* in the Absence of GAI and RGA. *Genetics,* 159**,** 767-776.

KOBAYASHI, M., SAKURAI, A., SAKA, H. & TAKAHASHI, N. 1989. Quantitative Analysis of Endogenous Gibberellins in Normal and Dwarf Cultivars of Rice. *Plant and Cell Physiology,* 30**,** 963-969.

KOJIMA, M., KAMADA-NOBUSADA, T., KOMATSU, H., TAKEI, K., KUROHA, T., MIZUTANI, M., ASHIKARI, M., UEGUCHI-TANAKA, M., MATSUOKA, M., SUZUKI, K. & SAKAKIBARA, H. 2009. Highly Sensitive and High-Throughput Analysis of Plant Hormones Using MS-Probe Modification and Liquid ChromatographyTandem Mass Spectrometry: An Application for Hormone Profiling in *Oryza sativa*. *Plant and Cell Physiology,* 50**,** 1201-1214.

KOORNNEEF, M., ELGERSMA, A., HANHART, C. J., LOENEN-MARTINET, E. P., RIJN, L. & ZEEVAART, J. A. D. 1985. A Gibberellin Insensitive Mutant of *Arabidopsis thaliana*. *Physiologia Plantarum,* 65**,** 33-39.

KOORNNEEF, M. & VEEN, J. H. 1980. Induction and Analysis of Gibberellin Sensitive Mutants in *Arabidopsis thaliana* (L.) Heynh. *TAG Theoretical and Applied Genetics,* 58**,** 257-263.

KREPPEL, L. K., BLOMBERG, M. A. & HART, G. W. 1997. Dynamic Glycosylation of Nuclear and Cytosolic Proteins. Cloning and Characterisation of a unique O-GlcNAc Transfrase with multiple Tetratricopeptide Repeats. *Journal of Biological Chemistry,* 272**,** 9308-9315.

LAEMMLI, U. K. 1970. Cleavage of Structural Proteins during the Assembly of the Head of Bacteriophage T4. *Nature,* 227**,** 680-685.

LARKIN, M. A., BLACKSHIELDS, G., BROWN, N. P., CHENNA, R., MCGETTIGAN, P. A., MCWILLIAM, H., VALENTIN, F., WALLACE, I. M., WILM, A., LOPEZ, R., THOMPSON, J. D., GIBSON, T. J. & HIGGINS, D. G. 2007. Clustal W and Clustal X version 2.0. *Bioinformatics,* 23**,** 2947-2948.

LAWIT, S. J., WYCH, H. M., XU, D. P., KUNDU, S. & TOMES, D. T. 2010. Maize DELLA Proteins dwarf plant 8 and dwarf plant 9 as Modulators of Plant Development. *Plant and Cell Physiology,* 51**,** 1854-1868.

LEE, H., GUO, Y., OHTA, M., XIONG, L., STEVENSON, B. & ZHU, J.-K. 2002a. *LOS2*, a genetic locus required for cold-responsive gene transcription encodes a bi-functional enolase. *EMBO J,* 21**,** 2692-2702.

LEE, S., CHENG, H., KING, K. E., WANG, W., HE, Y., HUSSAIN, A., LO, J., HARBERD, N. P. & PENG, J. 2002b. Gibberellin regulates *Arabidopsis* seed germination via *RGL2*, a *GAI*/*RGA*-like gene whose expression is up-regulated following imbibition. *Genes and Development,* 16**,** 646-658.

LEE, S., LEE, S., YANG, K.-Y., KIM, Y.-M., PARK, S.-Y., KIM, S. Y. & SOH, M.-S. 2006. Overexpression of *PRE1* and its Homologous Genes Activates Gibberellin-dependent Responses in *Arabidopsis thaliana*. *Plant Cell Physiol.,* 47**,** 591-600.

LI, K., WANG, Y., HAN, C., ZHANG, W., JIA, H. & LI, X. 2007. GA signaling and *CO*/ *FT* Regulatory Module mediate Salt-Induced Late Flowering in *Arabidopsis thaliana*. *Plant Growth Regulation,* 53**,** 195-206.

LIAO, W. B., RUAN, M. B., CUI, B. M., XU, N. F., LU, J. J. & PENG, M. 2009. Isolation and Characterization of a *GAI* / *RGA*-like gene from *Gossypium hirsutum*. *Plant Growth Regulation,* 58**,** 35-45.

LIU, T., GU, J.-Y., XU, C.-J., GAO, Y. & AN, C.-C. 2007. Overproduction of OsSLRL2 Alters the Development of Transgenic *Arabidopsis* Plants. *Biochemical and Biophysical Research Communications,* 358**,** 983-989.

LOPEZ-MOLINA, L., MONGRAND, S., KINOSHITA, N. & CHUA, N.-H. 2003. AFP is a novel negative regulator of ABA signaling that promotes ABI5 protein degradation. *Genes & Development,* 17**,** 410-418.

LOVEGROVE, A., BARRATT, D. H. P., BEALE, M. H. & HOOLEY, R. 1998. Gibberellin-Photoaffinity Labelling of two polypeptides in Plant Plasma Membranes. *The Plant Journal,* 15**,** 311-320.

LOVEGROVE, A. & HOOLEY, R. 2000. Gibberellin and Abscisic acid Signalling in Aleurone. *Trends in Plant Science,* 5**,** 102-110.

LU, C.-A., HO, T.-H. D., HO, S.-L. & YU, S.-M. 2002. Three Novel MYB Proteins with One DNA Binding Repeat Mediate Sugar and Hormone Regulation of α-amylase Gene Expression. *Plant Cell,* 14**,** 1963-1980.

MA, H., YANOFSKY, M. & MEYEROWITZ, E. 1990. Molecular Cloning and Characterization of *GPA1*, a G Protein α–Subunit Gene from *Arabidopsis thaliana*. *Proceedings of the National Academy of Sciences of the United States of America,* 87**,** 3821-3825.

MA, Y., SZOSTKIEWICZ, I., KORTE, A., MOES, D., YANG, Y., CHRISTMANN, A. & GRILL, E. 2009. Regulators of *PP2C* Phosphatase Activity Function as Abscisic Acid Sensors. *Science,* 324**,** 1064-1068.

MAEKAWA, T., MAEKAWA-YOSHIKAWA, M., TAKEDA, N., IMAIZUMI-ANRAKU, H., MUROOKA, Y. & HAYASHI, M. 2009. Gibberellin Controls the Nodulation Signalling pathway in *Lotus japonicus*. *Plant Journal,* 58**,** 183-194.

MARTI, C., ORZAEZ, D., ELLUL, P., MORENO, V., CARBONELL, J. & GRANELL, A. 2007. Silencing of *DELLA* Induces facultative Parthenocarpy in Tomato Fruits. *The Plant Journal,* 52**,** 865-876.

MASON, M. G. & BOTELLA, J. R. 2000. Completing the Heterotrimer: Isolation and Characterization of an *Arabidopsis thaliana* G protein γ-subunit cDNA. *Proceedings of the National Academy of Sciences of the United States of America,* 97**,** 14784-14788.

MASON, M. G. & BOTELLA, J. R. 2001. Isolation of a novel G-protein γ-subunit from *Arabidopsis thaliana* and its Interaction with Gβ. *Biochimica et Biophysica Acta (BBA) - Gene Structure and Expression,* 1520**,** 147-153.

MAURIAT, M. & MORITZ, T. 2009. Analyses of *GA20ox*- and *GID1*-over-expressing Aspen suggest that Gibberellins play two distinct roles in Wood Formation. *Plant Journal,* 58**,** 989-1003.

MAYMON, I., GREENBOIM-WAINBERG, Y., SAGIV, S., KIEBER, J. J., MOSHELION, M., OLSZEWSKI, N. & WEISS, D. 2009. Cytosolic activity of *SPINDLY* implies the existence of a DELLA-Independent Gibberellin-response Pathway. *Plant Journal,* 58**,** 979-988.

MCCUBBIN, A. G., RITCHIE, S. M., SWANSON, S. J. & GILROY, S. 2004. The Calcium-dependent protein kinase *HvCDPK1* mediates the Gibberellic acid Response of the Barley Aleurone through Regulation of Vacuolar Function. *The Plant Journal,* 39**,** 206-218.

MCGINNIS, K. M., THOMAS, S. G., SOULE, J. D., STRADER, L. C., ZALE, J. M., SUN, T. P. & STEBER, C. M. 2003. The *Arabidopsis SLEEPY1* gene encodes a putative F-box subunit of an SCF E3 Ubiquitin Ligase. *Plant Cell,* 15**,** 1120-1130.

MENA, M., CEJUDO, F. J., ISABEL-LAMONEDA, I. & CARBONERO, P. 2002. A Role for the DOF Transcription Factor *BPBF* in the Regulation of Gibberellin-Responsive Genes in Barley Aleurone. *Plant Physiol.,* 130**,** 111-119.

MENA, M., VICENTE-CARBAJOSA, J., SCHMIDT, R. J. & CARBONERO, P. 1998. An Endosperm-specific DOF protein from Barley, highly conserved in Wheat, Binds to and Activates transcription from the Prolamin-box of a native B-hordein promoter in Barley Endosperm. *The Plant Journal,* 16**,** 53-62.

MILTENYI, S., MÜLLER, W., WEICHEL, W. & RADBRUCH, A. 1990. High Gradient Magnetic Cell Separation with MACS. *Cytometry,* 11**,** 231-238.

MITCHUM, M. G., YAMAGUCHI, S., HANADA, A., KUWAHARA, A., YOSHIOKA, Y., KATO, T., TABATA, S., KAMIYA, Y. & SUN, T.-P. 2006. Distinct and Overlapping roles of two Gibberellin 3-oxidases in *Arabidopsis* Development. *The Plant Journal,* 45**,** 804-818.

MONTE, E., AMADOR, V., RUSSO, E., MARTINEZ-GARCIA, J. & PRAT, S. 2003. *PHOR1*: A U-Box GA Signalling component with a role in Proteasome Degradation? *Journal of Plant Growth Regulation,* 22**,** 152-162.

MOON, J., SUH, S. S., LEE, H., CHOI, K. R., HONG, C. B., PAEK, N. C., KIM, S. G. & LEE, I. 2003. The *SOC1* MADS-box gene Integrates Vernalization and Gibberellin signals for Flowering in *Arabidopsis*. *Plant Journal,* 35**,** 613-623.

MUANGPROM, A., THOMAS, S. G., SUN, T. P. & OSBORN, T. C. 2005. A novel Dwarfing mutation in a Green Revolution gene from *Brassica rapa*. *Plant Physiology,* 137**,** 931-938.

MUELLER, T. D. & FEIGON, J. 2002. Solution Structures of UBA Domains Reveal a Conserved Hydrophobic Surface for Protein–Protein Interactions. *Journal of Molecular Biology,* 319**,** 1243-1255.

MUNNIK, T., IRVINE, R. F. & MUSGRAVE, A. 1998. Phospholipid Signalling in Plants. *Biochimica et Biophysica Acta (BBA) - Lipids and Lipid Metabolism,* 1389**,** 222-272.

MURASE, K., HIRANO, Y., SUN, T. P. & HAKOSHIMA, T. 2008. Gibberellin-induced DELLA Recognition by the Gibberellin Receptor GID1. *Nature,* 456**,** 459-U15.

MURRAY, F., KALLA, R., JACOBSEN, J. & GUBLER, F. 2003. A role for *HvGAMYB* in Anther Development. *The Plant Journal,* 33**,** 481-491.

NAKAJIMA, M., SHIMADA, A., TAKASHI, Y., KIM, Y.-C., PARK, S.-H., UEGUCHI-TANAKA, M., SUZUKI, H., KATOH, E., IUCHI, S. & KOBAYASHI ET, A. 2006. Identification and Characterization of *Arabidopsis* Gibberellin Receptors. *The Plant Journal: For Cell And Molecular Biology,* 46**,** 880-889.

NAVARRO, L., BARI, R., ACHARD, P., LISON, P., NEMRI, A., HARBERD, N. P. & JONES, J. D. G. 2008. DELLAs Control Plant Immune Responses by Modulating the Balance of Jasmonic acid and Salicylic acid Signalling. *Current Biology,* 18**,** 650-655.

NOLAN, T., HANDS, R.E., BUSTIN, S.A. 2006. Quantification of mRNA using Real-time RT-PCR. *Nature Protocols,* 1**,** 1159-1582.

O'FARRELL, P. H. 1975. High Resolution Two-Dimensional Electrophoresis of Proteins. *Journal of Biological Chemistry,* 250**,** 4007-4021.

O'NEILL, D. P., DAVIDSON, S. E., CLARKE, V. C., YAMAUCHI, Y., YAMAGUCHI, S., KAMIYA, Y., REID, J. B. & ROSS, J. J. 2010. Regulation of the Gibberellin pathway by Auxin and DELLA Proteins. *Planta,* 232**,** 1141-1149.

OGAWA, M., HANADA, A., YAMAUCHI, Y., KUWALHARA, A., KAMIYA, Y. & YAMAGUCHI, S. 2003. Gibberellin Biosynthesis and Response during *Arabidopsis* Seed Germination. *Plant Cell,* 15**,** 1591-1604.

OH, E., KANG, H., YAMAGUCHI, S., PARK, J., LEE, D., KAMIYA, Y. & CHOI, G. 2009. Genome-Wide Analysis of Genes Targeted by *PHYTOCHROME INTERACTING FACTOR 3-LIKE5* during Seed Germination in *Arabidopsis*. *Plant Cell,* 21**,** 403-419.

OH, E., YAMAGUCHI, S., HU, J. H., YUSUKE, J., JUNG, B., PAIK, I., LEE, H. S., SUN, T. P., KAMIYA, Y. & CHOI, G. 2007. *PIL5*, a Phytochrome-interacting bHLH protein, Regulates Gibberellin Responsiveness by Binding Directly to the *GAI* and *RGA* Promoters in *Arabidopsis* Seeds. *Plant Cell,* 19**,** 1192-1208.

OLSZEWSKI, N., SUN, T. P. & GUBLER, F. 2002. Gibberellin Signalling: Biosynthesis, Catabolism, and Response Pathways. *Plant Cell,* 14**,** S61-S80.

PABINGER, S., THALLINGER, G., SNAJDER, R., EICHHORN, H., RADER, R. & TRAJANOSKI, Z. 2009. QPCR: Application for Real-Time PCR Data Management and Analysis. *BMC Bioinformatics,* 10**,** 268.

PACIOREK, T., SAUER, M., BALLA, J., WISNIEWSKA, J. & FRIML, J. 2006. Immunocytochemical technique for protein localization in sections of plant tissues. *Nature Protocols,* 1**,** 104-107.

PAGE, R. D. M. 1996. Tree View: An Application to Display Phylogenetic Trees on Personal Computers. *Computer applications in the biosciences : CABIOS,* 12**,** 357-358.

PARK, S.-Y., FUNG, P., NISHIMURA, N., JENSEN, D. R., FUJII, H., ZHAO, Y., LUMBA, S., SANTIAGO, J., RODRIGUES, A., CHOW, T.-F. F., ALFRED, S. E., BONETTA, D., FINKELSTEIN, R., PROVART, N. J., DESVEAUX, D., RODRIGUEZ, P. L., MCCOURT, P., ZHU, J.-K., SCHROEDER, J. I., VOLKMAN, B. F. & CUTLER, S. R. 2009. Abscisic Acid Inhibits Type 2C Protein Phosphatases via the *PYR* / *PYL* Family of START Proteins. *Science,* 324**,** 1068-1071.

PARK, S. H., NAKAJIMA, M., HASEGAWA, M. & YAMAGUCHI, I. 2005. Similarities and differences between the characteristics of gibberellin-binding protein and gibberellin 2-oxidases in adzuki bean (*Vigna angularis*) seedlings. *Bioscience Biotechnology and Biochemistry,* 69**,** 1508-1514.

PENFIELD, S., GILDAY, A. D., HALLIDAY, K. J. & GRAHAM, I. A. 2006. DELLA-Mediated Cotyledon Expansion Breaks Coat-Imposed Seed Dormancy. *Current Biology: CB,* 16**,** 2366-2370.

PENG, J. & HARBERD, N. P. 1997. Transposon-Associated Somatic *gai*-Loss Sectors in *Arabidopsis*. *Plant Science,* 130**,** 181-188.

PENG, J., RICHARDS, D. E., HARTLEY, N. M., MURPHY, G. P., DEVOS, K. M., FLINTHAM, J. E., BEALES, J., FISH, L. J., WORLAND, A. J., PELICA, F., SUDHAKAR, D., CHRISTOU, P., SNAPE, J. W., GALE, M. D. & HARBERD, N. P. 1999. `Green Revolution' genes encode Mutant Gibberellin Response Modulators. *Nature,* 400**,** 256-261.

PENG, J. R., CAROL, P., RICHARDS, D. E., KING, K. E., COWLING, R. J., MURPHY, G. P. & HARBERD, N. P. 1997. The *Arabidopsis GAI* gene defines a Signalling pathway that Negatively Regulates Gibberellin Responses. *Genes & Development,* 11**,** 3194-3205.

PHINNEY, B. O. 1983. *The History of Gibberellins.*, Praeger Publishers USA.

PIERIK, R., CUPPENS, M. L. C., VOESENEK, L. & VISSER, E. J. W. 2004. Interactions between Ethylene and Gibberellins in Phytochrome-mediated Shade Avoidance Responses in Tobacco. *Plant Physiology,* 136**,** 2928-2936.

PIERIK, R., DJAKOVIC-PETROVIC, T., KEUSKAMP, D. H., DE WIT, M. & VOESENEK, L. 2009. Auxin and Ethylene Regulate Elongation Responses to Neighbor Proximity Signals Independent of Gibberellin and DELLA Proteins in *Arabidopsis*. *Plant Physiology,* 149**,** 1701-1712.

PISKUREWICZ, U., TURECKOVA, V., LACOMBE, E. & LOPEZ-MOLINA, L. 2009. Far-Red Light Inhibits Germination through DELLA-dependent Stimulation of ABA Synthesis and ABI3 Activity. *Embo Journal,* 28**,** 2259-2271.

PRIKRYL, J., ROJAS, M., SCHUSTER, G. & BARKAN, A. 2011. Mechanism of RNA stabilization and translational activation by a pentatricopeptide repeat protein. *Proceedings of the National Academy of Sciences,* 108**,** 415-420.

PYSH, L. D., WYSOCKA-DILLER, J. W., CAMILLERI, C., BOUCHEZ, D. & BENFEY, P. N. 1999. The GRAS gene family in *Arabidopsis*: Sequence Characterization and basic Expression Analysis of the *SCARECROW-LIKE* Genes. *The Plant Journal,* 18**,** 111-119.

RAVENTOS, D., SKRIVER, K., SCHLEIN, M., KARNAHL, K., ROGERS, S. W., ROGERS, J. C. & MUNDY, J. 1998. *HRT*, a Novel Zinc Finger, Transcriptional Repressor from Barley. *J. Biol. Chem.,* 273**,** 23313-23320.

REID, M. S. & BIELESKI, R. L. 1968. A Simple Apparatus for vertical flat-sheet Polyacrylamide Gel Electrophoresis. *Analytical Biochemistry,* 22**,** 374-381.

REMINGTON, D. L. & PURUGGANAN, M. D. 2002. *GAI* homologues in the Hawaiian Silversword Alliance (*Asteraceae-Madiinae*): Molecular Evolution of Growth Regulators in a rapidly diversifying Plant Lineage. *Molecular Biology and Evolution,* 19**,** 1563-1574.

RHOADES, M. W., REINHART, B. J., LIM, L. P., BURGE, C. B., BARTEL, B. & BARTEL, D. P. 2002. Prediction of Plant MicroRNA Targets. *Cell,* 110**,** 513-520.

RIEFLER, M., NOVAK, O., STRNAD, M. & SCHMULLING, T. 2006. *Arabidopsis* Cytokinin Receptor mutants reveal Functions in Shoot Growth, Leaf Senescence, Seed Size, Germination, Root Development, and Cytokinin Metabolism. *Plant Cell,* 18**,** 40.

RIGAUT, G., SHEVCHENKO, A., RUTZ, B., WILM, M., MANN, M. & SERAPHIN, B. 1999. A Generic Protein Purification Method for Protein Complex Characterization and Proteome Exploration. *Nature BioTech,* 17**,** 1030-1032.

RITCHIE, S. & GILROY, S. 1998a. Calcium-Dependent Protein Phosphorylation may mediate the Gibberellic acid Response in Barley Aleurone. *Plant Physiol.,* 116**,** 765-776.

RITCHIE, S. & GILROY, S. 1998b. Gibberellins: Regulating Genes and Germination. *New Phytologist,* 140**,** 363-383.

RITCHIE, S., SWANSON, S. J. & GILROY, S. 2000. Physiology of the Aleurone Layer and Starchy Endosperm during Grain Development and Early Seedling Growth: New Insights from Cell and Molecular Biology. *Seed Science Research,* 10**,** 193-212.

ROHILA, J. S., CHEN, M., CERNY, R. & FROMM, M. E. 2004. Improved Tandem Affinity Purification Tag and Methods for Isolation of Protein Heterocomplexes from Plants. *The Plant Journal,* 38**,** 172-181.

ROSE, T., SCHULTZ, E., HENIKOFF, J., PIETROKOVSKI, S., MCCALLUM, C. & HENIKOFF, S. 1998. COnsensus-Degenerate Hybrid Oligonucleotide Primers for Amplification of Distantly Related Sequences. *Nucleic Acids Research,* 26**,** 1628-1635.

ROSE, T. M., HENIKOFF, J. G. & HENIKOFF, S. 2003. CODEHOP (COnsensus-DEgenerate Hybrid Oligonucleotide Primer) PCR primer design. *Nucleic Acids Research,* 31**,** 3763-3766.

ROZEN, S. & SKALETSKY, H. 1999. Primer3 on the WWW for General Users and for Biologist Programmers.

RUSHTON, P. J., MACDONALD, H., HUTTLY, A. K., LAZARUS, C. M. & HOOLEY, R. 1995. Members of a New Family of DNA-binding proteins Bind to a Conserved Cis-Element in the Promoters of α*-AMY2* Genes. *Plant Molecular Biology,* 29**,** 691-702.

SAIKI, R. K., GELFAND, D. H., STOFFEL, S., SCHARF, S. J., HIGUCHI, R. & AL., E. 1988. Primer-Directed Enzymatic Amplification of DNA with a Thermostable DNA Polymerase. *Science,* 239**,** 487.

SAMBROOK, J., FRITSCH, E. & MANIATIS, T. (eds.) 1989. *Molecular Cloning, A laboratory Manual*: Cold Spring Harbour Laboratory Press.

SANCHEZ-FERNANDEZ, R., ARDILES-DIAZ, W., VAN MONTAGU, M., INZE, D. & MAY, M. 1998. Gene note. Cloning of a novel *Arabidopsis thaliana RGA*-like gene, a putative member of the VHIID-domain transcription factor family. *Journal of Experimental Botany,* 49**,** 1609-1610.

SANTNER, A., CALDERON-VILLALOBOS, L. I. A. & ESTELLE, M. 2009. Plant hormones are Versatile Chemical Regulators of Plant Growth. *Nature Chemical Biology,* 5**,** 301-307.

SASAKI, A., ITOH, H., GOMI, K., UEGUCHI-TANAKA, M., ISHIYAMA, K., KOBAYASHI, M., JEONG, D. H., AN, G., KITANO, H., ASHIKARI, M. & MATSUOKA, M. 2003. Accumulation of Phosphorylated Repressor for Gibberellin Signalling in an F-box Mutant. *Science,* 299**,** 1896-1898.

SCHWECHHEIMER, C. & VILLALOBOS, L. 2004. Cullin-Containing E3 Ubiquitin Ligases in Plant Development. *Current Opinion in Plant Biology,* 7**,** 677-686.

SEO, M., NAMBARA, E., CHOI, G. & YAMAGUCHI, S. 2009. Interaction of Light and Hormone Signals in Germinating Seeds. *Plant Molecular Biology,* 69**,** 463-472.

SHEERIN, D. J. 2010. Characterisation of the Interactions of *RGL1*; a Negative Regulator of Gibberellin Signalling. *Thesis*.

SHEERIN, D. J., BUCHANAN, J., KIRK, C., HARVEY, D., SUN, X., SPAGNUOLO, J., LI, S., LIU, T., WOODS, V. A., FOSTER, T., JONES, W. T. & RAKONJAC, J. 2011. Inter- and Intra-Molecular Interactions of *Arabidopsis thaliana* DELLA protein RGL1. *Biochemical Journal,* 435**,** 629-639.

SHI, T., HUANG, H. & BARKER, M. S. 2010. Ancient genome duplications during the evolution of kiwifruit (*Actinidia*) and related Ericales. *Annals of Botany,* 106**,** 497-504.

SHIMADA, A., UEGUCHI-TANAKA, M., SAKAMOTO, T., FUJIOKA, S., TAKATSUTO, S., YOSHIDA, S., SAZUKA, T., ASHIKARI, M. & MATSUOKA, M. 2006. The Rice *SPINDLY* gene functions as a Negative Regulator of Gibberellin Signalling by Controlling the Suppressive Function of the DELLA protein, SLR1, and Modulating Brassinosteroid Synthesis. *The Plant Journal: For Cell And Molecular Biology,* 48**,** 390-402.

SHIMIZU-SATO, S. & MORI, H. 2001. Control of Outgrowth and Dormancy in Axillary Buds. *Plant Physiology,* 127**,** 1405-1413.

SIDAWAY-LEE, K., JOSSE, E. M., BROWN, A., GAN, Y. B., HALLIDAY, K. J., GRAHAM, I. A. & PENFIELD, S. 2010. *SPATULA* Links Daytime Temperature and Plant Growth Rate. *Current Biology,* 20**,** 1493-1497.

SILVERSTONE, A. L., CIAMPAGLIO, C. N. & SUN, T.-P. 1998. The *Arabidopsis RGA* Gene Encodes a Transcriptional Regulator Repressing the Gibberellin Signal Transduction Pathway. *Plant Cell,* 10**,** 155-170.

SILVERSTONE, A. L., JUNG, H. S., DILL, A., KAWAIDE, H., KAMIYA, Y. & SUN, T. P. 2001. Repressing a Repressor: Gibberellin-Induced rapid Reduction of the RGA protein in *Arabidopsis*. *Plant Cell,* 13**,** 1555-1565.

SILVERSTONE, A. L., MAK, P., MARTINEZ, E. C. & SUN, T. 1997. The New *RGA* Locus Encodes a Negative Regulator of Gibberellin Response in *Arabidopsis thaliana*. *Genetics,* 146**,** 1087-1099.

SILVERSTONE, A. L., TSENG, T.-S., SWAIN, S. M., DILL, A., JEONG, S. Y., OLSZEWSKI, N. E. & SUN, T.-P. 2007. Functional Analysis of *SPINDLY* in Gibberellin Signaling in *Arabidopsis*. *Plant Physiol.,* 143**,** 987-1000.

SIMPSON, G. G., DIJKWEL, P. P., QUESADA, V., HENDERSON, I. & DEAN, C. 2003. FY is an RNA 3' End-Processing Factor that Interacts with FCA to Control the *Arabidopsis* Floral Transition. *Cell,* 113**,** 777-787.

SONG, S., QI, T., HUANG, H., REN, Q., WU, D., CHANG, C., PENG, W., LIU, Y., PENG, J. & XIE, D. 2011. The Jasmonate-ZIM Domain Proteins Interact with the R2R3-MYB Transcription Factors MYB21 and MYB24 to Affect Jasmonate-Regulated Stamen Development in Arabidopsis. *The Plant Cell Online,* 23**,** 1000-1013.

SONG, Y., ZHANG, Y.-M., LIU, M.-Y., WANG, C.-Z., LIU, J., FENG, S.-Q., WANG, Y.-L. & CHEN, X.-S. 2012. Cloning and Prokaryotic Expression of *MdRGL* Gene from Spur-Type Apple (*Malus domestica* Borkh.). *China Agriculture Science,* 45**,** 1347-1354.

SPONSEL, V. M. 1995. Plant Hormones. Physiology, Biochemistry and Molecular Biology. *In:* DAVIES, P. J. (ed.) 2nd ed.: Kluwer Acedemic Publishers.

STEBER, C. M., COONEY, S. E. & MCCOURT, P. 1998. Isolation of the GA-Response Mutant *sly1* as a Suppressor of *ABI1-1* in *Arabidopsis thaliana*. *Genetics,* 149**,** 509-521.

STEFFENS, B., WANG, J. & SAUTER, M. 2006. Interactions between Ethylene, Gibberellin and Abscisic acid Regulate Emergence and Growth rate of Adventitious Roots in deepwater Rice. *Planta,* 223**,** 604-612.

STEVENSON, J. M., PERERA, I. Y., HEILMANN, I., PERSSON, S. & BOSS, W. F. 2000. Inositol Signalling and Plant Growth. *Trends in Plant Science,* 5**,** 252-258.

STONE, S. L. & CALLIS, J. 2007. Ubiquitin Ligases Mediate Growth and Development by Promoting Protein Death. *Current Opinion in Plant Biology,* 10**,** 624-632.

STRADER, L. C., RITCHIE, S., SOULE, J. D., MCGINNIS, K. M. & STEBER, C. M. 2004. Recessive-Interfering Mutations in the Gibberellin Signaling gene *SLEEPY1* are Rescued by Over-

expression of its Homologue, *SNEEZY*. *Proceedings of the National Academy of Sciences of the United States of America,* 101**,** 12771-12776.
SUN, T. P. 2010. Gibberellin-GID1-DELLA: A Pivotal Regulatory Module for Plant Growth and Development. *Plant Physiology,* 154**,** 567-570.
SUN, X., FREARSON, N., KIRK, C., JONES, W. T., HARVEY, D., RAKONJAC, J., FOSTER, T. & AL-SAMARRAI, T. 2008. An *E. coli* Expression System optimized for DELLA Proteins. *Protein Expression and Purification,* 58**,** 168-174.
SUN, X. L., JONES, W. T., HARVEY, D., EDWARDS, P. J. B., PASCAL, S. M., KIRK, C., CONSIDINE, T., SHEERIN, D. J., RAKONJAC, J., OLDFIELD, C. J., XUE, B., DUNKER, A. K. & UVERSKY, V. N. 2010. N-terminal Domains of DELLA Proteins Are Intrinsically Unstructured in the Absence of Interaction with GID1/Gibberellic Acid Receptors. *Journal of Biological Chemistry,* 285**,** 11557-11571.
SUN, X. L., JONES, W. T. & RIKKERINK, E. H. A. 2012. GRAS Proteins: The versatile Roles of Intrinsically Disordered proteins in Plant Signalling. *Biochemical Journal,* 442**,** 1-12.
SUZUKI, H., PARK, S. H., OKUBO, K., KITAMURA, J., UEGUCH-TANAKA, M., IUCHI, S., KATOH, E., KOBAYASHI, M., YAMAGUCHI, I., MATSUOKA, M., ASAMI, T. & NAKAJIMA, M. 2009. Differential Expression and Affinities of *Arabidopsis* Gibberellin Receptors can explain Variation in Phenotypes of Multiple Knock-out Mutants. *Plant Journal,* 60**,** 48-55.
SWAIN, S. M. & SINGH, D. P. 2005. Tall Tales from *sly* Dwarves: Novel Functions of Gibberellins in Plant Development. *Trends in Plant Science,* 10**,** 123-129.
SWAIN, S. M., TSENG, T. S. & OLSZEWSKI, N. E. 2001. Altered Expression of *SPINDLY* affects Gibberellin Response and Plant Development. *Plant Physiology,* 126**,** 1174-1185.
TESTOLIN, R. & FERGUSON, A. R. 1997. Isozyme Polymorphism in the Genus *Actinidia* and the Origin of the Kiwifruit Genome. *Systematic Botany,* 22**,** 685-700.
THOMAS, S. G., RIEU, I. & STEBER, C. M. 2005. Gibberellin Metabolism and Signalling. *Plant Hormones.* San Diego: Elsevier Academic Press Inc.
THORNTON, T. M., SWAIN, S. M. & OLSZEWSKI, N. E. 1999. Gibberellin Signal Transduction presents ...the SPY who *O*-GlcNAc'd Me. *Trends in Plant Science,* 4**,** 424-428.
TORII, K. U., MITSUKAWA, N., OOSUMI, T., MATSUURA, Y., YOKOYAMA, R., WHITTIER, R. F. & KOMEDA, Y. 1996. The *Arabidopsis ERECTA* Gene Encodes a Putative Receptor Protein Kinase with Extracellular Leucine-Rich Repeats. *Plant Cell,* 8**,** 735-746.
TRUONG, H.-N., CABOCHE, M. & DANIEL-VEDELE, F. 1997. Sequence and Characterization of two *Arabidopsis thaliana* cDNAs Isolated by Functional Complementation of a Yeast *gln3 gdh1* Mutant. *FEBS Letters,* 410**,** 213-218.
TSENG, T. S., SALOME, P. A., MCCLUNG, C. R. & OLSZEWSKI, N. E. 2004. SPINDLY and GIGANTEA Interact and Act in *Arabidopsis thaliana* pathways involved in Light Responses, Flowering, and Rhythms in Cotyledon Movements. *Plant Cell,* 16**,** 1550-1563.
TSENG, T. S., SWAIN, S. M. & OLSZEWSKI, N. E. 2001. Ectopic Expression of the Tetratricopeptide Repeat domain of SPINDLY causes Defects in Gibberellin Response. *Plant Physiology,* 126**,** 1250-1258.
TSUJI, H., AYA, K., UEGUCHI-TANAKA, M., SHIMADA, Y., NAKAZONO, M., WATANABE, R., NISHIZAWA, N. K., GOMI, K., SHIMADA, A., KITANO, H., ASHIKARI, M. & MATSUOKA, M. 2006. *GAMYB* Controls different sets of Genes and is differentially Regulated by microRNA in Aleurone cells and Anthers. *The Plant Journal,* 47**,** 427-444.
TYLER, L., THOMAS, S. G., HU, J. H., DILL, A., ALONSO, J. M., ECKER, J. R. & SUN, T. P. 2004. DELLA proteins and Gibberellin-Regulated Seed Germination and Floral Development in *Arabidopsis*. *Plant Physiology,* 135**,** 1008-1019.
UBEDA-TOMAS, S., SWARUP, R., COATES, J., SWARUP, K., LAPLAZE, L., BEEMSTER, G. T. S., HEDDEN, P., BHALERAO, R. & BENNETT, M. J. 2008. Root Growth in *Arabidopsis* requires Gibberellin / DELLA Signalling in the Endodermis. *Nat Cell Biol,* 10**,** 625-628.
UEGUCHI-TANAKA, M., ASHIKARI, M., NAKAJIMA, M., ITOH, H., KATOH, E., KOBAYASHI, M., CHOW, T.-Y., HSING, Y.-I. C., KITANO, H. & YAMAGUCHI ET, A. 2005. *GIBBERELLIN*

INSENSITIVE DWARF1 encodes a Soluble Receptor for Gibberellin. *Nature,* 437**,** 693-698.

UEGUCHI-TANAKA, M., FUJISAWA, Y., KOBAYASHI, M., ASHIKARI, M., IWASAKI, Y., KITANO, H. & MATSUOKA, M. 2000. Rice Dwarf mutant *d1*, which is Defective in the α-subunit of the Heterotrimeric G protein, affects Gibberellin Signal Transduction. *Proceedings of the National Academy of Sciences of the United States of America,* 97**,** 11638-11643.

UEGUCHI-TANAKA, M., NAKAJIMA, M., KATOH, E., OHMIYA, H., ASANO, K., SAJI, S., XIANG, H. Y., ASHIKARI, M., KITANO, H., YAMAGUCHI, I. & MATSUOKAA, M. 2007. Molecular Interactions of a Soluble Gibberellin Receptor, GID1, with a rice DELLA protein, SLR1, and Gibberellin. *Plant Cell,* 19**,** 2140-2155.

VANDENBUSSCHE, F., FIERRO, A. C., WIEDEMANN, G., RESKI, R. & VAN DER STRAETEN, D. 2007a. Evolutionary Conservation of Plant Gibberellin Signalling Pathway Components. *Bmc Plant Biology,* 7.

VANDENBUSSCHE, F., VANCOMPERNOLLE, B., RIEU, I., AHMAD, M., PHILLIPS, A., MORITZ, T., HEDDEN, P. & VAN DER STRAETEN, D. 2007b. Ethylene-Induced *Arabidopsis* Hypocotyl Elongation is dependent on but not mediated by Gibberellins. *Journal of Experimental Botany,* 58**,** 4269-4281.

VARBANOVA, M., YAMAGUCHI, S., YANG, Y., MCKELVEY, K., HANADA, A., BOROCHOV, R., YU, F., JIKUMARU, Y., ROSS, J., CORTES, D., MA, C. J., NOEL, J. P., MANDER, L., SHULAEV, V., KAMIYA, Y., RODERMEL, S., WEISS, D. & PICHERSKY, E. 2007. Methylation of Gibberellins by Arabidopsis *GAMT1* and *GAMT2*. *Plant Cell,* 19**,** 32-45.

VELASCO, R., ZHARKIKH, A., AFFOURTIT, J., DHINGRA, A., CESTARO, A., KALYANARAMAN, A., FONTANA, P., BHATNAGAR, S. K., TROGGIO, M., PRUSS, D., SALVI, S., PINDO, M., BALDI, P., CASTELLETTI, S., CAVAIUOLO, M., COPPOLA, G., COSTA, F., COVA, V., DAL RI, A., GOREMYKIN, V., KOMJANC, M., LONGHI, S., MAGNAGO, P., MALACARNE, G., MALNOY, M., MICHELETTI, D., MORETTO, M., PERAZZOLLI, M., SI-AMMOUR, A., VEZZULLI, S., ZINI, E., ELDREDGE, G., FITZGERALD, L. M., GUTIN, N., LANCHBURY, J., MACALMA, T., MITCHELL, J. T., REID, J., WARDELL, B., KODIRA, C., CHEN, Z., DESANY, B., NIAZI, F., PALMER, M., KOEPKE, T., JIWAN, D., SCHAEFFER, S., KRISHNAN, V., WU, C., CHU, V. T., KING, S. T., VICK, J., TAO, Q., MRAZ, A., STORMO, A., STORMO, K., BOGDEN, R., EDERLE, D., STELLA, A., VECCHIETTI, A., KATER, M. M., MASIERO, S., LASSERRE, P., LESPINASSE, Y., ALLAN, A. C., BUS, V., CHAGNE, D., CROWHURST, R. N., GLEAVE, A. P., LAVEZZO, E., FAWCETT, J. A., PROOST, S., ROUZE, P., STERCK, L., TOPPO, S., LAZZARI, B., HELLENS, R. P., DUREL, C.-E., GUTIN, A., BUMGARNER, R. E., GARDINER, S. E., SKOLNICK, M., EGHOLM, M., VAN DE PEER, Y., SALAMINI, F. & VIOLA, R. 2010. The Genome of the Domesticated Apple (*Malus* x *domestica* Borkh.). *Nat Genet,* 42**,** 833-839.

VILLASUSO, A. L. & MACHADO-DOMENECH, E. 2004. Gibberellin Signalling Pathway: Role of Phospholipids in Barley Aleurone. *Plant Growth Regulation,* 43**,** 101-108.

VRIEZEN, W. H., ACHARD, P., HARBERD, N. P. & VAN DER STRAETEN, D. 2004. Ethylene-Mediated enhancement of Apical hook formation in Etiolated *Arabidopsis thaliana* Seedlings is Gibberellin Dependent. *Plant Journal,* 37**,** 505-516.

WANG, F., ZHU, D. M., HUANG, X., LI, S., GONG, Y. N., YAO, Q. F., FU, X. D., FAN, L. M. & DENG, X. W. 2009. Biochemical Insights on Degradation of *Arabidopsis* DELLA Proteins Gained From a Cell-Free Assay System. *Plant Cell,* 21**,** 2378-2390.

WASHIO, K. 2003. Functional Dissections between *GAMYB* and Dof Transcription Factors Suggest a role for Protein-Protein Associations in the Gibberellin-Mediated Expression of the *RAMY1A* gene in the Rice Aleurone. *Plant Physiology,* 133**,** 850-863.

WEISS, C., GARNAAT, C., MUKAI, K., HU, Y. & MA, H. 1994. Isolation of cDNAs Encoding Guanine Nucleotide-Binding Protein β- Subunit Homologues from Maize (*ZGB1*) and *Arabidopsis* (*AGB1*). *Proceedings of the National Academy of Sciences of the United States of America,* 91**,** 9554-9558.

WEN, C. K. & CHANG, C. 2002. *Arabidopsis RGL1* Encodes a Negative Regulator of Gibberellin Responses. *Plant Cell,* 14**,** 87-100.

WESTON, D. E., ELLIOTT, R. C., LESTER, D. R., RAMEAU, C., REID, J. B., MURFET, I. C. & ROSS, J. J. 2008. The pea DELLA proteins LA and CRY are important Regulators of Gibberellin Synthesis and Root Growth. *Plant Physiology,* 147**,** 199-205.

WILLIGE, B. C., GHOSH, S., NILL, C., ZOURELIDOU, M., DOHMANN, E. M. N., MAIER, A. & SCHWECHHEIMER, C. 2007. The DELLA Domain of GA INSENSITIVE Mediates the Interaction with the GA INSENSITIVE DWARF1A Gibberellin Receptor of *Arabidopsis*. *Plant Cell,* 19**,** 1209-1220.

WILSON, R. N. & SOMERVILLE, C. R. 1995. Phenotypic Suppression of the Gibberellin-Insensitive Mutant (*gai)* of *Arabidopsis*. *Plant Physiology,* 108**,** 495-502.

WITTIG, I., BRAUN, H.-P. & SCHAGGER, H. 2006. Blue Native PAGE. *Nature Protocols,* 1**,** 418-428.

WITTIG, I., KARAS, M. & SCHÃ¤GGER, H. 2007. High Resolution Clear Native Electrophoresis for In-gel Functional Assays and Fluorescence Studies of Membrane Protein Complexes. *Molecular and Cellular Proteomics,* 6**,** 1215-1225.

WOODGER, F. J., MILLAR, A., MURRAY, F., JACOBSEN, J. V. & GUBLER, F. 2003. The Role of *GAMYB* Transcription Factors in GA-Regulated Gene Expression. *Journal of Plant Growth Regulation,* 22**,** 176-184.

XI, W. Y., LIU, C., HOU, X. L. & YU, H. 2010. *MOTHER OF FT AND TFL1* Regulates Seed Germination through a Negative Feedback Loop Modulating ABA Signalling in *Arabidopsis*. *Plant Cell,* 22**,** 1733-1748.

XIANG, H. Y., TAKEUCHI, H., TSUNODA, Y., NAKAJIMA, M., MURATA, K., UEGUCHI-TANAKA, M., KIDOKORO, S., KEZUKA, Y., NONAKA, T., MATSUOKA, M. & KATOH, E. 2011. Thermodynamic Characterization of OsGID1-Gibberellin Binding using Calorimetry and Docking Simulations. *Journal of Molecular Recognition,* 24**,** 275-282.

XIE, Z., ZHANG, Z. L., ZOU, X. L., YANG, G. X., KOMATSU, S. & SHEN, Q. X. J. 2006. Interactions of Two Abscisic acid Induced WRKY genes in Repressing Gibberellin Signalling in Aleurone Cells. *Plant Journal,* 46**,** 231.

XU, Y., LI, L., WU, K., PEETERS, A., GAGE, D. & ZEEVAART, J. 1995. The *GA5* Locus of *Arabidopsis thaliana* Encodes a Multifunctional Gibberellin 20-Oxidase: Molecular Cloning and Functional Expression. *PNAS,* 92**,** 6640-6644.

YAMAGUCHI, S. & KAMIYA, Y. 2000. Gibberellin Biosynthesis: Its Regulation by Endogenous and Environmental Signals. *Plant and Cell Physiology,* 41**,** 251-257.

YAMAGUCHI, S. & KAMIYA, Y. 2001. Gibberellins and Light-Stimulated Seed Germination. *Journal of Plant Growth Regulation,* 20**,** 369-376.

YAMAMOTO, Y., HIRAI, T., YAMAMOTO, E., KAWAMURA, M., SATO, T., KITANO, H., MATSUOKA, M. & UEGUCHI-TANAKA, M. 2010. A Rice *gid1* Suppressor Mutant reveals that Gibberellin is Not Always Required for Interaction between Its Receptor, GID1, and DELLA Proteins. *Plant Cell,* 22**,** 3589-3602.

YANG, G. X., SHEN, S. H., YANG, S. H. & KOMATSU, S. 2003. *OsCDPK13*, a Calcium-Dependent Protein Kinase gene from Rice, is Induced in response to Cold and Gibberellin. *Plant Physiology and Biochemistry,* 41**,** 369-374.

YASUMURA, Y., CRUMPTON-TAYLOR, M., FUENTES, S. & HARBERD, N. P. 2007. Step-by-Step acquisition of the Gibberellin-*DELLA* growth-Regulatory Mechanism during Land-Plant Evolution. *Current Biology,* 17**,** 1225-1230.

YU, H., ITO, T., ZHAO, Y. X., PENG, J. R., KUMAR, P. & MEYEROWITZ, E. M. 2004. Floral Homeotic Genes are Targets of Gibberellin Signalling in Flower Development. *Proceedings of the National Academy of Sciences of the United States of America,* 101**,** 7827-7832.

ZENG, Y. & PIWNICA-WORMS, H. 1999. DNA Damage and Replication Checkpoints in Fission Yeast Require Nuclear Exclusion of the Cdc25 Phosphatase via 14-3-3 Binding. *Molecular and Cellular Biology,* 19**,** 7410-7419.

ZENTELLA, R., ZHANG, Z.-L., PARK, M., THOMAS, S. G., ENDO, A., MURASE, K., FLEET, C. M., JIKUMARU, Y., NAMBARA, E., KAMIYA, Y. & SUN, T.-P. 2007. Global Analysis of DELLA Direct Targets in Early Gibberellin Signaling in *Arabidopsis*. *Plant Cell,* 19**,** 3037-3057.

ZHANG, Z. L., OGAWA, M., FLEET, C. M., ZENTELLA, R., HU, J. H., HEO, J. O., LIM, J., KAMIYA, Y., YAMAGUCHI, S. & SUN, T. P. 2011. SCARECROW-LIKE 3 Promotes Gibberellin Signalling by Antagonizing Master Growth Repressor DELLA in *Arabidopsis*. *Proceedings of the National Academy of Sciences of the United States of America,* 108**,** 2160-2165.

ZHANG, Z. L., XIE, Z., ZOU, X. L., CASARETTO, J., HO, T. H. D. & SHEN, Q. X. J. 2004. A Rice WRKY Gene encodes a Transcriptional Repressor of the Gibberellin Signaling Pathway in Aleurone Cells. *Plant Physiology,* 134**,** 1500-1513.

ZHAO, S. & FERNALD, R. 2005. Comprehensive Algorithm for Quantitative Real-Time Polymerase Chain Reaction. *J Comput Biol,* 12**,** 1047 - 1064.

ZHU, Y., NOMURA, T., XU, Y., ZHANG, Y., PENG, Y., MAO, B., HANADA, A., ZHOU, H., WANG, R., LI, P., ZHU, X., MANDER, L. N., KAMIYA, Y., YAMAGUCHI, S. & HE, Z. 2006. *ELONGATED UPPERMOST INTERNODE* Encodes a Cytochrome P450 Monooxygenase that Epoxidizes Gibberellins in a Novel Deactivation Reaction in Rice. *Plant Cell,* 18**,** 442-456.

ZIPPER, H., BRUNNER, H., BERNHAGEN, J. & VITZTHUM, F. 2004. Investigations on DNA Intercalation and Surface Binding by SYBR Green I, its Structure Determination and Methodological Implications. *Nucleic Acids Research,* 32**,** e103.